NASA TECHNICAL TRANSLATION

NASA TT F-635

NASA TT F-635

DYNAMICS OF THE RADIATION BELTS OF THE EARTH

by B. A. Tverskoy

"Nauka" Press, Moscow, 1968

NATIONAL AERONAUTICS AND SPACE ADMINISTRATION • WASHINGTON, D. C. • JUNE 1971

DYNAMICS OF THE RADIATION BELTS OF THE EARTH

By B. A. Tverskoy

Translation of "Dinamika Radiatsionnykh Poyasov Zemli." "Nauka" Press, Moscow, 1968.

NATIONAL AERONAUTICS AND SPACE ADMINISTRATION

For sale by the National Technical Information Service, Springfield, Virginia 22151
price $3.00

ANNOTATION

The first chapter of the monograph surveys contemporary ideas on the physical conditions in the earth's magnetosphere (the magnetic field, plasma, and electromagnetic pulsations of different frequencies). The second chapter contains a detailed explanation of data on the structure and dynamics of the earth's radiation belts.

The third chapter explains the theoretical investigation made of the transfer of trapped particles as a result of the effect of geomagnetic disturbances. The electric field induced by the disturbance is found, the particle drift equation is solved, and the diffusion factor is established. The different stationary and nonstationary processes involved in particle transfer in the magnetosphere are studied.

The application of transfer theory to the interpretation of the properties of the radiation belts is reviewed in the fourth chapter. It is shown that protons with energies of less than 30 Mev occur in the magnetosphere as a result of betatron acceleration upon transfer from the boundary. An explanation of diffusion waves of high-speed electrons is given.

The fifth chapter investigates the boundary of stability for the radiation belts and shows that the proton belt is stable, or slightly unstable. Electron intensities close to the boundary are stable, and electron escape is the result of excess intensity being thrown out into the ionosphere.

There are four tables, 37 illustrations, and a bibliography of 156 citations.

FOREWORD

There have been recent, great successes in the experimental research done in /6
near space. The structure of the geomagnetic field, deformed by the solar wind, has been clarified and detailed, systematic investigations of the fluxes of charged particles with different types of energies have been made, and research on the spectrum of electromagnetic oscillations and of waves in the magnetosphere have begun. The development of theoretical research on the physics of the magnetosphere can be characterized by the ever expanding use of the concepts of contemporary plasma theory.

The vast body of experimental material suggests that the formation of very high fluxes of high-energy, charged particles in the magnetosphere is primarily one of the manifestations of a complex set of processes involved in the interaction between the geomagnetic field and the solar plasma fluxes. Purely earth processes (electrostatic fields generated by ionospheric winds, as well as electromagnetic radiation from lightning discharges, and ionospheric turbulence) too have a significant part in the range of comparatively low energies ($\lesssim$10 keV).

But there are many basic problems to be solved before a complete theory for the dynamics of the magnetosphere can be postulated. It can only be hoped that when detailed measurements of the electrostatic and electromagnetic fields in near space are made these will be the basis for the successful construction of a semiphenomenological theory of the dynamics of charged particles. At the same time, the solutions to individual problems are definitely possible right now. Included among them, in particular, is the answer to the question of the occur- /7
ance of very high fluxes of very high fluxes of charged particles with energies $\gtrsim$ 100 keV on the earth's radiation belts.

As we know, there are no particles with energies such as these in the solar wind. On the other hand, the available data on electromagnetic fields indicate that it is impossible to accelerate to these energies because of a variety of statistical and impact mechanisms. Finally, the cosmic-ray albedo neutron decay is clearly inadequate to create the particle fluxes observed. The only possibility of radiation belt particle acceleration therefore reduces to adiabatic acceleration upon transfer to a region with a stronger field.

Evaluations indicate that at energies of $\lesssim$ 10 keV the transfer of ionospheric winds by electric fields is extremely effective. But at higher energies (and, correspondingly, at higher magnetic drift rates) this effect will only result in small adiabatic variations in the drift orbits of the particles. Here the transfer mechanism pointed out by Parker is much more effective; that is, the drift in electric fields that occurs as a result of forced oscillations of the boundary of the magnetosphere during geomagnetic disturbances.

There has been a recent, intensive development of this concept by scientists in a number of countries, and this has led to the explanation and prediction of many properties of the earth's radiation belts. The many experimental confirmations of this theory permit the hope that the basic mechanism involved in particle acceleration in the belts has been explained.

The mechanism involved in escape is a second, important, problem in the theory of belts. This question is closely allied with the stability of higher than normal radiation zones. Here too, substantial progress has been made.

Accordingly there has now been formulated a definite set of theoretical assumptions that provides an inherently noncontradictory explanation of the processes of acceleration and destruction of particles in radiation belts, one which has a great many direct and indirect confirmations. This monograph is devoted /8 to a systematic exposition of this theory.

The first two chapters are devoted to a survey of experimental data, and are based on materials published through mid-1966. The purpose of the survey is simply to record the present state of knowledge of physical conditions in the earth's magnetosphere and, in more detail, of knowledge of the radiation belts. Hence, many of the results which had played an important part in their time are not considered because they have been covered completely in subsequent research. Primary attention has been given to questions that must be answered in order to understand the physics of radiation belts, and particularly to those concerned with phenomena in the area of the plane of the equator because it is here that the main particle accumulation occurs.

Chapter III develops the general transport theory. Chapter IV applies results obtained to explain the observed properties of radiation belts. The

theory of belt stability is reviewed in Chapter V. Chapters III through V were written using materials obtained from original research performed by the author.

In conclusion, I would like to take this opportunity to express my warm appreciation to S. N. Vernov, A. A. Vedenov, M. A. Leontovich, L. P. Pitayevskiy, R. Z. Sagdeyev, V. A. Troitskaya and D. A. Frank-Kamenetskiy for much valuable advice in preparing the manuscript for printing.

B. A. Tverskoy

Table of Contents

Chapter I

Physical Conditions in the Earth's Magnetosphere

1. Introduction

Since the time of the famous work done by Stormer, Birkeland and Chapman on the theory of the aurora and magnetic storms, the problem of the effect of corpuscular radiation from the sun on the earth has become one of the major concerns of geophysics. This research began to develop very rapidly in 1957, when powerful rockets became available for direct studies of the physical processes taking place in space. The fundamentals of plasma physics were developed at about this same time as part of thermonuclear research. Noted in subsequent years was a tendency to synthesize the achievements of the altitude experiments and of plasma theory, the result of which has been the gradual evolution of an orderly physical picture of the phenomena taking place in near space. /9

Figures 1 and 2 are diagrams of the earth's magnetosphere, drawn primarily from experimental data. The section of the magnetosphere in the plane passing through the axis of the geomagnetic dipole, and the earth-sun line, is shown in Figure 1, with the equatorial section shown in Figure 2. The figures were drawn to scale to approximate the real proportions. As will be seen from the figures, there are six characteristic regions (A-F) with different properties. The boundaries between these regions are shown by heavy lines and (with the exception of the boundary between the B and E regions) are very sharp.

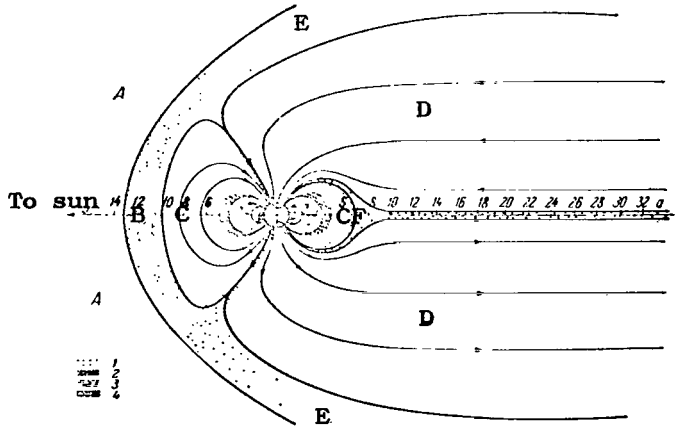

Figure 1. Diagram of the earth's magnetosphere (meridional section). /10

1 - outermost belt;
2 - outer electron zone maximum;
3 - proton belt maximum;
4 - inner electron belt.

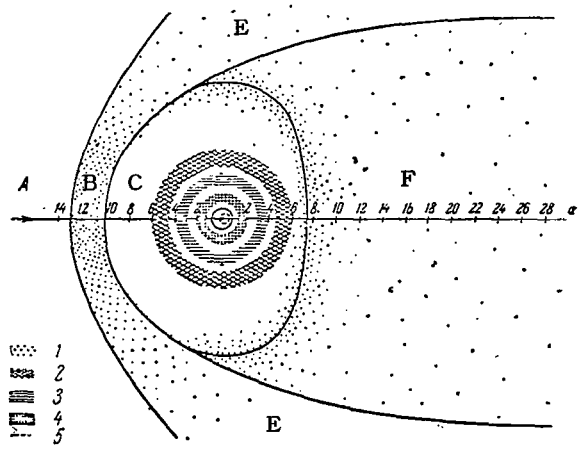

Figure 2. Diagram of the earth's magnetosphere (equatorial section). Designations for 1 through 4 are the same as for those shown in Figure 1. 5 - Aurora ring.

Region A is that of the undisturbed solar plasma flux (the solar wind). /11 Particle density is usually on the order of 10 cm^{-3}, the directed velocity is on the order to 300 to 700 km/second, but the random velocity is much lower. The flux carries a frozen-in magnetic field with an intensity of several gammas (1 $\gamma = 10^{-5}$ gs). The velocity is many times that of the Alfvén velocity.

The flux of the geomagnetic field results in the formation of a shock wave. As the solar plasma passes through the shock wave the random speeds of the particles increase, and the magnetic field becomes turbulent. The wave front has a perpendicular, or nearly so, flow velocity near the day boundary and the effect of thermalization is particularly great. Therefore, there is a region of hot plasma (region B) near the earth-sun line on the day side.

The shock wave becomes oblique as it moves away from the earth and is transformed into a Mach cone. Dissipation decreases and region B gradually becomes region E, in which the plasma flux resembles the undisturbed solar wind in its properties.

The disturbed solar wind deforms the geomagnetic field and squeezes it into a cavity called the magnetosphere. The magnetosphere breaks up into

three characteristic regions. The geomagnetic field lines in region C are qualitatively similar to those associated with a dipole, and the drift orbits of the particles close within the limits of the magnetosphere. This region is filled with corpuscular radiation, the average energy of which is considerably higher than that outside the magnetosphere. Region B is called the trapped radiation region.

The boundary of the trapped radiation region is projected along the field lines in the form of two narrow rings on the earth's surface (one in the northern, and one in the southern hemisphere). It is along these rings that the auroras usually flare in the ionosphere. The regions bounded by the aurora rings, and containing the earth's magnetic belts, are called the polar caps.

The field lines threading the polar caps close on the night side of the /12 magnetosphere at very great distances from the earth. No tendency of the field lines to close has been observed in the regions of the magnetosphere thus far investigated. Near the plane of the equator the field lines run parallel to this plane, but in opposite directions in the northern and southern hemispheres. The regions with fields of opposite signs are broken down into narrow layers in which the intensity is below the response limits of the most sensitive magnetometers in use today (0.25 γ).

The D region, in which the field lines spread out from the sun, is called the tail of the magnetosphere, and the thin F layer is called the neutral layer.

The distribution of fast particles in near space can be characterized by a series of maxima (radiation belts) encompassing the earth. Although the concept of the radiation belt is solidly entrenched in scientific usage, there is still no generally accepted classification of the belts, and this sometimes leads to misunderstandings. Today, when practically the entire particle spectrum has been investigated experimentally, it appears possible to construct a more precise classification of radiation belts.

From our point of view it is reasonable to distinguish four main zones. First, there is the outermost radiation belt, which on the day side coincides with the region of thermalized turbulent plasma, the B region, and on the

night side crosses the neutral F layer, which too is filled with hot plasma. The particles in the outermost belt escape into the ionosphere along the lines of force separating the trapped radiation region from the tail of the magnetosphere and enter the aurora ring. The average energy of the particles in the outermost belt is ~ 1 keV.

Somewhat closer to the earth is the outer electron belt, the maximum intensity of which is found to be from 4 to 5 earth radii, a, from the center of the earth (in the plane of the equator). Electrons with energies of ~ 50 keV form a quite heavily diffused maximum, but a very sharp peak of intensity /13 can be observed at energies of 200 keV, and higher.

Electron fluxes are minimal at distances of from 3a to 4a from the center of the earth. This is the region containing the absolute maximum for the proton belt. The proton belt is a single formation. Heavier fluxes of protons with energies greater than 100 keV are observed, beginning at the boundary of the trapped radiation region. Average energy, as well as the integral flow of protons, increases with approach to the earth, right up to the geocentric distance 3.5a in the plane of the equator. At lesser geocentric distances the average energy continues to increase, and is on the order of tens of MeV near the earth. The integral flow declines, however.

The intensity of electrons with energies ~ 100 keV, and higher, begins to increase once again at geocentric distances less than 3a. This formation, naturally, is called the inner electron belt. Much of this zone today is filled with electrons from high-level nuclear bursts.

A first approximation of the configurations of the belts outside the equatorial plane can be arrived at from the travel of the magnetic field lines. Each of the belts has a thin structure corresponding to the different spectral regions.

The picture described above is for the quiet solar wind, the characteristics of which remain stable over a long period of time ($\gtrsim$ several days). Variations in the radiation belts occur when the wind is disturbed by solar flares, or by active regions passing through the center of the sun (active regions that are sources of intensive corpuscular flows). Severe wind dis-

turbances cause magnetic storms.

Much of the nature of the radiation belts has now been explained. The night side of the outermost belt is probably the extension of the boundary layer between the geomagnetic field and the solar wind in the depth of the magnetosphere. The intensity in the trapped radiation regions is the result of the diffusion of particles from the outermost belt by the geomagnetic disturbances. The particles move into a region with a stronger field and are accelerated by the retention of the adiabatic invariants. /14

The transfer rate drops off rapidly as the earth is approached, and the different loss mechanisms begin to play a role. The result is the formation of the internal boundaries of the belts. It can be asserted, apparently, that the proton losses are primarily the result of ionized deceleration. Electrons escape much more rapidly, and this is associated with the electromagnetic wave scattering that takes place in the magnetosphere. There is reason to believe that these waves oscillate because of the instability of the radiation belts.

The experimental materials dealing with the physical phenomena in the magnetosphere are so vast that only a large group of writers, working together, would be able to put together anything resembling a complete outline of these questions. However, the task can be simplified greatly if we limit ourselves to consideration of only those phenomena (or more precisely, to those characteristics) of interest from the point of view of the possibility of accelerating particles to the energies observed in the radiation belts. The criteria for the selection should be general considerations concerned with the different types of accelerating mechanisms in plasma.

It appears that any of these mechanisms can be reduced to one of three classes: adiabatic, statistical, or shock acceleration.

Adiabatic acceleration is based on the retention of the adiabatic invariants for the particles when fields change slowly. Since the geomagnetic field is constant, on the average, the adiabatic acceleration can only play a role in forming the belts when there is particle transfer across the drift shells. At the same time, the particles, the points of reflection of which

are displaced toward the earth (that is, into a region with a stronger field) will be accelerated.

The displacement of the particles across the drift shells can only occur in an electric field. The field should be asymmetrical in longitude /15 and change with characteristic time, which is less than, or on the order of, the period of the magnetic drift of a particle over a distance on the order of the spatial scale of the electric field.

The first condition flows from the retention of the generalized moment of a pulse in axially symmetrical fields; the second from the adiabatic invariantness of the drift shell. Taking the general considerations, it is possible to significantly concretize the requirements for causing transfer and adiabatic acceleration to take place. The transfer theory is now widely disseminated and is the basis for the explanation of many properties of belts [1-15].

Statistical acceleration will only occur when the amplitudes of the electromagnetic and plasma oscillations are substantially in excess of the thermal noise levels. A special case of statistical acceleration is the Fermi mechanism (the reflection of particles from moving magnetic heterogeneities). Statistical acceleration can appear in the fluctuations of the invariant for the longitudinal effect with the magnetic moment retained, or in the breakdown of both invariants (depending on the wave frequency). Processes of the first type should lead to concentration of high-energy particles at low altitudes in a geomagnetic trap, something that has not in fact been observed. There are a great many other data (particularly concerning the spectrum of hydromagnetic oscillations at frequencies of from 1 to 10 Hz) that also point to the absence of Fermi acceleration in the belts.

It is possible to generate practically all types of waves in plasma with frequencies below the Langmuir frequency if one considers only the possible causes of acceleration. The phase velocities of these waves are $U_f = \omega/k$, and can be less than the speed of light, so what follows from the equations $\mathrm{rot}E = -(1/c)(\partial H/\partial t)$ is that the amplitude of the

magnetic field is $H \approx (c/U_f)\, E \gg E$ (E is the electric field amplitude). The only exception is the case of longitudinal, or almost longitudinal, /16
oscillations ([kE] $\ll$ kE, where k is the wave vector). The electric field is all that causes any change in the energy of the particle. If l_{eff} is used to designate the effective length of the resonant interaction of the particle with the wave, the change in energy, $\delta\varepsilon$, will be $\sim eEl_{eff}$. Change in pulse orientation (scattering) can be caused by the electric, as well as by the magnetic, fields with the electric force $f_E = eE$, and the Lorentz force $f_H \backsim e(v/c)H$. If particle velocity is $v \gg u_f$, the Lorentz force causing pure scattering is many times greater than the electric force. Consequently, the time to scatter a particle by an angle $\sim \pi$ is much shorter than the time during which the probable fluctuation of energy $\Delta\varepsilon$ will become of an order ε. Therefore, when $v > u_f$, particles will escape into the ionosphere with significant changes in energy.

Electrostatic waves of the ion sound type are much too slow, so the most probable cause of statistical acceleration (if it does in fact take place in radiation belts) can either be the Langmuir oscillations, or space radio radiation. The latter is of much too low power, however.

The hypothesis regarding the statistical acceleration of the electrons on radiation belts by plasma oscillations was advanced in [16]. The availability of experimental, or theoretical, data on the effective temperature of plasma waves in the magnetosphere allows one to evaluate the role of these processes in the formation of radiation zones. Consequently, waves of this type must be given special consideration in an analysis of the physical conditions in the magnetosphere when considered from the point of view of acceleration processes.

Despite the fact, noted above, that oscillations with frequencies below the plasma frequency cannot effectively accelerate particles, their probable role is a very large one in the dynamics of belts, since it is on waves of this type that particle scattering takes place [17-20]. We will, therefore, consider the data on these waves as well in what follows.

Finally, the third class of conceivable acceleration mechanisms is one of non-colliding shock waves. Plasma particles acquire high directional velocities in the case of strongly nonlinear movements and /17 simultaneously form unstable configurations (beams, as a rule). As the particles are scattered on the developing electromagnetic or electrostatic oscillations the directional velocities become partially random, and in the final analysis this results in irreversible heating. Let us emphasize the fact that instability is a necessary ingredient of the heating mechanism. Many papers have not taken this fact into consideration and the solutions to purely dynamic problems in which the acceleration is reversible ([21], for example) are called shock waves. The determining role played by instability in the case of shock heating was investigated in the work done by R. Z. Sagdeyev, and a detailed explanation can be found in [22].

Today, there is no doubt as to the principal possibility of impact heating. Non-colliding shock waves have been obtained in laboratory experiments and have been observed in space. Rigorous solutions to equations, in which the effect of instability [23] can be taken into consideration consistently, have been obtained for certain types of waves.

But there are no strong shock waves (with Mach numbers $\gtrsim 1.5$) within the radiation belts. This fact is confirmed by the spate of data from ground and high-altitude measurements, and in the final analysis can be explained by the vastness of the leading fronts of the solar wind disturbances. The width of a front such as this is $\sim (2 - 10) \cdot 10^{10}$ cm, which, at a velocity $\sim 10^{8}$ cm/second, will result in an increase in the time it takes the pressure to rise in the magnetosphere that will be on the order of several minutes. The basic period of the natural hydromagnetic oscillations of the magnetosphere is of the same order of magnitude. Compression is therefore adiabatic. The adiabatic nature of the compression manifests itself because the amplitudes of the natural oscillations caused by field deformations are much less in magnitude than are those of the static disturbance because of the shift in the boundary of the magnetosphere toward the earth.

This fact poses an important problem for the solar wind theory;

explanation of disturbances with broad fronts. The plasma pressure in the /18
undisturbed solar wind is much lower than the magnetic pressure. Therefore, according to [22], the width of the front should be on the order of c/Ω_0, where Ω_0 is the ion plasma frequency (this is the width of the front of a standing shock wave occurring as the solar wind flows over the magnetosphere). At the same time, it develops that impact heating has no significant role to play in the theory of radiation belts.

So, it is possible to narrow down very considerably the phenomena of primary interest from those included in general considerations of the nature of acceleration processes in plasma. The framework becomes even more rigid during an analysis of the dynamics of the radiation belts proper. But what must be borne in mind is that this approach to the problem is somewhat subjective in its nature, and is justified only for purposes of selecting the direction more detailed research is to take. The decisive criteria for the veracity of the particular conception remain the justification for the original premises, the quantitative explanation of available data, and confirmation of the conclusions flowing from the theory by experiment.

The next paragraphs of Chapter I will present contemporary ideas of what physical conditions are in the magnetosphere, taking the conditions cited into consideration.

2. The Geomagnetic Field

The geomagnetic field is the basic factor in the existence of radiation belts because it holds the trapped charged particles for a long period of time. Field sources are the currents in the earth's core. At great distances, the field is heavily deformed by the solar wind and is squeezed into a cavity extending into the night side, away from the sun. Ionospheric currents, and possibly the hypothetical ring current in the region of the outer radiation zone, the existence of which is assumed in order to explain certain of the phenomena occurring during /19
magnetic storms, contribute to the geomagnetic field, and these currents

are in addition to those flowing in the earth's core and on the boundary of the magnetosphere.

There are periods when solar corpuscular radiation is extremely stable, periods of approximately a week a year when solar activity is at a minimum. It seems that variations in the shape of the boundary of the magnetosphere are simply the result of the rotation of the earth's magnetic axis with respect to the geographic axis.

Ionospheric currents caused by friction between electrons or ions, and by winds of neutral particles, have a smooth diurnal path, primarily the result of changes in the degree of ionization with changes in illumination. The magnitude of the diurnal variation in the field, as recorded for these conditions at each of the magnetic observatories, is $\sim$ 20 - 50 γ. There is no ring current, or it is constant in magnitude.

The boundary of the magnetosphere is almost always at a definite distance from the earth during these quiet periods (according to the 1961-1963 data, at any rate). A frontal point, corresponding approximately to the intersection of the magnetosphere boundary and the earth-sun line, remains 10 to 11 earth radii, a, from the center of the earth. The stability of the boundary on magnetically quiet days suggests that the solar wind has a constant component.

Let us now review the experimental and theoretical data on the structure of the geomagnetic field under quiet solar wind conditions. The most detailed investigation of the shape of the boundary, and of field features at long distances, was made by the satellite IMP-1 with an apogee $\sim$ 200,000 km from the center of the earth ($\sim$ 30a) [24, 25]. Magnetometers carried by the satellites in the Elektron series, and by Explorer 12 and Explorer 14 too provided valuable information on the geomagnetic field at great distances from the earth [26-28].

What follows from the solar wind theory [41] is that radial expansion causes the solar plasma to become supersonic, and the velocity of the ordered particle motion in the earth orbit is many times that of the thermal spread. Therefore, a head shock wave and a Mach cone should appear /20

when the solar wind flows over the magnetosphere (if hydrodynamics are applicable to solar plasma motion). Theoretical studies [29, 30] have pointed this out. The shock wave is in a position close to the boundary of the magnetosphere in the vicinity of the frontal point (2a to 3a from it), so the pressure at the boundary corresponds, approximately, to the duplicate flux of the pulse in the solar wind (duplication results from the reflection of particles from the boundary). The shock wave is weak in the Mach cone region and the pressure at the boundary too is determined by the duplicate component of the flux of the pulse for an undisturbed wind in a direction normal to the boundary.

Therefore, the shape of the cavity in which the geomagnetic field is localized can be established, approximately, by solving the Laplacian for magnetic potential, U, with a dipole feature at the null and with a boundary condition

$$\frac{1}{8\pi}(\nabla U)^2 = 2mn_0 v_0^2 \sin^2\psi, \tag{2.1}$$

m is the proton mass;

n_0 and v_0 are the density and velocity of the solar wind in the undisturbed region;

ψ is the angle between the wind direction and a tangent to the plane at the boundary [29].

This holds even when there is a shock wave.

This problem can be solved beautifully by using the theory of the functions of a complex variable in the two-dimensional case (the dipole analogy here is a two-wire line with antiparallel currents([29]. Today, high-speed computers are used to develop a series of approximate methods for solving the three-dimensional problem concerning the shape of the boundary. Despite the fact that a firm basis for these methods has not been advanced, a comparison of the results obtained by numerical solution of the two-dimensional problem with the precise solution confirms the reliability of this approach.

The numerical investigation was made for a somewhat more general boundary condition

$$\frac{1}{8\pi}(\nabla U)_s^2 = 2mn_0v_0^2\sin^2\psi + P_0, \qquad (2.2)$$

where the constant static pressure, P_0, was added to the dynamic pressure. Solving for $P_0 \neq 0$ reduces to a closed model of the magnetosphere, and when $P_0 = 0$, the cylindrical tail stretches to infinity on the night side. /21

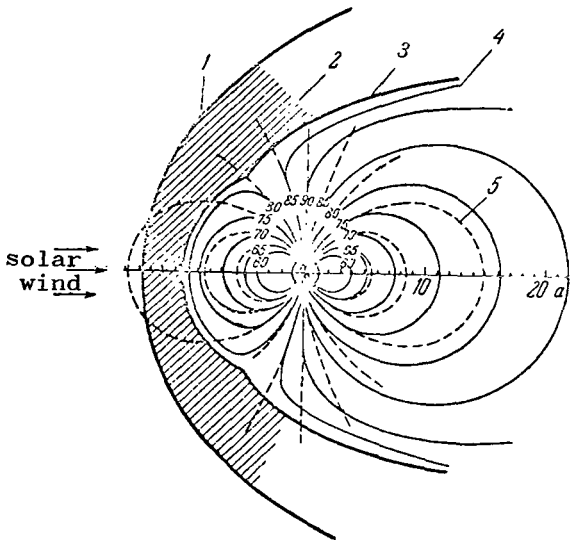

Figure 3. Path of the field lines of the geomagnetic field in the plane passing through the magnetic axis and the earth-sun line, computed with the boundary condition at (2.1) as the basis (elastic reflection of solar wind particles from the boundary of the magnetosphere).

1 - shock wave; 2 - region of thermalized solar plasma; 3 - boundary of the magnetosphere; 4 - field lines of the deformed, and 5 - dipole fields; the geomagnetic latitudes at which the respective field lines intersect the earth's surface are shown.

Figure 3 shows the results of the computations made in [31, 32] to determine the shape of the boundary and of the field when $P_0 = 0$ in the plane passing through the magnetic axis and the earth-sun line. Let us note that since for $P_0 = 0$ the parameters of the problem reduce to m, n_0, v_0 and $\mathfrak{M}$ (the magnetic moment of the earth), the only magnitude with the dimensionality of length, and a reasonable scale, that can be composed of these constants is /22

$$\Lambda' = \left(\frac{\mathfrak{M}}{mv_0^2n_0}\right)^{1/6}. \qquad (2.3)$$

In order of magnitude, Λ' corresponds to the distance from the dipole to the front point ($n_0^{-1/3}$), the width of the shock wave front, and the width of the boundary layer between the plasma and the field has no effect on the size and shape of the magnetosphere. Therefore, if Λ is selected as a unit of length, the solution should be universal in nature.

The spherical analysis made in [32] revealed that for reasonable values of Λ (7 to 11a, where a is the radius of the earth) in a spherical region with radius Λ the field can be established for all practical purposes by two harmonics

$$U = -h_0\left(\frac{\Lambda_0}{\Lambda}\right)^3 R\cos\theta + h_1\left(\frac{\Lambda_0}{\Lambda}\right)^4 R^2\sin\theta\cos\theta\cos\varphi, \qquad (2.4)$$

where R, θ and φ are the spherical coordinates with origin at the point of the dipole, the polar axis along the magnetic axis, and the origin of the φ reading at the noon meridian, respectively. These calculations do not take into consideration the non-coincidence between the magnetic and geographic axis or the tilt of the latter toward the plane of the ecliptic. However, these effects probably will provide but slight corrections to the equation at (2.4).

The potential at (2.4) can be written in a form in which the parameter Λ, the distance from the dipole to the frontal point, is introduced in place of Λ'. Λ, Λ_0, and R can be measured in earth radii, a. The average position of the boundary is designated by $\Lambda_0 \approx 10.8$. This entry for the parameters h_0 and h_1 describes the average value and the longitudinal variation in the θ component of the field of the external currents at the earth's equator. These magnitudes are 25γ and 2γ, respectively, for the models [31, 32]. The disturbance is $\approx$ 45 γ at the frontal point when $\Lambda = \Lambda_0$. The contribution of the rest of the harmonics when $R \leqslant \Lambda$ is less by almost one order of magnitude.

The hypothesis of a rapid convergence of the potential of the field /23
of external currents in the $R \leq \Lambda$ range was advanced in [5-7] and used to investigate particle motion in the radiation belts in the case of oscillations of the magnetosphere boundary. This was the basis for the construction of the transfer equation used in our papters [8-12], as well as in [15]. This hypothesis greatly simplifies the calculations. Since much of the experimental data confirms the theoretical conclusions based on the representation of the potential in the form at (2.4), it can be taken that the predominance of the first two harmonics is a real fact. However, the numerical values of the constants obtained in [31, 32] are

false. Moreover, the true structure of the magnetosphere differs greatly from the theoretical models described in the foregoing.

Although many important results concerning the structure of the magnetosphere were obtained as far back as 1959, the basic contribution to the solution to this problem was made by the research conducted with the satellite IMP-1 [24, 25]. This satellite, with an apogee of $\sim$ 30a, and with a slight tilt of its line of apsides* to the ecliptic, carried, in particular, very sensitive magnetometers. One (a so-called rubidium magnetometer), based on the principles of quantum electronics, was used to make highly accurate measurements of the Zeeman splitting of the spectral lines of rubidium vapors. This resulted in a determination of the magnitude of the H field intensity with an absolute error of $\pm$ 0.25 γ. Used as well were flux-gate magnetometers. These were somewhat less accurate in measuring the three components of the intensity vector. The interval between two successive measurements was $\sim$ 1 second.

The satellite was initially launched on the day side of the magnetosphere. Its apogee then gradually shifted to the night side as a result of the movement of the earth around the sun. The measurements made on the day side provided good confirmation of the theoretical results discussed in the foregoing. The satellite usually recorded a cold, stable, solar wind with a small, regular magnetic field with an intensity of about /24
5 γ near the apogee. The satellite, during its approach to the boundary of the magnetosphere, first intersected the stationary shock front, which is several hundred kilometers wide. The magnetic field became turbulent as it passed through the front, and its average magnitude increased by a factor of from 2 to 3. Plasma analyzers installed aboard this same satellite recorded thermalization of the solar plasma on the wave front (the random velocities of the particles became the same order of magnitude as the directional velocity). Significant ($\sim 2 \cdot 10^6$ $cm^{-2}sec^{-1}$) proton fluxes with energies $\gtrsim$ 10 keV developed [33].

---

* The line passing through the apogee and perigee; that is, the major semiaxis of the elliptical orbit.

Upon subsequent approach to the earth the satellite once again intersected the sharp (width > 1000 km) boundary, at which the average field intensity increased from 10 to 60 γ, approximately. The field was still seen to fluctuate, but at this point one can begin to discuss not only the average magnitude, but the average direction, which too changed slowly with further movement of the satellite. This is the transient layer and is the boundary of the magnetosphere. /25

Figure 4 shows typical readings by the magnetometers, obtained during one passage of the satellite through the region indicated near the frontal point [24]. The upper part of the figure shows the 10-second averages of field intensity values, and the angles between the field and the normal to the plane of the ecliptic (θ), as well as the angle between the projection of the field on this plane and the earth-sun line (φ), in accordance with geocentric distance. The lower graphic shows the mean square fluctuation for each of the three field components at 10-second intervals. The figure clearly shows the region of the quiet wind, the shock wave, the transient turbulent region, and the magnetosphere boundary.

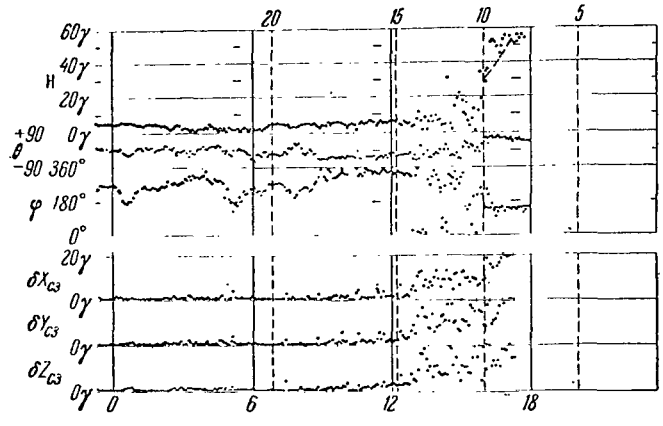

Figure 4. Example of a magnetogram obtained by the satellite IMP-1. Laid out along the axis of the abscissa is GMT in hours (lower) and the geocentric distance, R, in earth radii (upper). The shock front when R = 14a, and the boundary of the magnetosphere when R = 10a, are clearly seen.

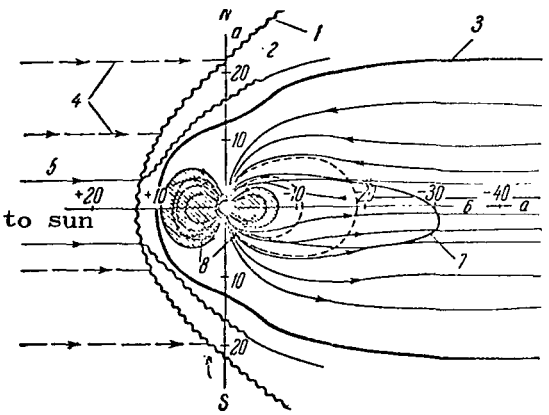

Figure 5. Meridional section of the magnetosphere from IMP-1 data.

1 - shock wave; 2 - thermalized plasma region; 3 - magnetosphere boundary; 4 - solar wind velocity; 5 - interplanetary magnetic field; 6 - neutral layer; 7 - satellite's orbit; 8 - trapped radiation region.

Figure 5 [25] is a summarized version of the position of the shock wave and of the boundary of the magnetosphere near the plane of the ecliptic, based on data from many loops. Authors have compared the results /26 with theoretical profiles obtained through numerical calculations in [34] (magnetosphere boundaries) and in [35] (shock wave). The jagged nature of the experimental curves indicates that with change in the strength of the solar wind comes a change in the position of the boundary and of the shock wave (the time inverval between adjacent points is about two days).

We should note that the results obtained in [24, 25] are good confirmation of the theory of shock waves in collisionless plasma [22]. According to [22], the width, δ, of the front of the shock wave, propagating at angle Θ to the magnetic field ($\sqrt{m/M} \ll \Theta \ll 1$), is approximately $c\Theta/\Omega_0$, where c is the speed of light, m and M are electron and ion mass, respectively, and $\Omega_0 = 4\pi e^2 N/M$ is the ion plasma frequency (more precisely, δ is on the order of several $c\Theta/\Omega_0$; see [22], pp. 68-69). This

assessment reduces to $\delta \sim 10^7$ cm in the case of solar wind parameters $N = 1$ to 10 cm^{-3}, $\Theta \approx 1/3$.

The width of the boundary layer between the solar plasma and the geomagnetic field corresponds to the theoretical calculations for an electrically neutral layer in which the charge separation field created by the difference in the Larmor radii of the electrons and ions is compensated for by the influx of cold electrons [36, 37]. In this case, the width of the layer will be on the order of that of the larmor ion radius.

The transition of the front shock into a Mach cone is observed as the apogee of the satellite moves away from the frontal point. The strength of the shock diminishes, and the effect of plasma thermalization gradually disappears. The satellite's orbit ultimately moves into the night side, and the line of apsides enters the tail of the magnetosphere. The theoretical result, in accordance with which the boundary of the magnetosphere on the night side should be almost cylindrical in form, is confirmed. However, the field structure is completely different than that expected. It seems that the cylindrical tail is halved by a narrow layer of hot plasma lying approximately (but not strictly) in the plane of the ecliptic. The field lines flow almost parallel to the layer, /27 but the field has opposite signs on different sides of the layer. The field strength is less than 0.25 γ (the threshold of sensitivity of the rubidium magnetometer) within the layer. The least geocentric distance at which the neutral layer is observed is 9a. There is no tendency to close the tail of the magnetosphere at greater distances.

The diagram of how the magnetosphere is built in the plane of the noon and midnight meridians is shown in Figure 5 [25]. The magnetic field at the surface of the neutral layer is approximately $\pm$ 20 γ and diminishes slowly with distance (approximately as 1/R). Layer width is almost 600 km. The magnetic pressure is equalized by the pressure of the plasma inside the layer.

Three points of view exist with respect to the nature of field deformation in the tail. The first of these explains the elongation of the field lines by the interaction of the solar wind with the field at the boundary of the magnetosphere [38-40]. The formation of a neutral layer by the hot plasma is attributed to the Joule heating during the destruction of the antiparallel fields as a result of instability. The two other hypotheses are based on different assumptions with respect to the breakthrough of the solar plasma into the tail of the magnetosphere. One of the breakthrough possibilities is associated with the fact that in the models of the type in [31, 32] the particle drift orbits leave the tail at the boundary layer, so it is possible for solar protons and electrons to flow into the tail of the magnetosphere (see Section 5). This effect was pointed out in [5] and [8]. It seems to us that it is possible to compare the plasma pressure in the tail with the pressure in the turbulent zone if the transparency of the boundary layer is high enough, beginning at some critical drift orbit. The pressure of the plasma will elongate the field lines on the night side.

Finally, the third hypothesis [42-44] involves a plasma breakthrough with so-called "neutral points." A precise solution to the two-dimensional problem dealing with the shape of the boundary between the dipole field and the plasma flux demonstrates that near some point on the surface of separation (in the Northern and Southern hemispheres) there is a branching of the field lines, with the branching in the form of break. The magnetic field vanishes at the point of branching. The suggestion was /28 made in [29] that solar particles can break into the magnetosphere through these neutral points. Basically, this effect is a special case of the mechanism reviewed in [5] and [8].

Future high-altitude investigations, as well as model experiments of the type described in [45] and [48], in which the magnetic dipole was fired from the plasma gun, should play a big part in revealing the true mechanism of how the tail of the magnetosphere is formed.

The question of the existence of a component of the magnetic field, h, in the "neutral" layer of the perpendicular layer is of interest. The strength of this field is not in excess of 0.25 γ, according to [25]. But there is little likelihood that $h \equiv 0$. The magnitude of h can be assessed regardless of any particular conception held with respect to the nature of the "neutral" layer. It need only be assumed that the plasma pressure in this transition region is not too anisotropic.

Experimentation [25] reveals that the radius of the section of the magnetosphere R, continues to increase, albeit very slowly, out to a distance of 30a. If the change in the magnetic flux in the tail attributable to the closure of the field lines through the neutral layer is ignored (it will be shown in what follows that this is a reasonable assumption), the absolute magnitude of the field strength in the northern and southern halves of the tail will change in accordance with the law

$$H(z) = H_0\left[\frac{R(z_0)}{R(z)}\right]^2;$$

where

z is a coordinate read from the center of the earth along the earth-sun line;

$z_0 \approx 15a$ is a distance beginning with which it can be assumed that $(dR/dz)\delta z \ll \delta z$, that is, the boundary can be considered to be close to cylindrical;

$R(z_0) \equiv R_0 \approx 20a$ is the radius of the tail when $z = z_0$;

$H_0 \approx 20\ \gamma$ is the field when $z = z_0$.

The magnetic pressure is balanced at the boundary by the normal component of the solar wind pulse stream [see (2.1)]. It is evident that /29

$$\sin\psi \approx \operatorname{tg}\psi = \frac{dR}{dz} \qquad (\psi \ll 1).$$

From whence

$$\frac{dR}{dz} = \left(\frac{H_0^2}{16\pi m n_\infty v_0^2}\right)^{1/2}\left(\frac{R_0}{R}\right)^2$$

and

$$R = R_0\left\{1 + \left(\frac{H_0^2}{16\pi m n_\infty v_0^2}\right)^{1/2}\frac{z - z_0}{R_0}\right\}^{1/3} \tag{2.5}$$

(the constant of integration is determined from the condition that $R = R_0$ when $z = z_0$). The magnetic field in the tail will change in accordance with the law

$$H = H_0\left\{1 + \left(\frac{H_0^2}{16\pi m n_\infty v_0^2}\right)^{1/2}\frac{z - z_0}{R_0}\right\}^{-2/3} \tag{2.6}$$

and decays much more slowly than does the field of the dipole, by agreement with the results contained in [25]. What follows from the equation at (2.6) is that the results obtained are valid out to distances ~ 300a, at which the H field drops off to the level of the magnetic field of the solar wind ($\approx$ 5 γ), and the nature of the boundary condition changes.

Let us now evaluate the magnitude of h at distances $\approx$ 20a. The equation at (2.6) tells us that a pressure $H^2/8\pi$ is acting at the boundary layer, the gradient of which when $z = z_0$ is

$$|\nabla P| \approx \frac{H_0^2}{6\pi R_0}\left(\frac{H_0^2}{16\pi m n_\infty v_0^2}\right)^{1/2}. \tag{2.7}$$

equating the density of the z-component of the Lorentz force $1/c \cdot jh$ by the order of magnitude of $|\Delta P|$, and considering that $j \approx c/2\pi \cdot H_0/\delta$, where δ is the width of the layer, we obtain

$$h \approx \frac{1}{3}\frac{\delta}{R_0}H_0. \tag{2.8}$$

When $\delta \approx$ 600 km, R_0 = 20a $\approx$ 130,000 km, and H_0 = 20 γ, the magnitude of h is /30 $\approx 3\cdot10^{-2}$ γ, and this does not contradict the results contained in [25] ($h \leqslant 0.25$ γ).

The magnetic flux, Φ, through the northern (or southern) part of the tail, according to the model, is equal to $\frac{1}{2}\pi R_0^2 H_0 \approx 5\cdot10^{16}$ maxwells. When $h = 3\cdot10^{-2}$ γ, and the average width of the layer is $\approx 2R_0$ = 40a, this flux will close at distance ~ 10^{12} cm (greater than 10^3a), and this confirms our original assumption concerning the negligibility of the small change in the flux resulting from the closure through the neutral layer at distance ~ z_0 from the earth. The magnitude ~ 10^3a characterizes the probable length of the magnetosphere tail on the condition that there is in fact a neutral

layer at great distances.

There are many questions concerned with the physics of the magnetosphere, including those concerned with the theory behind the earth's radiation belts, that require precise knowledge of the position and structure of the inner boundary of the neutral layer. There are grounds for believing that this boundary is a sharp one. For example, it is natural to assume that the auroras are caused by soft electrons breaking through the neutral layer* toward the earth. Analysis of IGY data (synchronized photography of the night sky by a worldwide network of stations) revealed that the auroras can be seen simultaneously at all longitudes in the northern and southern hemispheres. At that time the width of the lighted regions was usually $\sim 1^\circ$ of latitude, and sometimes measured ~ 1 km on a distance basis. If the aurora is a projection of the inner boundary of the "neutral layer" on the earth's surface along the field lines, the narrowness of the aurora indicates just how small the width of this boundary is. And analysis of the structure of radiation belts (Section 5) will lead to this same conclusion.

Data on the boundary of the neutral layer are still fragmentary. As has already been pointed out, the minimum distance at which this layer was /31
recorded by the satellite IMP-1 was 9a. Explorer 14 also recorded the change in the directions of the field lines near the plane of the geomagnetic equator. On magnetically quiet days the transition from a direction normal to this plane to one almost parallel to it took place at a distance of about 10a, and when geomagnetic disturbances were present the boundary shifted to 8a [28].

The computation for currents in the magnetosphere tail is also a significant reflection of the nature of the field in the radiation belt region. In [50] the model of the magnetosphere in [31, 32] (Figure 3) was supplemented by a plane current corresponding to the neutral layer. Current parameters were selected such that some of the characteristics of the high-latitude boundary of the radiation belts could be explained. Noted in [15] is the

* The energies of the particles trapped in the radiation belts are, as we know, obviously not high enough to excite an aurora of even moderate brilliance.

fact that the longitudinal asymmetry in this model is approximately double that in the model in [31, 32]. The true asymmetry is apparently even greater.

Up to this point we have analyzed only the currents flowing outside the radiation belt region. The question of the extent to which the field in this region can be considered a potential field arises. There are two mechanisms for forming currents in this particular region. First, there is the difference in potentials at the ends of the same field line that can result from the electric fields in the ionosphere. The currents will flow along the field lines. Second, there are the drift currents of fast particles in the radiation belts. The results of the calculations made in [51], using experimental data on the belts, are shown in Figure 6. A calculation made using the same formulas as those in [51], but based on a more detailed analysis of the readings made by the same fast particle sensors [52], yielded a curve with approximately the same shape, but the absolute magnitudes at all points were smaller by a factor of approximately 3.

The investigations made by the satellite Elektron 2 [26, 53] provide a qualitative confirmation of the existence of these disturbances. But since the magnetometers were only cut in at distances > 3a, the minimum was observed approximately in only three of the forty cases. The minimum apparently was located closer to the earth during the majority of the passes. The maximum negative anomalies at distances $\approx$ 3a were 100 to 150 γ at the quiet time. /32

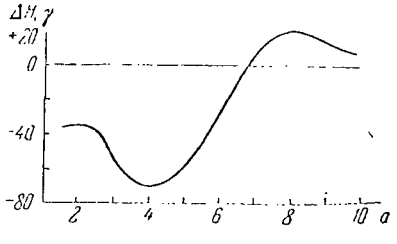

Figure 6. Disturbance Δ H of the geomagnetic field by drift currents of the proton belt near the plane of the geomagnetic equator. Geocentric distance is plotted along the axis of the abscissa.

The deflection of the measured field from the field of internal sources is almost always positive at distances > 5a near the plane of the equator, and > 7a on the high-latitude branches of the satellite's orbit. The sources of this positive anomaly apparently are the currents at the boundary of the magnetosphere [52]. The field they create

within the limits of the magnetosphere is a potential field, naturally.

Concluding this brief survey of present day conceptions of the quiet magnetosphere, let us formulate the basic conclusions that will be used in the development of the theory of belts in subsequent chapters.

1. The magnetic field in the region of trapped radiation in a quiet magnetosphere is practically a potential field.

2. The field of external currents within the limits of the radiation belt region probably can be approximated accurately enough by the sum of a homogeneous field and a quadrupole term describing the asymmetry of the day and night sides.

3. The deflection from the dipole field is relatively slight at distances $\leq 5a$ from the center of the earth.

4. The shape of the boundary, and the structure of the field in the magnetosphere, remain similar with changes in the strength of the solar wind, and the similarity factor is the parameter Λ. /33

Ground observations indicate that the geomagnetic field is changing constantly. Even when the sun is completely quiet for a long period of time, the geomagnetic field experiences a variation with an amplitude of $\sim$ 20-50 γ at each point during the day. These variations follow a specific law and correlate well with changes in the luminance of the atmosphere caused by the sun. It is known that the currents attributable to these variations flow in the E-layer of the ionosphere at altitudes of 100 to 110 km. In high-altitude investigations the sign of the tangential component of the disturbance changes when the rocket intersects the E-layer.

The opinion today is that the cause of these variations is winds in the ionosphere resulting from tidal or coriolis forces.* The friction be-

* The temperature on the day side is somewhat higher than on the night side in the ionosphere, the result of the dissimilar luminance, so there is a pressure gradient perpendicular to the force of gravity. When rotation occurs, the result is the appearance of steady-state fluxes parallel to the earth's surface.

tween the winds, which consists of neutral atoms, and the ions and electrons when there is a magnetic field present, causes a current to flow, the strength of which is proportional to the concentration of charged particles. Changes in concentration correlate with luminance conditions, so there is a daily motion in the field variations. See [55, 56] for details concerning daily variations.

Ionospheric currents probably play no significant role whatever in the dynamics of particles with energies > 100 keV, because the field disturbances they create, even near the earth, are always weaker than the dipole field and diminish rapidly with altitude, while the time scale precludes the possibility of resonant interaction with these particles. However, the same conclusion with respect to particles with energies of from 1 to 10 keV would be mistaken. It is known that in the high-latitude regions there is a heavy discharge of particles with energies of from 10 to 50 keV into the ionosphere, /34 and this can increase the degree of ionization sharply. These particles therefore often cause a significant redistribution and intensification of ionospheric currents, and these appear on ground magnetographs in the form of irregular oscillations of field components. The magnitudes of these oscillations increase sharply with increase in the magnetic latitude, and reach a figure of several thousand gammas ($\sim$ 10% of the dipole field) in the aurora region ($\pm 65^\circ$ latitude, approximately). The correlation between disturbance amplitudes is slight, even at nearby stations.

There is a good correlation between these disturbances and solar activity. There is usually a powerful flare on the sun approximately one day prior to a strong geomagnetic disturbance. This result also shows that the disturbance of ionospheric currents is associated with charged particles. The light effects of the flare ought to appear on the earth in 8 minutes, and this too is seen on the magnetograms in the form of small hooks.

Irregular field oscillations in the region containing the aurora zone can be observed almost daily. At the same time, there are narrow currents in which the approximations (quite rough) coincide with the outlines of the north and south zones of maximum frequency of auroras. The width of this horseshoe-shaped current is $\sim$ 100-500 km. The currents spill over the

polar caps at the ends of the "shoe" and over the low-latitude regions. It is possible that the currents are in part shorted through the magnetosphere. The amplitude of the disturbance is maximum near the current, naturally, and diminishes rapidly with distance from the current. Disturbances of this type are called polar storms, or bays (because of the resemblance between the shape of the magnetogram and the outlines of a coastal bay). The use of the abbreviation DP (polar disturbance), suggested by S. Chapman, is a recent innovation.

Irregular oscillations encompass the entire world in the event of strong disturbances. There are several methods that can be used to arrive /35 at a quantitative evaluation of geomagnetic activity. These are based on an analysis of long-term data, and accepted by all countries. The most widely used characteristic is the so-called K-index. The K-index is established from maximum deviations in field disturbance from the level corresponding to the quiet daily variation. Days are divided into eight 3-hour intervals, and the maximum deviation is determined for each of them at all of the world's magnetic observatories. Each station has its own scale for converting these amplitudes into the K-index. The thought behind the conversion is that given the same planetary nature of the disturbance, the amplitudes at the different stations will differ significantly, and will increase sharply as they move from the equator to the zones of aurora maxima.

Table 1 lists the association between the amplitudes of the 3-hour deviations of the field from the quiet level, and the corresponding K-indices for the geomagnetic latitude of $\approx 50°$. As will be seen from the table, the association between K and the amplitude is approximately logarithmic. Very strong disturbances (K = 9) correspond to amplitudes > 500 γ at the latitude of 50°. An amplitude > 2000 γ corresponds to this value for the K-index in the aurora region.

TABLE 1

Limits of change in amplitude (in gammas)	0	5	10	20	40	70	120	200	330	500
K-index	0	1	2	3	4	5	6	7	8	9

By international agreement, data on K-indices from the 12 stations located between 48° and 63° of geomagnetic latitudes in the northern and southern hemispheres making such determinations are forwarded to Göttingen for statistical processing and establishment of the planetary K-indices. These averaged magnitudes are also given for each 3-hour interval and designated K_p (K planetary). The K_p indices are measured on a 28 grade scale: /36 0_0, 0_+, 1_-, 1_0, 1_+, 2_-, etc., to 9_0. The parameter K_p thus characterizes the general planetary disturbance level.

Practice has demonstrated that the use of this magnitude to develop a qualitative (and sometimes even a quantitative) correlation between geomagnetic disturbances and other processes is extremely effective, despite the somewhat normal nature of the K_p index.

Let us emphasize the fact that irregular field oscillations evidence themselves in different forms at different stations. The K-indices, and the amplitudes corresponding to them, are therefore by no means characteristic of planetary currents. Yet this characteristic too is of great interest. The average disturbance can be established by averaging the longitudinal readings of stations with close magnetic latitudes, and this will eliminate the latitude effect. At the same time, and despite the comparatively slight correlation between the irregular oscillations, the average value is usually different from zero. It will, so far as the middle latitudes are concerned, appear as an increase, or a decrease, in the horizontal field component. The averaged longitudinal magnitude of the disturbance in the middle latitudes is designated D_{st} (storm disturbance).

It can now be proven that the magnitude of H is always associated with the compression of the magnetosphere. The absolute magnitude of this effect is slight, as a rule (10 to 40 γ). A disturbance of this type almost always changes the sharp front by a duration of $\sim$ 1 minute. The disturbance then slowly diminishes (on a time basis, on the order of one, or of several hours). Observed occasionally are sudden decays in the field, associated with rapid expansion of the magnetosphere.

Since the time of rise, or decay, of the field during these sudden pulses is short, they are distinct on the magnetograms. There are other

ways in which to investigate these processes. From our point of view, these effects are the basic mechanism for the acceleration of the particles in the radiation belts to energies above 100 keV. /37

In addition to the sudden pulses, the D_{st} variations contain field decays that occur more smoothly with respect to time, sometimes reaching magnitudes of several hundred gammas. Until comparatively recently there was, for all practical purposes, a generally accepted view that this attenuation was caused by the ring currents flowing near the plane of the equator at distances of from 4a to 5a from the center of the earth. However, investigation of the fluxes of fast particles, and of variations in the geomagnetic field at great altitudes, cast doubt on the existence of such heavy currents. Not precluded is the fact that a good deal of the current creating the D_{st} disturbance flows in the ionosphere and on the inner boundary of the tail.

The totality of the sharp increase in the K-index (that is, in irregular field oscillations), the intensification of the current in the polar electrojets, and the appearance of large negative D_{st} variations (the correlation between the first two phenomena and the third is almost always the case) is called a magnetic storm. This phenomenon is usually preceded by a sudden positive pulse (particularly in the case of intense storms). In this case the rapid rise in the field is called the sudden onset of the storm, while the period during which $D_{st} > 0$ is called the first phase. The period from the occurrence of D_{st} through zero to the arrival at field minimum is called the main phase of the storm, while the time of decrease in $|D_{st}|$ to zero and the decay of K_p to small values is called the restoration phase.

Until recently it was considered that the sudden onset and the three phases were necessary elements of the storm. This point of view has been revised in the past decade. It turns out that the main phase of the storm can develop, even without there being a sudden onset. These storms usually repeat with the period of rotation of the sun around its axis (27, 54, etc., days after a flare), so are called recurrent. At the same time, sudden pulses are recorded almost daily, yet are not usually accompanied by storms.

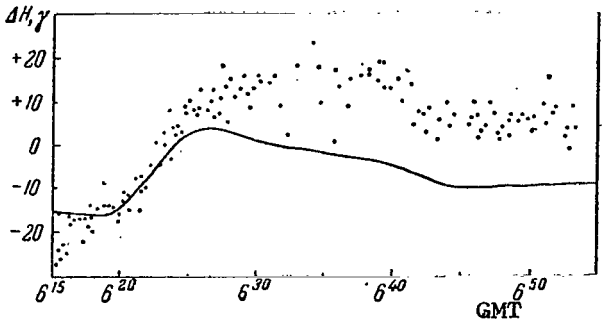

Figure 7. Sudden pulse. GMT in hours and minutes plotted on the axis of the abscissa. The magnetic disturbance at the earth's surface (the solid line) and at high altitude (dots) plotted on the axis of ordinates.

High-altitude measurements show that sudden pulses develop identically on earth, as well as in the magnetosphere, [27]. One example of a sudden positive pulse is shown in Figure 7, taken from reference [27], which demonstrates that the asymmetry of the geomagnetic field at great distances is itself great. According to ground data, the magnitude of the disturbance near the equator depends on the longitude φ in accordance with /38

the law

$$\Delta h \approx \bar{h}(1 + 0.44 \cos \varphi) \tag{2.9}$$

(the angle φ is read from the noon meridian). If it is taken that the displacement in the boundary from 11a to 8 to 10a corresponds to the average sudden pulse, and if the disturbance at (2.9) is represented in the form of the sum of the external currents and the intratelluric skin currents of the shielding, the ratio between the constants h_0 and h_1 in the equation at (2.4) can be found.

In a two-component model of the potential of the external currents at (2.4), the disturbance at the earth's equator when the skin effect is taken into consideration is in the form

$$\Delta h = \frac{3}{2} h_0 \left[\left(\frac{\Lambda_0}{\Lambda}\right)^3 - 1\right] + \frac{5}{3} h_1 \left[\left(\frac{\Lambda_0}{\Lambda}\right)^4 - 1\right] \cos \varphi. \tag{2.10}$$

From whence, as well as from the equation at (2.9), we obtain (Λ_0 = 11, Λ = 8 - 9), $h_1 \approx 0.25\ h_0$. The ratio h_1/h_0 has little dependence on Λ /39 (so that when Λ = 10, h_1/h_0 equals 0.27) so the relationship at (2.9) is quite reliable for establishing the degree of asymmetry.

This asymmetry evaluation can be confirmed by an analysis of the spatial dependence of the amplitude of the sudden pulses. The disturbance in space (near the plane of the equator) is

$$\Delta h(R, \varphi) = h_0\left[\left(\frac{\Lambda_0}{\Lambda}\right)^3 - 1\right] + h_1\left[\left(\frac{\Lambda_0}{\Lambda}\right)^4 - 1\right] R\cos\varphi$$

(R is in earth radii). From whence it will be seen that when $\varphi = \pm 90°$, the amplitude in space should be 2/3 $\bar{h}$ (as a practical matter when R = 3a the skin current field can be ignored). According to [27], the h(R)/$\bar{h}$ ratio is 0.7 (when R = 4a, $\lambda_m = 25°$, $\varphi = 90°$). At the same time, the magnitudes of h(R) should be greatly in excess of $\bar{h}$ for large R at the noon meridian because of the growth of the quadrupole harmonic with R. When $\Lambda = 9 - 10$, $\Lambda_0 = 11$ and R = 8a, we obtain h(8.0) /$\bar{h}$ = 2.8 - 2.5. According to [27], this ratio equals 2.3. Henceforth, we will use this evaluation of the asymmetry. Spherical analysis of the field of sudden pulses apparently is the method with the best prospects for investigating the geomagnetic field in the radiation belt region.

Sudden pulses, as has already been pointed out in Section 1, reflect the structure of the disturbance in the solar wind. The rapid rise in the field is linked with the passage of the leading edge of a wind disturbance with a width of $\sim 10^5 - 10^6$ km. This distance, which is considerably in excess of the width of the shock front ($\sim 10^2 - 10^3$ km), nevertheless is a negligible percentage (< 1%) of an astronomical unit. The slow decay of the field over a period of time on the order of several hours corresponds to a gradual restoration of the average characteristics of the solar wind. Asymmetry such as this is completely natural and regular, from the point of view of gas dynamics, because the steepness of the leading edge should increase as a result of the nonlinear effects.

Sudden pulses are not the only type of disturbance on the boundaries of / the magnetosphere. There are, in addition to the regular solar wind, disturbed during flares, stable plasma clouds thrown out of the action regions on the sun. The pulse flux in these clouds is higher than it is in the solar wind. The radius of the clouds' cross section is $\gtrsim 10^{12}$ cm. The interaction time with the magnetosphere when the cloud velocity is $\sim 10^8$ cm/seconds is $\gtrsim 10^4$ seconds, or several hours. These clouds cause the recurrent storms mentioned above.

There are no direct data on other types of disturbances at the boundary

of the magnetosphere. Because the general picture of the field at high altitudes has been given little study, the spatial variations are difficult to distinguish from the time variations (the exception being the sudden pulses, the temporary nature of which stem uniquely from a comparison made between satellite data and ground magnetograms).

The comparison made between the high-altitude and the ground data shows that the magnetic disturbance effect at long distances from the earth is much less than had been supposed. The most complete data on the association between high-altitude and ground disturbance effect were obtained by the satellites in the Elektron series [26, 53]. These results provided the final proof that the cause of severe disturbances of ionospheric currents (rise in the K_p-index) is variation in the solar wind. We have already pointed out that at long distances from the earth the difference, Δ H, between the measured field and the field resulting from the intratelluric sources is always positive. There is no question of the fact that this effect is linked with compression of the magnetosphere by the solar wind. Consequently, the increase in Δ H corresponds to a much more compressed field (approach of the boundary of the magnetosphere to the earth), and vice versa. Figure 8 [26] shows the values of Δ H at long distances, as well as the K_p-indices as a function of time. The correlation between K_p and Δ H is obvious.

Magnetic measurements [26, 53] (and this was the case in all preceding investigations) failed to develop any marked variations in the ring currents to which the reduction in the field near the earth during the main phases of /41
magnetic storms could be attributed. The magnetograms of the region of negative Δ H when K_p are large are no different from similar curves read during a quiet period. The boundary at which Δ H = 0 approaches the earth with increase in disturbance. This indicates that the currents causing field attenuation vary much less than do the currents at the boundary of the magnetosphere. Although the magnetic storms in the period from February through April 1964 (results [26] and [53] were obtained at that time) were relatively weak and make definitive conclusions premature, one must nevertheless point out that the problem of the main phases of magnetic storms has become very much more complicated. There is a need, apparently, for a

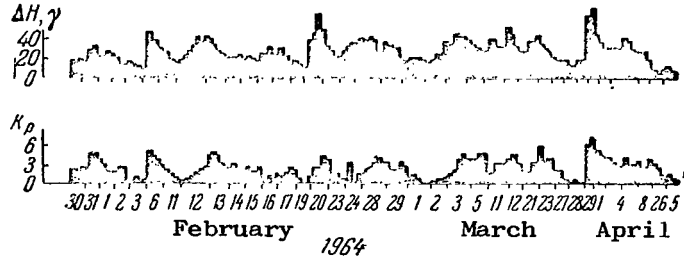

Figure 8. Correlation between the K_p-index and the disturbance of the geomagnetic field, ΔH, by currents at the boundary of the magnetosphere.

more detailed study of the possibility of localizing the ring currents created by the averaged D_{st} variation in the atmosphere.

The phenomenon that is probably the most puzzling of all the magnetic effects discovered in space is described in [26]. During the magnetic storm that occurred on 12 February 1964, and somewhat less distinctly during the storms on 21 February and 4 March 1964, there was recorded a brief (~10 minutes) reduction in the field by a very great magnitude (300 to 500 γ). All three events were observed in what was, approximately, the same magnetic shell (with a distance from the apex of the field lines to the center of the earth of ~ 4a) in the geomagnetic latitudes ~ 30 to 50°. No correlation /42 was found on the ground magnetograms between these phenomena and the world effects, but a correlation with the onset of intensification of polar electrojets was established.

The principal difficulties in understanding the nature of these effects are linked with the results of simultaneous measurements of particle fluxes over virtually the entire reasonable range of energies. In order to create the disturbed field observed (decay from ~ 1500 to 1000 γ), the particle energy density would have to be in excess of all the values ever observed in the belts by a factor of approximately 30. At the same time, in some sections of the proton spectrum, where intensity falls very rapidly with energy, the betatron decelerator would have to reduce the velocity of the calculation for the corresponding sensors by more than one order of magnitude in the event of a 30% decay in the field. Yet no such significant variations were observed in any of the sections of the spectrum. The nature of the effect remains an enigma. However, the purely local nature, the

briefness, and the slight probability of the occurrence of these phenomena ($\sim$ 10 minutes/month $\approx 2 \cdot 10^{-4}$), permit the assumption that their role in the dynamics of the belts is slight.

The boundary of the magnetosphere approaches the earth when there are magnetic disturbances. The neutral layer, judging from the results in [28], too turns out to be closer. Reference [15] (according to a citation made by one of the authors of the magnetic investigations made using IMP-1) notes great field changes in the tail. It has already been pointed out that the internal boundary of the neutral layer apparently is projected along the field lines the location of the ring of auroras in the ionosphere. The results of the analysis of the data obtained by synchronized photography of the night sky by the worldwide network of stations and sketched in [49] definitely point out the shift in the ring in the region of the lower latitudes with increase in the magnetic disturbance effect. Figure 2 (page 10) indicated diagramatically the link between the boundaries of the neutral layer and the ring of auroras. Some of the results [49] are shown in Figure 9 (the noon and midnight latitudes of the ring in terms of K_p). Although the /43 displacement of the auroras from the pole when magnetic field disturbances occurred has long been known, it was not until IGY data became available that a quantitative study of this effect was possible. Specifically, the fundamental fact of the existence of a ring of auroras simultaneously, at all longitudes, was established for the first time by [49] on the basis of an analysis of these data.

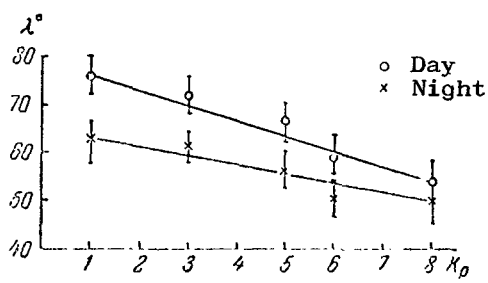

Figure 9. Noon and midnight latitudes of the aurora ring in terms of the magnetic activity level.

Since geomagnetic disturbances are the result of variations in the corpuscular radiation from the sun, it is natural to suppose that the level of such disturbances would change with the 11-year cycle of solar activity. Actually, the average daily K_p-indices clearly correlate with the number of sunspots. A

more detailed analysis reveals that the severe storms, with an average daily K_p-index $\gtrsim 5$, experience the greatest variations. There is little fluctuation in the frequency of moderate, and particularly of weak, storms. It is even possible that the maximum for these disturbances is delayed 3 to 4 years with respect to the maxima for the spots.

In conclusion, let us consider the question of the electric fields associated with geomagnetic disturbances. Since the time scales of the disturbances ($\gtrsim$ 1 minute) are large compared with the periods of the oscillations of the particles from the radiation belts between the points of reflection, these fields can only cause the adiabatic acceleration accompanying the transfer of the particles into the depth of the magnetosphere. /44

The present day picture of the magnetosphere, briefly described in this paragraph, points to the existence of two types of electric fields; curl fields, associated with variations in the geomagnetic field, and electrostatic fields occasioned by ionospheric disturbances. This book is primarily devoted to the investigation of the effects of the electric curl field.

Electrostatic fields occur in the ionosphere and are propagated throughout the magnetosphere because the field lines can be considered as practically equipotential, the result of the high conduction of the near space plasma along the field. If polarization is the result of steady-state winds, and if the field does not change with time, the latter will deform the drift orbits of the particles somewhat. This effect was reviewed in [57]. The estimate is that orbital disturbances will become significant at energies $\lesssim$ 10 keV. Variable fields, linked with ionospheric turbulence, can cause a transfer of particles across the drift shells. The effect will be marked when the spectrum of the turbulent electric fields contains pulsations of visible amplitude, the frequencies and scales λ of which are such that the "phase velocity" of the pulsations is $2\pi\lambda/\omega \sim v_d$, where v_d is the velocity of the magnetic drift of the particles. The fundamentals of the theory behind this transfer were developed in [14].

Let us point out that turbulent electric fields at high altitudes should cause turbulent convection of the plasma (and vice versa). The concept of the diffusion of the particles in the belts during convection in

the magnetosphere was reviewed in [1]. Because of the ionospheric currents, convection is forced. It can be assumed that in the magnetosphere proper there is convective instability, occasioned by the pressure gradient of the cold plasma and by diamagnetic effects [58]. However, large-scale movements of this type are suppressed by dissipations in the ionosphere [59]. Moreover, a comparison of the energy resources of the sources of free and forced convection reveals that the latter should be much more intensive. /45

Therefore, from the point of view of contemporary postulations with respect to the dynamics of the magnetosphere, the particle transfer mechanism can be linked with the curl fields of the worldwide geomagnetic disturbances, or with ionospheric turbulence. It is impossible at this time to explain their relative roles in the formation of the belts from general considerations because information on winds in the ionosphere is clearly inadequate. The study of the transfer as a result of the effect of the curl fields is quite detailed at this point, and the experimental data on this question are quite complete, but at the same time can not be considered as exhaustive. Research results are successful in explaining the dynamics of particles, the drift periods of which are $\lesssim$ 1 hour (corresponding to energies of $>$ 100 keV, approximately). Yet there are many difficulties encountered when one enters the area of large drift period values (of lesser energies). Specifically, some of the experimental data show that the transfer of these particles is more rapid (particularly during magnetic storms). Since, judging from the estimates made in [57], the effect of the polarization of the ionosphere becomes significant, particularly in the energy range $\sim$ 1 to 10 keV, it can be assumed that this mechanism plays an important role in this particular energy range.

The survey made in this paragraph of current data on the earth's magnetosphere is hardly complete. Our purpose was to describe the principal qualitative features of the earth's magnetic field necessary for an understanding of the structure of the geomagnetic trap, to give an overview of the research methods used today, and to describe some of the quantitative characteristics of field disturbance activity (K-index, K_p-index, and the like) widely used to analyze the link between the magnetic phenomena and

other processes in the magnetosphere.

More complete data on many of the questions concerned with the physics /46
of the magnetosphere can be found in the lectures given by S. Chapman [56] (1962), and in original papers [24-26, 50, 53] describing the principal results obtained after 1962.

3. Cold Plasma and Electromagnetic and Plasma Waves in the Magnetosphere

One of the most important characteristics of the physical conditions in the magnetospere, in addition to the magnetic field, is the distribution of the cold plasma, that is, of particles with average energies of from 0.1 to 10 eV, approximately. Cold plasma establishes many important parameters, important from the standpoint of the theory of radiation belts, and, in particular, the life of fast particles in terms of ionization losses and the index of refraction for various types of electromagnetic and plasma waves. And in turn, the index of refraction can be used to express the frequencies at which the resonant interaction between the corresponding types of waves with particles of specified energy takes place, as well as the conditions under which the radiation belts will be stable in terms of the rise times of the various waves.

The distribution of cold plasma, likely, is included among the less studied parameters of near space. Even at so comparatively a low altitude as 1,000 km, the measurements made using similar methods have produced an electron density, N_e, differing by a factor of 10. The apparent reason for these divergencies is not the fault of the particular methodology used (although all have known deficiencies), but is found in the great changeability in the properties of cold plasma in space and in time. In any case, monitored measurements of the profile of the electron density at altitudes of < 1,000 km, made using four different methods, by satellite, by rocket and by ground sounding, at the same time, and in the same place [60], yielded the same result. Specifically, the electron density at an altitude of 1,000 km is $10^4 cm^{-3}$. This magnitude is now accepted by most authors as the average electron density at the upper boundary of the ionosphere during years of reduced /47
solar activity (1961-1965).

An altitude of $\sim$ 1,000 km is considered to be the upper boundary of the ionosphere, because it is here that the total concentration of ions of atomic oxygen, nitrogen, and helium are approximately equal to the proton concentration. The earth's atmosphere at altitudes $>$ 1,200 km is practically 100% protons and electrons [61]. These results, as well as the data in [62], which agree with them, were obtained during years of low solar activity (1962-1964), when the apparent temperature of the upper atmosphere was approximately half that in years of maxima (1958-1959).

In what follows, we will only have need of information on the ionosphere during the investigation of the stability of the radiation belts, where the necessary information will reduce to an estimate of the reflection factor for certain types of waves reflected from the earth, with absorption in the ionosphere taken into consideration. This very special question will be dealt with in Chapter V.

A much broader spectrum of phenomena in the magnetosphere, and of the radiation belts, can be established by the density of the cold plasma at altitudes $\gtrsim$ 3,000 km from the earth's surface (or 1.5a from the center of the earth). Various estimates have been made, and show that near the plane of the equator the densities of ions and electrons is $N_i = N_e \approx 10^3$ cm^{-3} when $1.5a \leqslant R \lesssim 3.5a$. This result was obtained during years of maximum solar activity [63], as well as during years of minimum solar activity [64, 65]. A similar order of magnitude for N in this region is provided by an analysis of the propagation of extremely low frequency electromagnetic waves [66] and Alfvén waves [67] along the geomagnetic field lines. The accuracy of these results is low, so one discusses them as being of an order of magnitude of N. Judging from some of the data, the density of the cold plasma falls off sharply, to a magnitude $\lesssim 10^2$ cm^{-3} [63, 66] when $R > 3.5$ to 4a. The dependence N(R), used in various of the theoretical works on the subject, is most diverse in its nature (from $N \approx$ constant, to $N \sim R^{-4}$). There are the following definite positions so far as the theoretical point of view is concerned: /48

(a) along the magnetic field lines there is a hydrostatic equilibrium

$$(H\nabla P) = (gH)\rho, \tag{3.1}$$

where

H is the magnetic field intensity;

P is cold plasma pressure;

ρ is cold plasma density;

(b) the plasma is quasineutral ($N_i = N_e \equiv N$).

Moreover, there is the probability that at altitudes > 1,000 km, the temperatures of ions and electrons do not in any case decrease with distance from the earth along the field lines. It is possible that the electrons are isothermal above 3,000 km (but the temperature, T_e, can differ on different field lines). If it is assumed that the proton temperature, T_i, is constant along the field lines at these altitudes, the solution to the equation at (3.1) is trivial:

$$N = N_0 \exp\left[2M \frac{U(R_0) - U(R)}{T_i + T_e}\right], \tag{3.2}$$

where

N_0 is the density at altitude R_0, beginning at some attainable isothermal state;

U(R) is the gravitational potential;

M is the proton mass. The temperatures in the equation at (3.2) are measured in ergs.

The parameters N_0, T_i, and T_e, contained in the equation at (3.2), are constants along the field lines, but can be different on different lines. Hence, the distribution at (3.2) is not spherically symmetrical, generally speaking. The pressure gradients across the magnetic field can be balanced by the summed action of the force of gravity and the magnetohydrostatic forces. Transfer of heat and material across the field is magnetically very confined, and the movement is at a velocity of $(\nu_i/\Omega_H)^2$, or slower by a factor of $(\nu_e/\omega_H)^2$ than along the field (ν_i and ν_e are the frequencies of ion and electron collisions, Ω_H and ω_H are the respective cyclotron frequencies). These ratios are very small ($\lesssim 10^{-9}$) in the region of the radiation belt maxima.

The gravitational field cannot be taken as homogeneous at high alti-

tudes; $U(R) = - G_0 a^2/R$ (here the radius of the earth, a, and the distance, R, are measured in centimeters). The equation at (3.2) can be used to estimate the altitude movement of the density along the field lines if T_i and T_e are known. For example, if, in accordance with the experimental data in [68], it is taken that at high altitudes ($\sim$ 10,000 km from the earth's surface) $T_e = 8{,}000°$ in the plane of the equator, even when $T_i = 0°$, the density from 1.5a to the apex of the field line will not diminish by a factor of more than 3.5. If $T_i = T_e/2 \approx 4{,}000°$, let us say, the analogous density differential will only be $\approx$ 30% on the field line, the apex of which is 3a from the center of the earth. Thus, at temperatures $\sim$ 1 eV, the altitude movement of the density along the field lines is low, and the apparent dependence of N_0 on the magnetic latitude (and possibly on the longitude as well) plays a big part. /49

The transfer theory is the basis for saying that the computations concerned with the structure of the earth's radiation belts are completely analogous for any exponential dependence of N on the equatorial distance. References [5-12] assumed that when $R > 1.5a$ $N = \text{constant} \approx 10^3$ cm^{-3}. The results obtained with this very simple model were much closer to the experimental data than were the results in [15] for models with a rapid decay (such as R^{-4}). The data on the radiation belts are such that N(R) can be established by several independent methods, in principle, The results of this estimate, and the prospects for a more accurate determination of N through the dynamics of rapid particles will be discussed in Section 13. We will put $N = \text{constant} \approx 10^3$ cm^{-3} in what follows to estimate the index of refraction and the ionization losses.

Cold plasma pressure (10^{-9} ergs/cm^3) is negligibly small compared with $H^2/8\pi$ (10^{-8}ergs/cm^3 at the boundary of the magnetosphere, and approximately 10^{-5} to 10^{-6} ergs/cm^3 in the region of the outer zone). The pressure of the fast particles, despite the low density, exceeds the cold plasma pressure by one order of magnitude at the proton belt maximum.

A plasma frequency of $\omega_0 \approx 2 \cdot 10^6$ rad/sec ($3 \cdot 10^5$ Hz) corresponds to a density of $N_e = 10^3$ cm^{-3}. The electron cyclotron frequency, ω_H changes from $2 \cdot 10^6$ rad/sec near the equatorial plane when $R \sim 1.5a$, to $\approx 10^3$ rad/sec at

the boundary of the magnetosphere, so the inequality $\omega_H \ll \omega_O$ is virtually everywhere satisfied. When $R \ll 4a$, the ion plasma frequency is $\Omega_O < \omega_H$. So there is a broad, forbidden gap, $(\omega_H \leqslant \omega \leqslant \omega_O)$, in the spectrum of electromagnetic and electrostatic wave frequencies. The propagation of waves with frequencies $< \omega_H$ has a substantial magnetohydrodynamic character (the only exception is ion sound). The effect of the inertia of the cold electrons is even more noticeable at frequencies of $\sim \omega_O$ (but higher than ω_O). Finally, when $\omega \gg \omega_O$, the electromagnetic waves can be propagated practically as in a vacuum. As has already been pointed out in Section 1, electromagnetic waves with $\omega \gg \omega_O$ (cosmic and solar radio radiation) are of no interest so far as the theory of radiation belts is concerned. /50

Low frequency electromagnetic fields in the magnetosphere (with the exception of the forced oscillations reviewed in Section 2) are linked with natural hydromagnetic oscillations. The natural oscillations of the magnetosphere "core" (that is, of the region of trapped radiation) and of its tail can apparently be considered separately in some approximation. Obviously, the periods of the lowest harmonics of the poloidal oscillations (that is, oscillations with a radial and a latitudinal component of the velocity) of one order of magnitude are determined by the time required to propagate the disturbance from the surface of the earth to the boundary

$$T \sim \int_a^{R_b} \frac{dR}{u_a(R)}, \tag{3.3}$$

where

$$u_a = \frac{H(R)}{\sqrt{4\pi\rho}}$$

is the Alfvén velocity. Taking ρ = constant $\sim 10^{-22}$ to 10^{-23} g·cm^{-3}, that is, $N \approx 10^2 - 10^3$ cm^{-3} and $H = 2H_O(a/R)^3$ ($H_O \approx 0.3$ gauss is the field at the earth's equator), we obtain

$$T \sim \frac{1}{4}\left(\frac{R_b}{a}\right)^4 \frac{\sqrt{4\pi\rho}\, a}{H_0}. \tag{3.4}$$

This assessment is very rough, of course, because it does not take into consideration the latitudinal and longitudinal dependency of H and the current fields at the boundary. Still, there are a number of qualitative conclusions that can be drawn from the equation at (3.4). First of all, /51

the order of magnitude of T is $\sim$ 1 minute. Second, T is greatly dependent on the position of the boundary. Proceeding from these assessments, one can analyze the data on geomagnetic disturbances with periods on the order of several minutes and attempt to separate the types of oscillations that correspond, qualitatively, to these relationships. Since what is referred to here are the lowest of the harmonics. The pulsations with the specified frequency should be observed simultaneously over a considerable part of the earth's surface (comparison of amplitudes can be made difficult by the pick-ups in the ionosphere and by the skin effect at the earth's electrically heterogeneous surface). Experimental data concerning changes in the position of the boundary of the magnetosphere, as recorded by various of the satellites, have been published in recent years. There should be a strong dependence of T on R_b, as shown by the equation at (3.4) (although it is not mandatory that this dependence be in the form $T \sim R_b^4$), of course).

The analysis made by V. A. Troitskaya [69] shows that the regular micro-pulsations of the geomagnetic field in the frequency interval from $\sim$ 0.1 to 0.01 Hz satisfy the qualitative requirements indicated. These oscillations are recorded simultaneously by all stations on the illuminated side of the earth and have identical, stable frequencies for all stations. Reference [69] obtained an empirical ratio between T and R_b

$$T \approx 7 \cdot 10^{-4} \left(\frac{R_b}{a}\right)^5 \text{ second} \qquad (3.5)$$

that is close to the rough estimate at (3.4).

Changes in the frequencies of these pulsations usually take place intermittently, and are associated with sudden pulses of the geomagnetic field. At the same time, the amplitude of the oscillations increases sometimes, and the natural explanation is that the increase is due to the disturbance of the magnetosphere boundary. However, the amplitudes of the oscillations ($\lesssim 1\ \gamma$) are considerably smaller than the magnitude of the static jump made by the field while the sudden pulse lasts. /52

A detailed explanation of regular pulsations still runs head on into known difficulties (first of all, and this is not understood at all, why these pulsations are only observed on the illuminated side of the earth).

But even now there are ways seen to overcome these difficulties, and the conclusion in [69] that these oscillations are the lowest natural harmonics of the magnetosphere raises no doubts. The near future measurements of regular pulsations apparently will result in continuous monitoring of the position of the boundary of the magnetosphere from ground data.

Measurements of micropulsations in the frequency range from approximately 0.2 to 5 Hz have resulted in the detection of phenomena that differ in principle from the regular pulsations [70] reviewed in the foregoing. It turns out that long, quasi-monochromatic wave packets, repeating regularly with a period of $\sim$ 100 seconds, are often observed in this range. The magnetogram resembles a string of beads, and because of this similarity these pulsations have been called "pearls." From our point of view, the "pearls" are the result of weak instability in the proton zone [19, 20]. This question will be discussed in more detail in Chapter V.

There is no ground information on electromagnetic oscillations in the magnetosphere in the frequency interval from $\sim$ 10 to several hundred hertz. These frequencies are close to the cyclotron frequencies of the O^+, N^+, and NO^+ ions (that is, of the basic components of the ionosphere) so are very much absorbed. The first, and as yet the only, attempt to observe these oscillations at high altitudes was undertaken by the satellite Elektron 3 [71]. The data obtained are being processed. In the meantime, it has been explained that the amplitudes in the 30 to 300 Hz range are lower than is the case for the lower frequencies (1 to 10 Hz). Single pulses with amplitudes $\geqslant$ 5 γ are recorded once a minute, approximately. Pulses with amplitudes > 25 γ are not observed. One of the tasks of the experiment was to assess the effectiveness of the Fermi acceleration mechanism, reviewed as applicable to the radiation belts in [72]. The results in [71] indicate /53 that the Fermi acceleration cannot play a significant role in the spectrum of pulsations observed.

The ionosphere becomes relatively transparent at the apexes of the corresponding field lines in the range of frequencies from approximately 1 kHz to ω_H. The electromagnetic waves at these frequencies are an electron analog of Alfvén waves, and when $\omega \sim \omega_H$, their velocity is close

to $\frac{H}{2\sqrt{4\pi mN}}$ (m is the electron mass). Ground observations record intensive noises arriving in this range from the ionosphere (that is, from above), as well as from along the surface of the earth. In the latter case the waves are usually generated during thunderstorm lightning discharges, and are called atmospherics.

The echo of the lightning discharges in this particular range can often be received at a point linked with the thunderstorm area along the field line. The signal, moving over the long path from one hemisphere to the other, is drawn out because of the dispersion and is received by ear as a whistle, the tone of which descends with time. Phenomena such as these are called whistling atmospherics. It has sometimes been possible to observe a great many (up to 40) successive reflections of whistling atmospherics at magnetically linked points.

The investigation of whistling atmospherics is what made it possible to assess the density of cold plasma at high altitudes, even before space rockets and satellites were launched. The order of magnitude thus found ($N \sim 10^3$ cm^{-3}) was confirmed later on by the high-altitude measurements.

Certain types of instability in the radiation belts [17-2], as well as the lightning discharges can be sources of extremely low frequencies. We will return to this question in Chapter V. Let us note at this point that the ability of the electromagnetic waves in this range to propagate along bent geomagnetic field lines is not the trivial consequence of the law of dispersion, but can simply be the result of the presence of heterogeneities in the desnity at high altitudes (unique, extremely low frequency waveguides). However, the reality of this effect can be confirmed not only by more purposeful experiments. An analogous relay of waves at a frequency of 15.5 kHz, created with a frequency generator [73], was accomplished. /54

High altitude measurements in the extremely low frequency range are described in [74-76]. The receiver used in the first two of these references was a loop, and magnetic vector pulsations were recorded. Reference [74] reported the registration of waves with amplitudes $\sim 1\ \gamma$ (according to ground data, amplitudes in this range are not in excess of $10^{-3}\ \gamma$).

The maximum amplitudes in [75] did not exceed 10^{-2} γ, and this is more reasonable from the standpoint of the transparency of the ionosphere.

Reference [76] used a rod antenna for measurements (that is, the oscillations of the electric vector E were recorded). Recorded at altitudes of from 500 to 600 km were brief (3 to 10 minute duration) flashes of radiation with amplitudes of from 0.2 to 1 mv/cm, primarily at a frequency of 1.7 kHz. If these waves belonged to the type described above, these amplitudes would correspond to high frequency magnetic waves of from 10 to 100 γ. But waves such as these have never been observed in this range. This led the authors of [76] to conclude that their equipment had recorded electrostatic oscillations of the ion sound type.

The frequency at which the effect is expressed most clearly (1.7 kHz) is close to the ion plasma frequency for oxygen and nitrogen ;(O^+ or N^+) at altitudes of $\sim$ 500 km ($N_i \approx 5 \cdot 10^5$ cm^{-3}). In accordance with the dispersion equation for ion sound waves, the wave length should thus be on the order of a debye radius, and the phase velocity should be $\lesssim \sqrt{T_i + T_e/M_i}$, that is, 10^5 cm/sec. Resonance acceleration of particles has little effect at phase velocities as low as these. And cyclotron resonance, taking the Doppler effect into consideration ($k_\parallel v_\parallel \approx \omega_H$, where $k_\parallel$ and $v_\parallel$ are the projections of the wave vector and the particle velocities in a magnetic field, respectively; ω_H is the cyclotron frequency) when $v \sim c$ too is possible only when $k_\parallel \ll k$. Therefore, the role of the waves detected in [76] in the formation /55
of the radiation belts is slight (the more so because large amplitudes were observed primarily at low altitudes, 500 to 600 km, while the apogee of the orbit was found to be higher than 3,000 km).

There is, as has already been pointed out, a forbidden gap between the frequencies ω_H and ω_O (when $\Omega_O < \omega_H$) in the wave spectrum. Plasma oscillations were apparently recorded by the satellite Elektron 2 [64]. Measurements made at a frequency of 725 Hz showed that sometimes the effective temperature of the radiation in this frequency region rose by from 1 to 3 orders of magnitude as compared with the cosmic radio radiation background ($T_{eff} \approx 3 \cdot 10^7$ °K).

The increase is considerably smaller at higher frequency (1,525 kHz). The flares show no correlation with solar phenomena and geomagnetic activity, but quite definitely correlate with the rise in the fluxes of soft electrons (with energies $\sim$ 100 ev) in the earth's magnetosphere. The plasma frequency equals 725 kHz when $N_e = 5 \cdot 10^3$ cm^{-3}, and if the sources of the observed waves actually are plasma oscillations, their generation occurs at altitudes of from 1,500 to 2,000 km above the earth's surface.

The mean effective temperature of these oscillations (with the high pulse rate taken into consideration) apparently does not exceed 10^8°K. If it is taken that analogous processes take place throughout the magnetosphere, and if it is assumed that T_{eff} is proportional to $1/N_e$ (two points, f = 725 kHz and 1,525 kHz, satisfy this condition), the mean value of $\bar{T}_{eff}$ near the plane of the equator will be 10^9°K. According to the computations made in [16], these values for T_{eff} are too small to have any significant effect on the radiation belt. However, when the computations were made it was assumed that the average wave length was on the order of a Debye radius. The effectiveness of statistical acceleration increases in the case of longer waves. What follows from [16] is that in the case of electron energies $\sim T_{eff}/\log q$ ($\log q$ is the logarithm of the Debye shielding; in the magnetosphere $\log q \approx 25$) the acceleration is curtailed and the ionization losses begin to predominate. The mechanism in [16] therefore cannot play a significant role in the dynamics of electrons with energies $\gtrsim$ 100 keV. Thus although statistical acceleration cannot yet be entirely discarded in the considerations, it obviously is not a basic mechanism for the generation of fast particles. /56

We will conclude our survey of the physical conditions in the magnetosphere on this note. Let us recall that the purpose of the survey was to describe the most significant parameters and processes from the point of view of contemporary experimental and theoretical results, as well as to present the arguments that are the basis for what we consider to be the principal, and most likely, trends in the theory of particle acceleration in the radiation belts, the investigation of the transfer of particles across the drift shells. Consequently, many of the questions of great

interest to other branches of the physics of the magnetosphere (particularly those dealing with ionospheric processes and the properties of the solar wind), as well as many of the results of the morphological investigation of various phenomena, have not been dealt with in any detail. Nor were certain debatable questions, on which agreed opinion is lacking, touched upon.

Chapter II

/57

The Earth's Radiation Belts

4. Particle Drift in the Field of Intraearth Currents

It is desirable, before proceeding to an analysis of the experimental data on the radiation belts, to review the basic properties of the region in which high-energy particles are localized (those with energies $\gtrsim$ 40 keV). This region has a comparatively small volume and its boundary apparently coincides with the boundary of the tail of the magnetosphere. We will, in this paragraph, review kinematic questions for the most part (that is, the geometry of the particle drift orbits). The review is based on the drift theory, and primarily on the use of two of the first adiabatic invariants; that of the magnetic moment, and that of the longitudinal effect. The general theory of traps is now quite widely known, so only those questions in which the specifics of the geomagnetic field arise will be reviewed.

The trapped radiation region can be broken down, if somewhat conditionally, into an inner and an outer section, in the first of which the field is established by the intraearth currents, and in the second of which the currents on the boundary of the magnetosphere become substantial. A region, delimited by field lines a distance of approximately 5a from the center of the earth in the plane of the equator, and resting on the 63rd geomagnetic parallel, can be included in the inner region at a magnetically quiet time. During disturbances this boundary is shifted earthward somewhat, but even during /58 the most severe storms rarely gets closer than 3.5a in the plane of the equator. The field in the inner region is close to the dipole field at high altitudes.

The drift orbits of the particles in the field of the dipole lie in shells formed by the rotation of the field lines around the magnetic axis, the result of symmetry. The reflection points drift in circles with constant intensity. Let us consider first the time parameters of the drift. There is no need to consider the finiteness of the Larmor radius and of the cyclotron frequency so far as the majority of the questions dealing with the theory of the belts are concerned (except for problems of

stability). It can be taken that $r_H = 0$, and that $\omega_H \to \infty$. The period of the oscillations of the particles between reflection points, τ_θ, (the index θ signifies that the polar angle θ changes during oscillations) depends on particle velocity, v, the values for θ at the mirror point ($= \theta_m$) and on the parameter of the field line, L (the distance from the dipole to the apex of the field line; here, and in what follows L will be measured in earth radii, a, and is a dimensionless magnitude:

$$\tau_\theta = 6.3 \cdot 10^{-2} \frac{L}{\beta} f_\theta(\theta_m) \text{sec}, \qquad (4.1)$$

where $\beta = v/c$, and the function $f_\theta(\theta_m)$ changes monotonically from 1 when $\theta \to \pi/2$ to ≈ 2 when $\theta = 0$. Time τ_θ is usually used for estimates only, so it can be taken that $f_\theta = 1$. The order of magnitude of τ_θ for electrons is 0.1 to 1 second.

The velocity of the drift along the longitude, v_φ, in the case of particles with mirror points close to the equator is obviously $\sim \omega_H r_H \frac{\partial r_H}{\partial R}$ (where R is the radius vector, read from the dipole). Let us designate total particle energy in Mc^2 units (M is the mass of the particular particle) by ε, the pulse in Mc units by P (ε and P are dimensionless numbers and $\varepsilon^2 = P^2 + 1$), and the nonrelativistic cyclotron frequency eH/Mc by $\omega_H^{(0)}$. Taking it that $H \sim R^{-3}$, what we obtain is a drift velocity proportional to $\frac{P2}{\varepsilon} L^2$. The computations made in [77] reduce to the following expressions for the period of longitudinal drift $\tau_\varphi = \frac{2\pi a L}{v_\varphi}$: /59

$$\tau_\varphi = \begin{cases} \frac{44}{LE} f_\varphi(\theta_m) \min & (E \ll Mc^2), \\ \frac{22}{LE} f_\varphi(\theta_m) \min & (E \gg Mc^2), \end{cases} \qquad (4.2)$$

where E is the kinetic energy in MeV. The function $f_\varphi(\theta_m)$ established the dependence of τ_φ on the latitude of the mirror point. In the plane of the equator $f_\varphi = 1$, and when $\theta_m \to 0$, the function $f_\varphi \approx 1.5$. Tables and graphics for making a precise determination of τ_θ and τ_φ can be found in the survey in [78], if needed.

Comparing the equation at (4.1) with those at (4.2), we see that when $1 \leqslant L \leqslant\leqslant 10$ $\tau_\varphi \gg \tau_\theta$ right up to energies of $\sim$ 100 MeV. Therefore, the

longitudinal drift is much slower than the oscillations along the field line everywhere in the radiation belts.

If the processes leading to change in the adiabatic invariants, in energy ε, or in the number of particles in some field duct can be characterized by times $\tau \gg \tau_\theta$, a quasi-stationary particle distribution (changing over time $\gtrsim \tau \gg \tau_\theta$), uniquely linked with the angular distribution and the spectrum in the plane of the equator, can be established along the field lines. Let $f = f(\eta, P_\parallel, P_\perp)$, which is a function of the distribution that depends on the longitudinal and transverse components of the pulse with respect to the field, and on the changing coordinate along the field line of magnitude $\eta = H/H_{min}$, where H is the field at the particular point and H_{min} is the minimum value for the intensity on the field line. The function f should satisfy the kinetic drift equation. The general solution to this equation in the stationary case is, as is known, an arbitrary function of two drift intervals of the movement. It is convenient to select for the latter the absolute magnitude of the pulse, and the adiabatic invariant $\mu = (\sin^2 \alpha)/\eta$ (α is the angle between the velocity and the field line). Values must be assigned to this function when $\eta = 1$ in order to arrive at a unique determination of f (when $\eta > 1$ some of the particles cannot reach the point with given η, and their distribution /60 will not depend on $f(\eta)$).

If $f = f_0(P, \sin^2 \alpha_0)$, when $\eta = 1$, for arbitrary η the function can be determined by replacing the magnitude $\sin^2 \alpha_0$ in f_0 by $(\sin^2 \alpha)/\eta$. Thus the particle density at an arbitrary point on the field line is

$$n(\eta) = 2\pi \int_0^\infty \int_0^\pi P^2 f(P, \alpha) \sin \alpha \, d\alpha \, dP = \\ = 2\pi \int_0^\infty \int_0^\pi P^2 f_0\left(P, \frac{\sin^2 \alpha}{\eta}\right) \sin \alpha \, d\alpha \, dP. \tag{4.3}$$

Let us point out one important, special case. If $f_0 = \psi(P) \sin^\nu \alpha_0$, as will be seen quite readily

$$f(\eta, P, \alpha) = \psi(P) \eta^{-\nu/2} \sin^\nu \alpha. \tag{4.4}$$

The angular distribution and the spectrum are identical along the entire field line, but the particle density changes as $\eta^{-\nu/2}$. The distribution at (4.4) enables us to use simple expressions to approximate the experimental data, and is particularly convenient for making theoretical computations.

The relationships obtained contain no explicit dependence of η on the coordinates, so are valid for the dipole, as well as for any magnetic trap in which $H_{max} \gg H_{min}$. Moreover, in the case of the dipole, because of the axial symmetry, the values for the stationary function of the distribution are identical and along the lines H = constant and on the shells L = constant. In the case of an arbitrary injection of particles, this axially symmetrical distribution can be established in time $t \sim \tau_\varphi^2/\Delta\tau_\varphi$ ($\Delta\tau_\varphi$ is the divergence in the values for the drift periods for the injected particles, the result of the divergence in energies).

Computation for comparatively small deviations of the field of the intraearth currents from the dipole field will cause no qualitative changes in the picture of the drift. As MacIlvain has pointed out [79], the particle drift shells do not depend (or do so only slightly) on the latitude of the reflection point, even in this case. Proof is based on a /61 numerical analysis of drift shells in a real geomagnetic field. The field lines, and surfaces H = constant and $I = \int_z^{z^*} \sqrt{1 - H/H_m}\,dz$ = constant, were found using a computer and a specified scalar potential. The integral, I was taken along the field lines between points with equal field values. I is the second adiabatic invariant in a stationary field. The computation for the drift shells based on the computation of two invariants turned out, in practise, to be much more effective than the direct solution of drift equations. Analysis showed that particles with any α_0, initially located on the same field line, will drift over virtually the same surface. At the same time, as we know [80], lines H = constant on drift shells are lines of constant particle density.

However, the qualitative closeness of the nature of the particle drift in the dipole field and in the field of the intraearth currents by no means signifies that the differences are negligibly small. Whereas the approximation

of a non-central dipole (shifted approximately 500 km from the center of the earth in the direction of Eastern Siberia) can be used near the equatorial plane at altitudes $\gtrsim$ 3000 km ($R \geqslant 1.5a$), higher harmonics must be taken into consideration at lower altitudes.

Reference [79] introduced the magnetic shell parameter L, corresponding to the distance from the apex of the field line to the dipole at long distances from the earth, and pointed out a method for computing L in terms of the geographic coordinates of the point. This computation can be done on computers. Charts of the lines L = constant have now been published for distances from 0 to 3,000 km from the surface of the earth in 100 km increments. These charts can be used quite handily to determine the L value at any point with an accuracy, the limits of which are within the concept of the L-coordinate itself (1 to 2%). Figure 10 is an example of one such chart of the lines L = constant, H = constant at an altitude of 1,000 km. The charts were drawn in the Goddard Space Flight Center (USA).

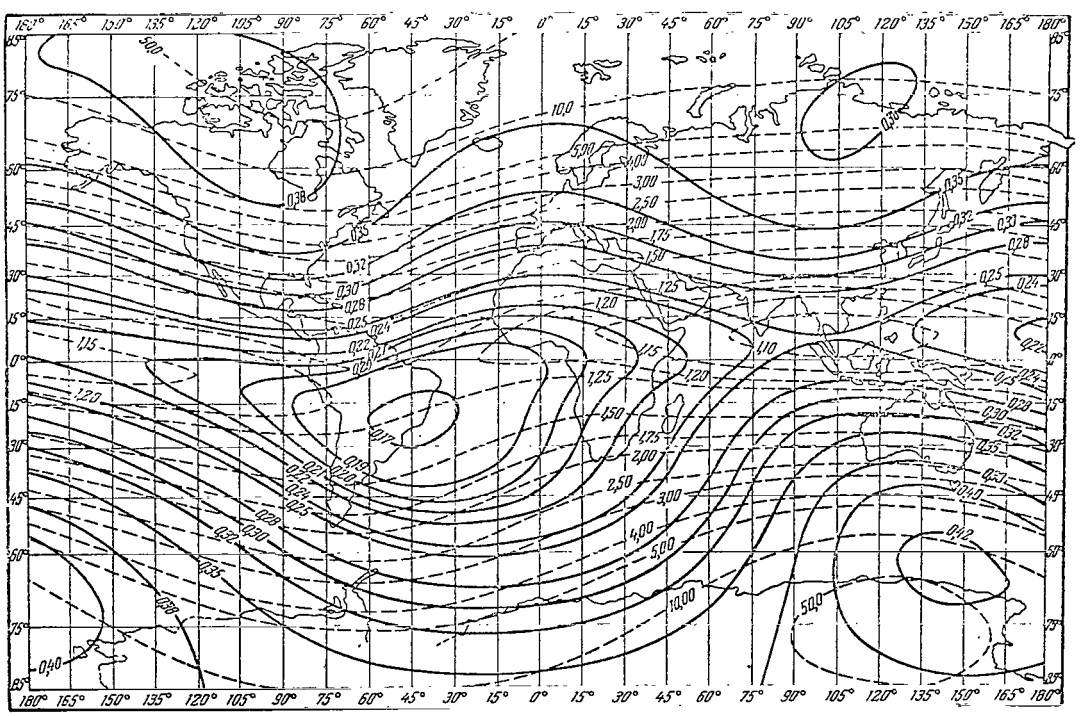

/62

Figure 10. Lines for L = constant (---), and H = constant (——) at an altitude of 1,000 km.

Commas represent decimal points.

The computation for the drift shells allows us to introduce a natural system of coordinates to describe the particulars in the radiation belts [79]. One of the coordinates is the parameter L, the other the field intensity H.* If there are no disturbances in the radiation belts during a period of time on the order of τ_φ, the intensity for given L and H will not depend on the longitude. The physical meaning behind the use of L and H as coordinates is that if H is taken as the field intensity at the mirror point for some particle, changes in L and H have completely different natures. Change in L is linked with the transfer of particles across the drift shells, and from this point of view field disturbances, the time scales of which are on the order of the drift period τ_φ, are the most effective (as was pointed out in [80], in the case of slow field variations, slow in terms of τ_φ, that is, the particle will follow the drift shell, and in the case of a return of the field to its original state, the original particle distribution is restored. Changes in the positions of the mirror points on the field lines are the result of an infringement of the first two adiabatic invariants, the magnetic moment, and the "longitudinal effect" $\int_{z_1}^{z_2} P_{\parallel}\, dz$. The magnetic moment is infringed as a result of the effects of disturbances with frequencies $\omega \lesssim \omega_H$, or with wave numbers $k \lesssim 1/r_H$. The infringement of the second invariant is linked with disturbances in which $\omega \lesssim \tau_\theta^{-1}$, or $m \lesssim \tau_\varphi/\tau_\theta$ (m is the number of the harmonic in the expansion of a disturbance field into a Fourier series in terms of the longitude). These scales are much smaller, and the frequencies much higher, than is the case for the infringement of L.

The experimental data on the belts at altitudes $\lesssim$ 2,000 km did not, practically, speaking lend themselves to quantitative analysis prior to the development of the L, H system of coordinates. At these altitudes the distribution of fast particles can be characterized by sharp gradients along the field lines (the result of the rapid decay in the density of cold plasma with altitude), as well as across the drift shells, the distances between which at low altitudes are much shorter than in the equatorial plane. However, the introduction of the MacIlvian system of coordinates

* The magnetic induction, B, which is, naturally, identically equal to H in the magnetosphere, is often used in place of the field, H.

made it possible to systematize the data and to find simple laws at once in completely chaotic sets of points.

Today, the different systems of coordinates based on the use of one of the systems of coordinate surfaces of L shells are widely used to analyze experimental data, as well as in theoretical works. The parameter L usually is measured in earth radii.

Thus, the stationary function of the distribution at high altitudes depends on three variables, L, P, and α, and can be established completely by the equatorial distribution.

Let us now consider changes in energy and angular distribution of radiation belt particles for the case of slow variations in the magnetic field, as compared with τ_θ. We will consider the dipole field to be the original field.

Variations can be reversible, and nonreversible, depending on the nature of the disturbance. In the case of reversible variations, the restoration of the original field is accompanied by the restoration of the original particle distribution, and in the case of nonreversible disturbances the parameter L, the pulse P, and the equatorial angle between the velocity and the field line, α_0, can have values different from the initial values at the end of the cycle.

Real geomagnetic disturbances usually cause reversible, as well as nonreversible, variations. Reversible changes in radiation belts can be linked to slow disturbances as compared with τ_φ ($\lesssim$ 1 hour), or with axially symmetrical portion of the disturaance for any time scales.

In the former case the reversibility is occasioned by the already noted invariantness of the drift shell [80], and although the shell can be deformed when changes occur in the field, the particle drift path follows the changes in the shell. The magnetic flux does not change /65 along the path of the particle's mirror point and is the particle's third adiabatic invariant in the magnetic trap [80].

In the case of disturbances that are axially symmetrical with respect to the magnetic axis, the reversibility follows directly from the law of

the conservation of the generalized moment of the pulse

$$M=\left[r\left(P+\frac{e}{c}A\right)\right]; \tag{4.5}$$

where r is the radius vector for the particle;

P is its pulse;

e is the charge;

c is the speed of light;

A is the field's vector potential.

The projection of M on the axis of symmetry is retained in the case of axial symmetry ($\frac{\partial A}{\partial \varphi} = 0$). The term $\frac{e}{c} A \gg P$ ($A \sim Hr$ and $\frac{cP}{eA} \sim \frac{r_H}{r} \ll 1$, where r is the field heterogeneity scale) in the drift approximation. From whence it follows that the magnitude

$$M_z = r \sin \theta A_\varphi, \tag{4.6}$$

where r, φ, and θ are spherical coordinates (the polar axis is directed along the magnetic axis), is maintained with an accuracy of within small oscillations in the case of Larmor rotation. However, the expression $r \sin \theta A_\varphi$ = constant is the field line equation, so what follows from the conservation of M_z is that in the case of axially summetrical fields the particle will move with the field lines and will return to the original shell when the disturbance is over. The theory of reversible variations near the plane of the equator was developed in [9].

The possibility that radiation belts are formed by some hypothetical process during which trapped particles regularly drift toward the earth was reviewed in [81]. What follows from the equation at (4.5) is that no such process can take place as a result of the electromagentic field because an axially symmetrical electric field $E_\varphi = -\frac{1}{c}\frac{\partial A_\varphi}{\partial t}$, the move- /66

ment in which is reversible, is needed for a regular, radial drift.

Nonreversible particle shifts take place under the effects of asymmetrical disturbances in the electric field with characteristic times $\tau \lesssim \tau_\varphi$. The average shift equals zero in the first approximation with respect to the amplitude of the disturbance, and the transfer is of the diffusion form. However, the average shift, squared with respect to the amplitude of the disturbance, does not equal zero.

The investigation of the concrete mechanism involved in the transfer is one of the basic tasks of the theory of radiation belts. It is of interest to investigate the change in the angular distribution and in the energy of the particles with change in the parameter L, and retention of the first two invariants. These results will be valid for any transfer mechanism if the time and space scales for the disturbances are sufficiently large.

Let us review this task in the relativistic case, taking it that at the beginning and at the end of the disturbance the field is a dipole field, and that the parameter for the magnetic shell will change from L to L' [82]. Expressing the adiabatic invariants $P/\sqrt{H}$ and $\int_{-l_0}^{+l_0} P_{\parallel}\, dl$ in terms of $P = \varepsilon\beta$ ($\beta = v/c$), and the field at the mirror point as H_m, we have

$$\frac{\varepsilon\beta}{\sqrt{H_m}} = \frac{\varepsilon'\beta'}{\sqrt{H'_m}}, \tag{4.7}$$

$$\varepsilon\beta \int_0^{l_0} \sqrt{1 - \frac{H(l)}{H_m}}\, dl = \varepsilon'\beta' \int_0^{l'_0} \sqrt{1 - \frac{H(l')}{H'_m}}\, dl', \tag{4.8}$$

where the integrals with respect to dl and dl' are taken along the field lines with parameters L and L', respectively. Expressing H and dl in terms of the magnetic latitude, λ at the reflections points by λ_0 and λ'_0, we obtain /67

$$\varepsilon\beta = \varepsilon'\beta' \left(\frac{L'}{L}\right)^{3/2} \frac{\cos^3\lambda'_0}{\cos^3\lambda_0} \sqrt{\frac{1+3\sin^2\lambda_0}{1+3\sin^2\lambda'_0}}, \tag{4.9}$$

$$\varepsilon\beta = \varepsilon'\beta' \left(\frac{L'}{L}\right)^{3/2} \frac{\Psi(\lambda'_0)}{\Psi(\lambda_0)}, \tag{4.10}$$

and

$$\Psi(x) = \int_0^x \sqrt{1 - \frac{\cos^6 x\,(1+3\sin^2\varphi)^{1/2}}{\cos^6\varphi\,(1+3\sin^2 x)^{1/2}}} \times \sqrt{1+3\sin^2\varphi}\cos\varphi\, d\varphi \approx 1.78x^2 - 0.79x^3. \tag{4.11}$$

The latter relationship is the analytical approximation of the results of the numerical tabulation of $\Psi(x)$, and is correct with an error of <1% in the segment $0 \leqslant x \leqslant \pi/2$. We find, through the equations at (4.9)-(4.11), that λ_0' can be determined through the equation

$$f(x) = \frac{\cos^3 x}{x^2 (1 - 0{,}44x) \sqrt[4]{1 + 3\sin^2 x}}. \tag{4.12}$$

and that

$$f(\lambda_0') = \sqrt{\frac{L}{L'}}\, f(\lambda_0). \tag{4.13}$$

The equation at (4.12) is easily solved with the help of the table of values for f(x) (Table 2). P' can then be established through (4.10). When $\lambda_0 = 0$, we always have $\lambda_0' = 0$, and $P' = P(1/1')^{3/2}$ (since $P_\parallel = 0$, change in $P = P$ can be determined by retaining the magnetic moment). When $\lambda_0 \to \pi/2$, on the other hand, $P_\perp = 0$, and $P' = PL/L'$ (the invariant for the longitudinal effect reduces to LP). It appears that when $\lambda_0 \leqslant 30°$ and when there is a change in L by a factor of 3 to 4, $P' \approx P(L/L')^{3/2}$ with an error of no more than 3%. Consequently, the total pulse of particles with reflection points near the plane of the equator changes with $P_\perp$. The latitude of the reflection points is $\lambda_0' \approx (L'/L)^{1/4}\lambda_0$. Analogous computations in the nonrelativistic case were cited in [13].

TABLE 2. /68

x	$f(x)$	x	$f(x)$	x	$f(x)$
0,38	6,13	0,70	1,08	1,00	0,21
0,40	5,41	0,72	0,98	1,02	0,19
0,42	4,80	0,74	0,88	1,04	0,17
0,44	4,27	0,76	0,80	1,06	0,15
0,46	3,80	0,78	0,72	1,08	0,13
0,48	3,40	0,80	0,65	1,10	0,11
0,50	3,05	0,82	0,58	1,12	0,10
0,52	2,74	0,84	0,52	1,14	0,08
0,54	2,46	0,86	0,47	1,16	0,07
0,56	2,21	0,88	0,42	1,18	0,06
0,58	1,99	0,90	0,38	1,20	0,05
0,60	1,80	0,92	0,34	1,22	0,04
0,62	1,63	0,94	0,30	1,24	0,04
0,64	1,47	0,96	0,27	1,26	0,03
0,66	1,32	0,98	0,24	1,28	0,02
0,68	1,20			1,30	0,02

Commas represent decimal points.

The majority of the particles in the radiation belts have reflection points in latitudes $\lambda \leqslant 30°$ (and, as a result, angles $\alpha_0 \geqslant \arcsin \eta^{-1/2}(\pi/3) = 36°$). The content of particles with specified energy in a field duct with a section of 1 cm^2, and when $\eta = 1$, can be established by the equatorial distribution $f_0(\varepsilon, \alpha_0, L)$. Since each particle intersects the equatorial plane twice in time τ_θ, the content can be established as

$$N \approx \pi \int_0^{\pi/2} f_0(\varepsilon, \alpha_0, L)\, v_\parallel \tau_0(\alpha_0, v) \sin \alpha_0 \, d\alpha_0 =$$

$$= \pi v \tau_0(\pi/2, v) \int_0^{\pi} f_0(\varepsilon, \alpha_0, L) \sin \alpha_0 \cos \alpha_0 f_0(\alpha_0) \, d\alpha_0, \qquad (4.14)$$

where $f_\theta(\alpha_0)$ is a function establishing τ_θ in terms of α_0. As has already been pointed out, $f_\theta(\alpha_0) \approx 1$. The content of particles $N_{(\gamma)}$ with $\alpha_0 \geqslant \gamma$ can be determined by the same integral in the limits from γ to $\pi/2$. When the distribution is isotropic

$$\frac{N(\gamma)}{N} \approx \frac{\int_\gamma^{\pi/2} f_0(\alpha_0) \sin \alpha_0 \cos \alpha_0 \, d\alpha_0}{\int_\gamma^{\pi/2} \sin \alpha_0 \cos \alpha_0 \, d\alpha_0} = 1 - \sin \gamma, \qquad /69$$

and if $\gamma = 36°$, $N(\gamma)/N \approx 60\%$, whereas if $f_0(\alpha_0) \sim \sin^2 \alpha_0$, then $N(\gamma)/N \approx 90\%$.

These particles make an even greater contribution to the density near the equatorial plane, on a percentage basis

$$n_e \sim \int_0^{\pi/2} f_0(\alpha_0) \sin \alpha_0 \, d\alpha_0$$

or in average form, for all directions of intensity nv; when $f_0 = 1$ (isotropic distribution) $n(\gamma)/n \approx 80\%$.

Therefore, one can, when studying the dynamics of the main mass of particles, introduce the function of the distribution $\Theta = \Theta(J, L, t)$ suth that the magnitude

$$dv = \Theta(J, L, t)\, dJ\, dL \qquad (4.15)$$

will provide the number of particles between shells L, L + dL in the interval of values for $J = PL^{3/2}$ from J to J +dJ and exclude the angular distribution [6]. The intensity of the particles with $P > P_0$ near the plane of the equator can be expressed in terms of Θ by the following

relationships

$$I_0(>P_0)=\frac{\hat{\alpha}}{2\pi W_0 L^2}\int\limits_{P_0L^{3/2}}^{\infty}\Theta(J,\ L,\ t)\,v(J,\ L)\,dJ, \tag{4.16}$$

where W_0 is the volume of the layer between the two shells with $L \approx 1$, a distance of 1 cm apart in the plane of the equator;

$v(J,L)$ is the velocity of the particle, expressed in terms of J and L;

$\hat{\alpha}$ is the functional of the angular distribution, very slightly dependent on the degree of anisotropy.

The dependence of $\hat{\alpha}$ on v for an approximation of the angular distribution by the law of $\sin^{v}\alpha_0$ is reviewed in [11]. When v = 0 (isotrophy), 2, 4, 6, 8, 10, $\hat{\alpha}$ is 1, 1.33, 1.60, 1.83, 2.04, and 2.2, respectively. If $\hat{\alpha}$ = constant $\approx$ 1.5, the error that is possible in the angular anisotropy observed in the radiation belts will be much lower than the indeterminacy in the absolute values of measured flows because of the experimental errors. /70

The introduction of the function Θ very greatly simplifies the investigation of the transfer processes while providing an accuracy that is quite adequate for comparison with the experiment.

5. The Boundary of the Trapped Radiation Region.

There is no expectation that a firm quantitative theory dealing with the physical phenomena associated with the formation of the tail of the magnetosphere can be postulated in the near future because the interaction of the geomagnetic field with the solar plasma is substantially nonlinear in this region. Because the problem is very asymmetrical, and because of the need for systematic computation of the collisionless dissipation that establishes the nature of the interaction between the plasma and the field, there are still unsurmountable difficulties in the path of quantitative investigation. There is reason to believe that study of plasma turbulence will, in the end, result in some simplified system of equations of the Navier-Stokes type, and of a thermal conductivity which, while approximate, will describe plasma dynamics with collisionless dissipation taken into consideration with adequate strictness.* Apparently, this is the only

* This has already been done successfully in certain special cases. See [22,23,83], for example.

basis on which a complete theory for the interaction between the solar wind the geomagnetic field can be developed successfully. The only approach that is possible today is a semi-empiracal one, based on a qualitative analysis of the experimental data.

Looking at the problem from the standpoint of the radiation belt theory, what is of great interest is the additional problem that concerns itself with the boundary of the trapped radiation region. References [84, 85] pointed out that at altitudes of $\sim$ 1,000 km the radiation belts have sharp latitudinal boundaries. The streams of electrons with energies $>$ 40 keV change by several orders of magnitude at distances of $\lesssim$ 100 km when these boundaries are intersected. Higher latitudes are located in the region on the day side of the boundary rather than on the night side. The day boundaries are located at $\pm 75^\circ$ to $\pm 77^\circ$, and the night boundaries are located at $\pm 67^\circ$ to $\pm 68^\circ$ during magnetically quiet periods. The boundaries will shift toward the equator (to $\pm 60^\circ$ on the night side) with increase in the disturbance. Measurements made near the plane of the equator [86] reveal that during quiet periods the belts of electrons with energies $\sim$ 40 keV coincide with the boundary of the magnetosphere on the day side of the boundary ($\sim$ 10a from the center of the earth at any point). The boundary is much closer ($\sim$ 7.5a) on the night side. The investigations made with the satellites in the Elektron series [87] in the morning and night regions of the magnetosphere traced the boundary over a wide range of latitudes and concluded that the boundary of the radiation belts coincides with the field lines and is projected along them from the plane of the equator to the ionosphere. These investigations also confirmed the shift of the trapped radiation boundary toward the earth during geomagnetic disturbances [88].

Accordingly the boundary of the region in which the fast particles are retained effectively is probably identical with the inner boundary of the tail of the magnetosphere.

Reference [6] and [8] demonstrated that the boundary of the geomagnetic trap does not coincide with the boundary of the magnetosphere, and that it should lie closer to the earth on the night side than on the day side. This conclusion follows directly from an analysis of drift orbits in the equatorial plane. These orbits were identified in [6] and in [8]

with the lines of equal geomagnetic field intensity. Similar considerations were developed in [98].

Obviously, the equatorial section of the boundary of the magnetosphere is not the lines for H = constant, because on the boundary $H^2/8_\pi$ is equal to the pressure of the solar wind, which is a maximum at the frontal point and decreases in the direction toward the east and west sides. Consequently, the line $H = H_s$ (H_s is the field at the frontal point) divides the equatorial /72 section into two regions. In one of these $H > H_s$, and the drift orbits will close within the magnetosphere. In the other region $H < H_s$, and the lines H = constant will enter the thin boundary layer between the geomagnetic field and the solar wind. This is a very turbulent layer because effective diffusion of the particles from interplanetary space into the magnetosphere, and vice versa, is possible. If there are no electrons with energies > 40 keV outside the magnetosphere (and this is usually what is observed during an experiment), they should also disappear from the $H < H_s$ region in time $\sim \tau_\varphi$. The field of external currents in the plane of the equator is parallel to the field of the earth dipole, but at equal distances from the earth is less intense on the night side than on the day side. Therefore, the line $H = H_s$ approaches the earth on the night side.

References [6] and [8] named the $H = H_s$ boundary the magnetosphere separatrix. The behavior patterns mentioned above are correct for particles with reflection points in latitudes $\lambda_m \leqslant 30°$, as well as for particles with zero longitudinal velocity drifting along the separatrix.

The magnetosphere is compressed during geomagnetic disturbances and the separatrix approaches the earth. Some of the particles that are initially outward of the separatrix can turn out to be on the closed drift orbits within the limits of the magnetosphere as the fluid returns to normal. A detailed analysis of the capture mechanism for the case of a flat magnetosphere boundary was made in [8] during a discussion of possible sources of radiation belt particles.

There are many difficulties encountered by the conception of a radiation belt boundary [6, 8], despite the fact that there is no question but what the above-reviewed phenomena should occur, at least from a qualitative point of view, and despite the partial confirmation provided by the

experimental data. The experiment demonstrates that the boundary of the radiation belts on the night side is virtually the same field line, regardless of the position of the particle reflection points (the results contained in [84] and [86] were published at a time when references [6] /73 and [8] were completed). Yet as will be seen quite readily from Figure 3,* the length of the field line passing through the noon point of the separatrix is considerably longer than that at the midnight meridian (the field line touching the boundary of the magnetosphere should be compared with the field line passing through the 70th parallel on the night side). Since the drift of particles from the reflection points near the earth is determined by the conservation of the longitudinal action, which in this case is proportional to the length of the field line, it would seem that these particles ought to drift over the lines that are more distant from the earth on the night side. Yet this has not been observed.

A second difficulty is linked with the morphology of the auroras. Obviously, what must follow from the considerations developed in the foregoing is a conclusion with respect to the excitation of the auroras over the entire region of the northern and southern polar caps (areas delimited by the projections of the separatrix along the field lines on the earth). Yet in point of fact only the boundary of the caps is lighted, and the width of the lighted belt sometimes is $\lesssim$1 km.

The discovery of the neutral layer [25] automatically eliminates these difficulties. The interpretation of the auroras using a model of the magnetosphere [25] was given above (#2,p.30). Naturally, the seeming independence of the boundary of the trapped radiation on the latitude of the particle mirror points can be explained in the same way. The deformation of the field lines in the tail reduces to the fact that when computing the longitudinal effect it is necessary to take into consideration the sections close to the great lengthening of the field lines in the plane of the midnight meridian, and particles with these second invariant values cannot drift on the day side, but must exit into the boundary layer. /74 The half-difference in the lengths of the field lines delimiting the region of trapped radiation is 8 to 15a (estimates derived from the most

* The results in [6] and [8] were based on a closed model of the magnetosphere (the unknown neutral layer was not considered at the time), so Figure 3 most closely corresponds to the field picture used in [6] and [8].

varied of models fall within these limits). If we take it that the width of the tail is $\sim 40a$, and that the magnetic field perpendicular to the "neutral" layer can be on the order of 10^{-5} gauss (see page 30), we obtain a magnetic flux between the boundaries of the trapped radiation regions with reflection points near the equator, and in the high latitudes, of $\Phi \lesssim 10^{15}$ maxwells. Let us now estimate the distance between these boundaries at the earth's surface. Taking it that the field is $H \approx 1$ gauss, and that the radius of the projection of the separatrix on the earth is $r = a\cos\lambda_m^{(s)}$, where the magnetic latitude of the boundary is $\lambda_m \approx 70°$, we obtain

$$\Phi \approx 2\pi a \cos\lambda_m^{(s)} \cdot \Delta z \cdot H,$$

from whence $\Delta z \lesssim 10^6$ cm, so both boundaries practically coincide. Similar results were obtained in [50] during an analysis of concrete models of the neutral layer.

What follows from these considerations is that near the neutral layer, and for a distance out to $\sim$ 15 to 22a, there should be a narrow zone in which the intensity of electrons with energies ~ 40 keV is increased, and this is what was observed in the experiments performed by the satellite Explorer 14 [91] (fig. 11).

The conception advanced in [6] and [8] with respect to the particle trapping mechanism in closed orbits within the magnetosphere during movement of the trap boundary in times of magnetic disturbances remains valid for the model in [25] as well. The effect of the extension of the field lines on the night side, and of the sharp attenuation of the field near the equatorial plane introduces a new element into the trapping mechanism, that of the possibility of strong betatron acceleration of the particles during the partial restoration of the field that takes place upon termination of the disturbance. As was pointed out in #2, even at comparatively short distances from the earth ($\sim$ 10 to 20a), the field in the "neutral" layer decreases to $\sim 0.3\gamma$ and is weaker here by a factor of 100 than at the boundary of the radiation belts. Since there are protons and electrons with energies of $\sim$ 10 keV and 1 keV, respectively, in the solar wind behind the shock front, the betatron acceleration could, in principle, cause trapping of protons with energies of tens of MeV and of relativistic /75

electrons. The basic limitation on the possibilities of these processes taking place is linked with the drift of the particles across the "neutral" layer and on into interplanetary space.

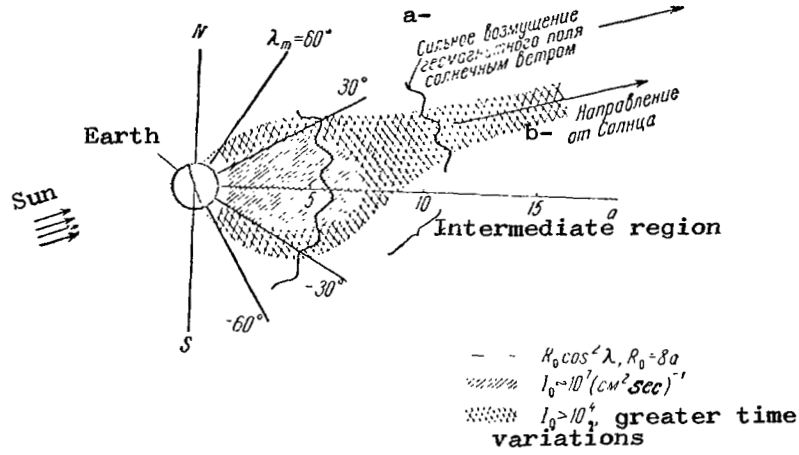

Figure 11. Regions of increased intensity of electrons with energies of 40 keV on the night side of the magnetosphere (section through the plane of the midnight meridian).

a- Strong disturbance of the geomagnetic field by the solar wind.
b- Direction from the Sun.

Let Z(z) be the scale of the heterogeneity of the normal component of the field, h, in the "neutral" layer. The rate of drift in direction y (toward the boundary of the magnetosphere) in the nonrelativisty case is $\sim \frac{v_\perp^2}{2\omega_H} \cdot \frac{1}{Z}$. The magnitude $\frac{v_\perp^2}{\omega_H}$ is the adiabatic invariant, so the drift rate therefore changes as the inverse scale of the heterogeneity of field h. The magnitude Z is large in the "neutral" layer ($\sim 10^2$a, apparently). /76 The least value of Z occurs near the boundary of the trapped radiation region, so trapping is determined by the particle drift during the time the field lines are "pulled in" from the tail in the radiation belt area. If Z_{min} is the minimum Z value, τ is the "pull in" time, and $Y \approx 40a$ is the width of the tail on the night side, the trapping condition is in the

form (τ is shorter than the drift time at distance Y)

$$\frac{v_{\perp}^2}{2\omega_H}\tau \leq YZ_{\min}. \qquad (5.1)$$

And from this we see just how great the significance of a thin structure of the region of the internal boundary of the tail of the magnetosphere, and of the time scales of its variations, is for the dynamics of the radiation belts. As has already been pointed out in #2, experimental data on this question are still extremely scarce.

Several interesting papers on the dynamics of the region of the magnetosphere under review appeared in 1966 [151-155], and should be considered, if briefly. Reference [151] noted that a great anisotropy in the angular distribution of the velocities of electrons with energies > 40 keV can be observed in the projection near the equator (see fig. 11) adjacent to the trapped radiation region on the night side. Here, as distinguished from the radiation belts, there is clear predominance of particles whose longitudinal component of the velocity with respect to the field is larger than the transverse component. This result is confirmed in [152], which further demonstrates that the field lines in the projection close through the equatorial plane. In the region in which the field component parallel to the equator changes sign, the absolute magnitude of the intensity does not become zero, but instead has a value of $\sim 1\gamma$, indicating the presence of an observable component normal to the plane of the equator, H. As has already been pointed out, trapped particles with reflection points in the high geomagnetic latitudes drift through the projection. Near the equatorial plane the direction of the velocities of these particles is close to the field lines, explaining the anisotropy detected in the velocity distribution.

The rapid variations in electron fluxes during the great magnetic storm of 17 April 1965, are described in [153,154]. As these papers point out, soon after the sudden onset of the storm, when L>5, the intensity of the electrons in the outer zone dropped sharply, and then, within a period of $\leq$ 1 hour, formed a new belt. The fluxes of electrons with energies above 300 keV rose to a magnitude exceeding the corresponding

value before the storm by one order of magnitude. Relativistic electrons with energies greater than 5 MeV appeared. There is a note in [154] that /77 the time required to form the new belt coincided with magnetic storms in the aurora zone. These phenomena can be understood qualitatively when based on the above-explained considerations concerning the betatron effects during the stretching out of the field lines from the trapped radiation region in the tail and their subsequent retraction. Judging from the results in [153,154], the inner boundary of the projection shifted to $L \approx 5$ at the onset of the storm, and this is entirely possible during a severe disturbance. Of great interest here is the movement of the boundary of the trapped radiation region to low altitudes during this particular storm.

Let us, finally, stop to consider [155], which provides us with a statistical analysis of the time shifts between the intensification of fluxes of electrons with energies > 100 keV near the boundary of the trapped radiation region on the night and day sides. It seems that on the day side this intensification is delayed by one hour as compared with the analogous effect on the night side. The delay time is close to half-period of the drift of the electrons with energies of 100 keV along the separatrix. The results in [155] also reveal that the injection of particles into the trapped radiation region occurs on the night side.

Reference [86] draws the equal intensity lines for electrons with energies >40 keV near the boundary of the trapped radiation region. Judging from these data, the width of the boundary near the equator is ~ 1 to $3 \cdot 10^3$km. Let us assume $\sim 3 \cdot 10^3$km is a typical value of Z_{min}. Values for τ can be very different. Field restoration time after the storm is $\sim 10^5$ seconds. On the other hand, great changes can take place in the currents flowing in the elctrojets (see #2) in just a few minutes as the polar storms develop. Since the polar electrojets are located along the projection of the boundary of the zone of trapped radiation on the earth's surface, and are the result of a sharp increase in the degree of ionization in the E-layer of the ionosphere because of the dropping of electrons with energies $\gtrsim 40$ keV,* it is natural to assume

* Electrons with lower energies are absorbed in the higher layers of the atmosphere.

that the DP-disturbance is associated with the acceleration of the electrons in the tail as the field lines in the trapped radiation region are retracted. Therefore, $\tau \sim 10^2$ seconds can be taken as the low limit of τ. Finally, the intensity of the H_s field in the trapped radiation region near the boundary is $\approx 50\gamma$. From whence, as well as from the equation at (5.1), it follows /78 that the maximum energies of particles trapped by this mechanism are

$$\frac{mv_{\perp}^2}{2} \leqslant \frac{e}{c} H_s \frac{YZ_{\min}}{\tau} \approx 1 \ MeV. \qquad (5.2)$$

(In the case of electrons, the drift rate for these energies is determined by the relativistic ratio and is larger than that in (5.1) by a factor of approximately 2, but this has no effect on the order of magnitude of the estimate at (5.2).) The limit energy is reduced to 100 to 10 keV in the case of smoother restoration ($\tau \sim 10^4$ to 10^5 seconds).

It seems that comparatively smooth and uneven periods alternate when the field varies, so that very jagged distribution of the intensity of electrons with energies $\sim$ 100 keV [89] in terms of L is often observed near the boundary of the trapped radiation region. Reference [89] further notes that there is a link between the appearance of teeth in the distribution of the fluxes of fast electrons and the development of polar storms.

Reference [90] reports that near the boundary of the radiation belts one can observe a sharp change in the electron spectrum (in the approximation of the exponential spectrum e^{-E/E_0}, the average energy changes from 20 keV for the inner to $\sim$ 3 keV for the outer region). The investigations were made at comparatively low altitudes (< 3000 km). The width of the region in which the spectrum changes is $\approx 1°$, according to the data in [90]. Fluxes of low-energy ($\sim$ 10 keV) electrons at the boundary were 10^{10} cm^{-2} sec^{-1} in individual cases. These electrons apparently escape into the magnetosphere from the turbulent region between the shock wave and the boundary of the geomagnetic field along the separatrix, and cause the field deformation in the tail. Some of these electrons are trapped in closed drift orbits with distance from the separatrix, and are accelerated to energies above 40 keV. And judging from the change that takes place in the average energy, the length of the field line is reduced by a factor of 2.7 (if the acceleration observed at low altitudes is associated with the conservation of the longitudinal effect). It is also possible that /79

the field is intensified by a factor of approximately 7 during partial retraction of the tail. In such case the particles observed at low altitudes should appear as a result of intensive scattering in the region near the equator.

The above-explained considerations enable us to link together much of the experimental data on the physical phenomena on the boundary of the trapped radiation region and reduce to reasonable values the basic numerical characteristics. In what follows it will be shown that many of the more subtle effects observed in orbit also agree with the particular point of view.

Let us point out that there are other views with regard to the particle trapping mechanism. Certain of the papers already mentioned [42-44] conjecture that analogous processes take place on the day side, rather than on the night side. Field attenuation is attributed to hypothetical current rings made up of particles breaking through the branching point, rather than near the plane of the equator. The protons that do break through are deflected eastward, and the electrons to the westward, because of the drift, and the result is the establishment of ring currents. However, the data obtained from the experiments conducted in space contradict the conceptions in [42-44]. The authors of these papers proceeded from the assumption that even during magnetically quiet periods protons with energies of from 60 to 100 eV, and an intensity of $\sim 5 \cdot 10^{10} cm^{-2} \cdot sec^{-1}$, would be found at the boundary of the magnetosphere. It will be readily apparent that these parameters correspond to a density of $\sim (3\text{-}4) \cdot 10^{3} cm^{-3}$ and a pressure of $\sim 5 \cdot 10^{-7} erg/cm^{3}$. A field of $\sim 300\gamma$ is needed to balance this pressure, whereas the field at the boundary of the magnetosphere is apparently between 60 and 70 γ during a magnetically quiet period. The boundary would therefore be at 6 earth radii from the center of the earth, and not at 11, when the pressure is $5 \cdot 10^{-7} erg/cm^{3}$.

A second contradiction between the conceptions advanced in [42-44] and the experiment is the absence of powerful proton fluxes in the region of the magnetosphere indicated by the authors. According to the data in [92], the intensities of protons with energies of from 0.1 to 10 keV

in the eastern high-latitude region did not exceed the instrument sensitivity threshold ($\sim 5 \cdot 10^7 cm^{-2} sec^{-1}$). Therefore, the totality of the hypothesis advanced in [42,44] is controversial. /80

The question of low-energy ($\sim$ 1 keV) particles is closely associated with the problem of the boundary of the trapped radiation region. The increased intensities of these electrons was first detected at long distance from the earth in the experiments conducted with the second Soviet space rocket [93]. Shortly after the geophysical rockets were launched into the ionosphere it was established that electrons with these energies are the cause of the excitation of the auroras [94,95]. Numerous investigations, conducted later on, at high, as well as low, altitudes (see [92] and the survey [96]), demonstrated that particles with average energies of $\sim$ 1 keV form the so-called outermost radiation belt and encompass the earth. The maximum for this belt lies near the boundary of the trapped radiation zone on the night side, and probably closes outside the magnetosphere (see Fig. 1) on the day side.

It is probable that the low-energy particles originate in the solar wind on the shock front and then penetrate the magnetosphere along the separatrix. Electrons with energies of $\sim$ 1 keV are observed as well in the trapped radiation region right up to $L \sim 5$ on the night side [97]. It is possible that the mechanism by which they penetrate this region is associated with the drift in the electrostatic fields excited by the ionospheric winds [57].

Thus, the experimental data indicate that during magnetic disturbances the outer part of the trapped radiation region is filled with particles with energies ranging from a few tens of keV up. It is probable that the trapping mechanics involves the stretching out of the field lines on the night side, the injection of particles from the solar wind into a greatly weakened field, and the betatron acceleration of these particles during the retracting of the field lines into the trapped radiation zone when the disturbance is over. And very different spectra of particles, with energies right up to $\sim$ 1 Mev, can be formed, depending on the field /81 restoration time dependence. Electrons and protons with energies of $\sim$ 1 keV and 10 keV, respectively, penetrate into the trap along the separatrix, even when there is no disturbance, because these particles are always

present in the region between the shock wave and the magnetosphere boundary. The trapping mechanisms described are probably the principal sources of radiation belt particles.

6. High-Energy Protons and the Earth's Magnetosphere

Sections #6 and #7 will present contemporary concepts of the earth's radiation belts (that is, of fluxes of charged particles with energies $\gtrsim$ 50 keV in the trapped radiation region). It must be remembered that information obtained since 1957, has been extremely uneven in distribution during the period.

The period 1957-1961, saw the establishement of the fundamental, qualitative features of belts, and of estimates of the orders of magnitude of fluxes of particles with different energies in different regions. These results are what made it possible, later on, to carry out more precise measurements (1962-1965), and these measurements, in turn, provided the materials needed to explain the nature of the belts. Although the levels of solar activity in the period 1957-1960 (unique maximum), and in the period 1961-1965 (decay and minimum of activity), were very much different, it seems that the properties of the radiation belts remained quite stable, on the average. But great care must be exercised when extrapolating the 1961-1965 data as applicable to an earlier period. Let us reiterate, therefore, that this survey is based on data obtained since 1961, so that strictly speaking, the picture, as reviewed, is that of a period of reduced activity.

Protons with energies of several tens of MeV were first detected as far back as the first launches of the artificial earth satellites [72, 78]. The satellite Explorer 12 discovered a powerful belt of relatively low-energy protons (from 100 keV to ~ 2 MeV) [99], the existence of which was then confirmed in the course of later experiments by Explorer 14 [86,100]. Some of the papers on the subject [5-10] advanced the suggestion that these protons resulted in the transfer from the boundary of the magnetosphere. Others [11,12] used these considerations to compute the equatorial distribution of protons with energies of from 100 keV to 40 MeV. The spectrum for L = 5 [99] was taken as the boundary condition. The results of subsequent measurements coincided with the theoretical curves,

/82

at least within the limits of accuracy for the experiment [11,12].

The most detailed investigations of protons with energies above 200 keV were made by the satellites in the Elektron series [87,101,102], and by Relay 1 (USA) [103,104]. The results [87,101,102] agree well with theory [11,12]. One paper [103] showed some divergence (maxima for protons with energies of from 1 to 5 MeV appeared at 0.5a closer to the earth), but a more detailed processing and analysis of these data [104] proved that the data in [103] were inaccurate. The final results of the measurements made by Relay 1 agree well with the other experiments, and with the theory.

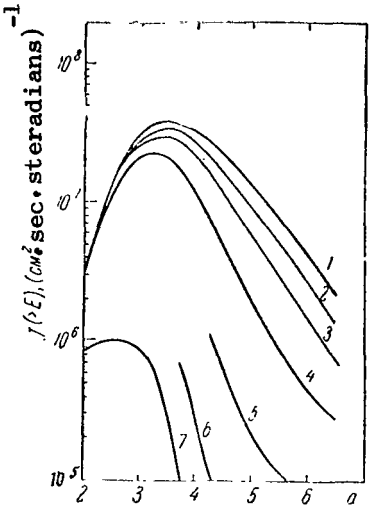

1 - E ≥ 98 keV; 2 - E ≥ 134 keV;
3 - E ≥ 168 keV; 4 - E ≥ 268 keV;
5 - E ≥ 49 keV; 6 - E ≥ 988 keV;
7 - E ≥ 1.69 MeV

Figure 12. Distribution of fluxes of protons with energies of from 100 keV to 1.7 MeV in the plane of the equator.

Figure 12 depicts the data on the distribution of protons with energies from 100 keV to 1.7 MeV in the plane of the equator. These data were obtained in 1961, but were not widely published until recently [99]. Figure 12 is taken from [15]. Figure 13 shows the distribu- /83 tion of protons with energies of from 1 MeV to 30 MeV obtained by the Elektron satellites (here too the data refer to the equatorial plane). As already mentioned, the results [104] agree well with this distribution. Finally, Figure 14 depicts the equatorial distribution of the highest energy protons obtained by the Elektron and Explorer 15 [105] satellites.

As will be seen from the figures, there is a definite behavior pattern in the movement of the intensity curves for protons of different energies, right up to energies of ~ 30 MeV. The steepness of the outer edge of the belt increases with increase in energy, and the maximum approaches the earth. The spectrum becomes more and more precise with reduction in L.

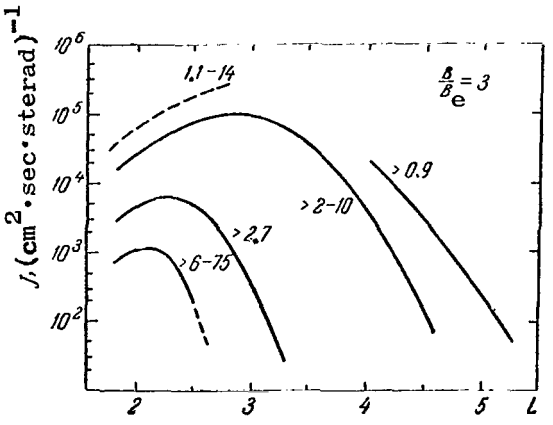

Figure 13. Distribution of protons with energies of from 1 MeV to 30 MeV near the equatorial plane (on the surface, where the field intensity is in excess of the equatorial value by a factor of 3.)

According to [99], the differential spectrum for protons close to the plane of the equator is in the form

$$\frac{\partial I_0}{\partial \varepsilon} = S_0 e^{-E/E_0}, \qquad (6.1)$$

where the average energy, E, depends on L and when L = 5 and 6 is equal to 120 and 69 keV, /84 respectively. The betatron ratio $\varepsilon_0(5)/\varepsilon_0(6) = H_0(5)/H_0(6)$ is well satisfied at these two points. Reference [13] computed the change in the energies of particles upon transition between drift shells when the first two adiabatic invariants (see #4) were retained, and the results obtained were used to analyze all of the data from the experiments in [99]. The investigation showed that for energies higher than some critical value $E_m(L)$, the magnitude E_0 changes in accordance with the theoretical results for all values of the equatorial angle between the velocity and the field lines. Consequently, if the adiabatic invariants are selected as the independent variables, the particle spectrum will be unchanged. This conclusion yields one of the most persuasive confirmations of the transfer conception.

A comparison of the data on the spectrum when L = 5 [99], and when L = 1.5 [106], will show that the law $E^0 \sim L^{-3}$ can be satisfied right up to L = 1.5, where $E_0 \approx 4$ MeV.

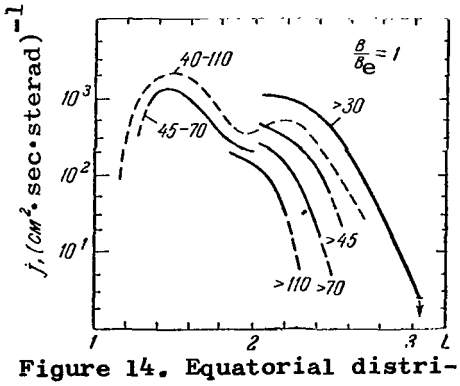

Figure 14. Equatorial distribution of protons with energies above 30 MeV.

The sharp difference in the structure of the proton belt in the energy intervals from 0.1 to 30 MeV, approximately, and when > 30 to 40 MeV will be seen distinctly in Figures 13 and 14. /85 The most significant difference is in the L ≈ 2.2 area, where the intensity of the protons with the highest energies

($E > 40$ MeV) form a second maximum [105]. The altitude movement of protons with an intensity of $E \lesssim 30$ MeV along the field lines can be established by the features of their spectrum reviewed in the foregoing. As [13] has pointed out, the distribution of particles with respect to the values of the first two invariants in the outer part of the proton zone is identical for all L and magnetic latitudes. What follows from the computations made in [13] and in [82], is that upon transfer of particles to an L-shell closer to the earth, while retaining the first two invariants, the energy will increase more slowly the higher the magnetic latitude of the mirror point (see #4). Hence, average particle energy decreases, and intensity falls, with increase in the magnetic latitude. This effect is more sharply defined the smaller the L.

Behavior patterns of this type were tracked over a wide range of L and magnetic latitude values by the Elektron satellites [87, 102]. If the altitude movement is represented, approximately, in the form $N \sim (H/H_0)^{-m}$ (H_0 is the field at the apex, and H is an arbitrary point on the particular field line), the magnitude m will increase from ≈ 0.8 when $L = 3$ to 4, to 2 when $L \approx 2$, at low geomagnetic latitudes. The exponent m does not remain constant along the field line, and at latitudes of $\sim 45°$ will increase to ~ 4 when $L \sim 3$. Similar conclusions were obtained from the data measured by Explorer 12 [52,99] and Cosmos 41 [107,108].

The altitude movement of the intensity of protons with energies of from 40 to 110 MeV in the region of the second maximum differs significantly from the above picture. In this case the rate of change in the intensity along the field line decreases with rise in the magnetic latitude (that is, the effective exponent m is reduced). The additional m maximum, clearly defined in the plane of the equator, virtually disappears at a magnetic latitude of $\sim 25°$ [105].

Time variations in the fluxes of protons near the plane of the equator are small, and even at $L \sim 5$, there is no more than a factor of 2 change in intensity [52, 135]. The high degree of stability of the equatorial distribution of protons is characteristic of all energies /86 from 100 keV to 100 MeV. A comparison between the 1961 data (Explorer 12

[52, 99, 15]), and the results obtained in 1962-1963 by Explorer 14 [100] and in 1964 (Elektron 1, Elektron 2, Cosmos 41 [107,35]), will find no significant differences, neither in position nor in shape, nor in absolute intensity magnitudes, despite the fact that the level of solar activity in 1961, was substantially greater than in 1962, and particularly in 1963-1964. Moreover, the distribution of the fluxes of protons with energies of from 1 to 20 MeV, computed theoretically in [11,12] from the 1961 data for L = 5 [99], coincide with the results of subsequent experiments with a high degree of accuracy.

The analysis made in [11, 12] lead to the conclusion that the second maximum for protons with energies > 40 MeV when L = 2.2 is probably unsteady, and is a diffusion wave that occurs in the year of the last maximum in solar activity as a result of the trapping of protons with average energies of $\sim$ 100 keV at the boundary of the radiation belts. A sharp increase in the flux of these protons at the boundary of the belts was observed during the severe magnetic storm at the end of September 1961 [108]. The investigation made by Cosmos 41 [107] reveals that analogous phenomena are observed even during weak storms (with intensities still $\sim 10^4$ $cm^{-2}sec^{-1}$ when $E_p > 400$ keV, which is lower than the flows recorded in the case discussed in [108] by almost two orders of magnitude).

The results in [107] and [108] confirm the hypothesis [11, 12] concerning the possibility of a sharp rise in the average flux of protons with energies $\sim$ 100 keV at the boundary of the belts in a year of maximum solar activity such as 1958-1959, when the number of severe storms was particularly high. There has been yet another, recent confirmation of this conception. Reference [109] reported that the movement of a second maximum toward the earth was detected. The magnitude of the shift ($\sim$ 0.1a in two years) cited in [109] is very close to the theoretical results in [11] and [12] concerning the velocity of diffusion waves.

Variations in fluxes of protons outside the equatorial plane when /87
$L \leqslant 5$ too are slight. Even at such comparatively low altitudes as 1,000 km, the fluxes of protons during magnetically quiet period, as well as during a severe magnetic disturbance ($K_p = 8$), differ by less than a

factor of 2, while the angular distribution remains practically unchanged [110]. An analogous conclusion when $L < 5$ is also correct at altitudes $\sim 10^4$ km from the earth's surface [107].

Significant variations of fluxes of protons with energies ~ 0.5 MeV are observed at $L > 5$, and these are associated with magnetic activity [107]. The intensity increased by three orders of magnitude during a storm when $L \sim 9$.

It is now generally recognized that the proton belt is the result of the transfer of particles across the drift shells. It is only in the energy range above 40 MeV that neutron decay begins to play a role. A more probable cause of the loss of protons with energies in > 0.5 MeV is ionization losses, and possibly that of overcharging in the region of lower energies. No data are available at this time to indicate proton scattering.* In fact, the results in [13] show that both proton adiabatic invariants are retained during transfer, so for all practical purposes there is no scattering.

Such are the principal characteristics of the distribution of fast protons in the magnetosphere.

7. High Energy Electrons

As distinguished from protons, the region of increased intensity of electrons with the same energies ($\gtrsim$ 100 keV) can be broken down into two distinct maxima, an outer, and an inner, belt. There is a gap between them, in which the intensity is lower than at the maxima located in the /88
region of the $L = 3$ to 3.2 shell, by from two to three orders of magnitude. The time variations at high altitudes are slight in the inner zone and in the gap. At the same time, great changes take place in the distribution of the electron intensity and spectrum in the outer zone, while the amplitudes of the variations reach three orders of magnitude for given L.

*Reference [111] reports a sharp decay in intensity of protons with E $\sim$ 35 MeV, and with small pitch angles when $L \gtrsim 2$ during the magnetic storm in September 1963. However, nothing similar has been observed, before or since, in any experiment, despite the fact that research on protons with these energies has been going on almost continuously since the end of 1957.

Electrons with energies of several tens of keV too probably form an outer and inner zone, but the gap is not nearly as deep as in the case of the higher energy particles, and the maxima are not as sharply expressed. Variations during which the intensity changes rapidly by one to two orders of magnitude are observed in the outer zone. The variations correlate with magnetic disturbance.

The dynamics of electron belts have specific features at low altitudes ($\lesssim$ 1000 km), and these are associated with the very definite dependence of the escape rate on the altitude, and with anomalies in the geomagnetic field. These questions will be reviewed at the end of the section.

Electron intensity in the inner zone and in the gap is stable at high altitudes, as has already been pointed out. This conclusion follows from the results of the measurements made of fluxes of electrons with energies from 0.2 to 1.6 MeV by Explorer 14, Explorer 15 [100, 105], Relay 1 [112], Elektron 1 and Elektron 2 [87]. However, it should be remembered that these data were obtained after Starfish, the high-altitude burst of July 1962, which changed the structure of the inner electron zone significantly. There are virtually no reliable data on electrons in this region prior to 1962 (see [113-114]).

All of these experiments established the fact that the minimum in the intensity of electrons with energies > 200 - 500 keV was located in the $L = 3 \pm 0.2$ region. Intensities measured in the same regions by different satellites coincided with one order of magnitude.

An analysis made in [20] (see #18) reveals that the experimental data on the distribution of electrons with energies $\gtrsim$ 500 keV agree with the theoretical curve for $I_0 \sim 10^9 - 10^{10} L^{-10}$ $(cm^2 \cdot cek)^{-1}$ when $1.5 \leqslant L \leqslant 3$, corresponding to the boundary of belt stability. The intensity along /89 the field lines changes as $(H/H_0)^2$ [20] when $1.6 \leqslant L \leqslant 2.5$.

Let us note, however, that although the relative changes in intensity with L are very close in all experiments indicated, the absolute magnitudes of the fluxes differ by a factor of from 2 to 5, according to the data provided by the different authors. It is not yet clear whether the cause of these divergencies is the slow changes in particle fluxes with time, or

equipment or orientation effects. The theoretical considerations of the nature of high-energy electrons will be reviewed in #13.

Huge variations, the nature of which is different for different portions of the spectrum, take place in the intensity in the region of the outer zone ($L \gtrsim 3.5$), even during relatively weak magnetic disturbances. There is reason to assert that the nonstationary state is the normal state for the outer zone, and that absence of variations, if only for a week, is a very rare event.

The experimental data show that in nature the variations can be broken down into three groups of electrons with energies above 40 keV: 40-100 keV, 200-600 keV, and from 600 keV to 1.6-2 MeV. The exact boundary between the first two groups is not known (but is known to lie between 100 and 200 keV). There are still no data on electrons with energies > 2 MeV in the outer zone.

The most characteristic feature of the dynamics of electrons with energies of from 40 to 50 keV in the outer zone is the clear correlation with magnetic activity. This effect was detected during the investigations made with Explorer 12 [115] and was confirmed in the experiments conducted with Explorer 15 [91] and [100]. Figure 15 [89] presents the data on fluxes of electrons with energies > 40 keV from October 1962 to March 1963, at the outer zone (L = 4.8) maximum, and the corresponding values of the daily sum of the K_p-indices. Sharp increases in the K_p-index (magnetic storms) are always accompanied by a burst of intensity of electrons with energies ~ 40 keV. Conversely, during long periods of low magnetic activity there is a monotonic decay in the fluxes of electrons. /90

These behavior patterns are seen with particular clarity in Figure 16 [100], which shows the distribution of the fluxes of electrons with energies >40 keV in terms of L in the plane of the equator in December 1962. As will be seen from Figure 15, in the first half of December the magnetic disturbance was moderate. A rather severe storm occurred on 17 December (in any case, the most severe one to occur while Explorer 14 was operable),

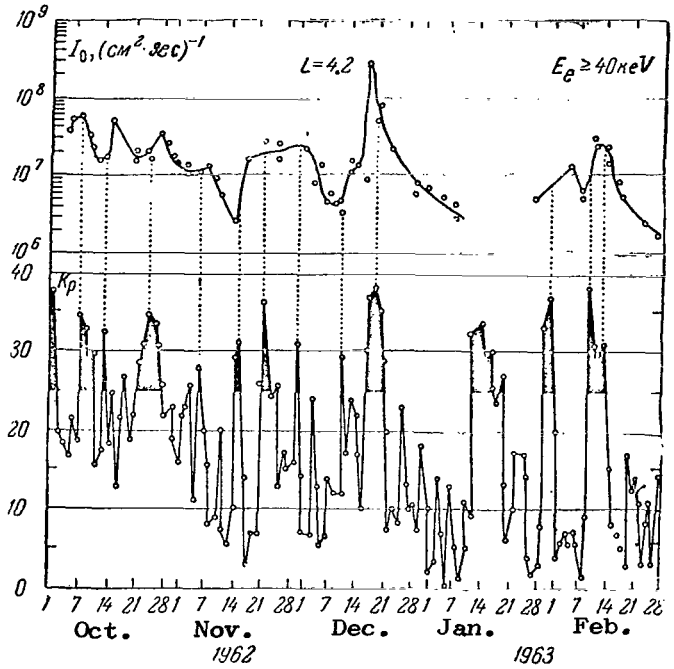

Figure 15. Comparison of fluxes of electrons with energies of 40 keV at the outer zone maximum with the level of magnetic activity between October 1962 and March 1963.

after which disturbance activity remained abnormally low until 10 January 1963. The first two curves (1 and 2) in Figure 16 (7 and 13 December 1962) are for the period prior to the storm, curve 3 (17 December) is during the storm, and the others (4 - 20 December, 5 - 24 December 1962, 6 - 8 January 1963) are for the period of low disturbance activity. We should point out that the intensity 4 x 10^8 cm^{-2}-sec^{-1} (curve 3) is the record for the time the satellite was operable (October 1962 - July 1963), while 10^6 10^6 cm^{-2}·sec^{-1} (curve 3) is the minimum for that same period. /91

Variations are particularly great in the outer zone ($L > 3.5$), as will be seen from Figure 16. There are practically no variations in the gap. The increase in intensity when $L > 3.2$ took place over a period of $\lesssim 1$ day. Analogous phenomena were observed during other magnetic storms, but amplitudes were lower.

Note that during the period of magnetic quiet (beginning of January 1963) there is a well-defined maximum for the fluxes of these electrons in the region near the equator close to the night boundary of the trapped

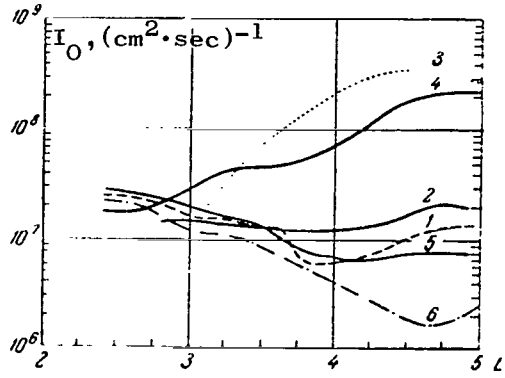

Figure 16. Equatorial distribution of electrons with energies > 40 keV in the outer zone (Dec 1962 - Jan 1963).

1 - 7 Dec; 2 - 13 Dec; 3 - 17 Dec; 4 - 20 Dec; 5 - 24 Dec; 6 - 8 Jan.

radiation region [91]. This confirms the considerations presented in #5 concerning betatron acceleration of electrons when the field lines are "retracted" from the tail into the trapped radiation region. /92

Geiger counters with the following recording thresholds were installed aboard Explorer 14, in addition to the counters with threshold energies of 40 keV for electrons and 500 keV for protons: 1) E_e > 230 keV, E_p > 4.5 MeV; 2) E_e > 230 keV, E_p > 500 keV; 3) E_e > 1.6 MeV, E_p > 20 MeV. Counters (1)

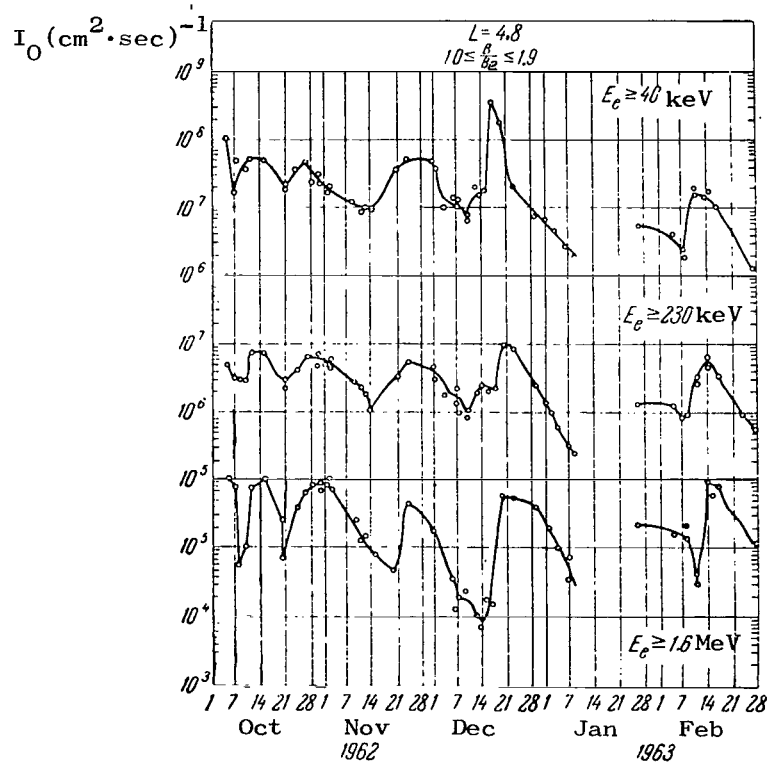

Figure 17. Variations in the intensity of electrons with energies > 40 keV, 200 keV, and 1.6 MeV at the outer belt maximum.

and (2) use different methods for cutting off electrons with energies /93
$\lesssim$ 200 keV; in the case of (1) by additional shielding of the counters so as to raise the threshold for protons, as well as for electrons; and in the case of (2) deflecting the electrons by a magnet, yet having no practical effect on protons with $E_p > 500$ keV penetrating the window. A comparison of the data in [100] with subsequent measurements of fluxes of protons with $E_p > 5$ MeV shows the counter (1) registered primarily electrons when $L \gtrsim 2.4$ (Explorer 14 data for $L < 2.4$ have not been published).

The readings of the three electron channels for the period October 1962 - February 1963, at the outer belt maximum (L = 4.8) are shown in Figure 17 [100]. The figure shows just how unstable the fluxes of electrons are in this region. Figure 18 shows the distribution of the fluxes of electrons and protons of the energies indicated for the end of 1962, beginning of 1963, and the picture is quite typical. Plotted on the axis of ordinates is the counting rate for the different sensors as a function of the geocentric distance in the region near the equator (the values of the parameter L and of the geomagnetic latitude are shown in the upper part of the figure). The true values of the intensities can be found by dividing the data in Figure 18 by the corresponding geometric factors (see the comment under the figure).

Electrons with $E_e > 40$ keV are distributed almost uniformly out to the boundary of the magnetosphere. Electrons with $E_e > 230$ keV and 1.6 MeV form a clearly defined peak in the $L \approx 4.8$ vicinity. Protons with energies > 500 keV caused the considerable difference in radings by counters with thresholds $E_e = 230$ keV, $E_p = 500$ keV and $E_e = 230$ keV, $E_p = 4.5$ MeV in the region of the gap.

As will be seen from Figure 17, the variations in the fluxes of electrons with energies of $\sim$ 200 keV are significantly less than in the case of higher ($E_e > 1.6$ MeV) and lower ($E_e \sim 40$ keV) high energy particles, and usually are not in excess of a three-fold deviation from the average on either side. These results apply to the belt maximum. Noticeable variations in the gap (when $L \lesssim 3.5$) are observed only during severe storms. Fluxes of electrons with energies > 1.6 MeV, according to the data in /94
[100], undergo variations that are on the same scale as those for $E_e \sim 40$ keV.

However, the nature of these variations, as well as their link with magnetic disturbance activity, is much more complex.

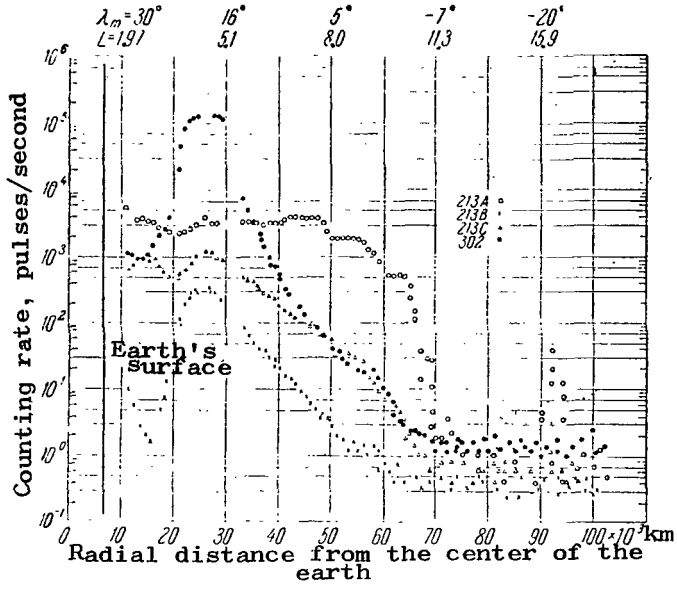

Figure 18. Counting rate for detectors with different threshold during the flight of Explorer 14, 6-7 October 1962. Absolute magnitudes of intensities for the readings from the respective detectors can be obtained by multiplying through the following magnitudes: 213A by $5 \cdot 10^3$; 213B by $1.7 \cdot 10^4$; 213C by $3 \cdot 10$; 302 by 10.

The fluxes of relativistic electrons diminish sharply during magnetic storms to a magnitude $\sim 10^4$ cm$^{-2} \cdot$ sec^{-1} at the maximum (see Fig. 17). In certain cases (prior to the 17 December 1962, storm, for example) this intensity can be established by the monotonic decay in the preceding storm during a relatively quiet period. There is no further decay during a storm, and the intensity remains at the $\sim 10^4$ cm$^{-2} \cdot$sec^{-1} level. /95

The intensity increases to $\sim 10^6$ cm$^{-2} \cdot$sec^{-1} when L $\sim$ 5 2 to 3 days after the storm. The peak that is forming moves into the small L region and gets progressively sharper. There were three cases of abnormally low levels of magnetic acitivity for several weeks after a storm during the operation of Explorer 14. And there was a long period of time over which the propagation of diffusion waves such as these could be observed and

the rates at which their fronts were moving in terms of L could be measured [109]. These results are of great importance to the transfer theory, because the wave velocities measured in [109] coincided with the values obtained through the theoretical computations in [11, 12]. This question will be reviewed in more detail in #13, where the respective figures from [109] will be included.

The origin of the diffusion waves has been observed much more frequently, the profile of the relativistic electrons shown in Figure 18 is a typical wave in the early stage. However, further development usually is broken up during the next storm. Note that the maximum fluxes in the waves were almost always $\sim 5 \cdot 10^5 - 10^6$ cm^{-2} $\cdot$ sec^{-1}, but that they never exceeded the magnitude 10^6 cm^{-2} $\cdot$ sec^{-1}.

Thus, the variations in the intensity of electrons with energies $\sim$ 40 keV and $\sim$ 1.5 MeV are not correlated. If it is considered that the flows of intermediate energy ($\sim$ 200 keV) particles are more stable, it can be said that during magnetic disturbances the energy density spectrum in the outer zone swings, as it were, relative to the point $E \approx 200$ keV. Figure 19 is illustrative of such changes in the spectrum (December 1962 - January 1963).

The wealth of material obtained by Explorer 14 continues to be processed and published. In addition to the papers cited above [28, 86, 91, 100, 109], let us also point out the articles [116, 117] that reviewed the dynamics of high-energy electrons ($E > 200$ keV) near the boundary of /96
the trapped radiation region.

The Elektron series of satellites provided a great deal of valuable information on the radiation belts at high altitudes. These satellites functioned under conditions of a deep minimum in solar and geomagnetic activity, the level of which was below that when Explorer 14 was in operation. The orbits of the satellites were such that measurements were made over a wide range of geocentric distances and geomagnetic latitudes (several of the first ascending half-loops are shown in Figure 20 [87]), and there were a number of cases when simultaneous readings were obtained at two points on the same field line.

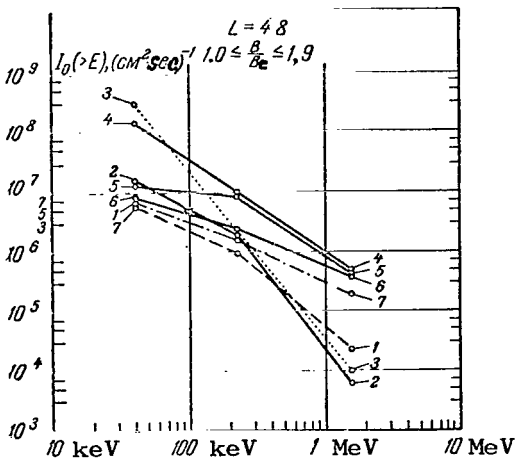

Figure 19. Variations in the electron spectrum in the inner zone in December 1962-January 1963.

1 -10 Dec.; 2 - 14 Dec.; 3 - 17 Dec.; 4 - 20 Dec.; 5 - 23 Dec.; 6 - 29 Dec.; 7 - 1 Jan.

This survey will confine itself for the most part to a review of the results obtained during the first two to three months of the flights of Elektron 1 and Elektron 2. Although these materials contain only a small part of the information obtained, they make it possible to /97 draw a number of conclusions concerning the dynamics of the outer electron belt.

The early 1964 level of magnetic disturbance activity was much lower than during the flight of Explorer 14. The result was a more stationary outer electron belt. Although variations were observed during virtually every pass, their amplitudes diminished, and sometimes the belt was stable for three or four days [87].

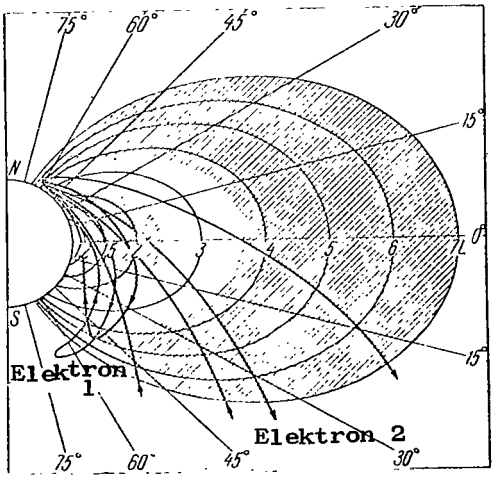

Figure 20. Examples of the paths of Elektron 1 and Elektron 2 in geomagnetic coordinates.

Figure 21 [87] is a typical picture of this stable distribution. The upper curve (fluxes of electrons with energies of 45 keV) was obtained at approximately this same time by the satellite IMP-1. The splitting of the curves when L is large reflects the difference in the structure of the boundary of the trapped radiation region on the east and west (morning and night) sides. The sharp break on the west side /98 was discussed in #5.

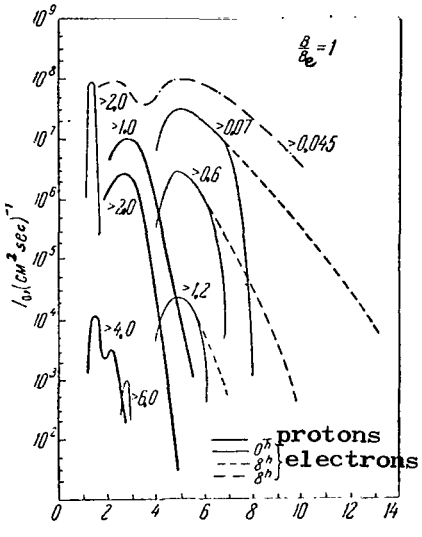

Figure 21. Distribution of electrons and protons with different energies (MeV) early in 1964.

The integral electron spectrum is in the flow N_0E^{-1} (intensity drops as the inverse of the energy) in the energy interval from 70 to 600 keV. The structure and the position of the maximum, as well as the absolute fluxes of electrons at these energies, are practically unchanged when compared with 1962-1963 (see Figs. 17 and 18).

There is a steep drop in the spectrum at energies above 600 keV, and when $E > 1.2$ MeV the intensity is equal to $\approx 10^4$ $cm^{-2} \cdot sec^{-1}$. This magnitude corresponds to the minimal flux of electrons with energies > 1.6 MeV observed in 1962-1963, and is lower than the maximal intensities during this same period by almost two orders of magnitude. Cosmos 41 (1964) carried a Geiger counter similar to the counter for electrons with $E > 1.6$ MeV carried by the American satellites. Cosmos 41 regularly intersected the equatorial plane in the region of the outer zone maximum ($L = 5$). The intensity of electrons with $E > 2$ MeV usually was not in excess of $2 \cdot 10^4$ $cm^{-2} \cdot sec^{-1}$ [107] while the satellite was in operation (several months). Thus, during long periods of low magnetic activity the fluxes of relativistic electrons was $\sim 10^4$ $cm^{-2} \cdot sec^{-1}$, which is lower than the peak intensity in the diffusion wave by two orders of magnitude. It has been pointed out [100, 109] that diffusion waves occur upon termination of magnetic storms. There were no severe storms between the end of January and the beginning of March 1964, probably explaining why there were no heavy fluxes of relativistic electrons. The intensity of electrons with $E > 1.2$ MeV in the outer zone increased after the storm of 5 March 1964, and the spectrum became more stable ($\sim N_0E^{-1}$ for E to 1.2 MeV) [87]. The results confirm the conclusion in [100] and in [109] that the increase in the fluxes of relativistic electrons in the outer zone is linked with magnetic storms.

/99

References [88, 89] provide a detailed study of the variations in position of the maximum, and of the boundary of the outer electron zone associated with the geomagnetic disturbance based on data obtained in January-February 1964, by Elektron 1 and Elektron 2. The position of the maximum, and of the boundary, is characterized by the parameter L, computed through the formulas for the dipole field. As the result show [88], the L_b (at the boundary) value computed in this manner from data from the upper and lower satellites differs, with the lower satellite fixing the boundary at lesser L. Yet the night boundary is very sharp.

This fact indicates that the field lines on the night side are somewhat further away from the earth than the dipole lines passing through the same latitude near the earth. Let us note that this conclusion follows from the form of the magnetic potential in the trapped radiation region obtained in #2 during the analysis of geomagnetic field disturbances. The field of external currents on the midnight meridian near the plane of the /100 equator is in the form $h = h_0 + h_1 L$, where $h_0 \approx 9\gamma$, but $h_1 \approx -4\gamma$. When $L > 2$ this field is antiparallel to the internal currents field, so the field lines apexes are further from the earth than the dipole line apexes. The displacement is a few tenths of a at geocentric distances ~8a.

The outer boundary of the belt usually approaches the earth with increase in magnetic activity. The position of the maximum is more stable,

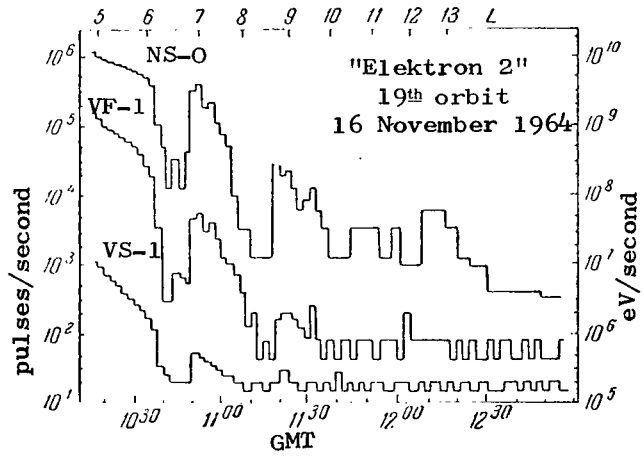

Figure 22. Irregular fluxes of electrons outside the limits of the trapped radiation region. NS-O is the energy flux incident to the crystal of the external scintillator; VF-1 is the rate at which the bremsstrahlung is counted; VS-1 is the Geiger counter reading.

yet considerable shift in the maximum (from $L \approx 4.8$ to $L \approx 4$) was observed during the storm of 19 February 1964.

Irregular fluxes of electrons with energies > 100 keV [117, 89] often were observed beyond the boundary of the belt. Figure 22 is an example of just such a distribution [89]. The irregular fluxes lasted from ~ 1 day to < 3 hours. The energy density spectrum was quite steep. There was not a single case, of all those observed during the first month of /101 the flight of Elektron 1 and Elektron 2 (~ 10), in which there were fluxes of electrons with energies greater than 400 keV. At the same time, the intensity of particles with $E > 100$ keV was $5 \cdot 10^5$ $cm^{-2} \cdot sec^{-1}$.

The jagged profile of the intensity on the outer boundary of the electron belt is probably an important characteristic of the acceleration mechanism, and it is upon the appearance of irregular fluxes that the formation of the belts begins. One possible reason for the occurence of irregular fluxes was pointed out in #5.

So, although the outer electron belt is a very nonstationary formation, its average characteristics remained stable in 1962-1964. Despite the sharp differences in the dynamics of electron and proton zones, their combination has a very important, common feature; increase in the intensity of high-energy particles with decrease in L, first of all, is associated with change in spectrum stability, and not with the increase in the density of particles of all energy levels. In the case of electrons we see that there is an approximately equal density of electrons with energies ~ 1 - 10 keV on both sides of the boundary of the trapped radiation zone. There is an uneven hardening of the spectrum at the boundary, and a sharp increase in the flux of electrons with energies to several tens of keV [40]. However, fluxes of electrons with energies of > 200 keV are still few (see Figs. 18 and 21). The intensity of electrons with energies in the tens of keV changes little with decrease in L, but there is a rapid increase in fluxes of particles with higher energies.

It has not been until recently that systematic investigation of the spectrum of electrons in the energy range above 2 MeV has been undertaken. Yet, as has been pointed out in [87], the energy desnity spectrum of the

electrons in the belts is much broader; when L = 2.7, there was a narrow peak of electrons with energies > 6 MeV, the intensity of which is $\sim 10^3 cm^{-2} \cdot sec^{-1}$. It is readily seen that there is the same tendency here toward an increase in particle energy with decrease in L. It can /102 be assumed that in the region of shells L ~ 3 to 3.5, there are peaks of of electrons with energies between 2 and 6 MeV, and that the set of curves for the distribution of electrons such as these resembles the analogous proton distribution (see Fig. 12).

The spectrum hardening effect with reduction in L is a characteristic feature of adiabatic acceleration during the transfer of particles across the drift shells. Since transfer can be observed directly by experiment (diffusion waves [100, 109]), there is every reason to assert that the formation of the outer belt of electrons with energies of at least > 200 keV is the result of transfer.

However, as distinguished from protons, the escapes of electrons to the outer zone are manifestly non-Coulomb in nature. Actually, according to [100] and [109], the transfer time for electrons in the gap region is on the order of one month. Obviously, the typical time for the losses should be of the same order of magnitude, otherwise the gap would disappear. The life of electrons with energies ~ 2 MeV in hydrogen plasma with a density of $\sim 10^3$ cm^3 is ~ 100 years. Therefore, it must be assumed that some very much more powerful loss mechanism acts in the gap region. The only such mechanism can be the interaction of the plasma with nonthermal oscillations, and the most probable cause of the oscillations is the instability of the radiation belts themselves.

The interaction with the waves should lead to effective scattering of the electrons in the dense layers of the atmosphere, and to the establishment of what is an almost isotropic angular distribution near the plane of the equator. As has been noted in #4, isotropy of the angular distribution results in the disappearance of the altitude movement of the intensity along the field lines. This is the phenomenon that takes place on the internal boundary of the outer belt [87], and confirms the hypothesis relative to the loss of electrons as a result of scattering.

According to this point of view, the loss of particles occurs at low altitudes, so the dynamics of the electron component of the radiation belts at low altitudes is of special interest for an understanding of the nature of electron escape. /103

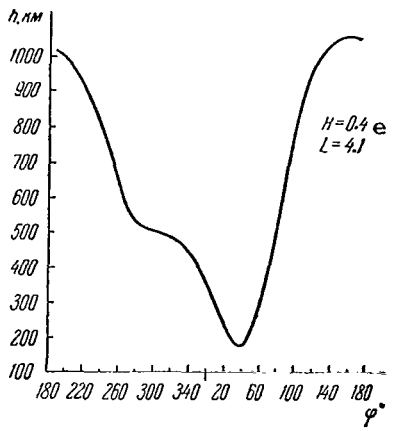

Figure 23. Altitude of lines H = 0.4e, L = 4.1 in terms of longitude in the southern hemisphere.

The intensity of electrons in the outer belt region, and in the gap, is stable at high altitudes. At low altitudes (1,000 km from the earth), the principal features of the distribution of electrons in the corresponding region of geomagnetic latitudes ($L \lesssim 3$ or $|\lambda_m| \lesssim 55°$) are determined by geomagnetic field anomalies (nondipole terms). Fig. 23 is an example of the altitude of the lines H = 0.4e, L = 4.1, in terms of longitude in the southern hemisphere. As will be seen, there is a sharp dip in the Atlantic Ocean area. Particles, the mirror points of which drift along this line, should be destroyed, or move into a higher orbit, during one drift orbit.

The result is longitudinal movement of the electrons; change in intensity on the line H = constant, L = constant, in terms of longitude. This effect was studied in [118 - 121]. The longitudinal movement is clearly expressed in the drift orbits of the mirror points (lines H = constant, L = constant), the minimum altitude of which above the earth (in the Atlantic Ocean area) is less than 350 km. The intensity is higher on the western limb of the anomaly (over South America) that in the center and on the eastern limb (Africa), and this corresponds to the direction of drift of the electrons. At an altitude $\approx$ 350 km the density of the cold particles is such that the mean square angle of scatter of the electrons with energies on the order of a few hundred keV upon passing through the anomaly corresponds to a shift of the mirror point to an altitude equal to the altitude of the change in atmospheric density by a factor of e. This scatter will go on for just a few drift orbits at high altitudes, and the longitudinal movement will disappear. /104

If it is taken that the difference in intensities at the inlet and outlet of the anomaly is what provides the magnitude of the escape, it is then possible to compute the average loss of particles, and to estimate particle life (in terms of the known store of electrons throughout the field duct). Estimates such as these [119] indicate that when $L \approx 2$, this life is $\sim 10^7$ seconds.

A sharp altitude movement of intensity along the field lines is observed in the inner belt when $L \lesssim 2$. When $L \approx 2$, the altitude movement begins to diminish, and at $L \approx 2.5$ to 3, the intensity at altitudes $\approx$ 1,000 km becomes about what it is in the plane of the equator [120,121]. This fact confirms the low anisotropy of the angular distribution of particles in the gap, and, consequently, the presence of an effective scatter mechanism. Longitudinal movement of intensity disappears when $L > 3$.

Since there is a significant altitude movement in the intensity when $L < 2$, the non-Coulomb scatter apparently disappears in this region. Let us note that analysis of the stability of radiation belts [20] (see #18) leads to an analogous conclusion.

The distribution of electrons when $L < 2.5$ is quite stable at low altitudes, but variation is observed in this region. There sometimes is a sharp increase in intensity within a narrow range of L values (on the order of a few tenths), according to [122]. Variations, correlated with magnetic activity when $L > 2.5$, are described in [123].

The outpouring of electrons from the belts occurs very frequently /105
in latitudes $> 50°$, and is virtually constant near the aurora zones. These phenomena were studied in detail during the experiments conducted with satellites Injun 1 [124, 85], and Injun 3 [125]. Investigations show that the outpouring is primarily of electrons with energies $\lesssim$ 50 keV, the intensity of which at altitudes $\sim$ 1,000 km sometimes increases rapidly to a magnitude on the order of that of the maximum fluxes at high altitudes. Data in [125] reveal that the intensities of electrons with energies of $>$ 200 keV change by but a few orders of magnitude at low altitudes, and that there is virtually no variation at energies $>$ 1.6 MeV. Injun 3 observed a few cases of very rapid isotropic behavior in the angular distribution (over 0.1 second).

Fluxes of thrown-out electrons are particularly heavy at the boundary of the trapped radiation region [85] and can be $\sim 10^7 cm^{-2} \cdot sec^{-1}$. At these intensities there are fluxes of X-rays $\sim 10^3$ quanta/cm^2-second, and these are readily recorded with equipment carried by balloon sondes. A great many authors have made such measurements. A statistical analysis [126] has shown that sometimes bursts of X-rays repeat periodically, and that the period is equal, approximately, to the time required for electrons with energies $\gtrsim$ 50 keV to oscillate between reflection points ($\sim$ 1 second). This conclusion has been confirmed many times since then (see [127], for example).

There is almost a constant outpouring in the aurora zone. The probability of the appearance of thrown out fluxes is maximum in the morning hours, local time. The outpouring increases sharply during geomagnetic disturbances, and is observed in all longitudes.

The life of electrons with energies of tens of keV is very short, particularly near the boundary of the trapped radiation region. The volume of a field duct with parameter L and a cross section of 1 cm^2 near the earth when L $\sim$ 5 to 7, is $\omega \approx 2aL^4 cm^3$ (when L is large the field near the earth is $2L^3$ larger than in the plane of the equator, and

$$\int_0^{\pi} \frac{H_e(L)}{H(L,\theta)} \frac{dz}{d\theta} d\theta = \frac{32}{35} L \approx L;$$

in the expression under the integral sign $H_e(L)$ is the field at the equator, $H(L, \theta)$ is the field at an arbitrary point on a field line with parameter L, dz is the differential in the length of the field line arc). Accordingly, in the case of average intensity, I_0, the store of particles in this duct will be $N \approx \frac{I_0}{c} \bar{\beta}^{-1} \cdot 2aL^4$. If the flux of electrons thrown out into the ionosphere is F, life will be $\tau = \frac{N}{F} = \frac{2I_0}{Fc} \bar{\beta}^{-1} aL^4$. /106

Typical values of I_0 and of F when L $\approx$ 7 during a period of severe magnetic disturbance are, respectively, 10^8 to 10^9 $cm^{-2} \cdot sec^{-1}$ and 10^6 to 10^8 $cm^{-2} \cdot sec^{-1}$, while $\beta = \frac{v}{c}$ for electrons with energies $\approx$ 50 keV is 0.4. From whence, $\tau \sim 3 \cdot 10^4$ seconds ($\sim$ 0.3 of a day). This time corresponds to the rate of restoration of the field at the beginning of the reverse phase of a magnetic storm and is shorter by many orders of magnitude than the typical

time of Coulomb scatter ($\sim$ 1 year for energy of 40 keV, and cold plasma density of $\sim 10^3$ cm^{-3}).

The throwing out of a large number of electrons increases the ionization of the E- and D-layers of the ionosphere, manifesting itself by an increase in the absorption of cosmic noise and radio signals reflected back to the earth from the F-layer maximum. Analysis of these phenomena reveals that on the night side of the earth there is yet another mechanism for increasing ionization; the intrusion into the ionosphere of high-speed protons from solar flares. But in such case the increase in ionization can be observed throughout the region of the northern and southern polar caps, and changes regularly with time.

The picture is an entirely different one when electrons pour out. The region of increased ionization is in the zone of the maximum frequency of appearance of auroras, and the time characteristics of the absorption of cosmic noise are significantly irregular. Therefore, data from ground stations measuring absorption of radio waves in the E- and D-layers uniquely establish the cause of the effect. Since data on ionospheric disturbances cover several decades, they can be used to analyze /107 the dynamics of the radiation belts as they pertain to changes in solar activity. It has turned out that the frequency with which electrons are thrown out into the ionosphere anticorrelates with the number of sun spots and the frequency of intense flares [128]. The frequency of such throw-out is maximum during years of minimum solar activity. This fact apparently is intimately associated with the data on the statistics of low-intensity magnetic storms, the frequency of which also anticorrelates with the number of spots.

Reference [128] drew no distinction between high and low power throw-outs (ionospheric sounding only makes it possible to establish the fact of an increase in ionization, but there is no way to estimate the magnitude of the effect [85]). Since weak storms are always more prevalent than severe ones, the number of throw-outs can be equated to the number of weak storms, based on the ionospheric sounding data.

The absolute magnitude of the throw-out can be estimated by measuring the absorption of cosmic noise [85]. The use of this methodology is

comparatively recent, however, so long-term data (on the order of two to three cycles of solar activity) are lacking. There is no doubt that in the future the study of such throw-out, using data on noise absorption, will become widespread, and thus permit analysis of the connection between throw-out and solar activity, with the absolute magnitude of the effect being taken into consideration.

We have reviewed the principal experimental data on the physical conditions in the earth's magnetosphere and in the radiation belts. Let us now proceed to a more precise formulation of the theoretical problems which must be solved in order to explain the nature of these phenomena.

One of the most important problems in the theory is to solve the one concerned with the formation of the tail of the magnetosphere. A number of qualitative considerations regarding the nature of the neutral layer, and the processes near the boundary of the captured radiation region, were reviewed in the foregoing. These considerations make it possible to pull together facts established experimentally, and to show with sufficient /108 persuasion, at least in our view, that particles are trapped in closed drift orbits within the limits of the magnetosphere when the boundaries of the belts are deformed. Sharp contraction of field lines, and increase in field intensity in the equatorial region upon "retraction" of the tail into the trap, cause considerable adiabatic acceleration of the trapped particles, the limit of which is determined practically by the ratio of the typical time for the "reaction" process to the particle drift period. Thus, the experiment shows that in the case of magnetic disturbances, the peripheral regions of the geomagnetic trap are filled with particles with energies considerably in excess of the energy of the particles in the turbulent zone between the boundary of the magnetosphere and the shock wave. Protons with energies $\sim$ 1 - 10 keV, and electrons with $E \sim 100 - 1000$ eV, can enter the trap, even when there are no disturbances.

A stricter theory of these phenomena should be based on the sequential computation of the effects of noncollision dissipation in plasma. There is no possibility of this approach to greatly asymmetrical and nonlinear problems at this time.

The experiment does indicate, however, that high-speed particles are present in the peripheral region ($L \gtrsim 5$) as well as in lesser L regions, but that the average energy of the particles increases with decrease in L. Consequently, the next problem the theory must face is how to explain the nature of the acceleration mechanism acting in the internal regions of the geomagnetic trap, where the drift orbits never come in contact with the interplanetary medium. As will be seen from the survey, there are no data as yet on the use of the autonomy of this sort of a mechanism. Quite the contrary, the majority of the facts indicate that filling of the internal regions of the trap is associated with the subsequent transfer of particles across the drift shells and with adiabatic acceleration during drift toward the earth. It is only in the internal electron zone, apparently, that there is an autonomous source (probably neutron decay) as well as retention of the remains of the artificial belt.

The only now known mechanism for the transfer of particles with /109
energies higher than 100 keV is the sudden pulses of the geomagnetic field, sharp compression, or expansions, of the magnetosphere during sudden changes in the strength of the solar wind. One should, apparently, consider ionospheric turbulence at lesser energies (1 to 10 keV). However, our knowledge of the spectrum of electromagnetic oscillations in the magnetosphere is still limited, and we cannot preclude other transfer mechanisms simply on the basis of what are purely empirical data. Therefore, the natural approach to the transfer problem is a theoretical development of the conception of sudden pulses, and a comparison of the results of the computations with the experiment. This trend is now being widely developed, and the respective investigations have proven successful.

Finally, the third problem in the theory of the belts is to explain particle escape, because the particles that do escape form the inner boundaries of the increased radiation zone. One of the causes of escapes - Coulomb collisions - is trivial.

Ionization losses apparently are the principal mechanism in the destruction of protons. However, experimental data on electrons in the outer zone show that there is a much stronger electron loss mechanism, one that caused scattering in the ionosphere. The experimental data lead to the assertion

that electron life decreases with increase in electron intensity (see Fig. 17). This fact uniquely demonstrates that the cause of electron destruction is lack of radiation belt stability. Consequently, we must make a theoretical investigation of the stability of the increased radiation zone.

So, three basic problems arise in the theory of radiation belts; injection, transfer, and stability. The first problem was reviewed qualitatively in #5. Subsequent chapters will deal with the other two problems.

Chapter III

The Transfer of Trapped Particles Across the Drift Shells During Sudden Pulses

8. Electromagnetic Disturbances During Sudden Pulses

E. Parker was first to review particle transfer during geomagnetic /11
disturbances of the sudden pulse type [2]. The disturbance time parameters are very asymmetrical, with a discontinuity occurring from 1 to 3 minutes after the pulse, and the return to normal lasting ~ 1 hour and longer. The longitudinal drift period for a particle with energy of ~ 1 MeV is ~ 10 minutes when $L \sim 4 - 5$. Thus, the discontinuity time is much shorter and the time to return to normal much longer, than the longitudinal drift period for the particles in the belts. Parker reviewed a model of a flat, ideally conducting magnetosphere boundary, and found the magnitude by which the particles are shifted by assuming that a particle will move along with the field line during the discontinuity, and by using geometric considerations. The movement during the second (slow) phase was found by retaining the third adiabatic invariant, the magnetic flux through the drift orbit from the mirror point. Parker, having found the resulting shift, computed the mean square shift of the particles and introduced it in the diffusion equation.

Subsequent papers [4, 5] showed that during a disturbance with a second order of amplitude there is an average shift of particles that too should be included in the transfer equation. Reference [4] reviewed the same model as that used in [2] and in [5], that is, the model for the case /11
of a field with an arbitrary, but adequately rapid, convergence for small L potentials. Reference [5], using symmetry considerations, showed that the quadrupole

$$h = -\frac{h_0(t)}{2} V R^2 \sin 2\theta \cos\varphi \qquad (8.1)$$

is the most effective, from the standpoint of harmonic transfer (here, and elsewhere in what follows, R will be measured in earth radii, the angle θ will be read from the magnetic axis, and the angle φ from the plane of

the noon meridian). The terms describing the homogeneous field, and the remaining quadrupole terms, do not cause transfer because they correspond to an axially symmetrical disturbance, or because they set up an electric field, the longitudinal components of which are antisymmetrical relative to the plane of the equator. In the latter case, the radial shifts in particle drifts in the opposite hemispheres have different signs and are mutually destructive. The terms with higher multipole orders are less effective because of the rapid convergence of the potential. As was pointed out in Section 2, contemporary models of the magnetosphere confirm, and give additional substance to, the assumption made in [5] with respect to the rapid convergence of the potential. It appears that a term of the type at (8.1) prevails over the other harmonics throughout the trapped radiation region.

The cause of transfer is the electric drift in a disturbed field. This is why [5] first found the electric field, E, generated by the sudden pulse, and then solved the equation for the movement of a particle in that field. The assumption of ideal conductivity along the field lines was resorted to in order to arrive at a unique determination of E, and it was shown that this requirement is equivalent to the condition used in [2] and 4]. The /112 average shift, as found in [5], differed from that found in [4] by the magnitude of the numerical coefficient. This difference was slight, at least from the point of view of analysis of the experimental data. Since both computational methods were equivalent, the discrepancy could only be the result of an arithmetical error in the quite cumbersome numerical computations. A check was made and showed that the error was in [5], and that the result in [4] was correct.

A recent explanation is that small positive and negative pulses, during which a non-stationary disturbance less than, or on the order of, the static asymmetrical field, h*, caused by the constant component of the solar wind, play a large role in transfer processes. Reference [129] generalized the transfer equation for the case of a discontinuous change in the amplitude in the equation at (8.1) from the arbitrary value $h^* \neq 0$, to some h_0. Accordingly, today the transfer equation has been deduced using different

methods, but arriving at identical results, and it has been shown that the original hypotheses correspond to real conditions in the magnetosphere quite accurately. Let us point out that the diffusivity can be obtained from a more general formula for an arbitrary h(t) dependence, in which the mean square shift is expressed in terms of the correlation function for the disturbance [14].

Since the computation for the electric field during a disturbance is of interest in and of itself, we will go through, at least in part, the development of the equation by the method in [5], and will, in order to illustrate the method in [4], compute $\overline{\Delta L^2}$ and $\overline{\Delta L}$, and construct the Fokker-Planck equation, instead of making the direct computation for the particle flux through the shell of L = constant [5].

Let us, in order to find E, introduce the vector potential A for the disturbance of field h, and let us set $E = -\frac{1}{c}\frac{\partial A}{\partial t}$. Let us seek A in the form $A_0 + \nabla\psi$, where A_0 is the vector potential for field h, and has no radial component, while $\nabla\psi$ describes the polarization of the plasma in the magnetosphere. Let us use the condition of ideal conductivity along the field lines to find ψ: (EH) = 0, where H is the sum of the field of the dipole, H_0, and of the disturbance, h. /11

Now, in the spherical coordinates R, θ, φ we have

$$H_{0R} = \frac{2H_e}{R^3}\cos\theta; \quad H_{0\theta} = \frac{H_e}{R^3}\sin\theta; \quad H_{0\varphi} = 0; \tag{8.2}$$

$$\begin{aligned} h_R &= -h(t)R\sin 2\theta\cos\varphi; \\ h_\theta &= -h(t)R\cos 2\theta\cos\varphi; \\ h_\varphi &= h(t)R\cos\theta\cos\varphi; \end{aligned} \tag{8.3}$$

$$A_{0R} = 0; \quad A_{0\theta} = \frac{ah(t)}{3}R^2\cos\theta\sin\varphi; \tag{8.4}$$

$$A_{0\varphi} = \frac{ah(t)}{3}R^2\cos 2\theta\cos\varphi,$$

where

$H_e \approx 0.3$ gauss, and is the field at the earth's equator.

Taking it that in the region considered $\eta(t) = \frac{h(t)}{H_e} \ll R^{-4}$ (that is,

that the disturbance is much less than the undisturbed field of the dipole), let us factor ψ powers of μ

$$\psi = \psi_1 + \psi_2 + \dots \quad (\psi_n \backsim \eta^n). \tag{8.5}$$

The equation (EH) = 0 will then convert into a chain of equations

$$(H_0\nabla\psi_1) = (H_0A_0); \quad (H_0\nabla\psi_2) = -(hA_0) - (h\nabla\psi_1);$$
$$(H_0\nabla\psi_3) = (h\nabla\psi_2) \quad \text{etc.} \tag{8.6}$$

The computation must be carried out with an accuracy within the terms $\sim \eta^2$, inclusive, in order to compute the transfer parameters.

As a first approximation we have:

$$2\cos\theta\frac{\partial\psi_1}{\partial R} + \frac{\sin\theta}{R}\frac{\partial\psi_1}{\partial\theta} = -\frac{ah(t)}{3}R^2\sin\theta\cos\theta\sin\psi, \tag{8.7}$$

from whence

$$\psi_1 = -\frac{aH_e\eta}{2l}R^3\sin\theta\sin\varphi + f\left(\varphi, \frac{\sin^2\theta}{R}\right). \tag{8.8}$$

The function f is the general solution to the equation at (8.7) without the right side. Reference [5] reviewed an analogous task with the finite dimensions of the earth taken into consideration. The ionosphere was taken as ideally conducting, and a magnetic field of the skin currents of the shielding, and a boundary condition $\psi R = 1^{=0}$, were introduced. The computation showed that taking the finite dimensions of the earth into consideration is of interest only when $L \leqslant 1.4$. At the same time it was shown that in the case of a point dipole it is necessary to put f = 0 in the equation at (8.8), as well as in the following approximations: /114

$$\psi_1 = -\frac{aH_e\eta}{2l}R^3\sin\theta\sin\varphi. \tag{8.9}$$

We have, in the succeeding approximation

$$2\cos\theta\frac{\partial\psi_2}{\partial R} + \frac{\sin\theta}{R}\frac{\partial\psi_2}{\partial\theta} = \frac{2a}{2l}\frac{\eta^2H_e}{2l}R^6\sin^2\theta\cos\theta\sin 2\varphi, \tag{8.10}$$

from whence

$$\psi_2 = -H_e\frac{a\eta^2}{168}R^7\sin^2\theta\sin 2\varphi. \tag{8.11}$$

The magnetic drift can be ignored during a field discontinuity, and it can be taken that a particle will move under the effect of a single electric field:

$$v_D = c\frac{[EH]}{H^2}. \tag{8.12}$$

Let us multiply through the equation at (8.12) vectorially by H, and let us take the rotor from the result. Taking it that $E = -\frac{1}{c}\frac{\partial A}{\partial t}$, rot A = h, $\frac{\partial H_0}{\partial t}$ = 0, and (EH) = 0, we obtain

$$\frac{\partial H}{\partial t} = \mathrm{rot}\,[v_D H], \tag{8.13}$$

that is, the condition that the field is frozen into the matter. Consequently, the particles will move along with the field lines, and in order to determine the change in the parameter L, it will be sufficient to consider the movement of particles with zero longitudinal velocity in the plane of the equator (θ = 0).

Using the preceding results, let us obtain the following expressions for the field when θ = 0: /115

$$H_{0R} = H_{0\varphi} = 0; \quad H_{0\theta} = \frac{H_e}{R^3}; \quad h_R = h_\varphi = 0; \quad h_0 = h(t)\cos\varphi; \tag{8.14}$$

$$E_R = \frac{aH_0}{c}\dot{\eta}\left(\frac{R^2}{7}\sin\varphi + \frac{\eta}{12}R^6\sin 2\varphi\right); \quad E_\theta = 0;$$

$$E_\varphi = \frac{aH_0}{c}\dot{\eta}\left(\frac{8}{21}R^2\cos\varphi + \frac{\eta}{42}R^6\cos 2\varphi\right). \tag{8.15}$$

With the equations at (8.14) and (8.15) as a base, we can investiage the movement of particles during a disturbance.

#9. Movement of Particles During a Sudden Pulse and Transfer Parameters

The magnetic drift determines the movement of particles in an undisturbed field. The field intensity along the field lines is minimal in the equatorial plane when $L \lesssim 5$. This is why particles with zero longitudinal velocity drift on the plane along the lines H = constant. Henceforth, we shall designate the polar coordinates in the plane of the geomagnetic equator by R and φ, and we shall designate the third adiabatic invariant by L. Since the magnetic flux in the dipole field can be expressed in terms of L

$$\left(\Phi = 2\pi\int_L^\infty \frac{H_e a^2}{L^3} L\,dL = -\frac{2\pi H_e a^2}{L}\right)$$

let us find L through the following relationship:

$$-\frac{2\pi H_e a^2}{L}=\int_0^{2\pi}\int_{R_L(\varphi)}^{\infty}\frac{H_e a^2}{R^3}\,dR\,d\varphi+\int_0^{2\pi}\int_0^{R_L}h_\theta(R,\varphi)\,R\,dR\,d\varphi. \tag{9.1}$$

The right side of the equation at (9.1) establishes the magnetic flux over the contour $R_L(\varphi)$, along which $H = H_0 + h$ = constant. The first integral yields the dipole field flux over this contour. So as not to complicate the computations we have used the flux that vanishes over the entire plane of the magnetic equator by an analysis of the features of the expression under the integral sign when $R \to 0$, and we have replaced the flux over the /116 inner region of the contour with a flux over the outer part with opposite sign. The second integral yields the field flux for currents at the magnetosphere boundary.

Since all computations should be carried out with precision to terms $\sim h^2$, inclusive, let us seek $R_L(\varphi)$ in the form

$$R_L(\varphi)=L+f_1(L,\varphi)\,\eta+f_2(L)\,\eta^2. \tag{9.2}$$

We shall take only the average value of the magnitude $R_L - L$, in the second approximation because the complement in the form $f(L)\sin m\varphi$ or $f(L)\cos m\varphi$ $(m \neq 0)$ will provide only a small correction to the mean square shift.

The form of the functions $f_1(L,\varphi)$ and $f_2(L,\varphi)$ is determined by the condition $H(R_L(\varphi))$ = constant, and by the relationship at (9.1). Taking it that

$$H=\frac{H_e}{R^3}+hR\cos\varphi, \tag{9.3}$$

we can determine the contour H = constant. Setting $R_H(\varphi) = R^{(0)} + \eta R^{(1)}(R^{(0)}\varphi) + \eta^2 R^{(2)}(R^{(0)})$, and using the method of successive approximations, we obtain:

$$\frac{3H_e}{R^{(0)4}}\eta R^{(1)}+hR^{(1)}\cos\varphi=0 \tag{9.4}$$

and

$$R^{(1)}=\frac{1}{3}R^{(0)5}\cos\varphi. \tag{9.5}$$

In the second approximation

$$\frac{3H_e}{R^{(0)4}}\eta^2 R^{(2)}(R^{(0)}) + \frac{6H_e}{R^{(0)5}}\eta^2 R^{(1)2}\overline{\cos^2\varphi} + h\eta R^{(1)}\overline{\cos^2\varphi} = 0, \tag{9.6}$$

from whence, considering that $\overline{\cos^2\varphi} = 1/2$, we obtain:

$$R^{(2)}(R^{(0)}) = \frac{1}{6}R^{(0)10} \tag{9.7}$$

and, finally,

$$R_H(R^{(0)}, \varphi) = R^{(0)} + \frac{1}{3}\eta R^{(0)5}\cos\varphi + \frac{1}{6}\eta^2 R^{(0)10}. \tag{9.8}$$

Now, by substituting the equations at (9.8) and at (9.3), in the equation at (9.1), let us establish the link between $R^{(0)}$ and L. Computation of the integral yields: /117

$$R^{(0)} = L\left(1 - \frac{5}{18}\eta^2\right) \tag{9.9}$$

and accordingly,

$$R_L(\varphi) = L + \frac{1}{3}\eta L^5\cos\varphi - \frac{1}{9}\eta^2 L^{10}. \tag{9.10}$$

In the case of a slow change in the parameter η, the particles on the circle R = L when η = 0 will drift over contours, the shapes of which can be determined through the relationship at (9.10).

Later on we shall also need formulas expressing L in terms of R, φ and η. There are readily obtainable from the equation at (9.10). Let us introduce the letter designations

$$R_L(\varphi) = L + a_1\eta L^5\cos\varphi + b_1\eta^2 L^{10} \tag{9.11}$$

$\left(a_1 = \frac{1}{3},\ b_1 = -\frac{1}{9}\right)$. Let us seek L = L (R, φ, η) in the form:

$$L = R + a_1'\eta R^5\cos\varphi + b_1'\eta^2 R^{10}. \tag{9.12}$$

Substituting the equation at (9.12) in that at (9.11), and equating the terms with identical powers of η, we obtain

$$a_1' = -a_1; \quad b_1' = -b_1 + \frac{5}{2}a_1^2$$

and

$$L = R - a_1\eta R^5\cos\varphi + (5/2a_1^2 - b_1)R^{10}. \tag{9.13}$$

The sequence in which subsequent computations are made is as follows. First, we determine the particle shift with initial coordinates R*, φ*, in the case of a rapid (compared with the magnetic drift) change in the amplitude of the asymmetrical harmonic of the outer currents from η* to η. The computations will be based on the equation for the particle's electric drift, without taking the magnetic drift into consideration. Then we substitute the values for R_L (φ) when η = η* as the initial coordinates and determine the particle shifts for the same L in terms of φ ≡ φ*. Substituting the final values for the coordinates in the equation at (9.13), we find the magnitude of δL in terms of φ* and L, and, finally, averaging all /118 values of φ* from 0 to 2 π, we compute $\overline{\delta L^2}$ and δ L.

The equations for the electric drift in the E field, established in Section 8, are in the components of forms

$$\dot{R} = -\frac{c}{a}\frac{E_\varphi}{H_{0\theta}+h_0} = \dot{\eta}R^3\frac{\frac{8}{21}R^2\cos\varphi+\frac{1}{42}\eta R^6\cos 2\varphi}{1+\eta R^4\cos\varphi}, \tag{9.14}$$

$$R\dot{\varphi} = \frac{c}{a}\frac{E_R}{H_{0\theta}} = \frac{1}{7}\dot{\eta}R^5\sin\varphi. \tag{9.15}$$

Since change in φ in the first approximation does not change L (see equations (9.10) and (9.12)), the second equation can be adequately considered in a linear approximation. Dividing both sides of the equations by $\dot{\eta}$, and developing the right side of the equation at (9.14) in η with an accuracy that of the average value of a term proportional to η, we obtain:

$$\frac{dR}{d\eta} = -\frac{8}{21}R^5\cos\varphi+\frac{4}{21}\eta R^9, \tag{9.16}$$

$$\frac{d\varphi}{d\eta} = \frac{1}{7}R^4\sin\varphi. \tag{9.17}$$

Let us seek the solution in the form $R(R_0, \varphi_0, \eta) = R_0 + \eta R^{(1)}(R_0, \varphi_0) + \eta^2 R^{(2)}(R_0)$, $\varphi = \varphi_0 + 1/7\ R_0^1 \sin\varphi_0$. Substituting in the equation at (9.16), averaging the terms of the first order of smallness with respect to η in terms of φ, and equating the coefficients of the various powers η to zero, we obtain:

$$R = R_0 + a_2R_0^5\cos\varphi_0 + b_2R_0^9;\quad \varphi = \varphi_0 + \gamma\eta R_0^4\sin\varphi_0. \tag{9.18}$$

where $a_2 = -\frac{8}{21}$, $b_2 = \frac{128}{441}$, $\gamma = \frac{1}{7}$.

Let us now pass on from the arbitrary constants R_0, φ_0 when $\eta = 0$, to R^*, φ^* when $\eta = \eta^*$. Since it is sufficient to know the change in φ in the first approximation,

$$\varphi = \varphi^* + \gamma R^{*4}(\eta - \eta^*)\sin\varphi^*, \quad \varphi_0 = \varphi^* - \gamma R^{*4}\sin\varphi^*. \tag{9.19}$$

Let us put $R_0 = R^* + \alpha_1 \eta R^{*5}\cos\varphi^* + \alpha_2 \eta^2 R^{*9}$. Substituting R_0 in the equation at (9.18) when $\eta = \eta^*$, and with the equation at (9.19) taken into consideration, we obtain: /11

$$a_1 = -a_2, \quad a_2 = \frac{5}{2}a_2^2 - \frac{a_2\gamma}{2} - b_2$$

and

$$R = R^* - a_2 R^{*5}\eta^*\cos\varphi^* + \frac{5}{2}\left(a_2^2 - \frac{a_2\gamma}{2} - b_2\right)\eta^{*2}R^{*9}. \tag{9.20}$$

Expressing the magnitudes R_0 and φ_0 in terms of R^* and φ^*, in the equation at (9.18), for arbitrary:

we have

$$R = R^* + a_2(\eta - \eta^*)R^{*5}\cos\varphi^* - \\ - \frac{a_2}{2}(5a_2 - \gamma)\eta^*(\eta - \eta^*)R^{*9} + b_2(\eta^2 - \eta^{*2})R^{*9}. \tag{9.21}$$

The relationships at (9.19) and (9.21) thus yield the particle shifts during rapid change in the amplitude of the asymmetrical harmonic from arbitrary η^* to η.

Now let us consider particles with identical values for L_0 for the parameter L when $\eta = \eta^*$. According to the equation at (9.11), we should put

$$R^* = L_0 + a_1\eta^*\cos\varphi^* L_0^5 + b_1\eta^{*2}L_0^9. \tag{9.22}$$

Substituting the equation at (9.22) in that at (9.21), we obtain $R'(L_0, \varphi^*, \eta)$:

$$R'(L_0, \varphi^*, \eta) = L_0 + [a_1\eta^* + a_2(\eta - \eta^*)]\cos\varphi^* L_0^5 + \\ + \left\{b_1\eta^{*2} + \frac{5}{2}a_1a_2\eta^*(\eta - \eta^*) - \right. \\ \left. - \frac{a_2}{2}(5a_2 - \gamma)\eta^*(\eta - \eta^*) + b_2(\eta^2 - \eta^{*2})\right\}L_0^9. \tag{9.23}$$

In accordance with the values found for φ (φ^*, R^*, η) (9.19) and R' (L_0, φ^*, η) (9.23), let us, through the equation at (9.13), determine the change in L: $\Delta L = L' - L_0$

$$\Delta L = (a_2 - a_1)(\eta - \eta^*)\cos\varphi^* L_0^5 + \\ + \left\{(b_2 - b_1)(\eta^2 - \eta^{*2}) - \frac{5}{2} a_1 a_2 (\eta - \eta^*)^2 + \right. \\ \left. + \frac{\gamma}{2}(\eta - \eta^*)(a_1\eta + a_2\eta^*) - \frac{5}{2}(\eta - \eta^*)(a_2^2\eta^* - a_1^2\eta)\right\} L_0^9. \tag{9.24}$$

Averaging ΔL^2 and ΔL with respect to φ^*, let us find the transfer parameters. When averaging in the case of $\eta^* \neq 0$, it must be remembered that different values of φ^* are not equally likely. The probability of a particle remaining on the arc $(\varphi^*, \varphi^* + d\varphi^*)$ of the curve at (9.22) obviously is

/120

$$dw = \frac{R^*(L_0, \varphi^*)}{v_{\varphi_{md}}(R^*, \varphi^*)}, \tag{9.25}$$

where

$v_{\varphi_{md}}$ is the φ-component of the rate of magnetic drift.

Since the magnitude $\Delta L \sim \eta$, the disturbance v_{md}, because of the field h^*, need only be considered in the first order of magnitude with respect to η. In the case of particles, the points of reflection of which lie near the plane of the equator, this can be limited to the θ-component of the field disturbance. The average values of $\overline{\Delta L^2}$ and $\overline{\Delta L}$ can be determined through the formulas

$$\overline{\Delta L^2} = \frac{1}{\overline{T}_{md}} \oint_{R_L(\varphi^*, \eta^*, L)} \Delta L^2(L, \varphi^*, \eta) \cdot \frac{R^*(L, \varphi^*)}{v_{\varphi_{md}}(R^*, \varphi^*)} d\varphi^*, \tag{9.26}$$

$$\overline{\Delta L} = \frac{1}{\overline{T}_{md}} \oint_{R_L(\varphi^*, \eta^*, L)} \Delta L(L, \varphi^*, \eta) \cdot \frac{R^*(L, \varphi^*)}{v_{\varphi_{md}}(R^*, \varphi^*)} d\varphi^*, \tag{9.27}$$

where

$$T_{md} = \oint_{R_L(\varphi^*, \eta^*, L)} \frac{R^*(L, \varphi^*)}{v_{\varphi_{md}}(R^*, \varphi^*)} d\varphi \tag{9.28}$$

is the period of the magnetic drift. We have omitted the index "0" in the case of L.

Taking it that the particles drift along the line H = constant, we can put $v_{\varphi_{md}} = A \frac{\partial H}{\partial R}\Big|_{R = R_L(\varphi^*, \eta^*)}$, where the factor A does not depend on the coordinates. Differentiating the relationship

$$H = \frac{H_e}{R^3} + h^* R \cos\varphi^*$$

with respect to R, and substituting the expression for R_L, we obtain

$$v_{\varphi_{md}} = A'\left(1 - \frac{12a_1+1}{3}\eta^*\cos\varphi^* L^4\right), \tag{9.29}$$

where $A' = -\frac{3H_e}{L^4}A$, which, like A, does not depend on the coordinates (when L = constant). /121

Substituting the equations at (9.29) and (9.22) in equations (9.26) - (9.28), we find the transfer parameters:

$$\left.\begin{aligned}
\overline{\Delta L^2} &= \tfrac{1}{2}(a_2 - a_1)^2(\eta - \eta^*)^2 L^{10};\\
\overline{\Delta L} &= \Big\{(b_2 - b_1)(\eta^2 - \eta^{*2}) - \tfrac{5}{2}a_1a_2(\eta - \eta^*)^2 + \\
&\quad + \tfrac{\gamma}{2}(\eta - \eta^*)(a_1\eta + a_2\eta^*) - \\
&\quad - \tfrac{5}{2}(\eta - \eta^*)(a_2^2\eta^* - a_1^2\eta) + \\
&\quad + \tfrac{15a_1+1}{6}(a_2 - a_1)\eta^*(\eta - \eta^*)\Big\} L_0^9.
\end{aligned}\right\} \tag{9.30}$$

The numerical values for the constants are: $a_1 = 1/3$; $a_2 = -8/21$; $b_1 = -1/9$; $b_2 = 128/441$; $\gamma = 1/7$. From whence, putting $(\eta - \eta^*) = \Delta\eta$, we have

$$\overline{\Delta L^2} = \frac{25}{98}(\Delta\eta)^2 L^{10}, \tag{9.31}$$

$$\overline{\Delta L} = \frac{50}{49}(\Delta\eta)^2 L^9. \tag{9.32}$$

The relationships at (9.31) - (9.32) establish one average and mean square particle shifts for a given pulse. The transfer factors $D = \frac{d\overline{\Delta L^2}}{dt}$ and $U = \frac{d}{dt}\overline{\Delta L}$ will yield the relationships

$$D = \tfrac{1}{2}\left\langle\frac{1}{T}\overline{\Delta L^2}\right\rangle, \quad U = \left\langle\frac{1}{T}\overline{\Delta L}\right\rangle, \tag{9.33}$$

where T is the time between two successive pulses, and the angle brackets designate the average for many pulses.

Introduced in Section 4 was the distribution function $\Theta = \Theta(J, L, t)$, giving the number of particles with $J = PL^{3/2}$ per unit interval of values for the invariant J, and per unit interval for L values. The change in this function versus time as a result of transfer can be described by the Fokker-Planck equation /122

$$\frac{\partial\Theta}{\partial t} = \frac{\partial^2}{\partial L^2}D\Theta - \frac{\partial}{\partial L}U\Theta \quad + \text{the terms characterizing the other processes.} \tag{9.34}$$

There is another method, the direct computation of the particle flux, F, through a shell with specified L [8], that will reduce to this same equation. The flux is in the form

$$F = -\left\{ D\frac{\partial \Theta}{\partial L} + \left(\frac{\partial D}{\partial L} - U\right)\Theta \right\}. \tag{9.35}$$

which is readily obtainable from the equation at (9.34).

If the notation

$$D_0 = \frac{25}{196}\left\langle \frac{1}{T}(\Delta\eta)^2 \right\rangle, \tag{9.36}$$

is introduced, the equation at (9.35) will take the form

$$F = -D_0 L^{10}\left(\frac{\partial \Theta}{\partial L} + \frac{2}{L}\Theta\right). \tag{9.37}$$

The first term in the equation at (9.37) is the shape of the diffused flux, and is proportional to the gradient Θ, while the second term describes the regular flux. As will be seen from the equation at (9.37), the regular flux is directed toward the earth. The function Θ is proportional to nL^2, where n is the particle density. In the stationary condition, where there is no flux, particle density for given J is not constant (as in the case of diffused equilibrium), but increases with decrease in L as L^{-4}. Consequently, the transfer resulting from sudden pulses reduces to a concentration of particles near the earth.

Let us review the physical conception of the results obtained in more detail. As will be seen from the formulas at (9.18) and (9.21), during the fast phase of the cycle the particles on the day side (small φ) are shifted in a direction toward the earth when the magnetosphere is compressed, or, conversely, move away from the earth upon expansion (the factor $a_2 = -8/21$ is negative). The picture is the reverse on the night side ($\varphi \sim 180°$). At the same time, the lines for L = constant move as if to meet the particles [see the equation at (9.10)]. During compression, /123 therefore, the particles that were on the day side initially fall into a path with lesser, and on the night side with greater, L, as compared with the original L.

Since field disturbance changes slowly after a discontinuity as compared with the period of longitudinal particle drift the L values are

"frozen" and the particles are diverted into new drift orbits. The protons, or the electrons, drifting initially in an infinitely narrow shell, are distributed on some layer of finite thickness. In the first approximation, half of the particles move away from the earth, and half approach it. Diffusion is the result. The amplitude of the shift δL, is proportional to E/H, and since $E \sim L^2$, a $H \sim L^{-3}$, $\delta L \sim L^5$, and the diffusivity is $D \sim \delta L^2 \sim L^{10}$.

It is obvious that the further a particle with given φ is from the earth at the onset of the disturbance, the greater will be its shift. Particles entering some drift shell start from greater distances than do those leaving the shell. A regular flux is directed toward the earth, therefore. The region from which particles make the transfer into the particular shell is larger than the region occupied by the particles leaving the shell. The order of magnitude of the regular flux can be determined by the change in δL at a distance δL, that is, $\partial \delta L / \partial L \cdot \partial L$. If we take it that δL is $\sim L^5$ in the first approximation, the average flux obtained is $\sim L^9$.

There is no need, in many of the problems reducing to the Fokker-Planck equation, to have computations accurate to within the square terms, inclusive, and the average value $\overline{\delta x}$ of the independent variable x turns out to be linked with the mean square changes in $\overline{\delta x^2}$ by the simple relationship.

$$\frac{\delta x}{\delta T} = \frac{1}{2} \frac{\partial}{\partial x} \frac{\overline{\delta x^2}}{\delta T}. \tag{9.38}$$

The Fokker-Planck equation

$$\frac{\partial f(x, t)}{\partial t} = \frac{1}{2} \frac{\partial^2}{\partial x^2} \frac{\overline{\delta x^2}}{\delta T} f(x, t) - \frac{\partial}{\partial x} \frac{\delta x}{\delta T} f(x, t) \tag{9.39}$$

thus reduces to the diffusion equation /124

$$\frac{\partial f}{\partial t} = \frac{1}{2} \frac{\partial}{\partial x} \left(\frac{\overline{\delta x^2}}{\delta T} \frac{\partial f}{\partial x} \right). \tag{9.40}$$

Parker's paper [2] suggests, in particular, that the transfer caused by sudden pulses can be described by an equation of the type at (9.40).

This conclusion is false in this particular case, however. The relationship at (9.38) holds when the probability of direct and inverse pro-

cesses is equal. For this to happen in our problem, there must be a probability of transition from layer (L, L+dL) to (L', L'+dL') equaling the probability of transition from (L', L+dL') to (L, L+dL). Yet there are no bases for this assertion. Direct and inverse processes are two events, in the successive course of which the system returns to its original state. We know that the inverse picture of the movement in a magnetic field can be realized only when there is a change in field sign. If, therefore, after a sudden pulse the geomagnetic field were to change sign, the particles would drift in the opposite direction as a result of that change. In the event of a precise repetition in the inverse sequence, and with opposite sign for the temporary disturbance, the particles, at the moment the discontinuity occurs, would prove to be at those points in space to which they had moved during the discontinuity at the time of the "direct" process. They will return to their original orbits during sudden changes in the "inverse" process.

But since the geomagnetic field retains its sign for the period of time of interest in the theory of radiation belts, there is no detailed equilibrium, and the problem of transfer must be considered within the Fokker-Planck approximation, rather than within the diffusion approximation. Particle movement should, at the same time, be considered with an accuracy to within that of the square terms, inclusive.

As will be seen from the results obtained, the transfer factor does not depend on the invariant J. This conclusion is linked with the unique time dependence of the field disturbance and is limited by a definite interval for particle drift periods, $\tau\varphi$. As has already been pointed out, /125
this effect takes place when ($\sim$ 1 minute) and much shorter than the period of field return to normal ($\sim$ 1 hour). At the same time, movement during the discontinuity is caused by the electric drift, and during subsequent stages by the conservation of the third adiabatic invariant. In neither case does the movement depend on particle energy. Figure 24 shows proton energy, E_p, in terms of L for constant J (solid curves), and the energy values, $E_{p_{1,2}}$, for which the drift period equals one minute and one

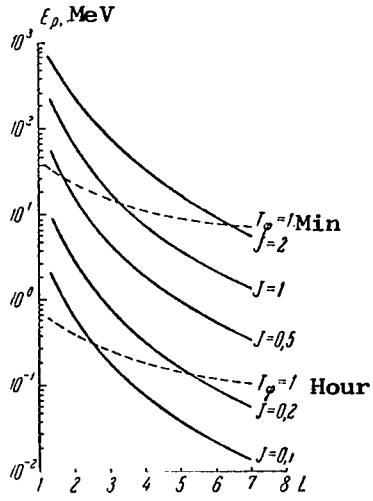

Figure 24. Proton energy in terms of L for constant J.

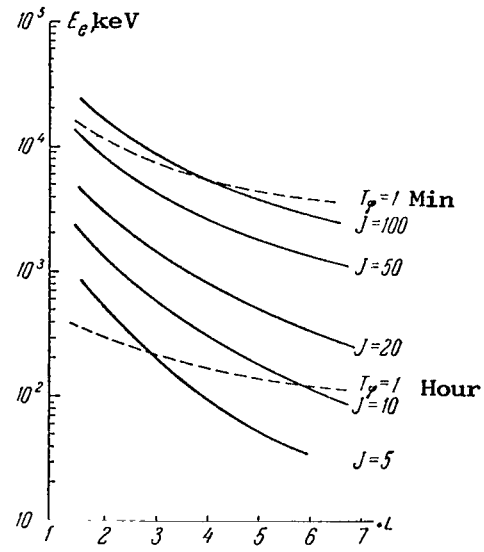

Figure 25. Electron energy in terms of L for constant J.

minute and one hour (the dotted curves). Figure 25 shows analogous relationships for electrons. As will be seen, the main mass of particles in the belts are located in the energy intervals permitting the approximation reviewed in the foregoing.

As has already been pointed out in Section 3, the ground stations almost always register the lowest harmonics of the natural hydromagnetic oscillations of the magnetosphere in the frequency band from $\sim 10^{-2}$ to 10^{-1} Hz, and further that the frequency changes according to the position of the magnetosphere boundary. The disturbance spectrum therefore contains harmonics with a definite amplitude right up to 0.1 Hz, and it can be expected that transfer will take place with great effectiveness right up to energies corresponding to $\tau_\varphi \sim 10$ sec (100 MeV when $L \approx 2$). Small $\tau\varphi$ such as these are characteristic only of inner zone protons, for the disturbances in the inner zone, even in the case of natural oscillations, /126 are practically potential (the hydromagnetic wave propagation time from the $L \approx 2$ envelope to the earth is on the order of one second, and in the case of frequencies $\sim$ 0.1 to 0.01 Hz, the cold plasma inertias in this region can be ignored). The dependence of transfer factors on L in the

case of frequencies ($\overline{\Delta L^2} \sim L^{10}$, $\overline{\Delta L} \sim L^9$). However, generally speaking, the magnitude D_0 will depend on the energy. There are no data available at this time on the spectrum of natural oscillations needed to establish this dependency. However, detected during the study of the radiation belts was an effect that qualitatively predicted the theoretical effect; movement of a second peak of protons with energies ~ 50 MeV [109]. The rate of /127
movement corresponds to the value for D_0 characteristic of lower energy particles. There is, therefore, some basis for believing that the magnitude D_0 does not depend on the energy right up to values $\tau\varphi \approx 0.5$ minute (the period of drift for protons with energies ~ 50 MeV when $L \approx 2$). This effect will be reviewed in more detail in Section 13.

10. Estimate of the Parameter D_0 from Sudden Pulse Data.

As will be seen from the relationship at (9.36), if constant D_0 is to be computed using sudden pulse data, it is necessary to know the frequency with which pulses appear in terms of the amplitude and degree of asymmetry of the disturbed field. There were no such data until recently, because from the point of view of the theory of geomagnetic disturbances the ionospheric currents, and the currents flowing during the main phases of storms, were more important subjects for analysis. Because of the lack of needed information, earlier papers on transfer identified sudden pulses with sudden onsets of magnetic storms, something that was in fact very rare. Therefore, the magnitude D_0, as estimated in [2] and in [6], proved to be very greatly reduced, despite the fact that [2] used the Chapman-Ferraro model (a flat magnetosphere boundary), which provides a strong asymmetry, and the particle shift was assumed to be very great (five earth radii from the center of the earth).

The study of sudden pulses made considerable progress in the years that followed, particularly when the important role they play in the dynamics of the radiation zones was explained. As has already been noted in Section 2, pulse data can also be used to determine the potential of the magnetic field of currents flowing at the magnetosphere boundary.

Reference [27], reviewed in detail in Section 2, contains the degree of asymmetry of the disturbance at the earth's equator as

$$\Delta h = \bar{h}(1 + 0{,}45\cos\varphi).$$

From whence the following relationship between the average observed disturbance, h, and the magnitude Δh_0 in the equation at (9.36) is obtained after computing the skin current field (see # 2): /128

$$\Delta h_0 \approx 0{,}27\bar{h}.$$

This same reference [27] also pointed out that positive pulses are observed daily, but that the frequency of negative pulses is lower by a factor of approximately 2. Still, [27] contains no data on frequency in terms of amplitude. These data do appear in [15], and Table 3 is from that paper. The data were obtained by averaging the period from 1958 through 1961, and include only positive pulses (including sudden onsets of magnetic storms).

TABLE 3

$\bar{h}$, γ	No. of events per year
> 100	0.5
60 - 100	1.8
40 - 60	2.3
20 - 40	21
5 - 20	61
2	720

To compute D_0 from the data in Table 3, let us put

$$D_0 = \frac{25}{196}\frac{1}{T}\frac{(0{,}27)^2}{H_e^2}\sum \nu_i(\bar{h}_i)^2,$$

where

T = 1 year = $3.1 \cdot 10^7$ seconds;

$H_e = 3.1 \cdot 10^4$ γ is the dipole field at the earth's equator;

ν_i is the number of pulses with amplitude h_i in one year.

The result obtained is $D_0 \approx 2 \cdot 10^{-14}$ seconds.

A computation made for the magnitude D_0, using these same data, but another model of the magnetosphere as a base [15], yielded a D_0 value smaller than that we obtained by a factor of 10. This is explained by the low degree of asymmetry of the field disturbance used in [15], wherein $h_0/\bar{h} \approx 0.08$ was used for this model, rather than 0.27. The model in [15] point out that the asymmetry is actually much greater.

We should point out that our paper [11] found a value $D_0 = 5 \cdot 10^{-14}$ second^{-1} from data on the structure of the proton belt. This method can be used to establish the D_0/N ratio, where N is the cold electron density at high altitudes. The D_0 value indicated corresponds to $N = 10^3 \text{cm}^{-3}$. Thus,

the estimates based on magnetic data and on proton belt structure are very /129
close and only differ by a factor of 2.5. It could be assumed that N = 400 cm^{-3}, and then both estimates would coincide. But recent experimental data provide a D_0 *in pure form from* the rate at which diffusion waves are propagated [109]. These data, as will be shown in Section 14, are in better agreement with the magnitude $D_0 = 5 \cdot 10^{-14}$ $second^{-1}$. Investigation of proton transfer apparently in this way will provide a means for estimating the distribution of cold plasma at high altitudes. This question will be reviewed in detail in Section 21.

The divergence in the D_0 estimates based on magnetic measurement data and on the investigation of the radiation belts is not so great that special significance need be attached to it. This is all the more so because the parameters used to compute D_0 are not accurately enough known. Table 3 lists no pulses with amplitudes from 2 to 5 γ, for example. Nor have negative pulses been taken into consideration. Also to be noted is that D_0 depends on $\bar{h}$ as the square. Yet Table 3 points to the possibility of there being significant fluctuations in D_0. It is readily seen that the average amplitude of $\bar{h}$ corresponding to $D_0 \approx 2 \cdot 10^{-14}$ sec^{-1} and 800 pulses per year, is on the order of 10γ. Therefore, a pulse with an amplitude of 40γ is equivalent to an increase in D_0 by a factor of 16, and when $\bar{h}$ = 100γ by two orders of magnitude. Powerful pulses are relatively infrequent. Fluctuations in D_0 average out pretty well in the sufficiently deep regions of the magnetosphere where the typical transfer times (see the next section) are greater than, or on the order of, one year. However, the effect of fluctuations in D_0 should play a big role on the more distant shells.

The first three amplitude intervals in Table 3 correspond to severe magnetic storms, and the appearance of pulses (with amplitudes >40γ) $\approx$ 40%. It can be expected, therefore, that the factor D_0 will undergo modulation with an amplitude $\sim$ 25% of the average value with an 11-year cycle. However, as has already been noted in Sections 2 and 7, weak disturbances anticorre- /130
late with strong ones, so the modulation index should be lower. Judging from the data on the proton belt, the modulation index is small, and has no effect on the intensity distribution within the limits of experimental accuracy (see Section 13).

The solar cycle, therefore, should manifest itself first of all in changes in the probability of large fluctuations in D_0. The average value of D_0 can be considered stable.

11. Basic Solutions of the Transfer Equation

Let us now review the basic solutions of the transfer equation

$$\frac{\partial \Theta}{\partial t} = D_0 \frac{\partial}{\partial L} L^{10}\left(\frac{\partial \Theta}{\partial L} + \frac{2}{L}\Theta\right). \tag{11.1}$$

Some problems that take sources into consideration also will be investigated at the end of this section.

The equation at (11.1) describes net transfer, it being assumed that in the region under consideration the sources of particles, losses, and processes leading to change in the magnitude of the invariant J, are absent. In the stationary case $\left(\frac{\partial \Theta}{\partial t} = 0\right)$ we have:

$$\Theta = A(J) L^{-2} + B(J) L^{-9}, \tag{11.2}$$

where

A and B are arbitrary functions of the invariant J.

The first term in the equation at (11.2) corresponds to a zero particle flux [see the equation at (9.37)], while the second is a constant flux (not dependent on L) with direction from the earth when $B > 0$. The second term differs from zero when there are particle sources in the region of small L (smaller than those in the region under consideration). The first term describes the equilibrium condition established when there is some stationary intensity at the outer boundary of the region. Taking it that the intensity I_0 is proportional to ΘL^{-2} [see the equation at (4.15)], what is observed is a considerable concentration of particle density ($n \sim L^{-4}$). The concentration is linked with the regular flux. The stationary state is /131
established when the outward diffusion balances this flux.

Now let us consider the nonstationary processes. Let us suppose a distribution in the form $\Theta(L_b, t) = \Theta(J) + \theta(J) e^{i\omega t}$, where $|\theta| \leqslant |\Theta|$ and $\omega > 0$, is maintained at some boundary $L = L_b$. The solution comprises two terms, the first of which is linked with the average value of $\Theta(L_b)$,

and reduces to the above-considered stationary solution $\left(\bar{\Theta}=\Theta_0(J)\cdot\left(\frac{L_b}{L}\right)^2\right)$. The second term describes the variation. The greatest interest is in solutions corresponding to frequencies low enough that near the boundary the equilibrium ($\Theta \sim L^{-2}$) is established. In this case the problem reduces to the solution of the equation

$$\frac{\partial\tilde{\Theta}}{\partial t}=D_0\frac{\partial}{\partial L}L^{10}\left(\frac{\partial\tilde{\Theta}}{\partial L}+\frac{2}{L}\tilde{\Theta}\right)$$

with limit conditions

$$\left.\begin{aligned}\tilde{\Theta}_{L\to\infty}&\to\theta(J)\left(\frac{L_b}{L}\right)^2 e^{i\omega t},\\ \Theta_{L\to 0}&\text{ is bounded.}\end{aligned}\right\}\qquad(11.3)$$

Let us seek our solution in the form $\Theta=0_0(J)\left(\frac{L_b}{L}\right)^2 e^{i\omega t}\psi(L)$. The function ψ satisfies the equation

$$\frac{i\omega}{D_0}\psi=L^2\frac{d}{dL}L^8\frac{d\psi}{dL}\qquad(11.4)$$

with the conditions $\psi_{L\to\infty}=1.1$, and $\psi_{L\to 0}$ is bounded. Let us write the equation at (11.4) in the form

$$\frac{d^2\psi}{dL^2}+\frac{8}{L}\frac{d\psi}{dL}-\frac{i\omega}{D_0}L^{-10}\psi=0\qquad(11.5)$$

and let us set $\xi = L^{-4}$, $\Psi = \xi^{7/8} Z(\xi)$. The equation at (11.5) reduces to a Bessel equation of order 7/8:

$$Z''+\frac{1}{\xi}Z'+\left(-\frac{i\omega}{16D_0}-\frac{49}{64}\frac{1}{\xi^2}\right)Z=0,\qquad(11.6)$$

and its solutions are cylindrical functions of the argument /132

$$x=\sqrt{\frac{-i\omega}{16D_0}}\,\xi=\frac{1-i}{4\sqrt{2}}\sqrt{\frac{\omega}{D_0}}\,\xi.\qquad(11.7)$$

What follows from the condition of boundedness when $L \to 0$ ($\xi \to \infty$) is that the sought-for solution is a Hankel function of the second kind. When $x\to 0$ $H_\nu^{(2)}\approx -\left(\frac{x}{2}\right)^{-\nu}\frac{i}{\Gamma(1-\nu)}$. Taking it that when $L\to\infty$ ($\xi \to 0$) $\psi \to 1$, we obtain:

$$\psi=i\left(-\frac{i\omega}{64D_0}\right)^{7/16}\Gamma\left(\frac{1}{8}\right)L^{-7/2}H_{7/8}^{(2)}\left(\sqrt{\frac{-i\omega}{16D_0L^8}}\right)\qquad(11.8)$$

and

$$\tilde{\Theta}=i\left(-\frac{i\omega}{64D_0}\right)^{7/16}\Gamma\left(\frac{1}{8}\right)L_b^{-7/2}0(J)\times$$
$$\times\left(\frac{L_b}{L}\right)^{11/2}H_{7/8}^{(2)}\left(\sqrt{\frac{-i\omega}{16D_0L^8}}\right).\qquad(11.9)$$

It is of interest to estimate the "depth of penetration" of an oscillating disturbance of the intensity at the magnetosphere boundary. A rough estimate (the argument for Hankel function of the order of one) shows that the "depth of penetration" will change as $\omega^{1/8}$. The higher the frequency, the further the shell on which marked variations are taking place from the earth.

A more detailed analysis should include the particle spectrum. It is obvious that the effect of betatron acceleration is to shift the region of pronounced disturbances toward the earth. Let us consider, for example, a stepped spectrum $\theta \sim J^{-n}$. The flux of particles with pulse > P will then be proportional to $\int_{PL^{3/2}}^{\infty} v(J, L)\theta(J)\,dJ$. In the relativistic case (v = c = constant), when $\theta \sim J^{-n}$, this integral is proportional to $L^{-\frac{3(n-1)}{2}}$. Taking it that the particle density is $n \sim L^{-2}$ ⊕ (see Section 4) we find that the variation in the intensity of particles with pulse greater than P is /133

$$I_0(>P) = C(P)L^{-\frac{15+3(n-1)}{2}} H_{7/8}^{(2)}\left(\sqrt{\frac{-i\omega}{16D_0L^8}}\right)e^{i\omega t} \qquad (11.10)$$

(C is a factor not dependent on L and t).

The function I_0 (> P) oscillates with change in L, and the amplitude has a maximum for some finite L (when $L \to \infty$ and $L \to 0$ the function I_0 (> P) vanishes). Let us find the position of this maximum. It is obvious that since the factor $L^{-\frac{15+3(n-1)}{2}}$ increases rapidly with decrease in L, the maximum for the amplitude will be located in the domain of large values for the Hankel function argument, where an asymptotic expansion can be used. Therefore

$$I_0(>P) \approx \approx C(P)L^{-\frac{7+3n}{2}} e^{-\sqrt{\frac{\omega}{32D_0L^8}}} \sin\left(\omega t - \sqrt{\frac{\omega}{32D_0L^8}} + \delta\right), \qquad (11.11)$$

where

δ - is the wave phase. The amplitude maximum is

$$L^{-\frac{7+3n}{2}} \exp\left\{-\sqrt{\frac{\omega}{32D_0L^8}}\right\}$$

and is expanded for

$$L_m = \left(\frac{\omega}{2D_0}\right)^{1/8}\left(\frac{2}{7+3n}\right)^{1/4}. \qquad (11.12)$$

As will be seen from the equation at (11.12), the position of the maximum is little dependent on the energy spectrum. Greater variations in the intensity are observed in the L_m region.

The nature of the variations [see the equation at (11.11)] is as follows. Initially, on shells with L somewhat larger than L_m, there occurs a peak of intensity that will move toward L_m, increasing in amplitude, pass through the shell L_m, and then begin to diminish. After time π/ω, the picture will be repeated, but with the opposite sign. The phase velocity of a wave in the L_m region is determined by the differentiation of the argument for the sine in the equation at (11.11):

$$\omega\, dt + \frac{1}{L^5}\sqrt{\frac{\omega}{2D_0}}\, dL = 0,$$

from whence

$$V = \frac{dL}{dt} = \sqrt{2D_0\omega}\, L^5 \qquad (11.13)$$

and

$$V(L_m) = -\left(\frac{\omega}{2D_0}\right)^{5/8}\sqrt{2D_0\omega}\left(\frac{2}{7+3n}\right)^{1/4}. \qquad (11.14)$$

By way of an example, let us consider periods of 11 years and 1 month. The first period corresponds to the 11-year cycle, the second qualitatively characterizes the average frequency at which severe magnetic storms occur in a year of maximum solar activity. Let us say that $D_0 = 5 \cdot 10^{-14}$ sec^{-1}. In the first case $\omega \approx 2 \cdot 10^{-8}$. When $n \sim 3$, we have $L_m \approx 2.7$ and $V(L_m) \approx 3 \cdot 10^{-3}$ a/day. In the second case $L_m \approx 5$, and $V(L_m) \approx 0.7$ a/day, respectively. These examples characterize the time scales for change in intensity as a result of transfer on the various L shells.

However, periodic changes in conditions on the boundary are not as characteristic of the belts as are discontinuous, irregular, changes with a broad frequency spectrum. It is of interest to explain, in particular, how the stationary distribution will change during discontinuous changes in conditions on the boundary.

If one considers the effects accompanying a discontinuity such as

this in the region of the outer zone and close to the earth ($L \leqslant 5$), it can be taken that the boundary is at infinity, and no particular error will be introduced. In this case the problem has no constant with the dimensionality of length* (neither in the equations, nor in the boundary and initial conditions), so there should be a self-similar solution that depends on one variable $\xi = \xi(L, t)$. One can, in particular, put $\xi = D_0 tf(L)$. The function f is selected from self-similarity considerations; when the variable ξ is substituted in the equation at (11.1), the coefficients too should be functions of ξ.

It will be seen quite readily that /135

$$\frac{\partial F(\xi)}{\partial t} = \frac{dF}{d\xi} \cdot \frac{\partial \xi}{\partial t} = D_0 f(L) \frac{dF}{d\xi};$$

$$\frac{\partial F}{\partial L} = \frac{dF}{d\xi} \cdot \frac{\partial \xi}{\partial L} = D_0 t \frac{df}{dL} \frac{dF}{d\xi};$$

$$\frac{\partial^2 F}{\partial L^2} = \frac{\partial}{\partial L} D_0 t \frac{df}{dL} \cdot \frac{dF}{d\xi} = D_0^2 t^2 \left(\frac{df}{dL}\right)^2 \frac{d^2F}{d\xi^2} + D_0 t \frac{d^2f}{dt^2} \frac{dF}{d\xi}$$

where

F is any function of ξ.

The sought-for solution will obviously be in the form

$$\Theta = 0(J) L^{-2} F(\xi), \tag{11.15}$$

where

$F(\xi) \to 1$ when $\xi \to \infty$, and

$F(\xi) \to 0$ when $\xi \to 0$.

A stationary condition, corresponding to the new boundary conditions, has been established on sufficient distant shells, but there has still been no success in progressing to small disturbances. Substituting the equation at (11.15) in that at (11.1), we obtain the following equation:

$$\frac{dF}{d\xi} = \frac{D_0^2 t^2 \left(\frac{df}{dL}\right)^2 L^{10}}{f(L)} \frac{d^2F}{d\xi^2} + \frac{D_0 t \left(L^{10} \frac{d^2f}{dL^2} + 8L^9 \frac{df}{dL}\right)}{f(L)} \frac{dF}{d\xi}. \tag{11.16}$$

The form of the factors in the right hand side of the equation at (11.16) in terms of t is such that it follows that the first is proportional to

* The radius of the earth, a, selected as a unit of length, is purely conventional. As a scale unit it is commensurate with the dimensions of the trapped radiation region.

ξ^2, while the second is proportional to ξ, or

$$\left(\frac{df}{dL}\right)^2 L^{10} = \alpha f^3(L), \tag{11.17}$$

$$L^{10}\frac{d^2f}{dL^2} + 8L^9\frac{df}{dL} = \beta f^2(L). \tag{11.18}$$

The only general solution of the equation at (11.07), and of that at (11.18) that contains no constant with the dimensionality of length is $f(1) = kL^8$, so, without loss of generality it can be put that k = 1. Accordingly,

$$\xi = D_0 t L^8 \tag{11.19}$$

and

$$64\xi\frac{d^2F}{d\xi^2} + (120\xi - 1)\frac{dF}{d\xi} = 0. \tag{11.20}$$

The solution satisfying the conditions $F_{\xi \to \infty} \to 1$, $F_{\xi \to 0} \to 0$, is /136

$$F = (8)^{-7/4} \cdot \frac{1}{\Gamma(7/8)} \int_0^{\xi} \eta^{-\frac{15}{8}} e^{-\frac{1}{64\eta}} d\eta. \tag{11.21}$$

The function Ⓜ is in the form of a single diffusion wave propagating toward the earth. The wave front is very steep. The function F diminishes as $e^{-\frac{1}{64D_0tL^8}}$. for small ξ. The position of the wave front is determined by the point of inflection in the profile. As will be seen from the equation at (11.20), when $\left(\frac{d^2F}{d\xi^2} = 0\right)$ or, with the equation at (11.19) taken into consideration

$$L_f = \left(\frac{1}{120D_0t}\right)^{1/8}. \tag{11.22}$$

The relationship at (11.22) can be considered as the characteristic for the time of propagation of the disturbance from the boundary of the magnetosphere to the L shell because of the transfer

$$\tau_D(L) = \frac{1}{120D_0L^8}. \tag{11.23}$$

The rounded value $\tau_D = 10^{-2}\ (D_0L^8)^{-1}$ was used in papers [5-12]. A difference of 20% is negligibly small, given the present level of knowledge of the belts.

Based on the equation at (11.22), the velocity of the self-similar diffusion wave front is

$$\dot{L}_f = 15 D_0 L^9 \qquad (11.24)$$

and is proportional to L^9. Let us note that an analogous dependence of the wave velocity on $L(L \sim L^9)$ is present in the case of the periodic boundary condition considered in the foregoing. If ω is expressed in the equation at (11.14) in terms of L_m (from the equation at (11.12)), we will have a law in the form at (11.24).

The formulas for L_f, τ_D and $\dot{L}_f(L)$ are correct for waves containing particles with identical J. Particles with the specified energies are always recorded in practice, so, generally, speaking, it follows that attention during the analysis should be given to the particle spectrum of waves observed during an experiment. Wave velocity increases somewhat in the case of soft spectra, the result of betatron effect, causing an additional increase in the number of high-energy particles with decrease in L. /137

However, an analysis of concrete examples reveals that the dependence of L_f, τ_D and $\dot{L}_f(L)$ on the spectrum is slight (just as in the case of periodic disturbances). After the various computations made for the structure of the proton belt are compared, one can assert that if a certain radiation belt is formed by transfer, and if the source at the boundary is stationary, the maximum intensity of particles with energies greater than E will be on the shell, the time of transfer to which, $\tau_D(L)$ (see the equation at (11.23)), will equal the escape time for particles with this energy. This conclusion is obvious, qualitatively speaking, but the computations show that the error in the determination of L_m by this estimate is just a few percentage points (see Section 12). The relationships at (11.22) - (11.24) therefore are the basic qualitative analysis of the radiation belts, from the point of view of the transfer theory, at any rate.

Table 4 lists the values for $\tau_D(L)$, computed through the formula at (11.23) when $D_0 = 5 \cdot 10^{-14}$ sec^{-1}.

TABLE 4

L	1,5	2	2,5	3	3,5	4
$\tau_D(L)$, sec	$6,5 \cdot 10^9$	$6,5 \cdot 10^8$	10^8	$2,5 \cdot 10^7$	$7,5 \cdot 10^6$	$2,6 \cdot 10^6$
L	4,5	5	5,5	6	7	
$\tau_D(L)$, sec	10^6	$4 \cdot 10^5$	$1,8 \cdot 10^5$	$1 \cdot 10^5$	$2,5 \cdot 10^4$	

Commas represent decimal points.

When L = 1.5, transfer time is almost 200 years, but this diminishes /138 to just a few days in the region of the outer belt (L = 5). As has already been pointed out in Section 10, there is a fluctuation in D_0 by one order of magnitude, and more, approximately once a month. A 20-fold increase in D_0 (corresponding to a pulse with an amplitude of $\sim 40\gamma$) will shift the diffusion front $L \approx 4$ in the course of a day. This is why fluctuations in D_0 play a significant role right up to such L. Even more powerful pulses are observed occasionally. One pulse is the equivalent of 100 days when the amplitude is 100γ, given an average disturbance effect level, and the front is shifted directly into the gap region.

Let us note, however, that fluctuations in the magnitude of D_0 do not always cause variation in intensity. If there is equilibrium distribution of the form at (11.2), change in the absolute magnitude of D_0 will not distort the front. Variations can be observed when there are deviations from the law postulated by the equation at (11.2) (on the front of a diffusion wave, or in a region where particle loss is the primary factor, for example).

In concluding our analysis of self-similar solutions, let us note that self-similarity is retained even when the boundary intensity changes with time in accordance with an arbitrary power law $t^n (n > 0)$. The solution must be sought in the form $\Theta = \theta(J) L^2 t^n F(\xi)$, in the same way that ξ is sought in formula at (11.19). The equation for F (ξ) reduces to a degenerate hypergeometric one. The solution is very close to that of (11.21) for $n \lesssim 3$, as well as for a region of change in L by a factor of from 2 to 3. The shape of the self-similar diffusion wave therefore proves to be quite stable in terms of variations in the law for change in boundary intensity

versus time.

The particular solutions reviewed show that the transfer processes in the magnetosphere can be characterized by a definite time-L relationship. Significant changes in intensity on the shell take place in time $t \sim (D_0 L^8)^{-1}$. in the case of nonstationary processes. Nor does the proportionality factor $\sim 10^{-2}$ depend to any great degree on the concrete statement of the problem, or on the particle spectrum. These conclusions can also be confirmed by the general solution of the problem with initial conditions as set forth in what follows.

Let us find Green's function for the equation at (11.1) [2, 11]. Let us first make the same substitution for the variables that we made in solving the problem with periodical conditions at the boundary $\left(\Theta = L^{-2}\psi,\ x = \frac{1}{4}L^{-4},\ \psi = x^{7/8}Z\right)$, and let us set $D_0 t = \tau$. The equation is /139

$$\frac{\partial Z}{\partial \tau} = \frac{\partial^2 Z}{\partial x^2} + \frac{1}{x}\frac{\partial Z}{\partial x} - \left(\frac{7}{8}\right)^2 \frac{1}{x^2} Z, \tag{11.25}$$

the general solution of which can be given in the form

$$Z = \int_0^\infty e^{-\sigma^2\tau} I_{7/8}(\sigma x) A(\sigma)\, d\sigma \tag{11.26}$$

(the positive sign for the order of the Bessel function provides for convergence when $L \to \infty$). When $\tau = 0$, the equation at (11.26) should pass to the initial condition $Z_0(x)$

$$Z_0(x) = \int_0^\infty I_{7/8}(\sigma x) A(\sigma)\, d\sigma. \tag{11.27}$$

From the Fourier-Bessel theorem

$$A(\sigma) = \int_0^\infty I_{7/8}(\sigma x') Z_0(x')\, x'\, dx' \tag{11.28}$$

and further,

$$Z(x, \tau) = \int_0^\infty \int_0^\infty Z_0(x')\, e^{-\sigma^2\tau} I_{7/8}(\sigma x) I_{7/8}(\sigma x')\, x'\sigma\, d\sigma\, dx'. \tag{11.29}$$

Integrating the equation at (11.29) with respect to σ, we get

$$Z(x, \tau) = \int_0^\infty Z_0(x')\, g(x, x', \tau)\, dx', \tag{11.30}$$

where

$$g(x, x', \tau) = \frac{x'}{2\tau} \exp\left(-\frac{x^2 + x'^2}{4\tau}\right) I_{7/8}\left(\frac{xx'}{2\tau}\right) \tag{11.31}$$

(see [130] 6.633.2); $I_{7/8}$ is the Bessel function of the imaginary argument.

Considering that $x=\frac{1}{4L^4}$, $x'=\frac{1}{4L'^4}$, $\Theta=(2)^{-7/4}L^{-11/2}Z$ and $Z_0=\Theta_0 2^{7/4}L'^{11/2}$, /140

we obtain

$$\Theta=\int_0^\infty \Theta(L')G(L, L', \tau)dL', \tag{11.32}$$

where Green's function is

$$G(L, L', \tau)= \\ =\frac{L^{-11/2}L'^{-7/2}}{2^{13/8}\tau}\exp\left\{-\frac{1}{64\tau}\left(\frac{1}{L^8}+\frac{1}{L'^8}\right)\right\}I_{7/8}\left(\frac{1}{32\tau L^4L'^4}\right). \tag{11.33}$$

By substituting $\tau - \tau'$ for τ in the equation at (11.33), we can construct a solution of the problem with source Q (L', τ'):

$$\Theta=\int_0^\tau\int_0^\infty Q(L', \tau')G(L, L', \tau-\tau')dL'd\tau'. \tag{11.34}$$

Density of Q sources is established in a manner similar to that used to establish Θ. The magnitude

$$dQ=Q\,dL\,dJ$$

yields the number of particles with invariant J in the interval J, J + dJ, produced in unit time between a shell with parameters L and L + dL.

Let us now consider the problem with the δ-form initial condition $\Theta_0 \sim \delta$ (L - L_0). The equations at (11.32) and (11.33) give us

$$\Theta(L, \tau)= \\ =\frac{CL_0^{-7/2}}{2^{13/8}}L^{-11/2}\exp\left\{-\frac{1}{64\tau}\left(\frac{1}{L^8}+\frac{1}{L_0^2}\right)\right\}I_{7/8}\left(\frac{1}{32\tau L^4L_0^4}\right). \tag{11.35}$$

When $L^4 \ll L_0^4$ and $\tau \gtrsim \frac{1}{32L_0^8}$, the argument for the Bessel function is small so $I_{7/8}(\xi) \approx \alpha\,\xi^{7/8}$ (α is a constant not dependent on L and τ). Therefore

$$\Theta \approx C^*\tau^{-\frac{15}{8}}L^{-9}\exp\left(-\frac{1}{64\tau L^8}\right); \tag{11.36}$$

where C* is dependent only on J.

The asymptotic solution of the problem with an arbitrary initial /141 condition localized in the $L \gtrsim L_0$ region when $\tau \to \infty$ is in the same form.

Let us now pass on to the intensity of particles with a pulse > P. For purposes of simplicity, we will take it that $C^*(J) \sim J^{-n}$, and we will look at the relativistic section of the spectrum (v = c). In this case the intensity in the plane of the equator, I_0 (> P), is proportional to the magnitude

$$L^{-2}\int_{PL^{3/2}}^{\infty}\Theta\,dJ, \qquad \text{or}$$

$$I_0(>P)=S_0\left(\frac{P}{P_0}\right)^{-(n-1)}\tau^{-\frac{15}{8}}L^{-\gamma}\exp\left(-\frac{1}{64\tau L^8}\right). \tag{11.37}$$

where

S_0 and P_0 are constant magnitudes, and

$$\gamma=\frac{3}{2}(n-1)+11=\frac{3n+19}{2}. \tag{11.38}$$

The solution of (11.37) describes a single diffusion wave. Differentiating the equation at (11.37) with respect to L, and equating the first and second derivatives to zero, we find the coordinats of the maximum, L_m, and of the leading and trailing phase fronts, $L_{f_{1,2}}$:

$$-\gamma L_m^{-(\gamma+1)}+\frac{1}{8\tau}L_m^{-(\gamma+9)}=0, \tag{11.39}$$

$$\gamma(\gamma+1)L_{f_{1,2}}^{-(\gamma+2)}-\frac{2\gamma+9}{8\tau}L_{f_{1,2}}^{-(\gamma+10)}+\frac{1}{64\tau^2}L_{f_{1,2}}^{-(\gamma+18)}=0 \tag{11.40}$$

and

$$L_m=\left(\frac{1}{8\gamma\tau}\right)^{1/8}, \tag{11.41}$$

$$L_{f_1}=\left(\frac{1}{\alpha_1\tau}\right)^{1/8}, \tag{11.42}$$

$$L_{f_2}=\left(\frac{1}{\alpha_2\tau}\right)^{1/8}, \tag{11.43}$$

where

$$\alpha_1=4(2\gamma+9+\sqrt{32\gamma+81}), \tag{11.44}$$

$$\alpha_2=4(2\gamma+9-\sqrt{32\gamma+81}). \tag{11.45}$$

But here too, the dependence of the parameter L_m and of L_{f_1} and L_{f_2} on the spectrum is very weak. For example, when $n \to 2$, the magnitude L_m (for given ξ) is only 7% smaller than when n = 8, despite the fact that the difference in the spectrum is colossal.

As will be shown in the next chapter, waves of this type have been observed repeatedly in the relativistic region of the spectrum of electrons in the outer zone. The magnitude of n in this section of the spectrum is apparently close to 2 to 3, so $\gamma \approx 14$, and $\alpha_1 \approx 240$ and $L_{f_1} \approx \left(\frac{1}{240D_0t}\right)^{1/8}$.

Accordingly, a diffusion wave resulting from a pulse injection of

particles at large L is propagated somewhat more rapidly than in the case of a discontinuous change in the boundary condition [$L_f = \left(\frac{1}{120 D_0 t}\right)^{1/8}$ see the equation at (11.22)]. As a matter of fact, when pulse injection occurs the trailing phase front is diffused, and this causes an additional shift of the maximum, and of the leading front in the small L region.

Readily obtainable from the equation at (11.42) when n ~ 3 to 5 is

$$\dot{L}_{f_1} \approx 30 D_0 L^9. \qquad (11.46)$$

Substituting the equation at (11.41) in that at (11.37), we find that the intensity at the maximum changes as $\tau^{\frac{\gamma-15}{8}}$ and that the maximum increases monotonically when n > 11/3. This is linked with the betatron acceleration of the particles moving toward the earth. At the same time, the total number of particles, determined by the integral

$$\int_0^\infty \Theta \, dL \sim \int_0^\infty \tau^{-15/8} d\left(L^{-8}\right) \cdot e^{-\frac{1}{64\tau} L^{-8}},$$

diminishes as $\tau^{7/8}$.

The examples reviewed show that in regions where there are no particle sources one can introduce a typical transfer time of $\tau_D(L) \approx 0{,}01 (D_0 L^8)^{-1}$. This time corresponds to the propagation of a disturbance on a shell with parameter L, and is the fundamental characteristic of transfer.

Now, let us consider the stationary problem with sources. Since this problem is of the greatest interest, at least from the present point of view, in the dynamics of the protons of neutron decay, we will restrict ourselves to the special form of density of sources $Q = Q_0 L^{-\mu} J^{-\nu}$. This is the prevailing relationship in the case of a step energy function, and of the step relationship of the total number of particles nascent in a unit of volume to L. Based on the computations made [131], the protons resulting from the cosmic-ray albedo neutron decay satisfy these conditions. /143

The transfer equation is in the form

$$D_0 \frac{\partial}{\partial L} L^{10} \left(\frac{\partial \Theta}{\partial L} + \frac{2}{L} \Theta\right) = - Q_0 L^{-\mu} J^{-\nu}. \qquad (11.47)$$

It is obvious that the equation at (11.47) is accurate for sufficiently

large L, at which the transfer time is much shorter than the times of Coulomb, and other losses not associated with the transfer, and will yield the asymptotic form of the distribution at large L. The effect of losses at small L can be taken into consideration qualitatively by using the boundary condition that requires Ⓜ to vanish at some L_i. We will consider the finiteness of the dimensions of the magnetosphere by using an analogous condition for some $L_e > L_i$. Keep in mind that under real conditions the parameters L_e and L_i can depend on particle energy. L_i, for example, will be smaller the higher the energy, since lifetime increases with increase in energy. But in the case of protons with energies of several tens of MeV the ionization loss time can be compared with the transfer time only at the ionosphere boundary ($L \approx 1.3$), so $L_e = 1.3$ can be taken as L_i for all energies with this order of magnitude because upon a further reduction in L the ionization loss time diminishes rapidly, the result of the sharp increase in the cold particle density.

The parameter L_i is determined by the condition that particles with specified energy and low longitudinal velocity be maintained in the magnetosphere. As a rough approximation, this condition is an equality with orders of magnitude those of the Larmor radius $\frac{mc^2P}{eH} = \frac{mc^2P}{eH_e}L^3$ /114/

and of the scale of the heterogeneity of field aL:

$$L_i(P) \approx \left(\frac{eH_e a^3}{3mc^2P}\right)^{1/2} \tag{11.48}$$

(let us remember that in this book P is measured in mc units, where m is the rest mass for the particle).

If we put $P = JL^{-3/2}$, the analogous estimate for $L_i(J)$ is readily obtained

$$L_i(J) \approx \left(\frac{eH_e a}{3mc^2J}\right)^2. \tag{11.49}$$

However, the corresponding values of L_i are very great ($\sim$ 6 to 10), even for protons with energies $\sim$ 50 to 100 MeV ($P \approx 1/3$). Hence, the effective value at the boundary of the trapped radiation region ($L_i \approx 7$) can be taken as L_i. As we will see in what follows, when there is a stable source spectrum the magnitude L_i plays no special role. The general solution of

the equation at (11.47) is in the form

$$\Theta = C_1(J)L^{-2} + C_2(J)L^{-9} - \frac{1}{(\mu+6)(\mu-1)}\frac{Q_0}{D_0}J^{-\nu}L^{-(\mu+8)}. \qquad (11.50)$$

Since the boundary values L = L_e and L_i are assumed identical for all J, the function of C_1 and C_2 in terms of J should be in the form $J^{-\nu}$. Factoring on the basis of boundary conditions

$$\Theta = \frac{Q_0}{D_0}\frac{1}{(\mu+6)(\mu-1)}J^{-\nu}\times$$
$$\times\left\{\frac{\left[L_e^7 L_i^{-(\mu-1)} - L_i^7 L_e^{-(\mu-1)}\right]L^{-9} - \left[L_i^{(\mu-1)} - L_e^{-(\mu-1)}\right]L^{-2}}{L_e^7 - L_i^7} - L^{-(\mu+8)}\right\}. \qquad (11.51)$$

We obtain the integral particle spectrum from the equation at (11.51) through the formula at (4.16). If the velocities are considered as nonrelativistic (v = cP = $cJL^{-3/2}$), and putting $\hat{\alpha}$ = 1.5, we have (v > 2): /145

$$I_0(>P) = \frac{1{,}5Q_0c}{2\pi D_0(\mu+6)(\mu-1)W_0(\nu-2)}P^{-(\nu-2)}L^{-\frac{3\nu-1}{2}}\times$$
$$\times\left\{\frac{\left[L_e^7 L_i^{-(\mu-1)} - L_i^7 L_e^{-(\mu-1)}\right]L^{-9} - \left[L_i^{-(\mu-1)} - L_e^{-(\mu-1)}\right]L^{-2}}{L_e^7 - L_i^7} - L^{-(\mu+8)}\right\}. \qquad (11.52)$$

Parameters μ and v are associated with the exponent of the sources within the energy spectrum. Upon the determination of Q we have

$$dN = QL^{-\mu}J^{-\nu}\,dL\,dJ, \qquad (11.53)$$

where dN is the number of particles nascent per second in the layer (L, L+dL) with J in the interval (J, J+dJ). Let us now pass on to the number of particles nascent in the volume dW and in the energy interval dε. The volume of the (L, L+dL) layer is W_0L^2dL. Setting $J = \sqrt{2\varepsilon}\,L^{3/2}$ in the equation at (11.53) (the kinetic energy is measured in Mc^2 units) we obtain

$$dN = W_0L^2q(L,\varepsilon)\,dL\,d\varepsilon = Q_0L^{-\mu}(2\varepsilon)^{-\nu/2}L^{-3\nu/2}\sqrt{2}\,L^{3/2}\varepsilon^{-1/2}d\varepsilon$$

and

$$q = \frac{Q_0}{W}2^{-\frac{\nu-1}{2}}L^{-\mu-\frac{3\nu+1}{2}}\varepsilon^{-\frac{\nu+1}{2}}. \qquad (11.54)$$

Let us set

$$q = q_0L^{-\mu'}\varepsilon^{-\nu'}. \qquad (11.55)$$

The density of the particle sources is usually represented in the form at (11.55). A comparison of the equation at (11.54) with that at (11.55) results in

$$Q_0 = q_0 W_0 2^{\frac{\nu-1}{2}};\ \nu = 2\nu' - 1;\ \mu = \mu' - 3\nu' + 1. \qquad (11.56)$$

As will be seen from the equation at (11.52), if $\nu > 2$, the numerical factor is positive when $\mu > 1$, and $\mu < -6$, but when $-6 < \mu < 1$ it is negative. The case of $\mu > 1$ corresponds to $\mu' > 3\nu'$. Considering the fact /146 that $L_e \gg L_i$, we find that the intensity depends on L as $L^{-\frac{3\nu+1}{2}-9} = L^{-(3\nu'+8)}$ far away from the boundaries. The physical import of this solution is readily understood from consideration of the limit case $\mu' \gg 3\nu'$. Source density diminishes very rapidly with increase in L. It is obvious that particle intensity with given P on given L forms as a result of three processes; production of particles with given P on given L, diffusion of particles with large initial P from a region of lesser L, and diffusion of particles with lesser initial P from the more distant shells. The second process has a basic role to play when $\mu' > 3\nu'$.

When $\mu < 6$ (that is, when $\mu' \leq 3\nu' - 7$), the intensity far away from the boundaries diminishes as $L^{-\frac{3\nu+5}{2}} = L^{-3\nu'+1}$. In this case the intensity on the particular shell is determined primarily by diffusion from more distant regions.

Finally, the intermediate case of $3\nu' - 7 < \mu' < 3\nu'$ reduces to an asymptotic law for the decay of the intensity

$$I_0(>P) = \frac{1{,}5 Q_0 c P^{-(2\nu'+3)}}{2\pi D_0 W_0 (2\nu' - 3)(\mu' + 7 - 3\nu')\sqrt{(3\nu - \mu')}} \cdot L^{-(\mu'+8)}. \qquad (11.57)$$

In this case the appearance of protons with given energy is the result primarily of the decay of neutrons of the same energy on the given shell, while diffusion for large and small L has little to do with the intensity. The decay law does not depend on the spectrum within the limits of change in ν indicated. The physical import of the equation at (11.57) is trivial; the intensity is proportional to the source density, $q \sim L^{-\mu'}$, and to the typical transfer time, which depends on L as L^{-8}. In the problem dealing

with the decay of neutrons $\mu' \approx 2$ to 3, while $v' \approx 2.5$ [131]. At the same time, $3v' - 7 = 0.5 < \mu'$, $3v' = 7.5 > \mu'$, so the solution is in the form at (11.57). Intensity diminishes as L^{-10} to L^{-11}. The role of the neutron mechanism in the formation of the radiation belts will be reviewed in Section 13 (protons) and Section 14 (electrons).

This section reviewed the basic solutions of the transfer equation in the regions of space in which loss of particles can be ignored. Let us now review problems in which losses are taken into consideration. /147

12. Particle Transfer from the Boundary of the Magnetosphere with Ionization Losses Taken into Consideration

There are particle escapes of another nature that play a role in the formation of the radiation belts, and this is in addition to transfer and the betatron effects that accompany transfer. The cause of the escapes can be the Coulomb collisions that result in the particles decelerating to thermal energies, and in the case of electrons to scattering in the dense layers of the atmosphere. Yet another possible escape mechanism is scattering on the different types of hydromatic and plasma waves.

Let us consider the effect of ionization losses on the formation of the proton belt. The typical time of proton deceleration attributable to Coulomb collisions is proportional to the cube of the pulse. Therefore, when a proton with given $J = PL^{3/2}$ drifts into the depth of the magnetosphere, its lifetime will increase as $L^{-9/2}$ when cold plasma density is constant. Transfer time increases much more quickly, as L^{-8}. Consequently beginning at some L, where the transfer time can be compared with the deceleration time, the rise in the intensity should be arrested, and the intensity will begin to diminish for lesser L.

Let us assume that we know the proton spectrum on the boundary of the region within the limits of which the field asymmetry is small ($L \approx 5$ to 6). Using the solution of the stationary problem without sources and losses [see the equation at (11.2)], we can formulate the following limit condition:

$$\Theta_{L\to\infty} = F(J)L^{-2}, \tag{12.1}$$

where the form of the function F is determined by the particular spectrum.

The stationary distribution should satisfy the equation

$$\left(\frac{\partial\Theta}{\partial t}\right)_i = D_0 \frac{\partial}{\partial L} L^{10}\left(\frac{\partial\Theta}{\partial L} + \frac{2}{L}\Theta\right), \tag{12.2}$$

where /148

$\left(\frac{\partial\Theta}{\partial t}\right)_i$ is the rate of change in Θ because of ionization losses (scattering of fast protons upon collisions with cold particles can be ignored). It is obvious that

$$\left(\frac{\partial\Theta}{\partial t}\right)_i = \frac{\partial}{\partial J}\dot{J}\Theta. \tag{12.3}$$

The derivative $\dot{J}$ is computed for constant L, so is $\dot{P}L^{3/2}$. In the nonrelativistic case

$$\dot{P} = \frac{v}{c} = -\frac{1}{\tau_c}\frac{1}{P^2}, \text{ where}$$
$$\tau_c = \frac{mMc^3}{4\pi e^4 N \ln\Lambda}, \tag{12.4}$$

e and m are the electron charge and mass, respectively; M is the proton mass; c is the speed of light; N is the cold electron density in cm^{-3} units; log Λ is the logarithm of the Debye shielding. Under magnetospheric conditions ($N \sim 10^3$ cm^{-3}, $T \sim 1$ eV) $\log\Lambda \approx 20$. Thus

$$\dot{J} = \dot{P}L^{3/2} = -\frac{L^{9/2}}{\tau_c}\frac{1}{J^2}$$

and the equation of (12.2) will become

$$\frac{\partial}{\partial L} L^{10}\left(\frac{\partial\Theta}{\partial L} + \frac{2}{L}\Theta\right) + \frac{L^{9/2}}{D_0\tau_c}\frac{\partial}{\partial J}\frac{\Theta}{J^2} = 0. \tag{12.5}$$

Readily seen is that the equation at (12.5) has particular solutions of the form

$$\Theta_\sigma = \psi_\sigma(L) J^2 e^{-\sigma J^3}, \tag{12.6}$$

and from which we can construct the general solution of the problem with an arbitrary spectrum and large L

$$\Theta(J, L) = J^2 \int_0^\infty \psi_\sigma(L) e^{-\sigma J^3} f(\sigma)\, d\sigma. \tag{12.7}$$

The function $\psi\sigma(L)$ satisfies the equation

$$\frac{d}{dL}L^{10}\left(\frac{d\psi_\sigma}{dL}+\frac{2}{L}\psi_\sigma\right)-\frac{3\sigma L^{9/2}}{D_0\tau_c}\psi_\sigma=0. \tag{12.8}$$

If the cold electron density and, as a result, time τ_c depend on L in terms of a power law, the equation at (12.8) reduces to a Bessel equation. We shall, in what follows, review the case of N = constant [11, 12]. The model $N \sim L^{-4}$ was investigated, and the charge exchange taken into account, in [15]. For comparison and analysis of the results [11, 12, and 15] see Section 13. /149

The substitutions $\xi = L^{-7/4}$, $\psi\sigma = \xi^{22/7}\varphi$ reduce the equation at (12.8) to a Bessel equation of the second order for the imaginary argument. The solution, limited when $L \to 0$ (corresponding to transfer from the boundary) is the MacDonald function:

$$\psi_\sigma = L^{-11/2}K_2\left(L^{-7/4}\sqrt{\frac{48}{49}\frac{\sigma_0}{D_0\tau_c}}\right). \tag{12.9}$$

Accordingly,

$$\Theta_\sigma = J^2 e^{-\sigma J^3}L^{-11/2}K_2\left(L^{-7/4}\sqrt{\frac{48}{49}\frac{\sigma_0}{D_0\tau_c}}\right). \tag{12.10}$$

When $x \to 0$, the function $K_2(x) \approx \frac{2}{x^2}$ and

$$\Theta_{\sigma_{L\to\infty}} = \frac{49}{24}\frac{D_0\tau_c}{\sigma}J^2 e^{-\sigma J^3}L^{-2}. \tag{12.11}$$

The function f (σ) in the equation at (12.7) can be found through the equations at (12.11) and (12.1). We have

$$\frac{49}{24}D_0\tau_c J^2\int_0^\infty \frac{d\sigma}{\sigma}f(\sigma)e^{-\sigma J^3} = F(J),$$

so the function $\frac{24}{49}\frac{1}{D_0\tau_c}\frac{F(J)}{J^2}$ is the Laplace transform $1/\sigma$ f(σ) in terms of the variable J^3. The function f(σ) is found through the inversion formula, or in tables of Laplace transforms. Let $F(J) = cJ^{-\nu}$, for example. Taking it that $\int_0^\infty x^\mu e^{-xy}\,dx = \frac{1}{y^{\mu+1}}\Gamma(\mu+1)$,

$$f(\sigma) = \frac{24}{49}\frac{c}{D_0\tau_c\Gamma\left(\frac{\nu+2}{3}\right)}\sigma^{\frac{\nu+2}{3}}.$$

is readily obtainable.

From whence

$$\Theta(L,\ J) = \qquad \text{/150}$$

$$= \frac{24}{49}\frac{cJ^2L^{-11/2}}{D_0\tau_c\Gamma\left(\frac{\nu+2}{3}\right)}\cdot\int_0^\infty \sigma^{\frac{\nu+2}{3}} e^{-\sigma J^3} K_2\left(L^{-7/4}\sqrt{\frac{48}{49}\frac{\sigma}{D_0\tau_c}}\right)d\sigma. \qquad (12.12)$$

the integral at (12.12) can be expressed through the Whittaker function ([130], 6.643.3):

$$\Theta(L,\ J) = \frac{7}{4}\Gamma\left(\frac{\nu+8}{3}\right)\frac{c}{\sqrt{3D_0\tau_c}}L^{-15/4}\times$$

$$\times\exp\left\{\frac{6}{49}\frac{1}{D_0\tau_c L^{7/2}J^3}\right\}W_{-\frac{2\nu+7}{6},\,1}\left(\frac{12}{49}\frac{1}{D_0\tau_c L^{7/2}J^3}\right). \qquad (12.13)$$

For large L, when the argument of the Whittaker function tends to zero, the function $W_{k,m}(x)$, diverges as $x^{-m+1/2}$ (in the case of integral, or half-integral, m, logarithmic divergence is also possible, but the term in the form $x^{-m+1/2}$ increases more rapidly) ([132], Vol. 2, Chap 16). From whence it will be seen that when $L \to \infty$ the solution assumes the asymptotic form at (1.12); $\Theta \sim L^{-9}J^{-\nu}$.

When $L \to 0$ (large values of the argument) the asymptotic expansion of W can be used [132]. And the function Θ is in the form

$$\Theta \backsim J^2 L^{\frac{7\nu+2}{6}}. \qquad (12.14)$$

At the same time, the magnitude $\left(\frac{\partial\Theta}{\partial t}\right)_c = \frac{\partial}{\partial J}\dot{J}\Theta = 0$, because $\dot{J} \sim \dot{J}^{-2}$. The result at (12.14) shows that in the case of large values for the argument the particles with given J are primarily the result of the deceleration of the higher energy particles.

The numerical investigation based on the integral of the W representation reveals that the position of the maximum for the intensity of particles with pulse larger than P can be established by the variable

$$x_m = \frac{6}{49}\frac{1}{D_0\tau_c L^{7/2}J^3(L,\ P)}, \qquad (12.15)$$

while the magnitude x_m is but slightly dependent on the spectrum. Thus, /151 when $\nu = 3$, $x_m \approx 4$, and when $\nu = 10$, $x_m \approx 6$. We can therefore assert (taking into consideration the fact that $J = PL^{3/2}$) that

$$L_m(P) = \left(\frac{1}{40D_0\tau_c P^3}\right)^{1/8}. \qquad (12.16)$$

and the possible error will be a few percentage points. Since the transfer time on shell L is $\tau_D(L) = \frac{1}{100 D_0 L^8}$, and the time for total deceleration of a particle with initial pulse P is equal to $\tau_P = \frac{1}{3}\tau_c P^3$, the relationship at (12.16) means that the approximate equality

$$\tau_D(L_m) \approx \tau_P. \tag{12.17}$$

occurs at the maximum. The relationship at (12.17) is more general than the one at (12.16), and is applicable to the case of an arbitrary dependence of τ_c (that is, the cold atmosphere density) on L. This conclusion will be justified in the next section when the computations are compared with different models of the atmosphere [11, 12, and 15].

On this note we will conclude our analysis of the basic solutions of the transfer equation and will go on to an interpretation of the properties of the radiation belts.

Chapter IV

The Role of Transfer in the Formation of Earth's Radiation Belts

13. The Proton Belt

Judging from the experimental data, there are three sources of high- /152
speed protons in the magnetosphere: trapping near the boundary of the belts of solar wind protons with energies of from 1 to 10 keV; trapping of harder protons (those with energies ~ 100 keV) during magnetic storms; and the cosmic-ray albedo neutron decay. The first two of these sources result in the formation of a definite proton spectrum on the boundary, with the intensity the result of transfer from the boundary in the deeper regions of the magnetosphere. The neutron source acts throughout the magnetosphere.

The solar wind can be taken as a stationary source of protons because wind intensity is at the average level most of the time.

After passage through the shock front the protons will be heated to a temperature on the order of several keV. The protons will be accelerated to energies of several tens of keV in the L ~ 6 region (field ~ 150γ) during transfer from the region between the shock front and the magnetosphere boundary where the magnetic field intensity is ~ 10γ. The dipole approximation is correct with further decrease in L, and the average particle energy near the plane of the equator should increase as L^{-3}.

Using the relationship at (12.16), we can estimate the position of the maxima for intensities of protons with different energies (assuming constant cold atmosphere density). The position of the L_m maximum is /153
linked with the energy by the simple relationship $L_m \sim \varepsilon^{-3/16}$.

More detailed information on the structure of the proton zone can be obtained if the proton spectrum on the outlying shells is known. Explorer 12 established the spectrum of protons with energies of from 0.1 to 1.7 MeV on the L = 5, and L = 6.1, shells near the equatorial plane [99]. The spectrum is in exponential form ($I_0(>E) = Ae^{-E/E_0}$), and the average energy, E_0, when L = 5 and L = 6.1 was 120 keV and 64 keV, respectively. More detailed analysis of the data obtained from this experiment established the spectra of protons with these energies over a wide region in space [52]. It turned out that in the case of high energies the asymptotic form of

the spectrum is everywhere exponential, and the average, E_0, for various L and geomagnetic latitudes corresponds to the conservation of magnetic moment and longitudinal effect [13]. Specifically, $E_0 \sim L^{-3}$ near the plane of the equator.

The structure of the proton belt was computed in [11, 12], using the spectrum in [99] when L = 5.

$$\frac{dI_0}{dE} = Ae^{-E/E_0}, \qquad (13.1)$$

where E_0 = 120 keV, A = 10^5 (cm^2-sec-steradian-keV)$^{-1}$ when 100 keV$\leqslant$E$\leqslant$ 1 MeV. Protons with energy of $\sim$ 1 MeV for L = 5 accelerate to energies of $\sim$ 40 MeV during the drift to the shell with L $\approx$ 1.5 (in the center of the inner zone). So it was of interest to investigate the distribution of protons right up to these energies. Here let us note that the fluxes of protons with energies $\sim$ 10 MeV in the inner zone exceed by far the capabilities of the neutron mechanism, making it necessary to seek new sources of such protons.

The computations used a D_0 factor equated to the position of the maximum for protons with energies greater than 500 keV. The cold atmosphere density was considered constant. The experimental data, the greater part /154 of which were published after the computations in [11-13] were made, virtually coincided with the theoretical curves.

Similar computations for protons with energies from 100 keV to 1.7 MeV were made in [15]. The factor was established using the theoretical model in [31] as a basis, a model providing a greatly reduced degree of disturbed field asymmetry. The density of the cold electrons at great distances was taken in [15] as equal to 50 cm^{-3}, and diminished when L $\sim$ 1.5 to 3 (from $\sim 10^3$ cm^{-3} when L $\sim$ 1.5), as L^{-4}. Taken into consideration in addition to the ionization losses was the charge exchange, the role of which for proton energies of from 100 to 200 keV can be compared with ionization losses. The results in [15] matched those in [11], as well as the experiment at great distances, where losses are insignificant. However, positions of maxima differed significantly from observed positions.

The results in [15] are nevertheless of great methodological interest because they enable us to estimate the dependence of the proton belt structure on the atmosphere model.

Let us review the results obtained in [11, 12]. The curves shown below were obtained from a somewhat more accurate numerical method than that in [11, 12]. The spectrum at (13.1) was approximated by the sum of four expressions of the form $E \cdot \exp\left\{(-E/E_n)^{3/2}\right\}$ for E_n = 100, 200, 400 and 800 keV. By a corresponding selection of numerical factors, one can thus approximate the equation at (13.1) with an error that will be no more than a few percentage points in the interval of energies from 100 keV to 1 MeV. At the same time, the spectrum with respect to J has the form of the sum of the expressions $J^2 \exp\left\{-(J/J_n)\right\}^3$, for which there is the comparatively simple solution of (12.10). However, these results almost completely coincide with those obtained in [11, 12].

Let us use the position of the maximum for protons with E > 500 keV: L_m (500 keV) = 3.2, known from many of the references, to define the magnitude D_0 more precisely. Substituting numerical values in the equation at (12.16), we obtain

/155

$$D_0 = 4 \cdot 10^{-17} N \qquad (13.2)$$

(D_0 is in sec^{-1}, N is in cm^{-3}). When $N = 10^3 cm^{-3}$, $D_0 = 4 \cdot 10^{-14} sec^{-1}$. This result, as has already been noted in #10, is close to the estimate made using the magnetic data ($2 \cdot 10^{-14} sec^{-1}$).

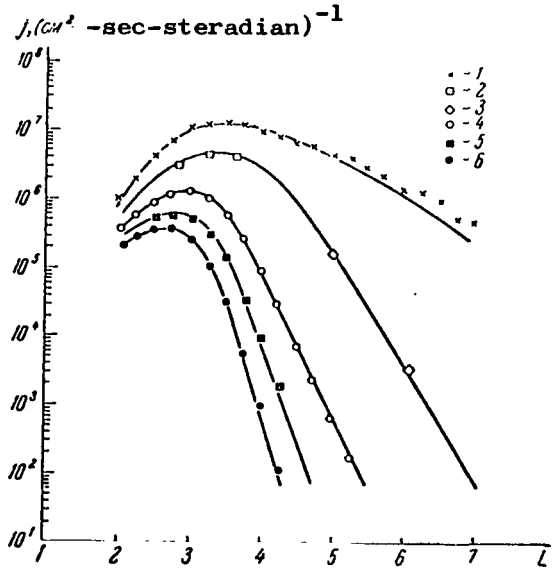

Figure 26. Theoretical and experimental data on fluxes of protons with energies of from 100 keV to 2 MeV in the plane of the equator.

1 - j(> 100 keV)[99];
2 - 3j(> 500 keV)[100];
3 - j(> 500 keV)[99];
4 - j(> 1 MeV)[101];
5 - j(> 1.7 MeV)[15];
6 - j(> 2 MeV)[101].

Figure 26 shows the theoretical and experimental data on the structure of the proton zone in the energy interval from 100 keV to 2 MeV. The solid curves were obtained by computation. The measurement data are plotted using the different symbols shown.

The experimental data were obtained by different types of equipment, /156 and measurement conditions differed because of orientation effects. Hence, the absolute magnitudes cited by the different authors can differ by a factor of from 1 to 2. At the same time, the relative magnitudes should have the same dependence on L because of the high degree of stability of the proton zone. In most of the experiments, the results of which are shown in the figure, the period during which data were gathered was longer than, or on the order of, the period of rotation of the satellite around its geometric axis. This resulted in the readings of the directional sensors pretty much averaging out, so that in fact the average intensity in all directions was measured. The only exception is [99], which contains data on the orientation and cites values for the intensity along a normal to the field line, and for the angular distribution. The average intensity corresponding to these data is equal to half the intensity along the normal to the field line.

In order to compare the relative course of the intensity, the experimental data were multiplied through by normalization factors selected such that the experimentally measured intensities would be equal to the theoretical. In the case of the curves for $E > 100$ keV, $E > 500$ keV, and $E > 1.7$ MeV [99] and $E > 1$ MeV and 2 MeV [101] the factors were close to one, and for $E > 500$ keV [100] the theoretical value was higher than the experimental by a factor of approximately 3. It should be remembered that in the experiments in [99] and [100] the intensity was measured by luminescent counters and semiconductor sensors. The energy threshold was established by pulse magnitude and was extremely critical. The registrations cited in [100] were by a Geiger counter and the threshold was established by the thickness of the window. Registration effectiveness was taken equal to one. It appears that effectiveness actually was much lower because when $L \sim 3$, the average energy of the protons was on the order of 500 keV, so that the main mass of protons falling on the counter had energy near the threshold. Given conditions such as these, the effectiveness of the Geiger counter is usually a few tens of percent. /157

Thus, the experimental data coincide with the results of the theoretical computations, within measurement accuracy limits. The measurements made of fluxes of protons with energies larger than 5 and 9 MeV were also confirmed by the theory.

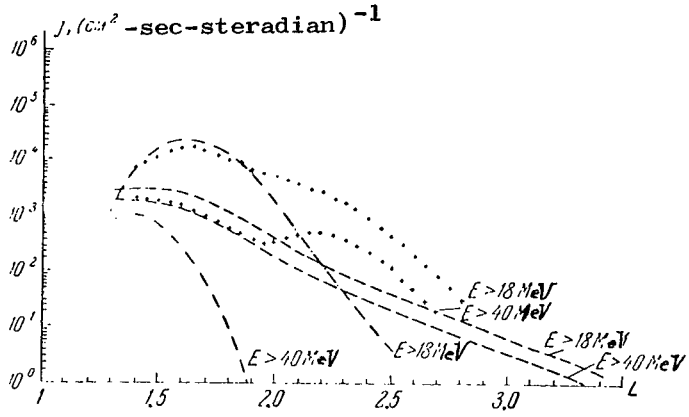

Figure 27. Comparison of theoretical and experimental data on fluxes of protons with energies larger than 18 and 40 MeV.

Now let us consider the high energy region. Figure 27 shows the results of computing fluxes of protons with energies larger than 18 and 40 MeV [11, 12]. The dotted lines are used to plot the distribution of intensities which should be established as a result of the cosmic-ray albedo neutron decay, with transfer taken into consideration (see #11). The dashed-dotted curves are for transfer from the magnetosphere boundary. The experimental data in [104] have been plotted for purposes of comparison. Figure 28 shows the comparison with measurements made by the Elektron satellites.

As will be seen, the measured fluxes of protons with energies of 18 and 30 MeV are close to the computed values corresponding to transfer from the boundary in the vicinity of the main maximum ($L < 2$). It is only at energies greater than 40 MeV that neutron decay begins to prevail. /158

A comparison of theory with experiment leads to the conclusion that the principal source of protons, right up to energies of 30 MeV, is the transfer from the boundary of the magnetosphere. Protons with initial energies $\lesssim$ 100 keV will accelerate to energies of scores of MeV during transfer to a stronger field region. This automatically reduces the

difficulty encountered by the neutron theory in trying to explain the heavy fluxes of protons with E ~ 10 MeV.

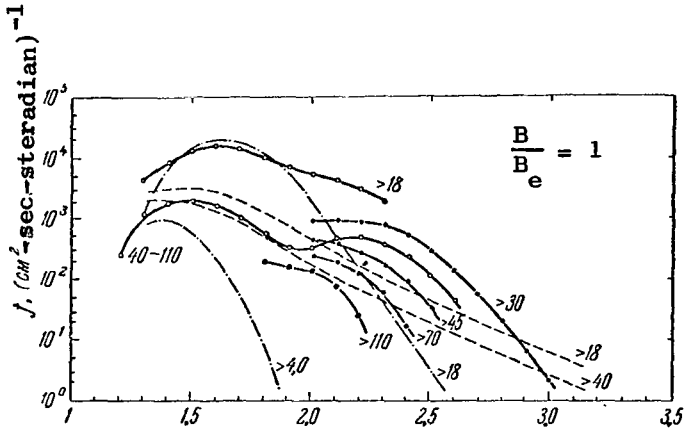

Figure 28. Comparison of theoretical results with data from measurements made of hard protons by the satellites in the Elektron series.

As will be seen from figures 27 and 28, when $2.5 > L > 2$, neither the neutron mechanism, nor the stationary transfer agree with the experiment. There is, in this region of space, an additional maximum for protons with energies of from 20 to 70 MeV. The proton spectrum in this region is much harder than the spectrum for electrons moving from the boundary, but softer than the neutron decay proton spectrum.

The additional maximum can be characterized by an abrupt altitude movement along the field line. For example, the maximum disappears at energies larger than 40 MeV by the 25° geomagnetic latitude, and the intensity diminishes with L as L^{-10}, something that is characteristic of the neutron mechanism (see #11). /159

Expressed in [11, 12] was the assumption that the additional maximum is not stationary, and is associated with the flares of intensity of protons with energies in the hundreds of keV during magnetic storms. The experimental data on these flares were presented at the end of #6, and show that there is reason to believe that in 1956-1960, the number and power of these flares was uniquely high. The displacement of the second maximum toward the earth can be observed as time passes, according to the hypothesis advanced in [11, 12]. The rate at which this displacement

occurs is difficult to determine because the drift period for protons with energies in the tens of MeV when $L \approx 2$ is on the order of one minute and the numerical value of D_0 can differ from the magnitude obtained above. Experimentation shows that in the specified range of drift periods the rate of transfer is of about the same magnitude as it is when $\tau_\varphi \sim 10$ minutes. It has been reported [109] that the maximum for protons with $E > 40$ MeV shifted from $L = 2.25$ at the end of 1962, to $L = 2.15$ at the end of 1964, that is, the rate at which the maximum moved when $L = 2.2$ was ≈ 0.05 a year (1.7×10^{-9} a/sec.). In accordance with the equation at (11.41), the maximum diffusion wave ($\gamma \approx 14$) rate is $14D_0L^9$, and when $D_0 = 5 \times 10^{-14}$, $L = 2.2$, the magnitude $L_m \approx 10^{-9}$ a/sec. The experiment thus confirms the interpretation made in [11, 12] that the additional maximum for the protons is a diffusion wave. Moreover, the data in [109] make it possible to find the transfer rate in the region of small drift periods, where the frequency spectrum of the electric fields is unknown.

The transfer theory provides a complete, quantitative explanation of the structure and dynamics of the belt of protons with energies greater than 100 keV with ionization losses taken into consideration. The exact coincidence between the theoretical and experimental results makes it possible to be more precise concerning the question of the distribution of cold plasma at high altitudes.

Figure 29 is the theoretical dependence of the position of the maxima for protons with different energies, computed assuming constant density of the cold atmosphere ($L_m \sim E^{-3/16}$). The experimental data corresponding /160 to energies of 0.5, 1, 1.7, 2, 5, 9, 10, 18, and 30 MeV plot right on the theoretical straight line. The experimental data in [104] lead to an analogous L_m-E relationship.

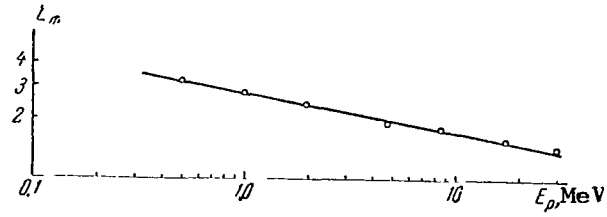

Figure 29. The positions of maxima for protons of different energies in terms of E_p in the plane of the equator.

The distance between adjacent maxima is very greatly dependent on the model of the atmosphere. In [15] the maxima for protons with energies of 0.5, 1, and 1.7 MeV satisfy the relationship $L_m \sim E^{-1/8}$. In the case of the model in [15], when $L \leqslant 3.5$, the density of the atmosphere changes as L^{-4}, so the life is $\tau_p \sim P^3 L^4$. Equating τ_p in an order of magnitude $\tau_D(L_m) \sim L^8$, we obtain $L_m \sim P^{-1/4} \sim E^{-1/8}$. The difference in the laws $L_m \sim E^{-3/16}$ and $L_m \sim E^{-1/8}$ is great enough to show up in the experimental data on maxima positions.

A more detailed analysis of the data in Figure 29 and in [104] shows that the experimental data on the position of proton maxima can superpose from 1-1/2 to 3-1/2 earth radii with no greater change in density than a factor of 2 to 3.

So far as the absolute magnitude of the density is concerned, proton data suggest that it can only be established in combination with the constant D_0. The next section will review the experimental data that permit an independent determination of D_0 with an accuracy within the factor $\leqslant 2$. This D_0 is close to 5×10^{-14}, which reduces to a magnitude of $N \approx 10^3$ cm^{-3}. These estimates of N and the N-L relationship agree with much of the experimental data. /161

Study of the proton belt provides valuable information on the nature of the physical processes in the earth's magnetosphere, and is persuasive confirmation of the important role of transfer caused by sudden pulses in the formation of the radiation zones.

The region of increased intensity of high-speed protons is formed, in essence, by a single mechanism, so it makes no sense to separate inner and outer proton belts.

Finally, let us consider the question of the existence of a belt of high-speed α-particles. It is highly likely that the solar wind contains helium nuclei, as well as heavier elements, in addition to protons. Transfer, and ionization losses, therefore should form belts of the corresponding nuclei as well. These considerations are at the basis of certain features of the belt of α-particles predicted in [12]. The ionization loss formula readily provides nonrelativistic particles with charge Z

and atomic weight A, such that for given energy E, the deceleration time $\tau_c(E)$ is proportional to $A^{-1/2} \times Z^{-2}$. In the case of helium (A = 4, Z = 2) the deceleration time is shorter by a factor of 8 than that for a proton with the same energy. Therefore, in accordance with the equation at (12.16), the maxima for α-particles with energy E will lie at distances that are $(8)^{1/8} \approx 1.3$ greater than for the corresponding protons. Detection and investigation of a belt of α-particles therefore will make it possible to make an independent verification of the hypothesis concerning the destruction of heavy particles in the belts as a result of ionization losses.

A comparison between the proton and α-particle spectra in the magnetosphere is also of great interest from the point of view of the acceleration mechanism theory, a mechanism that heats solar wind particles behind the shock wave. So, if acceleration is the result of the Fermi mechanism, spectra of injection of protons and α-particles with identical velocities are similar. Then the distribution of these particles in the magnetosphere would be completely similar as well [12]. Specifically, intense fluxes of α-particles with energies $\sim$ 100 MeV would have to be observed /162
in the middle of the inner belt. In the case of other acceleration mechanisms (that of acceleration to cyclotron resonance, for example) the law of similitude for spectra of particles with various Z and A has a definite dependence on the shape of the spectrum of turbulent pulsations with different scales, and it can be proven that the α-particle spectrum will be much softer.

Van Allen, in his report to the Belgrade conference on solar-ground communications (August 1966), said that a belt of α-particles with energies of from 2 to 4 MeV had been detected during the investigations conducted with the satellite Injun 3. The apogee of this satellite (2,500 km) was quite high, and the idea was to use values near the equator to estimate the density of the cold plasma. The maximum for the belt was between L = 3 and L = 3.5 (cited in the Van Allen and Frank abstracts of reports). From the above results, the maximum for protons with energies of 2 MeV lies at L = 2.6 (approximately 1.3 closer than for α-particles). Accordingly, the position of the peak for α-particles with energies greater than 2 MeV

agrees well with the hypothesis concerning the destruction of heavy particles as a result of ionization losses. The making of detailed measurements of fluxes of α-particles of different energies at high altitudes is of great interest.

14. The Outer Electron Belt

The experimental data (#6 and #7) show that there are significant differences in the structure and dynamics of proton and electron belts. Electrons with energies $\geqslant$ 100 keV form two distinctive belts, separated by a gap, as distinguished from the proton zone. The outer belt, which lies at L = 4.5 to 4.8, is an extremely nonstationary formation and undergoes great variations, the nature of which differ in different parts of the spectrum.

On the other hand, since the period of longitudinal drift of electrons in the outer zone have the same orders of magnitude as do those for the protons, it is clear that transfer ought to play a big role in the dynamics of the electron belt as well. /163

Known from experimentation is the fact that at the boundary of the trapped radiation region the average intensity of electrons with energies in the tens of keV is $\sim 10^7$ particles-cm^{-2}-sec^{-1}, and that the average energy is $\sim$ 25 keV [90]. If it is assumed, as in the case for protons, that the principal loss mechanism is ionization deceleration, it can be shown that transfer should lead to the formation of a strong peak of relativistic electrons when L < 2. If we take it that the field at the boundary is 50 to 70γ, and 4,000 to 8,000γ, when L $\sim$ 1.5 to 2 (that is, larger by a factor of 100), we find that the average energy in the region of the maximum would increase to 1 MeV. The intensity, which increases as L^{-4} with decrease in L, should reach $\sim 10^9$ cm^{-2}-sec^{-1}.

Since transfer undoubtedly does take place, the distribution of intensities of electrons in fact observed can be explained only by the presence of a non-Coulomb loss mechanism that reduces particle life significantly. The only possible mechanism of this type is the statistical interaction with the electromagnetic oscillations that results in the diffusion of the particles into pulse space, and, in particular, to their scattering in the dense layer of the atmosphere.

The discussion of the experimental data on the spectrum of high frequency electric and magnetic fields in the magnetosphere (#3) pointed out that the most probably mechanism providing for escape of electrons is "magnetic scattering," accompanied by no significant changes in particle energies. The sources of the waves causing the scattering can be the different processes taking place in the lower layers of the atmosphere (lightening discharges, acoustic oscillations, small-scale turbulence, and the like), or the instability in the radiation belts themselves. In the latter case scattering will be extremely effective because the unstable oscillations automatically have frequencies at which interaction with the particles is the most significant.

The structure of the electron belts can be interpreted in different /164
ways, depending on the nature of the wave sources. If it is taken that the causes of escape are the waves moving from the ionosphere, and that, as a result, the life of electrons is some specified function of L and of energy E, the outer belt maximum should be considered as a region in which the typical transfer time, in order or magnitude, corresponds to particle lifetime.

If this is the case, electron intensity in the inner zone can no longer be considered as resulting from transfer, and some other mechanism for the generation of particles in this region must be postulated. It might be acceptable, true enough, to suppose that in the inner belt the lifetime increases sharply, but data on decay from the artificial radiation belts refute this hypothesis.

On the other hand, if it is postulated that electron escape is the result of instability of the belts, the observed profile of the intensity should correspond to the stability boundary. Investigations of radiation belt stability (see Chapter V) shows that this viewpoint agrees with much of the experimental data, and is a basis for considering that this loss mechanism plays a main role, along with transfer, in the formation of electron belts. The possible effect of waves from outside sources, outside with respect to the belts that is, cannot yet be estimated because there are virtually no data on the spectrum of waves such as these.

Let us point out that the two approaches taken to the interpretation of electron escape from the belts are not in conflict. It can be shown, for example, that the occurrence of instability is associated only with a comparatively narrow section of the spectrum containing the main mass of electrons, and that the intensity in the region of higher energies is inadequate to build up the waves corresponding to them (see #19). At the same time, the high-energy electrons will be scattered because resonance conditions will change as waves are propagated along the field lines from the plane of the equator to the earth (wavelength and cyclotron frequency /165 increase, while the longitudinal velocity of the particle decreases). The lifetime of the high-speed particles will be determined in this case by the intensity of electrons with lower energies.

Noted in #4 was the fact that in the region of the outer electron belt are three groups of particles with significantly different properties; electrons with energies of several tens of keV, those with several hundred keV, and those with $\gtrsim$ 1 MeV.

Generally speaking, the dynamics of the electrons included in the first group cannot be included with the framework of the theory expounded because drift periods corresponding to energies $\sim$ 10 keV are several hours long. It is possible that the electric fields associated with ionospheric winds [57] ought to be taken into consideration when investigating the transfer of these particles.

The question of escape of electrons with energies of hundreds of keV and higher, has certain vague areas, but it is nevertheless possible to assert that the cause of their acceleration is transfer related to the effect of sudden pulses.

Electrons with energies of several hundred keV can be considered as a proton belt analog. Their sources are the electrons with energies of tens of keV at the magnetosphere boundary, the intensity and spectrum of which are relatively stable. Figure 30 shows a typical distribution of electrons with energies from 40 keV to $\sim$ 1 MeV, recorded by Elektron 2 and Explorer 18 (E_c > 40 keV)[89]. The particular loop passed through the east (morning) portion of the magnetosphere, where the real geomagnetic field is close to the dipole field. Analysis of the data obtained in the

course of a number of such passes shows that at the outer side of the belt the average energy of the electrons will change according to the adiabatic ratio (approximately as L^{-3}). On the night side, where the field attenuates much more rapidly than does the dipole field at great distances, the average energy rises with a decrease in the radial distance, and does so more rapidly than does L^{-3} [133].

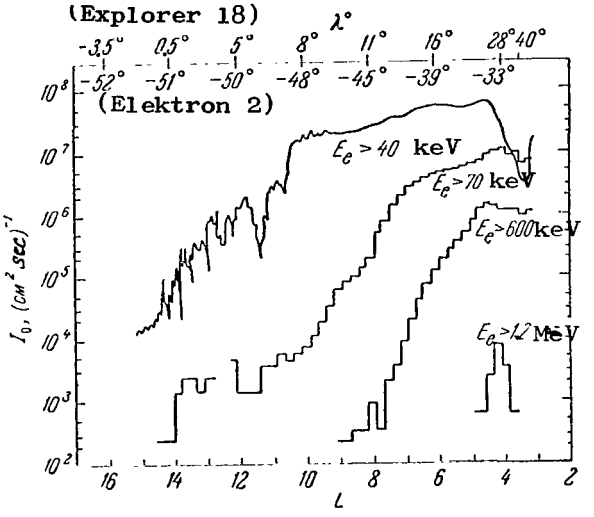

Figure 30. Electrons in the outer zone.

Figure 31 shows the dynamics /166 of the belt of electrons with energies > 200 keV in a period of moderate magnetic activity. This figure was constructed from data in [100]. See Figure 15 for the corresponding K_p values. Note that variations in intensity are relatively slight. The average value for the flux of electrons at the maximum $\bar{I}_0 \approx 2 \cdot 10^6$ cm^{-2}-sec^{-1}, changes from $0.5\bar{I}_0$ to $2\bar{I}_0$ as limits. The maximum itself is usually located between L = 4.2 and L = 4.8.

The variations during the period 28 January - 7 February 1963, can be explained by the fluctuations in the parameter D_0. The outer portion of the belt should remain unchanged, the maximum should shift toward the earth, and the intensity at the maximum should increase, when D_0 is increased and there are no changes in lifetime and conditions on the boundary. An analogous variation will take place when there is an increase in the lifetime, but no change in D_0 or in the conditions on the boundary. According to the above estimate that $D_0 \approx 5 \cdot 10^{-14}$ sec^{-1}, the typical transfer time when $L \approx 4.5$ is $(100\ D_0 L^8)^{-1} \approx 10^6$ sec $\approx$ 10 days, and corresponds to the time /167 over which the particular variation was observed.

The change in intensity between 14 and 28 February 1963, can be interpreted as the result of the increase in the power of the sources during

the moderate storm of 14 February (curve 4) and the return to the usual conditions when the storm was over.

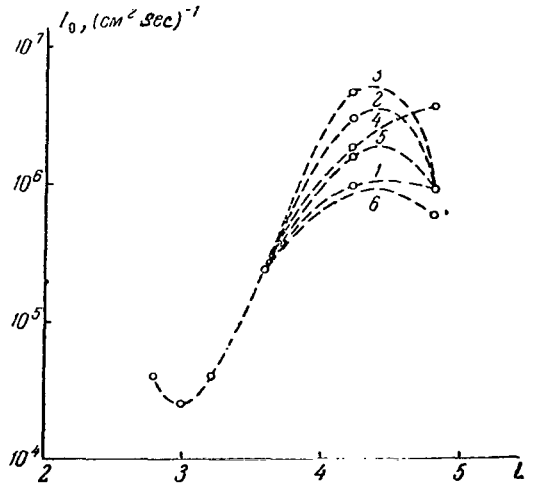

Figure 31. Dynamics of the belt of electrons with energies > 200 keV in a period of moderate magnetic activity.

1 - 28 Jan.; 2 - 1 Feb.; 3 - 7 Feb.; 4 - 14 Feb.; 5 - 21 Feb.; 6 - 28 Feb. 1963.

Figure 32 shows the variation that took place during the severe storm of 17 December 1962, as well as during the period following the storm (the figure was constructed from data in [100]). Prior to the storm (curve 1) the intensity at the maximum was 10^6 cm^{-2} · sec^{-1}. A sharp increase in intensity occurred at all $L \geqslant 3$ during the storm. The profile of the inner boundary of the belt that resulted corresponds to that of the diffusion wave at (11.21) (see Fig. 33), and the wave front is located at $L \approx 4$. /168

If the front had been propagated to L = 4, during the two day period (the storm's duration), the factor D_0 should have been $\frac{1}{120L_f^8\tau_D(L)} \approx 6 \cdot 10^{-13}$ sec^{-1} according to the equation at (11.2).

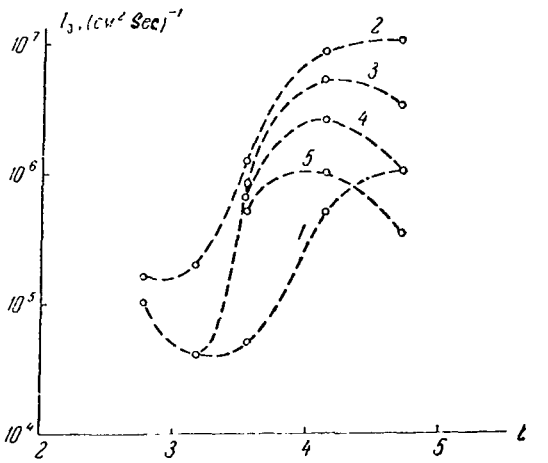

Figure 32. Variations in the belt of electrons with energies > 200 keV during a severe magnetic storm.

1 - 14 Dec.; 2 - 21 Dec.; 3 - 28 Dec.; 4 - 1 Jan.; 5 - 7 Jan. 1963.

Consequently an abrupt flare of intensity of electrons in the outer zone can be explained by the increase in D_0 during the storm by an order of magnitude, and by the simultaneous increase in the fluxes of electrons with energies in the tens of keV at the boundary. The latter effect was detected experimentally during these same passes through the outer zone by Explorer 14 [100]. So far as the tenfold increase in D_0 is concerned, all that is needed is one sudden pulse

with an amplitude of $\sim 40\gamma$, or several pulses $\sim 20\gamma$ during the storm.

There was a drop in intensity later on. A profile of intensity close /169 to that shown in Fig. 31 for moderate magnetic activity formed at the inner boundary ($L < 3.6$) during the week. No movement of the front toward the earth was observed, and it is natural to assume that the excess electrons in this region poured out into the ionosphere. The order of magnitude of the lifetimes of electrons with energies ~ 200 keV when $L < 3.6$ is some 10 days, according to these data.

Transfer serves to explain the evolution of the belt when $L > 3.6$. The intensity of the sources at the boundary decreased after the storm, and transfer led to the excess electrons being washed out of the belt. As will be seen from the figure, the front of an evacuation diffusion wave such as this reaches the $L \approx 4$ shell in 20 days. The value $D_0 \approx 5 \cdot 10^{-14}\ \text{sec}^{-1}$ corresponding to this parameter is equal to the average D_0 value, found earlier in many of the other data.

The experimental data on the electrons in the outer zone with energies on the order of hundreds of keV thus agree well with the transfer conception. In any case, up to this point there has never been a result that could lead to basic difficulties.

Now let us review the data on relativistic electrons. Most of the results obtained in this portion of the spectrum involve energies larger than 1.6 MeV. The intensity of electrons with energies > 5 MeV in the outer belt apparently does not exceed the cosmic ray background ($\sim 10\ \text{cm}^{-2} \cdot \text{sec}^{-1}$). At the same time, the fluxes of electrons with energies > 1.6 MeV when $L = 4$ to 5 often reach a magnitude of $\sim 10^6\ \text{cm}^2 \cdot \text{sec}^{-1}$. This is why the relativistic electrons observed in the outer zone have a very soft spectrum (extrapolation by the exponential law e^{-E/E_0} gives an average energy of $E_0 \leqslant 300$ keV). If it is taken that these electrons too occur as a result of transfer from the boundary of the trapped radiation region (where the field is $\sim 50\gamma$), the initial particle energy should be /170 300 to 500 keV. The intensity of the electrons with these energies at the boundary of the belts does not usually exceed the cosmic ray background. Electrons such as these are often observed during magnetic storms [116], however.

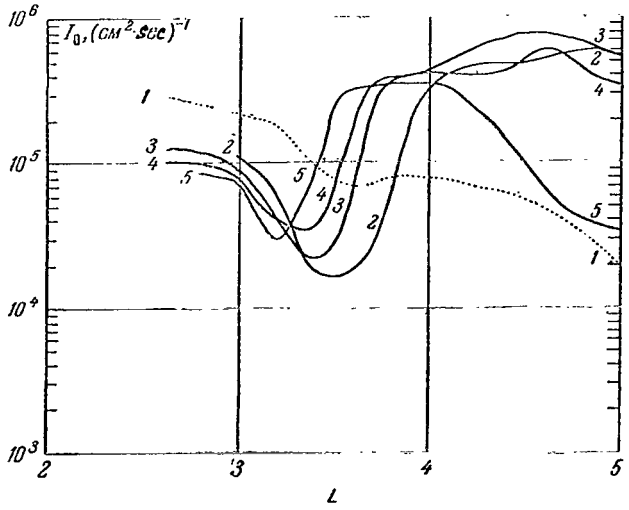

Figure 33. Example of a diffusion wave of relativistic electrons in the outer zone.

1 - 7 Dec.; 2 - 20 Dec.; 3 - 23 Dec.; 4 - 29 Dec. 1962; 5 - 8 Jan. 1963.

This fact appears in the special features associated with the dynamics of outer zone relativistic electrons. During lengthy periods of low magnetic activity (during the first months of the flights of Elektron 1 and Elektron 2, for example), the fluxes of electrons with energies above 1 MeV are low ($\sim 10^4$ cm^{-2} · sec^{-1} at the outer zone maximum). After several magnetic storms there are powerful peaks of relativistic electrons, the intensities of which reach 10^6 cm^{-2} · sec^{-1} when $L \sim 5$. If storms follow each other at $\lesssim$ 10 day intervals, the picture becomes very complicated. The peak apparently disappears during the storm, and a new maximum is formed when the storm is /171 over.

A diffusion wave will be observed if the magnetic activity is low for one month after a storm. One such phenomenon is described in [100]. Fig. 33 [100] is the profile of intensity of electrons with $E > 1.6$ MeV in the plane of the equator for December 1962-January 1963. Explorer 14 recorded two other diffusion waves, and these have been analyzed in [109]. An analogous phenomenon was observed in the high geomagnetic latitudes in the course of the investigations made by the Soviet Cosmos 41 [134].

Since the injection of electrons with subrelativistic energies at the boundary of the belts is pulse-like in nature, these diffusion waves belong

to the type at (11.37). The basic difference between the experimental results and the relationship at (11.37) is that in the real wave the intensity at the maximum is a decreasing function of time. This is quite natural when the losses are those with a typical time of $\tau_s \sim 10$ days.

This is the basis for the supposition that lifetime of relativistic electrons, τ_s, in the outer zone has little dependence on L (when $L < 4$ in any case). If so, and if losses are taken into consideration, the diffusion wave can be described, approximately, by the expression at (11.37) multiplied by e^{-t/τ_s}, while the movement of the maximum, and of the leading and trailing edges of the wave can be established through the relationships at (11.40)-(11.45), as usual.

The velocity of the leading edge when $D_0 = 5 \cdot 10^{-14}$ sec^{-1} is $V_f = L_f \approx 1.5 \cdot 10^{-7} L^9$ (a/day). Fig. 34 shows this (the solid curve), as well as the plot of the experimental data from [109]. The $L > 3$ points correspond to the diffusion waves observed by Explorer 14, while the $L \sim 2$ point is the rate at which the second maximum for the high-energy protons is shifted (see #10). We see that the law for the change in $L_f(L)$, as well as the absolute magnitude of the rate, agree well with the theoretical result. /172

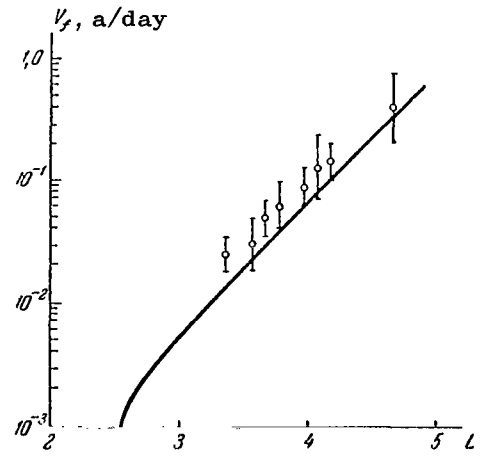

Figure 34. Theoretical and experimental data on the diffusion wave's leading edge velocity in terms of L.

Now let us consider the data in [134]. There was a maximum of electrons with energies > 2 MeV two days after the storm of 7-8 September 1964, when $L = 5.5$. It has shifted to $L \approx 5$ 5 in 10 days, and to $L = 4.3$ in 20 days. The position of the maximum, in accordance with the equation at (11.41) ($\gamma \approx 15$), can be established by $L_m = \left(\frac{1}{120 D_0 t}\right)^{1/8}$, from whence $D_0 = \frac{1}{120 L_m^8 t}$. Substituting numerical values L_m for t, we find that $D_0 \approx 5 \cdot 10^{-14}$ sec^{-1} (at the 2 and 20 day points), and that $D_0 \approx 3 \cdot 10^{-14}$ sec^{-1} (t = 10 days).

The data in [134] therefore confirm our estimates for the constant D_0 and show that at the end of 1964, this magnitude had the same value as it did at the end of 1962, beginning of 1963 [109].

Investigation of diffusion waves results in the direct determination /173 of D_0. Since these results lead to the same D_0 magnitude as does the analysis of the structure of the proton belt, the estimate for the average density of the cold atmosphere ($N = 10^3$ cm^{-3}) cited in #10, is confirmed.

The close coincidence in D_0 values, found in the different experimental data in the $1.5 \leqslant L \leqslant 6$ region, shows that sudden pulses actually are the basic mechanism for the acceleration of particles in the earth's radiation belts. And the experimental data also show that electron escape is not linked with Coulomb collisions, but occurs much more rapidly. The next chapter is devoted to a study of the nature of escape.

Chapter V

Radiation Belt Stability

15. Present Status of the Radiation Belt Stability Problem

Numerous investigations reveal that the only time unbound hot plasma /174
is stable in a magnetic field is when very rigid conditions are met. The only practically reliable way to guarantee stability is to find the ion and electron distribution functions in terms of particle energy. Some slight spatial heterogeneity of the plasma, or anisotropy in the angular distribution of particles, will result in intensification of the electric and magnetic fields in terms of time.

The development of instability is usually characterized by the increment γ, the inverse time of rise of the amplitude by a factor of e. The magnitude γ can be established by using very different plasma characteristics, depending on the principle involved in the occurrence of instability.

Magnetohydrodynamic and drift instabilities are among the comparatively slow, large-scale, instabilities. Magnetohydrodynamic instability is the analog of heat convection (for a detailed survey see [59]). Diamagnetic forces, working to eject the hot plasma into a weaker field region, play the role of the force of gravity. The physical mechanism involved in the development of convection instability is that of the increase in the electric polarization of the nonuniform plasma versus time. The electric field causes particle drift into a weaker field region in the case of instability. /175

According to [59], convective instability takes place in the dipole field when the plasma pressure decreases from L more rapidly than L^{-8}. If the geomagnetic trap is filled with particles because of transfer from the boundary caused by sudden pulses, particle density diminshes as L^{-4}, and average particle energy diminishes as L^{-3} (see #11). Consequently, pressure P will change as L^{-7}, and the plasma formed by this mechanism is convectively stable.

Spatial heterogeneity, in addition to causing convective instability, leads to the development of what are known as drift instabilities, during which waves with phase velocities equal to the current velocity for some

group of particles in the trap, build up. This type of instability is similar to that studied in the case of the slightly heterogeneous field. It can be shown that drift instabilities will develop at very much shallower pressure gradients than will convective instabilities [136].

The development of very much higher speed instabilities takes place as a result of certain special features of the particle distribution function. If, for example, there are, in an electron component, two or more groups of particles that are on the whole moving relative to each other (there are electron beams), the buildup of Langmuir oscillations with an increment on the order of the electron plasma frequency will begin. Electrostatic oscillations, with an increment on the order of the ion plasma frequency, also will build up when there is relative movement of electrons and ions at a velocity in excess of the electron sound velocity. There are a number of other variants of beam instability, summaries of which can be found in [137] and [138].

Anisotropy in the angular distribution of particles too will result in instability. When a magnetic field is present, electromagnetic waves, the frequency and polarization of which are determined by the nature of the anisotropy and by the particle velocity spectrum, are generated.

All instabilities, other than convective, are resonant in nature. /176
Participating in the buildup of the waves are particles, the velocities of which are near the wave's phase velocity (the Cherenkov resonance), or particles that are in cyclotron resonance with the wave when there is an external magnetic field.

Waves are always subject to energy losses in bounded systems. These losses are the result of radiation, dissipation at the boundary, etc. Development of instability is stabilized to some degree as a result. But there are certain critical values of the total number of hot particles below which (for a specified configuration of field and plasma) losses of wave energy exceed the rate at which energy is transferred from the plasma to the wave.

Today we can say that considerable progress has been made in the theory of plasma instability, and we can also say that present-day methods of

plasma physics are such that we cannot only establish the boundary of stability, but we can also investigate the dynamics involved in the development of instability in the case of super-critical concentration of plasma, taking into consideration the inverse effect of the waves on particles, and the nonlinear interaction of waves with each other [83, 140, 141]. This approach is possible in a linear approximation when there is a definite link between the frequency and the wave vector, and the increment of instability is small compared with the frequency. In the case of hydrodynamic turbulence, however, this particular approximation is inapplicable because here the dispersion law is determined by what are substantially nonlinear processes.

The plasma in the radiation belts is substantially nonuniform and anisotropic. It can therefore be expected that the plasma will prove to be unstable. The study of belt stability has begun to draw more and more attention in recent years. Drift instability of the proton belt, and cyclotron instability (associated with the anisotropy in the angular distribution) investigations are of greatest interest. Beam instabilities can play a known role at low altitudes, where the fluxes of electrons incident to the ionosphere when electron throw out is heavy, are considerably in excess of those reflected. There are no beams at high altitudes, however. /177

Chang, Pearlstein, and Rosenbluth made a detailed study of the drift instability of the proton zone [139]. This paper investigated the buildup of large-scale electrostatic oscillations of the magnetosphere. It was taken that the electric field is normal to the magnetic field at high altitudes because of the high degree of conductivity along the field lines, and the dissipation of currents in the ionosphere was taken into consideration. Once a stability criterion was established, the distribution of proton pressure was taken as close to the true pressure (pressure $P \sim L^{-6}$). The final result is in the form

$$n_{crit} \approx N_{ion} \frac{\Delta a}{2\pi a} L^{-1/2} \frac{m}{\sqrt{(L-1)(4L-3)}}, \qquad (15.1)$$

where n_{crit} is the critical density of the high-speed protons;

a is the radius of the earth;

$\Delta a \approx 5 \cdot 10^6$ cm is the thickness of the layer of the ionosphere in which dissipation takes place;

N_{ion} is the density of cold electrons in this layer;
$m \geq 1$ is the harmonic number (the solution was sought in the form $\sim e^{im\varphi}$, where φ is the longitude).

On the illuminated side of the earth $N_{ion} \approx 2 \cdot 10^5$ cm^{-3}, which is two orders of magnitude higher than the observed concentration. The critical concentration is significantly lower in the case of the night ionosphere parameters ($N_{ion} \approx 5 \cdot 10^3$ cm^{-3}). However, when estimating the stability of the large-scale disturbances ($m \sim 1$), it is obvious that the average longitudinal value $N_{ion} \approx 10^5$ cm^{-3}, must be taken.

Analysis of drift instability of the proton belt [139] therefore leads to the conclusion that the fluxes of high-speed protons observed in this region are well below the critical fluxes. Electric field drifts that occur during disturbances are scattered rapidly through the ionosphere. This conclusion agrees well with the results in #13, and what follows is that proton escape is linked primarily with ionization losses.

/178

Cyclotron instability, associated with anisotropy in the angular distribution of plasma particle velocities in a magnetic field, was forecast theoretically by R. Z. Sagdeyev and V. D. Shafranov [142] and was then observed experimentally in magnetic trap experiments [143, 144]. This instability, as applicable to radiation belts, was reviewed in [17-20]. A model with a homogeneous field was investigated in [17, 18]. Particle escape into the ionosphere was modeled by introducing a forbidden cone. It was assumed that waves incident to the ionosphere were completely absorbed. The problem of electron throw-out was solved in a quasilinear approximation (that is, with the inverse effect of waves on particles taken into consideration). The results [18] show that instability is very effective when maximum fluxes of electrons with energies on the order of several keV are observed in the belts. During the time it takes a wave to follow its path along the field line its amplitude rises from the level of the thermal noise to the magnitude reached for the scattering of electrons with an energy of $\sim$ 10 keV at an angle of $\sim \pi$. It follows, therefore, that cyclotron instability can play an important role in the dynamics of the Earth radiation belts.

The boundary of the cyclotron instability for real radiation belts, with the field heterogeneity and the ionospheric absorption taken into consideration, was investigated in [19, 20]. It was found that the critical intensity-L distribution corresponded quite accurately with the true profile of the electron belts. Specifically, the gap between the outer and inner belts corresponds to the minimum for ionospheric absorption of waves built up by high-speed electrons.

The principal results set forth in [19, 20] are presented below.

16. Basic Equations

Cyclotron instabilities are the result of waves and particles being in resonance at the Larmor frequency, with the Doppler effect considered. And in the case of soft particle spectra, the waves that are built up most /179 readily are those for which the wave vector, k and the group velocity, u_g, are parallel to the field line (see [138], p.75, for example). This geometry has resonance in the form

$$ckP_{\parallel} - \omega = \Omega, \tag{16.1}$$

where k and ω are the wave vector and the wave frequency, respectively;

$\Omega = \frac{qH}{\mu c}$ is the cyclotron frequency for a nonrelativistic particle;

μ and q are its mass and charge, respectively;

c is the speed of light;

$P_{\parallel}$ is the pulse component parallel to the field.

Here, and henceforth, we will take it that the pulse is measured in μc units, and that P is thus a dimensionless magnitude.

The resonant interaction of the particles with the wave reduces to absorption when there is an isotropic angular distribution of particles. If the angular distribution is anisotropic, however, instability will develop in an infinite plasma when particles, as high-speed as desired, are present. According to [142], unstable waves have circular polarization, and the manner of their build up depends on the direction of rotation of the electric field vector and on the nature of the anisotropy. If $\overline{\varepsilon}_{\perp} > \overline{\varepsilon}_{\parallel}$ ($\overline{\varepsilon}_{\perp}$ and $\overline{\varepsilon}_{\parallel}$ are the average energies of the longitudinal and transverse movements), and this is so in the belts, the protons build up to an Alfvén wave, the vector E for which rotates laterally with respect to the Larmor rotation of the protons, and the electrons build up to a

high-speed magnetic sound wave, in which the direction of rotation of the vector E is in the opposite direction. If there are, at one and the same time, protons and electrons that satisfy the condition of resonance at (16.1), when $\bar{\varepsilon}_\perp > \bar{\varepsilon}_\parallel$, the electrons will hamper the build-up of the Alfvén wave, the protons will hamper the build-up of the high-speed magnetic sound wave, the resultant effect must then be established by taking both plasma components into consideration.

Since the ratio of cyclotron absorption to build-up speed when $\frac{\varepsilon_\perp - \varepsilon_\parallel}{\varepsilon_\perp} \sim 1$ can be established by the magnitude of $\frac{\omega}{\Omega - \omega}$, frequencies $\omega \ll \Omega$ are of great interest, at least from the point of view of instability. As a practical matter, ω can be omitted when $\omega < \Omega/3$ in the resonance condition, and the dispersion equations for waves can be greatly simplified. We obtain ($\omega \ll \Omega_H$) /180

$$\omega = ku_a, \tag{16.2}$$

for Alfvén waves, where $u_a = \frac{H}{\sqrt{4\pi\rho}}$ is the Alfvén velocity. For a high-speed magnetic sound wave in the range $\omega_H \gg \omega \gg \Omega_H$

$$\omega = \omega_H \frac{c^2 k^2}{\omega_0^2}, \tag{16.3}$$

and when $\omega \lesssim \Omega_H$

$$\omega = ku_a. \tag{16.4}$$

Here ω_H and Ω_H are used to designate the Larmor frequencies for electrons and ions (more precisely, the absolute magnitudes of these frequencies), and $\omega_0 = \sqrt{\frac{4\pi e^2 N}{m}}$ is used to designate the plasma frequency. The magnitudes of e and m are electron charge and mass, respectively, and N is the number of cold electrons per cm^3.

The major contribution to the build-up of a wave with specified frequency in the case of soft spectra is made by the region near the equator, where field intensity on the field line is minimal: then resonance with particles of lesser energies is possible, as will be seen from the equation at (16.1). Therefore, without embarking on a detailed analysis, it is possible to make a number of estimates of the order of magnitude of the frequencies and lengths of the waves that are most dangerous from the instability standpoint. The following numerical values will be used for the estimates:

the magnetic field at the earth's equator is $H_e \approx 0.3$ gauss; the Larmor frequencies of the ions and electrons in the plane of the equator are $\Omega_H = \Omega_{H_0} L^{-3} \approx 3 \cdot 10^3 L^{-3}$, $\omega_H = \omega_{H_0} L^{-3}$, $\omega_0^2 = \text{constant} = 3 \cdot 10^{12}$ sec^{-2}, $u_a = u_o L^{-3} = 2 \cdot 10^9 L^{-3}$. The values ω_0^2 and u_a correspond to a cold plasma density of $N = 10^3$ cm^{-3}.

Let us consider the outer proton zone. At the maximum ($L \sim 3$ to 4) $c\overline{P} \sim 10^9$ cm-sec^{-1} $\gg u_a \approx 5 \cdot 10^7$ cm-sec^{-1}, such that the resonant frequency $\omega = \Omega_H \frac{u_a}{c\overline{P}}$ [see the equations at (16.1) and (16.2)] is much less than Ω_H, and is several radians per second in order of magnitude. The inner zone ($L \lesssim 2.5$) contains electrons with $\overline{P} \sim 1$. What derives from the equations at (16.1) and (16.3)is that $\omega \approx 4 \cdot 10^7 L^{-9}$ sec^{-1} everywhere lies in the interval $\omega_H \gg \omega \gg \Omega_H$, so that the use of the relationship at (3.16) is justified. However, in the outer zone ($L \sim 4$) the relativistic electrons ($P \approx 4$) build up much lower frequencies ($\sim$ 20 rad/sec), less than Ω_H. It can be proven that for all frequencies of interest the approximation of geometric optics is applicable with a high degree of accuracy everywhere except in the lower layers of the ionosphere. /181

Reviewed here are waves for which the wave vector, k, and the group velocity, u_g, are directed along the magnetic field lines (only in the ionosphere is the vector k deflected from the direction of the field and does it approach the vertical, the result of the sharp increase in the index of refraction). The existence of waves such as these in systems with curved field lines is not a trivial fact. But in the case of the magnetosphere waves of this type do exist, because at conjugate points (at opposite ends of a field line) one often observes repeated echoes of lightning discharges (so-called whistling atmospherics), the frequency ranges of which (1 to 10 kHz) correspond to the high-speed magnetic-sound waves. What follows from the Hamilton equations

$$\mathbf{r} = \mathbf{u}_g = \frac{\partial \omega}{\partial \mathbf{k}}; \quad \mathbf{k} = -\frac{\partial \omega}{\partial \mathbf{r}}; \quad \omega = \frac{e}{mc} \frac{k\,(\mathrm{kH})}{\omega_0^2}$$

is that if u_g is directed along a field line the vector k should have this same direction. There apparently are density nonuniformities at high altitudes that create unique waveguides in which the index of refraction is only dependent on the coordinates along the field line [145]. Waveguides in which the wave vector for the Alfven waves too is directed

along the field lines (u_g is always oriented along H in the case of Alfvén waves) can exist when there is this stratification.

Let us introduce an orthogonal coordinate system, x, y, z in which the lines x = constant and y = constant coincide with the beam trajectories, while z is the length of the arc of these lines read from the plane of the equator. Since the beam trajectories everywhere above the ionosphere coincide with the field lines, the Lame parameters h_x, h_y, $h_z = 1$, satisfy the obvious relationship $h_x h_y = \eta^{-1}(z)$, where $\eta(z)$ is the ratio of the magnetic field intensity, H(z), at the given point on the field line to the field, H_0, when z = 0. We note that in the dipole field, $\eta(z)$ is expressed in terms of the polar angle, θ, read from the magnetic axis, and does not depend on L

/182

$$\eta = \frac{\sqrt{1+3\cos^2\theta}}{\sin^6\theta}. \tag{16.5}$$

The Maxwell equations for transverse waves, the parameters of which depend only on z and on t (as $e^{i\omega t}$), reduce to

$$\operatorname{rot}\operatorname{rot}\mathbf{E} = \frac{4i\pi\omega}{c^2}(\mathbf{j}_0 + \mathbf{j}), \tag{16.6}$$

where j_0 is the cold particle current density;

j is the high-speed particle current density (we ignore the displacement current). The equation at (16.6) in components has the form

$$\left.\begin{aligned} \frac{1}{h_y}\frac{\partial}{\partial z}\frac{h_y}{h_x}\frac{\partial}{\partial z}h_x E_x &= \frac{4i\pi\omega}{c^2}\{\sigma_0 E_x + \sigma_H E_y + \hat{\sigma}_0 E_x + \hat{\sigma}_H E_y\}, \\ \frac{1}{h_x}\frac{\partial}{\partial z}\frac{h_x}{h_y}\frac{\partial}{\partial z}h_y E_y &= \frac{4i\pi\omega}{c^2}\{-\sigma_H E_x + \sigma_0 E_y - \hat{\sigma}_H E_x + \hat{\sigma}_0 E_y\}, \end{aligned}\right\} \tag{16.7}$$

where

h_x, h_y, are Lame parameters;

σ_0 and σ_H are the diagonal and Hall components of the conductivity tensor;

$\hat{\sigma}_0$ and $\hat{\sigma}_H$ are the corresponding operators describing the high-speed particle current.

We will take it that in the geometric optics approximation the operators $\hat{\sigma}_0$ and $\hat{\sigma}_H$ act on the phase of the wave only. Let us make the substitution

$$\mathbf{E} = \sqrt{\eta}\,\psi = \frac{\psi}{\sqrt{h_x h_y}}$$

and let us retain only the zero terms and the terms of the first order

of smallness in the "quasiclassical" expansion at (16.7) (that is, the terms with $\frac{\partial^2\psi}{\partial z^2}$ and $\frac{\partial\psi}{\partial z}$); the result we obtain is /183

$$\left.\begin{aligned}\frac{\partial^2\psi_x}{\partial z^2} &= \frac{4i\pi\omega}{c^2}\{\sigma_0\psi_x + \sigma_H\psi_y + \hat{\sigma}_0\psi_x + \hat{\sigma}_H\psi_y\},\\ \frac{\partial^2\psi_y}{\partial z^2} &= \frac{4i\pi\omega}{c^2}\{-\sigma_H\psi_x + \sigma_0\psi_y - \hat{\sigma}_H\psi_x + \hat{\sigma}_0\psi_y\},\end{aligned}\right\} \qquad (16.8)$$

from whence it will be seen that the system at (16.8) is the solution for the type of waves with circular polarization $\psi_x = \psi$; $\psi_y = \pm i\psi$, and the function ψ is satisfied by the equation

$$\frac{\partial^2\psi}{\partial z^2} = \frac{4i\pi\omega}{c^2}\{(\sigma_0 \pm i\sigma_H)\psi + (\hat{\sigma}_0 \pm i\hat{\sigma}_H)\psi\}. \qquad (16.9)$$

Bear in mind that the factors σ_o and σ_H depend on the direction of rotation of the plane of polarization to the extent that both signs in front of ψ_y are permissible only when $\omega < \Omega_H$. When $\omega > \Omega_H$ only waves with $\psi_y = -i\psi_x$, in which the rotation corresponds to the Larmor rotation for the electrons, exist. (For a detailed analysis of the properties of waves, traveling waves, and magnetic field, see [146], p. 28).

In the range of frequencies $\omega \ll \Omega_H$ and $\Omega_H \ll \omega \ll \omega_H$, the Equation at (16.9) can be written in the form

$$\frac{\partial^2\psi}{\partial z^2} + k_0^2 q^2(z)\psi = \frac{4i\pi\omega}{c^2}(\hat{\sigma}_0 \pm i\hat{\sigma}_H)\psi, \qquad (16.10)$$

where $k_0^2(\omega)$ is the wave number corresponding to the frequency, ω, in the equatorial plane, and the dimensionless factor $q(z)$ describes the change in the index of refraction with z.

Since the concentration of high-speed particles in the belts is low, and their pressure is many times less than $H^2/8\pi$, they cause no significant changes in the relationship between ω and k. Hence the high-speed particle current can be considered as a small disturbance. In the zero approximation, we have

$$\frac{\partial^2\psi}{\partial z^2} + k_0^2 q^2(z)\psi_0 = 0. \qquad (16.11)$$

The geometric optics approximation is correct everywhere except in the lower regions of the ionosphere, and the solution of the equation at /184 (16.11) is in the form

$$\psi_0 = \frac{1}{\sqrt{q}}\left\{A\exp\left(ik_0\int_0^z q(\zeta)\,d\zeta\right) + B\exp\left(-ik_0\int_0^z q(\zeta)\,d\zeta\right)\right\}. \qquad (16.12)$$

If the coordinates of the effective boundaries of the region in which the conditions of applicability of geometric optics are not met are designated by $\pm l$, the solution near these boundaries will be in the form

$$\psi_{\substack{0\\ z\to l}} = \frac{1}{\sqrt{q}}\left\{A\exp\left[ik_0\int_0^l q(\zeta)\,d\zeta - ik_0 q(l)(l-z)\right] + \right.$$
$$\left. + B\exp\left[-ik_0\int_0^l q(\zeta)\,d\zeta + ik_0 q(l)(l-z)\right]\right\}, \qquad (16.13)$$
$$\psi_{\substack{0\\ z\to -l}} = \frac{1}{\sqrt{q}}\left\{A\exp\left[-ik_0\int_0^l q(\zeta)\,d\zeta + ik_0 q(l)(l-z)\right] + B\exp\left[ik_0\int_0^l q(\zeta)\,d\zeta - ik_0 q(l)(l-z')\right]\right.$$

(in the second equality we have put $z' = -z$, and have taken into consideration the evenness of the function $q(\zeta)$).

Let us suppose that we know the exact solution to the problem of the reflection of a plane wave that flows from a region with an index of refraction N = constant, corresponding to $q(l)$, from the lower layers of the ionosphere, from the neutral atmosphere, and from the surface of the earth. The factors A and B in the equations at (16.13) can each be expressed in terms of the other by changing the phase $\Phi(\omega)$ and the reflection factor $R(\omega)$. Since the solution will be sought in the form $\sim e^{i\omega t}$, the term with A in the first equation at (16.13) describes the reflected wave, and the term with A in the second, the incident wave.

We have, therefore

$$Ae^{ik_0\int_0^l q(\zeta)\,d\zeta} = \sqrt{R}\,e^{i\Phi}Be^{-ik_0\int_0^l q(\zeta)\,d\zeta},$$
$$Be^{ik_0\int_0^l q(\zeta)\,d\zeta} = \sqrt{R}\,e^{i\Phi}Ae^{-ik_0\int_0^l q(\zeta)\,d\zeta}, \qquad /185$$

from whence flows the following "quantization rule"

$$e^{2ik_0\int_0^l q(\zeta)\,d\zeta} = Re^{2l\Phi}e^{-2ik_0\int_0^l q(\zeta)\,d\zeta}$$

or

$$k_{0n} = \left(\frac{n\pi + \Phi(\omega)}{2} - \frac{i}{4}\ln R(\omega)\right)\cdot\left(\int_0^l q(\zeta)\,d\zeta\right)^{-1}. \qquad (16.14)$$

The eigenfunctions ψ_{0n} accordingly have the form

$$\psi_{0n} = \frac{A_n}{\sqrt{q}}\begin{cases}\cos\left(k_{0n}\int_0^z q(\zeta)\,d\zeta\right),\\ \sin\left(k_{0n}\int_0^z q(\zeta)\,d\zeta\right).\end{cases} \qquad (16.15)$$

The decrement

$$\delta_n = \frac{\partial \omega}{\partial k} \operatorname{Im} k_n = \frac{1}{2T_n} \ln \frac{1}{R}, \tag{16.16}$$

where

$$T_n = \left(\frac{\partial \omega}{\partial k}\right)^{-1}_{k=k_n} \int_{-l}^{l} q(z)\, dz \tag{16.17}$$

is the time required for the wave packet with average frequency ω_n to move between the reflection points [$(\partial\omega/\partial k)(1/q(z))$ is the packet's group velocity]. The result at (16.16) has a clear physical import; after m reflections, the amplitude of the wave is reduced by a factor of $(\sqrt{R})^{-m} \approx e^{(1/2T)(\log 1/R)}$. Attenuation also takes place when $\partial\omega/\partial k < 0$, /186 since $R > 1$.

In fact, the incident and reflected waves are characterized by the symbol k in the determination of R. When $\partial\omega/\partial k < 0$, the flux of energy is directed opposite to k, so the incident wave is reflected from the point of view of the transfer of energy, and therefore has less amplitude.

The functions of ψ_{On} yield approximate values for the precise functions in the region above the lower boundary of the ionosphere. Given these conditions, the precise functions satisfy the equation at (16.11) (remember that in deriving (16.11) from (16.1) we ignored the second derivative of η; clearly, consideration of the field heterogeneity in the region between the earth's surface and the ionosphere will provide only negligibly small corrections). Precise functions of ψ_n vanish when $z = \pm z_0$; that is, at the earth's surface. By using this boundary condition, and the equation at (16.11), it can be proven quite readily that ψ_n is orthogonal with weight $q^2(z)$. Hence, the perturbation theory can be used in computing increments. At the same time, it is sufficient to use the approximate functions of ψ_{nO}, for the concrete computations of matrix elements because high-speed particle currents flow at high altitudes.

Therefore, from the equation at (16.10)

$$\delta k^2 = \frac{4i\pi\omega}{c^2} \frac{\int_0^t \psi_{n0}(z)(\hat{\sigma}_0 \pm i\sigma_H)\psi_{n0}(z)\, dz}{\int_0^t \psi_{n\eta}^2(z)\, q^2(z)\, dz} \tag{16.18}$$

and

$$\delta\omega = \frac{1}{2k}\frac{\partial\omega}{\partial k}\delta k^2, \tag{16.19}$$

so that in order to compute the increments it is necessary to determine the operators for the conductivity tensor, occasioned by the high-speed particles. Let us consider this problem in the relativistic case. /187

As before, we will designate particle charge and mass by Q and μ, making no distinction between ions and electrons. Since the z axis is selected in the direction of the field, $H > 0$, and the cyclotron frequency, Ω, has the same sign as Q. The distribution function will depend on the pulses, measured in μc units. The undisturbed function $F(P_z, P_\perp, z)$ can be considered even for P_z.

The kinetic equation for the disturbed function f in cylindrical coordinates P_z, $P_\perp$, and φ in pulse space is in the form

$$\begin{aligned} i\omega\varepsilon f + cP_z\frac{\partial f}{\partial z} - \Omega\frac{\partial f}{\partial\varphi} &= -\frac{Q}{\mu c}\left\{\varepsilon\left[(E_x\cos\varphi + E_y\sin\varphi) - \right.\right. \\ &- \left.\frac{icP_z}{\omega}(E_x\cos\varphi + E_y\sin\varphi)\right]\frac{\partial F}{\partial P_\perp} + \\ &+ \left.\frac{icP_\perp}{\omega}\frac{\partial F}{\partial P_z}\frac{d}{dz}(E_x\cos\varphi + E_y\sin\varphi)\right\} \end{aligned} \tag{16.20}$$

(here we have used the relationship $h = ic/\omega \operatorname{rot} E$, and have set $\varepsilon = \sqrt{P^2+1}$). For circular polarization ($E_x = E$, $E_y = \pm iE$), we have

$$\begin{aligned} &i\omega\varepsilon f + cP_z\frac{\partial f}{\partial z} - \Omega\frac{\partial f}{\partial\varphi} = \\ &= -\frac{Q}{\mu c}\left\{\left(\varepsilon E - \frac{icP_z}{\omega}\frac{dE}{dz}\right)\frac{\partial F}{\partial P_\perp} + \frac{icP_\perp}{\omega}\frac{dE}{dz}\frac{\partial F}{\partial P_z}\right\}e^{\pm i\varphi}, \end{aligned} \tag{16.21}$$

from whence it follows that the functions of $f = f_0 e^{\pm i\varphi}$, and that f_0 is satisfied by the equation

$$\begin{aligned} &cP_z\frac{\partial f_0}{\partial z} + i(\varepsilon\omega \pm \Omega)f_0 = \\ &= -\frac{Q}{\mu c}\left\{\left(\varepsilon E - \frac{icP_z}{\omega}\frac{dE}{dz}\right)\frac{\partial F}{\partial P_\perp} + \frac{icP_\perp}{\omega}\frac{dE}{dz}\frac{\partial F}{\partial P_z}\right\}. \end{aligned} \tag{16.22}$$

The components of the current density, $j = Q\int vf\, d^3P$ can thus be expressed by the magnitude /188

$$j = Qc\pi\int_0^\infty\int_{-\infty}^\infty f_0\frac{P_\perp^2}{\varepsilon}dP_z\,dP_\perp. \tag{16.23}$$

That is, $j_x = j$, $j_y = \pm ij$. In the geometric optics approximation

$$\left(E = \mathscr{E}(z)\,e^{ik_0\int_0^z q(\zeta)\,d\zeta}\right)$$

$$j = \frac{i\pi Q^2}{\mu}E\int_0^\infty\int_{-\infty}^\infty\frac{\dfrac{\partial F}{\partial P_\perp^2} + \dfrac{ckP_z}{\omega\varepsilon}\left(\dfrac{\partial F}{\partial P_\perp^2} - \dfrac{\partial F}{\partial P_z^2}\right)}{ckP_z + \omega\varepsilon \pm \Omega}P_\perp^2\,dP_z\,dP_\perp^2. \tag{16.24}$$

In order to compute the increment, we must find the real part of (16.24), and this can be determined by bypassing the singularity of the denominator. Putting

$$E=\frac{A_n}{\sqrt{q}}\cos k_n\int_0^z q(z)\,dz,$$

we obtain $\operatorname{Im} j_n=-\frac{\pi^2Q^2}{\mu ck}\frac{A_n}{\sqrt{q^3}}\cos k_n\int_0^z q(\zeta)\,d\zeta\times$

$$\times\int_0^\infty\left[\frac{\partial F}{\partial P_\perp^2}\pm\frac{\Omega}{\omega_n\varepsilon}\left(\frac{\partial F}{\partial P_\perp^2}-\frac{\partial F}{\partial P_z^2}\right)\right]P_\perp^2\,dP_\perp^2,\qquad P_z=\frac{\Omega}{ckq(\zeta)}$$

(for purposes of simplicity, we have put $\omega\ll\Omega$). An analogous result is obtained for the case of odd functions. From whence it is easy to find the matrix element of the magnitude $\frac{4l\pi\omega}{c^2}(\hat{\sigma}_0+i\hat{\sigma}_H)\psi=\frac{4i\pi\omega}{c^2}\sqrt{\eta}j$ and

$$\operatorname{Im}\delta k^2=\frac{4\pi^3Q^2\omega}{\mu c^3\Lambda k}\int_0^l\int_0^\infty\left[F\pm\frac{\Omega P_\perp^2}{\omega\varepsilon}\left(\frac{\partial F}{\partial P_\perp^2}\right)_\varepsilon\right]dP_\perp^2\frac{d\zeta}{q^2(\zeta)},$$

$$P_z^2=\frac{\Omega^2}{c^2k^2q(\zeta)}.\qquad(16.25)$$ /189

Here we have omitted the indices n, y, k, and ω, and have transformed the expression with F somewhat (integrated the first term by parts, and used the identity $\partial F/\partial P^2-\partial F/\partial P_z^2\equiv(\partial F/\partial P_\perp^2)_\varepsilon$), (the sign $(\quad)_\varepsilon$ indicates that the partial derivative is taken for constant ε, or, what is the same thing, P), and we have put

$$\Lambda=\int_0^l q(\zeta)\,d\zeta.$$

In the equation at (16.25) the upper sign corresponds to the Alfvén, the lower to the accelerated magnetic-sound, wave. Since, in the case of instability $\operatorname{Im}\delta k^2>0$, the Alfvén waves can be built up by protons ($\Omega>0$) with $\overline{P_\perp^2}>\overline{P_\parallel^2}$, or by electrons with the opposite type of anisotropy. Accelerated magnetic-sound waves, on the other hand, are built up by protons with $\overline{P_\perp^2}<\overline{P_\parallel^2}$, or by electrons with $\overline{P_\perp^2}>\overline{P_\parallel^2}$. In the case of a homogeneous field and constant cold plasma density the result at (16.25) is transformed into the nonrelativistic case in the corresponding formulas in [142]. The expression $(\partial\omega/\partial k^2)\delta k^2$ is the ratio of the work done by particles on the field in some field duct in unit time to the field energy in that same duct. The instability condition is determined by comparing the increment $\gamma(\omega)$ with the corresponding decrement $\delta(\omega)$.

Before continuing on to an analysis of stability in the different

regions of the Earth radiation belts, let us point out two important, special cases of the formula at (16.25). We know that the angular distribution of particles near the plane of the equator can be approximated quite well by the law of $\sin^{2\nu}\alpha$ (α is the pitch angle). This sort of distribution has /190
two interesting properties; it remains fixed along the field line, and the particle density changes as $\eta^{-\nu}$ (see #4). In variables P, $P_\perp$, the distribution function of this type is in the form

$$F = F_0(P^2)\left(\frac{P_\perp^2}{P^2}\right)^\nu \eta^{-\nu}(z). \tag{16.26}$$

The first term in the brackets in the equation at (16.25) can be ignored when $\nu \gg 1$ and $\omega \ll \Omega$. Substituting the equation at (16.26) in that at (16.25), we obtain

$$\gamma(\omega) = -\frac{1}{2k}\frac{\partial\omega}{\partial k}\operatorname{Im}\delta k^2 =$$
$$= \pm\frac{2\pi^3 Q^2\nu}{\mu c^3 k^2 \Lambda}\frac{\partial\omega}{\partial k}\int_0^l\int_0^{\infty'}\frac{\Omega(\zeta)\eta^{-\nu}}{q^2(\zeta)}\left[\frac{F_0(P^2)}{\varepsilon}\left(\frac{P_\perp^2}{P^2}\right)^\nu\right]dP^2\,d\zeta, \tag{16.27}$$
$$P^2 = P_\perp^2 + \frac{\Omega^2(z)}{c^2 q^2(\zeta)\,k^2}.$$

If, moreover, $F_0(P^2)$ is a step function, $F_0(P^2) = CP^{-2\lambda}$ when $P \geq P_0$, then for frequencies corresponding to resonance with the particles when $P_z \geq P_0$, what follows from the equation at (16.27) is that in the nonrelativistic case ($\varepsilon = 1$)

$$\gamma(\omega) = \pm\frac{Q}{|Q|}\frac{2\pi^3 Q^2\nu}{\mu c^2 k\Lambda}\frac{\partial\omega}{\partial k}C\int_0^l\frac{\eta^{-\nu}(\zeta)}{q(\zeta)}\left(\frac{|\Omega(z)|}{ckq(z)}\right)^{(-2\lambda-3)}d\zeta\times$$
$$\times\int_0^\infty x^\nu(1+x)^{-(\lambda+\nu)}dx, \tag{16.28}$$

and in the ultrarelativistic case ($\varepsilon \approx P$)

$$\gamma(\omega) = \pm\frac{\dot{Q}}{|Q|}\frac{2\pi^3 Q^2\nu}{\mu c^2 k\Lambda}\frac{\partial\omega}{\partial k}C\int_0^l\frac{\eta^{-\nu}(\zeta)}{q(\zeta)}\left(\frac{|\Omega(\zeta)|}{ckq(\zeta)}\right)^{-(2\lambda-1)}d\zeta\times$$
$$\times\int_0^\infty(1+x)^{-(\lambda+\nu+1/2)}dx. \tag{16.29}$$

Subsequent investigation was based on tne use of the formulas at (16.26) - (16.29).

17. Outer Proton Zone Stability and a Possible Mechanism for the Generation of Type Pc 1 Geomagnetic Micropulse /191

Let us first consider outer proton zone stability. The high-speed proton spectrum is very nearly Maxwellian and the angular distribution is virtually isotropic when $L \geq 6$, It can be described by a law in the form at (16.26) for $\nu \approx 1$ in the vicinity of the belt maximum. Let us put

$$F = \frac{3n}{2\pi^{3/2} P_0^3 \eta(z)} \frac{P_\perp^2}{P^2} e^{-\frac{P_\parallel^2}{P_0^2}}, \qquad (17.1)$$

where

n = $\int F d^3P$ is the proton density near the plane of the equator;

P_o is an average pulse.

The parameters n and P_o are functions of L, so $P_o \sim L^{-3/2}$. Since there are no electrons satisfying the condition of resonance with Alfvén waves, it is sufficient to consider a single proton component.

Let us use $u_o \approx 2 \cdot 10^9$ cm/sec to designate the Alfvén velocity corresponding to the field at the earth's equator, $H_e \approx 0.3$ gauss, and $N = 10^3$ cm^{-3} as the cold proton density. Then, at the apexes of the corresponding field lines $u_a = u_o L^{-3}$ and $\omega = k u_o L^{-3}$. The function $q(z) = \eta^{-2}(z)$ when the density is constant along the field line. Expressing $\eta(z)$ and the element of the length of the arc in terms of the polar angle θ and L, we obtain $\eta = \frac{\sqrt{1+3\cos^2\theta}}{\sin^6\theta}$, $dz = L \sin\theta \sqrt{1+3\cos^2\theta}\, d\theta$

(a is the radius of the earth). From whence $\Lambda = aL\int_0^{\pi/2} \sin^7\theta d\theta = (16/35)aL$. The lower limit of the integration can be selected as 0 because the contribution of small θ to the integral is negligibly small. The same limits are taken to compute the increment.

Further, let us put $\Omega_H = eH/Mc = \Omega_H^{(0)} \eta L^{-3}$, where $\Omega_H^0 \approx 3 \cdot 10^3$ rad/sec is the cyclotron frequency of the protons in the field $H_e \approx 0.3$ gauss. Putting $\varepsilon = 1$ in the equation at (16.27), and substituting for F in the form at (17.1) we obtain the following equation after simple transformations /192

$$\gamma(\omega) \approx 2.5\Omega_0 \frac{n\alpha}{N} P_0 \int_0^{\pi/2} \int_0^{\infty} \eta^2(\theta) \frac{x}{x + \alpha\eta^4(\theta)} e^{-[x+\alpha\eta^4(\theta)]} \times$$

$$\times \sin\theta \sqrt{1+3\cos^2\theta}\, dx\, d\theta, \qquad (17.2)$$

where

$$\alpha = \frac{\Omega_H^{(0)} u_0^2}{\omega^2 c^2 P_0^2 L^{12}}, \qquad (17.3)$$

and $\Omega_o = \sqrt{\frac{4\pi e^2 N}{M}}$ is the ion plasma frequency.

Numerical investigation of the integral at (17.2) leads to the following approximate expression

$$\gamma(\omega) \approx 1.1\Omega_0 \frac{n}{N} P_0 \sqrt{\alpha}\, e^{-\alpha}, \qquad (17.4)$$

and the maximum increment corresponds to the frequency

$$\omega(P_0) = \sqrt{2}\, \frac{u_0}{cP_0} \Omega_H^{(0)} L^{-6}. \qquad (17.5)$$

The magnitude of $n \sim 0.1$ cm^{-3} at the belt maximum ($L \approx 3.5$ to 4), while $P_o \sim 2 \times 10^{-2}$ (corresponding to a velocity $\approx 6 \times 10^8$ cm/sec). The corresponding frequency is $\omega(P_o) \approx 6$ rad/sec (~ 1 Hz), and the increment is $\gamma \approx 3 \times 10^{-2}$ sec^{-1}. This means that instability would develop in ~30 seconds if there were no ionospheric absorption. Intensive scattering in turbulent field pulsations should lead to the establishment of an isotropic angular distribution. If the distribution remains anisotropic, the instability will be stabilized by wave absorption, or particle lifetime will prove to be so short that in $\sim\gamma^{-1}$ second the protons with small pitch angles will be thrown out and anisotropy will be restored. Readily seen is that if the angular distribution $\sim \sin^2\theta$, 30% of the trapped particles must be thrown out in time $\sim\gamma^{-1}$ (this is the difference in the particle reserve for the distributions $\sim \sin^0\theta$ and $\sin^2\theta$). Consequently, if it is assumed that stabilization is lacking, one must suppose that protons have a lifetime ~100seconds that is clearly unrealistic. /193

Let us, for purposes of estimating the decrement, use the values for the reflection factor, R, computed in [147]. In the case of frequencies ~ 1 Hz, $R \approx 0.2$, and the time is

$$T = 2\int_0^l \frac{dz}{u_a} = \frac{2L^4 a}{u_0}\int_0^{\pi/2} \frac{1}{\eta}\frac{dz/La}{d\theta}\,d\theta \approx \frac{L^4 a}{u_0} = 0.3L^4.$$

So when $L \approx 4$, and $\omega = 6$, the decrement δ, in accordance with the equation at (16.16), is $\delta \approx 2 \cdot 10^{-2}$sec^{-1}. The increment decreases exponentially at lower frequencies, and at higher frequencies does so as $1/\omega$. At the same time, the decrement will change but slightly (according to [147] $\sqrt{R} \sim 1/\omega$, but $\delta \sim \log\sqrt{R}$). The effect of stabilization increases in both cases. Stabilization also is intensified with distance from the maximum for the intensity of the outer proton zone, toward larger, as well as toward smaller, L.

Thus, the computation made shows that the outer proton belt is stable, but that at the maximum the intensity of the high-speed protons near the boundary is unstable. It follows, therefore, that in the region of small energies $\lesssim$100keV the intensity cannot be very greatly in excess of the observed magnitude. On the other hand, instability plays no major role in proton escape for the fluxes observed and their destruction is linked primarily with ionization losses.

It is possible that the stability condition is upset in the case of geomagnetic field or ionospheric disturbances. The build up of Alfvén waves will begin in a narrow band of frequencies near $\omega(P_0)$, and wave packets oscillating from one hemisphere to the other with a period $T(L) \approx 0.3L^3$ seconds will be observed at the earth's surface. Since the change in the magnitude of P_0 in the outer proton zone is proportional to $L^{-3/2}$, $\omega(P_0) \sim L^{-4.5}$, the product $\omega T \sim L^{-1/2}$ is only very slightly dependent on L. The appearance of the waves is most probable in the region of geomagnetic latitudes corresponding to L_m from 3 to 4, approximately (that is, to the proton zone maximum). /194

The development of an instability such as this has a number of interesting features associated with the drift of the disturbance along the field line (in this case at Alfvén velocity) (see [83], p. 212). It appears that a number of important conclusions can be drawn on the basis of an analysis of a simple model with a homogeneous field and constant Alfvén velocity. Let us assume that at some moment in time the medium has become unstable with respect to waves with wave vector k in the interval between k_1 and k_2, and that absorption takes place outside this interval. If the interval of instability is sufficiently narrow, and if the increment γ is small compared with the frequency, it can be put that

$$\gamma(k) = \gamma_0 \frac{(k - k_1)(k_2 - k)}{k_1 k_2}. \tag{17.6}$$

The maximum value for the increment, corresponding to the wave vector $k_0 = (k_1 + k_2)/2$ is

$$\gamma_{max} = \gamma_0 \frac{(k_2 - k_1)^2}{4k_1 k_2}. \tag{17.7}$$

The distribution of a plane monochromatic wave can be determined through the relationship

$$f_k = e^{ik(x - vt) + \gamma(k)t}, \tag{17.8}$$

where f_k is some characteristic of the disturbance (one of the components of the electric field, for example), and $\gamma(R)$ can be determined through the equation at (17.7).

Let a single pulse, arbitrary in shape, traveling in the positive direction ($k > 0$), and sufficiently abundant in harmonics with $k \sim k_0$, occur at the initial moment. This latter conditions means that the pulse width is $\Delta x \lesssim 1/k_0$. The k harmonic outside the instability interval will attenuate with time, and only waves with $k \sim k_0$ will be retained in the

Fourier spectrum F(k). Since it is assumed that the interval (k_1, k_2) is sufficiently narrow, it can be put that $F(k) \approx F(k_0)$ in the Fourier integral $f(x,t) = \int_0^\infty F(k) f_k(x,t) dk$, and the lower limit can be replaced by $-\infty$. We obtain the following asymptotic expression for f(x,t) /195

$$f(x, t) = F(k_0) \int_{-\infty}^{+\infty} \exp\left\{ ik(x - vt) + \gamma_0 t \frac{(k-k_1)(k_2-k)}{k_1 k_2} \right\} dk. \qquad (17.9)$$

An elementary computation yields

$$f(x, t) \sim \frac{1}{\sqrt{t}} e^{ik_0(x-vt)} \exp\left\{ \gamma_0 t \frac{(k_2-k_1)^2}{4k_1k_2} - \frac{k_1k_2}{4\gamma_0 t}(x-vt)^2 \right\}, \qquad (17.10)$$

where

$k_0 = (k_1 + k_2)/2$. The increment of $\gamma = (k_2-k_1)^2/4k_1k_2$ is $\gamma(k_0)$. As we see from the equation at (17.10), the disturbance has a definite spatial period; the distance between the adjacent nulls is π/k_0. The quickest rise in amplitude (with increment γ_{max}) takes place when x = vt. The unstable region is localized near the point x = vt, and when $|x - vt| \to \infty$ there is attenuation with a decrement of $(k_1k_2v^2)/4\gamma_0 - \gamma_0 \cdot (k_2-k_1)^2/4k_1k_2$ (this expression is always positive for the assumptions made with respect to the smallness of γ_0 and k_2-k_1. The width of the region in which the amplitude diminishes from the maximum value (when x = vt) by a factor of e, increases in proportion to $\sqrt{t}$.

Accordingly, when conditions of cyclotron stability of the proton belt in the magnetosphere are upset, the result should be the occurrence of almost monochromatic wave packets oscillating along the field lines from hemisphere to hemisphere. Initially, the amplitudes of these waves will rise exponentially versus time, and the widths of the packets will increase as $\sqrt{t}$. As the waves build up they will begin to scatter the protons with ever-increasing intensity. Reduction in the angular anisotropy of the protons will result in a decay in the increment to zero, and then to the attenuation of the waves.

The fundamental properties of the instability reviewed (order of magnitude of the frequencies, narrowness of the spectrum, oscillation along the field lines, the slight dependence of the frequency-oscillation period product on L, scattering, polarization) correspond to well-known micropulses of the Pc1 type ("pearls") [70, 148]. The literature on the subject has repeatedly expressed the view that "pearls" are generated /196

by the cyclotron instability from almost monoenergic proton beams with energies on the order of hundreds of keV. Beams such as these have not been observed experimentally, however. Moreover, since the velocities of protons such as these are greatly in excess of the thermal velocities of cold plasma electrons, the beams should result in a very much more rapid instability (one with a frequency on the order of (ω_0) and an increment of $\gamma \sim (n/N)\omega_0$, where ω_0 is the Langmuir frequency, and n and N are the concentrations of hot and cold particles, respectively).

As we have pointed out in the foregoing, the fundamental properties of "pearls" provide a good explanation of the cyclotron instability of the real proton belt, as well as of the general laws for the development of instability on traveling waves. Further investigation of "pearls" can provide valuable information on the dynamics of the outer proton zone, as well as on the distribution of cold plasma at high altitudes. Of particular interest is an explanation of the concrete causes of upsets in proton belt stability conditions. Also of interest is the estimate of the scatter of protons on the "pearls," and the role of scatter in the variations that take place in the intensities of protons at low altitudes.

18. Inner Electron Zone Stability

There were no detailed investigations of the spectra of electron fluxes in the inner zone prior to the end of 1962, as we know (at least, not at high altitudes). The results of the work done in 1962-1963 [100, 105, 112], as well as the preliminary analysis of the data obtained by the Elektron satellites, revealed that the distribution of electrons with ~500 keV established for $L \lesssim 3$ was extremely stable. The disturbance caused by artificial injection rapidly disappears, and some standard distribution is restored. /197

According to the prevailing viewpoint, the relaxation time (~30 days) is the lifetime of the electrons in the inner zone when $L > 2$ and stable distribution is maintained by some sort of stationary acceleration mechanism. But no reasons for the nature of this mechanism have been advanced as yet. Known mechanisms (decay of neutrons and transfer from the boundary of the magnetosphere) obviously cannot provide the fluxes observed for approximately one month when $L \sim 2$.

There is another possible explanation of the structure of the inner zone; fluxes of electrons correspond to the stability boundary. Here lifetimes can be established by the ionization losses, but when the existing level is exceeded, instability develops, leading to rapid relaxation. It will be shown in what follows that this viewpoint agrees well with the experimental data.

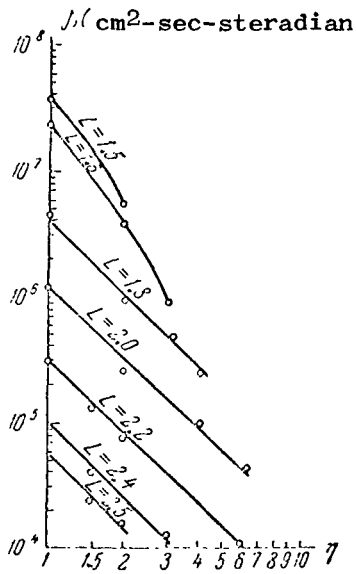

Figure 35. Distribution of electrons with energies >500 keV in the inner zone.

Figure 35 shows the distribution of fluxes of electrons with energies ≥500 keV in terms of L and η. The figure was constructed using the data in [112], obtained between May and September, 1963. We should point out that practically the same distribution in the plane of the equator was observed in December, 1962 [105]. As the figure shows, /198 the intensity changes along the field lines in a manner such that the formula at (16.27) (v=2) can be used.

If the angular distribution is specified, the spectrum of the particles in terms of L corresponding to the boundary of stability for all frequencies $\omega \leq \frac{\nu\omega_H}{\nu+1}$. can be established uniquely. (When $\omega > \frac{\nu\omega_H}{\nu+1}$ the cyclotron absorption suppresses the instability regardless of particle concentrations). The distribution obtained in this manner describes the inner zone structure established upon the injection of powerful fluxes of electrons over a broad interval of energies exceeding the critical value. In the case of a homogeneous field, the equation for the stability boundary, $\gamma(\omega) = \delta(\omega)$, is the Volterra integral equation of the first kind, with respect to the function F, and is of the form

$$\int_0^\infty I_0(y) F(x+y)\, dy = \varphi(x), \tag{18.1}$$

where $x = \frac{\omega^2_H}{c^2k^2}$, $y = P^2_\perp$, and the function $\varphi(x)$ is established by the dependence of the decrement on ω and by the dispersion equation $\omega = \omega(k)$. The equation at (18.1) can be solved quite readily by substituting $y = \xi - x$, by a Laplace transform in terms of x, and by the application of the convolution theorem. The uniqueness of the solution follows. In a heterogeneous field, the build up is primarily the result of the region near the apex of the field line, where the heterogeneity is slight. It is therefore probable that there is also uniqueness of solution. When this assumption is accepted, it is easy to find $F_0(L, R)$.

The computation for the decrement, δ, which is proportional to ω, is in the Appendix. As will be seen from the equation at (16.21), in the ultrarelativistic case, $F_0(P)$ corresponds to $\gamma(\omega)$. Let us seek $F_0(P)$

in the form $CP^{-2\lambda}$. Substituting for γ *) in the equation at (16.29), we find that $\gamma(\omega) \sim \omega^{\lambda-1}$, from whence (since $\delta \sim \omega$), $\lambda \sim 2$ and /199

$$\gamma(\omega) = \frac{8\pi^3 e^2 \omega C L^6}{m\omega_H^{(0)2}} \int_0^\infty x^2 (1+x)^{-4,5}\, dx \int_0^l \eta^{-4,5}\, dz \Big/ \int_0^l \eta^{-1/2}\, dz$$

or, after the computation for the integrals,

$$\gamma(\omega) \approx \frac{\pi}{20} \frac{\omega_0^2}{\omega_H^{(0)2}} \frac{n_0}{N} P_0 L^6 \omega, \qquad (18.2)$$

where the constant, C, is expressed in terms of the magnitude $n_0 P_0$ [$C = (n_0 P_0 / 2\pi)$; n_0 is the number of particles with pulse $P > P_0$ per cm^3. The intensity of particles with pulse larger than P is thus $n_0 P_0 / P$].

The spectrum n (>P)~1/P causes divergence in energy density when $P \to \infty$, so can be realized only within a limited energy region. But for given frequency ω the magnitude of γ can be determined on the basis of particles with $P \gtrsim P(\omega) = \sqrt{\frac{\omega_H^{(0)3} L^{-9}}{\omega_0^2}}$. It can be shown

that particles with $P_\perp^2 > 3P^2(\omega)$ only contribute about 10%. So it is sufficient to assume that the spectrum being established has the form $n \sim P^{-1}$ in the energy interval ϵ from $P(\omega)$ to $2P(\omega)$, in order to use the formula at (18.2) for given ω. In the case of pulse injection, this condition reduces to the creation of superhigh fluxes of particles in this energy interval.

Equating (18.2) to the $\delta(\omega)$ obtained in the Appendix, we see that /200 the boundary value for the intensity, cn_0, is

$$I_{0\ \mathrm{crit}} = cn_0 \approx \frac{10}{\pi} \sqrt{N_e N}\, \frac{v_0 c}{\varkappa a P_0} \frac{\omega_H^{(0)}}{\omega_0^2} L^{-8,5} \left(\frac{L}{L-1}\right)^{3/4}. \qquad (18.3)$$

---

*) $|\Omega| = \omega_H^{(0)} L^{-3} \eta(z)$, $q = \eta^{-1/2}$,

$$ck = \omega \sqrt{\frac{\omega}{|\Omega|}} = \omega_0 \sqrt{\frac{\omega}{\omega_H^{(0)}} \frac{L^3}{\eta}} \quad \text{and} \quad v = 2.$$

Let us compare the result with the data obtained by experiment. The most complete investigations of the inner zone to date have been those of fluxes of electrons with energies larger than 450-500 keV [105, 112]. This energy value agrees well with the conditions for applicability of the relationship at (18.3). Electrons with energy of 500 keV can be considered ultrarelativistic (P = 1.73 and ε = 2), but it is also probable that the supercritical intensity was reached over a quite wide range of energies larger than 500 keV during injection.

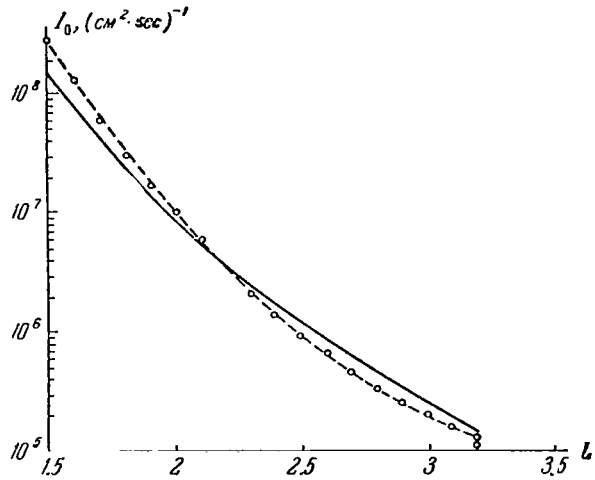

Figure 36. Critical values of fluxes of electrons with energies >500 keV in the equatorial region in the inner zone.

Figure 36 shows the values of the fluxes of electrons in the plane of the equator in a direction perpendicular to the field line. Intensities are expressed in $cm^{-2}sec^{-1}$ units. The solid curve was computed through the formula at (18.3). The dashed curve corresponds to experimental data contained in [105] and [112], obtained between January and September, 1963. We took it that $v_0 \approx 10^4 sec^{-1}$ (this was the magnitude introduced for an altitude of 110 km in [149]), and $\omega_H^0 = 5 \cdot 10^6$ rad/sec, $N = 10^3 cm^{-3}$, and $N_e = 10^4 cm^{-3}$. Since the accuracy of these parameters is relatively poor, no attempt has been made to impute any particular significance to the coincidence between absolute magnitudes computed and fluxes measured. But it is important to point out that the theory does yield a correct order of magnitude for the intensity and well describes its change with L. Further, we note that in the small L region, the approximation that

N = constant $\approx 10^3$ is obviously inapplicable when computing the integral $\int q(z)\,dz$. But since this integral is contained in the denominator as both a decrement and an increment, they cancel during the determination of n.

Now let us consider in more detail the spectrum of electrons in the inner zone. As has already been noted, at this time, along with /201 natural radiation, this region contains the remains of the artificial radiation belts. Moreover, there is a continuous influx of electrons from the cosmic-ray albedo neutron decay. There is no information on other sources of electrons in this region. The power of the source of electrons attributable to neutron decay close to the plane of the equator is in the form $Q = Q_0$ (L^{-2} to L^{-3}), where $Q_0 \approx 10^{-11}\text{cm}^{-3}\text{sec}^{-1}$ [131]. In accordance with the formula at (18.3), the critical intensity is $I_{0\,crit} \approx S_0 P_0 L^{-9}/L$, where $S_0 \approx 5 \cdot 10^9 \text{cm}^{-2}\text{sec}^{-1}$. Let us estimate the intensity that would gather as a result of neutron decay during the time of ionization losses, taking it for simplicity's sake that the average energy of these electrons is equal to 300 keV. When cold electron density is $N = 10^3\text{cm}^{-3}$, the lifetime is equal to $2 \cdot 10^8$ seconds, and $2 \cdot 10^{-3}$ (L^{-2} to L^{-3}) electron/cm^3 will gather near the plane of the equator, comparable to an intensity of $5 \cdot 10^7$ (L^{-2} to L^{-3}) $\text{cm}^{-2}\text{-sec}^{-1}$. Comparing this magnitude with the critical intensity, we see that there is some boundary value /202 $L = L_{crit}$ near 2 such that when $L < L_{crit}$, the neutron mechanism is inadequate to create critical fluxes, but that when $L > L_{crit}$, neutron decay, conversely, overflows the belt.

What follows then is that when $L < L_{crit}$, there is no instability, and that electron destruction is the result of ionization losses, or of scattering in whistling atmospherics. Lifetime is long in this region, so the remains of the belt resulting from the Starfish burst will be conserved here for a long time.

The spectrum of electrons of artificial origin is very rigid (average energy 1 MeV). Neutron decay makes but a small contribution to the total intensity.

There is a substantial change in the picture when $L > L_{crit}$, because instability is constant and the excesses of electrons from the neutron decay are thrown out into the ionosphere. The lifetime of these electrons, as is readily seen, will be on the order of

$$\tau = \frac{I_0 cr}{cQ} = \frac{S_0}{cQ_0}(L^{-6} - L^{-7})_{sec} \approx 2 \cdot 10^{10}(L^{-6} - L^{-7})_{sec}$$

and, when L = 3, is shortened to a magnitude $\sim 10^7$ seconds. We note that these estimates are sensitive to the magnitude of Q_0. It is possible that the true value of τ is several times shorter than this.

An important factor in the scattering of particles in the waves in an inhomogeneous magnetic field is the change in resonance conditions along the field line. As was pointed out above, instability develops more readily near the equatorial plane. As the waves are propagated earthward, there is a reduction in the wave vector k, the cyclotron frequency increases, and more and more energy particles reach resonance with the wave. Consequently, the instability generated by the neutron decay electrons will wash out higher energy electrons.

Since the amplitude of the magnetic disturbance rises with approach to the earth, the typical scatter time, τ_s, is very little dependent on particle pulse. Estimates based on numerical computations of the mean square change in the longitudinal component of a pulse in one oscillation along a field line reveal that τ_s increases in proportion to $\sqrt{P}$, and possibly even more slowly than that. /203

Therefore, in the $L > L_{crit}$ region the remains of the artificial belt should disappear much more rapidly than when $L < L_{crit}$. Within a few years from 1962, the spectrum of electrons in this region will consist of two significantly different components. A stationary component, the result of the neutron decay, is cut off at an energy of ~ 800 keV. A second, slowly dissipating, stable component, is the remains of the artificial belt.

These semiqualitative conclusions now have been partially confirmed. Detailed measurements of the spectra of electrons at altitudes up to

3800 km, made in August, 1964, are described in [150]. The absolute predominance of the stable component (the remains of the artificial belt) was recorded at L < 1.7. Two components, the neutron, and the stable, with a typical discontinuity in the spectrum for 800 keV, were clearly discernible in the L region from 1.7 to 2.2. Figure 37 shows the spectra when L = 1.5 and 2.2 [150].

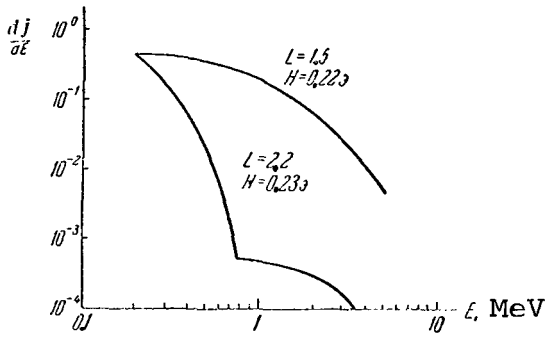

Figure 37. Differential electron spectra at low altitudes in the inner belt.

It is of great interest to make analogous measurements near the plane of the equator, where all the fundamental laws relating to the structure of the belts show up most clearly. With these data as a point of departure, it is possible to explain the dynamics of the throw out of electrons in the inner zone, as well as to make more precise the power of the injection of electrons from neutron decay.

Now, let us estimate the amplitudes of the waves needed to scatter electrons with an energy ~ 300 keV in $\sim 10^7$ seconds. The theory of traps tells us that lifetime in a trap equals the scatter time, τ_s, at an angle of $\sim \pi$, multiplied by the logarithm of the screw ratio (40, when L = 3). Scatter time, τ_s, is linked with the amplitude of the resonant wave, h, by the simple relationship: /204

$$\tau_s \approx \frac{1}{\omega_H}\left(\frac{H}{h}\right)^2 \qquad (18.4)$$

(ω_H = eH/mc is the cyclotron frequency, H is the undisturbed field). Putting $\tau = \log 40 \cdot \tau_s = 10^7$ seconds, substituting values for H and ω_H when L = 3, in the plane of the equator ($H \approx 10^{-2}$ oersted, $\omega_H \approx 2 \cdot 10^5 \text{sec}^{-1}$), we find that $h \approx 10^{-8}$ oersted. Consequently, electromagnetic oscillations with a frequency on the order of 1 kHz (the condition of resonance with the electrons from the neutron decay) and an amplitude of $\approx 10^{-8}$ oersted,

should always exist on the shells with $L \approx 3$ near the plane of the equator. Cosmic rays are the source of energy for these waves, in the final analysis.

Although the accuracy of the computations made is not very high, the result of indeterminancy in the values of a number of the parameters, the basic properties of the inner zone are described with adequate clarity. Specifically, explanations to many of the effects linked with the artificial injection of particles, as well as the features of spatial distribution, and of the electron spectrum, have been obtained.

In concluding this section, let us consider the question of the limits of applicability of the results obtained. Throughout the computations, it was assumed that the frequencies were very much lower than the electron cyclotron frequencies at the apexes of the field lines, but that such frequencies were still sufficiently high, and that ion currents could be disregarded in the dissipation computations. /205

In so far as the resonant frequencies of electrons with pulse $\sim P$ are concerned, $\omega = \frac{\omega_H^{(0)}}{L^3} \frac{c^2k^2}{\omega_0^2} \frac{1}{L^9P^2}$ (because $ck \approx \frac{\omega_H^{(0)}}{L^3P}$). The condition $\omega \ll \omega_H = \frac{\omega_H^{(0)}}{L^3}$ is equivalent to the inequality

$$PL_{\max}^3 \gg \frac{\omega_H^{(0)}}{\omega_0} \approx 1.7 \qquad (18.5)$$

and when $P = \sqrt{3}$ is everywhere correct where it can be taken that $N = \text{constant} \sim 10^3 \text{cm}^{-3}$ (that is, when $L \gtrsim 1.5$). The condition at (18.4) is more correct for particles with $P > \sqrt{3}$. The second condition reduces to the requirement that $\omega > \Omega_H^{(0)} \left(\frac{m}{M}\right)^{1/4}$. Absorption is minimal at these frequencies, and when ω falls below the value cited, there is a rapid increase in the Joule dissipation of ion currents. When $M = 16$, (O^+ ions) the low limit for frequency is $\approx 2 \times 10^3$ rad/sec. Therefore

$$L_{\min}^9 P^2 \lesssim 2 \cdot 10^4, \qquad (18.6)$$

and this is correct when $P^2 = 3$, right up to $L \approx 3$. The corresponding limit shifts earthward with increase in P. The latter estimate shows that the minimum for the intensity of particles with energies ~ 500 keV should be found for $L \approx 3$, and this, as we know, corresponds to the data from the experiment. Section 19 is devoted to a consideration of magnetic scattering in the gap between the belts.

19. Outer Electron Zone Stability. Gap Between the Belts. /206

Whenever frequency ω is reduced below the critical value $\Omega_H^{(0)}\left(\frac{M}{m}\right)^{1/4}$ absorption increases sharply, and reaches a maximum (almost 100%) when $\omega \approx \Omega_H^{(0)} \approx 200$ rad/sec. Wave velocity is determined by the equation at (16.3) when $L \geqslant 2.5$ (where the ion cyclotron frequency at the apex of the field line is less than 200 rad/sec). Change in frequency from $\sim 10^3$ to ~ 200 rad/sec is accompanied by an increase in the decrement by a factor of approximately 1000. Absorption remains high ($\log 1/R \sim 1$) right up to frequencies of ~1 rad/sec. The dependence of $\log 1/R$ on ω in the frequency range from 200 to 1 rad/sec can be approximated by the law $\log 1/R \approx 4.5\left(\frac{\omega}{\omega_H}\right)^{1/3}$.

Since the resonant frequency $\omega(P)$, corresponding to particles with pulse P, changes as L^{-9}, the transition from minimum to maximum absorption takes place within a very narrow region from L_{min} to $\sim 10^{1/9} \cdot L_{min} = 1.3 \cdot L_{min}$. For particles with $P \sim 1$, (energy $\approx$ 200 keV), $L_{min} \approx 3$, so the maximum should agree well with the data from the experiment when $L \approx 4.2$.

The order of magnitude held stable at the maximum for the intensity of particles with pulses from P to 2P is $\approx 100 \cdot I_{0\ min}(P)$, where $I_{0\ min}$ is the intensity at the minimum, determined through the formulas in Section 4. (The decrement increases by a factor of approximately 300, with the factor $L^{-2.5}$ taken into consideration, while the coefficient in the case of the increment decreases by a factor of 3.) This estimate also agrees well with the experimental data ($I_{0\ max}$ $(P > 1) \sim 10^7$ $cm^{-2}sec^{-1}$).

The transfer theory holds that the mechanism that forms the outer electron zone reduces to filling the region corresponding to the maximum wave absorption. Severe scattering of particles should be observed on the inner boundary of this region. This apparently serves as the practical explanation for the isotropic angular distribution detected in the $L \sim 2.5$ to 4 region during the investigations made by Elektron 1 and Elektron 2. /207

Finally, let us consider the region that is the gap between the inner and outer belts ($2.8 \leqslant L \leqslant 3.2$). Intensity of electrons with $P \sim 1$ is minimal in this region. Here the fluxes of electrons with energies $>$ 230 keV ($P \approx 1$) are 3 to $5 \cdot 10^4$ cm^{-2}-sec^{-1}, while the fluxes of electrons with energies $>$ 1.6 MeV ($P \approx 4$) are approximately 10^4 $cm^{-2}sec^{-1}$, according to [100]. Higher values for the intensities are cited in [105]: $\approx 10^5$ when $P >$ 1.73 (energy 500 keV) and $\approx 10^4$ for energies larger than 5 MeV (the latter result raises some doubts because [105] does not describe the principles upon which the detection of these electrons against the background of the bremsstrahlung are based; the presence of intensities such as these have not yet been confirmed).

The Elektron satellites detected a narrow peak of very hard electrons with energies larger than 6 MeV when $L = 2.8$. Their intensity at the maximum was $\approx 10^3$ $sec^{-2}sec^{-1}$.

Analysis of the cyclotron instability of radiation belts shows that:

a. cyclotron instability, of all known plasma instabilities, is the one that develops most readily;

b. the outer proton belt is stable, but the fluxes are close to critical at the maximum, and small disturbances in the magnetic field, or in the ionosphere, can generate waves corresponding to type Pc1 micropulsations;

c. the stable level of electron fluxes in the inner zone, and the gap, correspond to the critical value;

d. the transition from the inner electron zone to the outer is the result of a sharp increase in the absorption of the waves generated during instability;

e. the neutron mechanism maintains unattenuated oscillations in the gap, sharply reducing the lifetime of high energy electrons ($\gtrsim$ 200 keV).

This leads to the general conclusion that the cyclotron instability is the basic non-Coulomb mechanism involved in particle escape from the belts, and, with transfer, plays an important role in the formation of radiation zones. The investigation of cyclotron instability cited in [156] also leads to this conclusion. /208

APPENDIX

The Logarithmic Decrement for Waves with $\omega \gtrsim \Omega_H$ in the Magnetosphere

Experiment reveals that absorption of whistling atmospheric type waves is slight. The reflection factor can therefore be determined as

$$R = 1 - \frac{q}{S_k}, \tag{1}$$

where

$\dot{q}$ is the energy dissipated in a column with a cross-section of 1 cm^2 in 1 second;

S_k is the projection of the Umov-Poynting vector on the vertical. Since the night boundary of the lower ionosphere is extremely sharp (the electron concentration changes by a factor of e at an altitude of $\sim$ 1 km, which is shorter than the wavelengths considered), let us consider the problem of the reflection of a wave from a plane boundary. The density of neutral atoms above this boundary will change in accordance with the law $\sim e^{\varkappa z}$. The collision frequency too will change; $\nu = \nu_0 e^{-\varkappa z}$. The electron density, N, will be taken as constant. We can also say that $\nu_0 \ll \omega_H$.

Let us limit ourselves to the normal incidence case, because the index of refraction undergoes a sharp increase in the ionosphere. Since the index of refraction drops sharply below the ionosphere, we can say that when z = 0, the magnetic field disturbance vanishes (more precisely, its tangential components). But the electric field has an antinode, and changes as cos kz.

From equations

$$(i\omega + \nu)\mathbf{v} + \omega_H [\mathbf{v}\mathbf{n}] = -\frac{e}{m}\mathbf{E}; \tag{2}$$

$$i[\mathbf{k}\mathbf{h}] = \frac{4\pi e N}{c}\mathbf{v}; \tag{3}$$

$$[\mathbf{k}\mathbf{E}] = \frac{\omega}{c}\mathbf{h} \tag{4}$$

(n is a unit vector along the magnetic field), it follows that /20

$$\omega = \omega_H \frac{c^2 k^2 \cos\chi}{\omega_0^2}, \tag{5}$$

where X is the angle between H and the vertical. From the equation at (3),

it will be seen that

$$(\mathbf{kv}) = 0$$

Multiplying the equation at (2) by mNv in scalar fashion, we obtain

$$\mathrm{Re}(jE) = mNv^2\nu_0.$$

Putting $v = v_0 \cos kz$, and considering that $\varkappa/k \gtrsim 1$, we obtain

$$\dot{q} = \frac{2\nu_0 m v_0^2 N}{\varkappa}. \tag{6}$$

We will ignore the terms with ω and v in the equation at (2) in the computations for the vector S. Expressing E and h in terms of v, we have

$$S_k = \frac{c}{4\pi}\frac{(\mathbf{k}[\mathbf{EH}])}{k} = \frac{m^2c^2\omega_H^2(kn)^2}{4\pi e^2\omega k} v^2$$

and

$$R = 1 - \frac{2\omega_0^2\nu_0\omega}{c^2\varkappa\omega_H^2\cos^2\chi}. \tag{7}$$

Putting $\omega_H = \omega_H^{(0)}\sqrt{1+3\cos^2\theta}$, where $\omega_H^{(0)}$ is the frequency at the earth's equator, θ if the polar angle, and considering that

$$ck = \omega_0\sqrt{\frac{\omega}{\omega_H\cos\chi}}, \quad \cos\chi = \frac{H_r}{H} \text{ and } L\sin^2\theta = 1,$$

after uncomplicated transformations, we obtain

$$R = 1 - \frac{\omega_0\nu_0\sqrt{\omega\omega_H^{(0)}}}{\sqrt{2}\,c\varkappa\omega_H^{(0)2}\cos^{3/2}\theta}. \tag{8}$$

The group velocity of a wave with frequency ω at high altitudes is

$$u_g = \frac{\partial\omega}{\partial k} = \frac{2c\sqrt{\omega\omega_H^{(0)}}}{\omega_0} L^{-3/2}\sqrt{\eta}$$

and

$$T = 2\int_0^t \frac{dz}{u_g} \approx 0.6\,\frac{aL^{2,5}}{c}\,\frac{\omega_0}{\sqrt{\omega\omega_H^{(0)}}}.$$

/210

From whence, when $1 - R \ll 1$, the decrement is

$$\delta(\omega) = \frac{1}{2}\frac{\ln 1/R}{T} = \frac{1}{2\sqrt{2}}\sqrt{\frac{N_e}{N}}\frac{\nu_0}{\varkappa a}\frac{\omega}{\omega_H^{(0)}} L^{-2,5}\left(\frac{L}{L-1}\right)^{3/4}.$$

From the equation at (8), what follows is that when $\omega \sim 10^5$m the amplitude of the wave will attenuate by a factor of e after approximately 10 reflections. This result agrees well with the data from observations of atmospherics (over 40 reflections can be observed occasionally while the signal is weakening by two orders of magnitude [145]).

Conclusion

/211

The investigation made shows that there are two physical processes, transfer of particles across the drift shells, caused by the effects of sudden pulses, and the cyclotron instability of the radiation belts, that have a great deal to do with the dynamics of the fluxes of particles with energies larger than 100 keV in the trapped radiation zone.

Known from the experiment is that:

(a) on the outer edges of the proton and electron belts the average particle energy changes with L in accordance with the law of adiabatic invariance of the magnetic moment ($P \sim L^{-3/2}$);

(b) the typical time for the transfer of particles on a shell with parameter L is proportional to L^{-8};

(c) the numerical value of the diffusion factor, D_0, established by using the most varied of data, always comes out the same ($D_0 \approx 5 \cdot 10^{-14}$ sec^{-1}).

So it is possible to use purely empirical means to construct a transfer equation which should coincide with the equation we have deduced (Sections 9 and 10) (with an accuracy to within that of the numerical factor for the term describing the regular flux). Moreover, if the magnitude of the regular flux is estimated with respect to the concentration of energy protons when L = 1.5, the equation can be constructed practically uniquely.

Strictly speaking, what follows from this is that the transfer is caused by nonstationary electric fields, longitudinally asymmetrical, the amplitudes of which are proportional to L^2 (because the transfer rate is proportional to L^9), while the frequency spectrum has a broad plateau in the region of periods from 0.5 minute to several hours (becuase the transfer /212 rate in these limits does not depend on the drift period). It is impossible to obtain more concrete information on the nature of electric fields from the transfer equation.

Experimental data on geomagnetic disturbances lead to the assertion that one of the basic causes of the generation of these fields is sudden pulses, and the numerical magnitude of the transfer rate corresponds to

values that stem from the dynamics of the belts. It is only at very short drift periods, τ_φ ($\lesssim$ 1 minute), that the natural oscillations of the magnetosphere begin to play a role, and at least right up to τ_φ = 0.5 minute, the value of D_0 remains the same as it is in the case of large τ_φ.

We can find a D_0 magnitude averaged over a great many different time intervals, depending on the nature of the experimental data. For example, data on diffusion waves of relativistic electrons yield a D_0 value in a period of low magnetic activity that ranges from several days to a month. The data on the stationary proton belt provide a magnitude that is averaged from 100 days (when $L \approx 3.5$) to 100 years (when $L \approx 1.5$).

It is extremely noteworthy that all D_0 values obtained in this manner coincide with an accuracy factor $\lesssim 2$. This means that relatively weak, but at the same time, very frequent, disturbances of the quiet solar wind play a dominant role in transfer.

Short-lived increases in D_0 (sometimes many tenfold) are observed during magnetic storms. Still, when the time these "flares" in D_0 during storms are averaged, the time turns out to be short compared with the overall effect of many weak pulses. Thus, the principal accelerating mechanism creating the Earth radiation belts is a comparatively simple, stable, process of particle transfer that is the result of the effects of sudden pulses.

The proton belt is formed by transfer and ionization losses. The fact /213 that there has been success in correctly forecasting the distribution of protons right up to energies of tens of MeV at a single point throughout the trapped radiation region for the proton spectrum in the energy interval from 100 keV to 1 MeV is sufficiently persuasive of the advantage of this conclusion. Moreover, the proton belt appears to be stable in terms of different types of instability.

Proofs of the diffusion nature of the outer electron zone, while not exhaustive, are still quite persuasive. First, the change in the average energy of electrons with L on the outer edge of the belt too, is established by the betatron ratio. Second, the fluxes of electrons with energies in the tens of keV observed at the boundary are sufficient to fill the

outer zone because of transfer. Finally, the nonstationary processes in the outer zone (diffusion waves of relativistic electrons) are subordinate to relationships stemming from the transfer theory.

Since the maximum for the outer electron belt is located on comparative distant shells, it is much more sensitive to fluctuations in source power, and in the magnitude of D_0, than are the proton peaks, and therefore undergoes random variations. This fact in no way contradicts the transfer conception, however.

The maximum for the outer electron zone is located for large L (≈ 4.5). Escape is non-Coulomb in nature, and destruction of electrons takes place much more rapidly. It is known that the amplitudes of waves that are effective in scattering electrons are small. Moreover, in the case of pulse injection of electrons into a region of reduced intensity, what is usually observed ia rapid decay to some level which then remains stable for a long period of time. This is characteristic of instability escape; smallness of amplitude is compensated for by the resonant interaction of the waves with /214
the particles, while the stable level correspond to the stability boundary.

General considerations concerning the various mechanisms involved in plasma instability indicate that the most dangerous type of instability for the electron zone is the build-up of extremely low frequency waves as a result of the anisotropy of the angular distribution of electron velocities.

The level of intensity at which the increment of instability equals the logarithmic decrement for the waves during passage through the ionosphere corresponds to the stability boundary.

Computation shows that the distribution of intensity of electronc corresponding to the stability boundary practically coincides with the observed structure of the electron belts. And the gap between the belts corresponds to a region of minimal absorption of waves built up by electrons with energies of several hundred keV.

The gap is filled with neutron decay electrons when $2 \leqslant L \leqslant 3.5$. The neutron mechanism is insufficient to create critical intensity when $L < 2$. The electrons observed in this region are the remains of the artificial radiation belts.

Accordingly, use of the cyclotron instability provides a complete interpretation of the electron belts (at least for energies larger than 100 keV).

The theory of belts that has developed is the basis for obtaining many results of interest for other geophysical problems. Analysis of the structure of the proton belt, for example, leads to the conclusion that the average density of the cold plasma on the magnetic shells with $1.5 \leqslant L \leqslant 3.5$ at altitudes $> 3{,}000$ km from the surface of the earth are of the order of 10^3 cm^{-3} and changes by no more than a factor of 2 from $L = 1.5$ to $L = 3.5$.

Investigation of the stability of the proton belt has made it possible to advance an extremely probable hypothesis as to the nature of the unique, almost monochromatic pulsations of the geomagnetic field, of the so-called "pearls." The principal characteristics of the "pearls" stemming from the /215 theory agree well with observation data.

The overwhelming majority of the experimental data on the radiation belts agrees well with the theory that has developed, and it can therefore be asserted that the nature of the physical processes leading to the formation of radiation belts has, in principle, been explained.

There remain a number of questions, answers to which require further experimental and theoretical investigation.

The most important problem is the one concerned with the structure and dynamics of the neutral layer, and the outermost radiation belt associated with it. Clearly, it is in this region that the throw out of high-speed particles into the ionosphere and leading to the appearance of auroras, of polar current systems, and to the heating of the upper atmosphere, takes place. The currents flowing in this region make a significant contribution to the world component of geomagnetic disturbances. Finally, the outermost belt is a source of particles that go to form the increased radiation zones closer to the earth, the result of transfer.

Investigation of transfer of particles with energies of from 1 to 10 keV, the result of the effect of electric fields generated by winds in the ionosphere, is of great interest to the theory of magnetic storms

and auroras.

One of the most important problems of the radiation belt theory is the study of the dynamics of electron throw out based on a quasilinear approximation and a theoretical computation of the lifetime. This problem can be solved only with the help of modern computer techniques. Specifically, an explanation of the cause of the rapid disappearance of relativistic electrons from the outer zone during magnetic storms is of great interest.

The link between this effect and accelerated transfer, or with scattering as a matter of fact, is still unclear. In this connection, let us point out that amore detailed study of the dynamics of relativistic electrons /216 during high-altitude experiments is needed.

More careful investigations of electric and magnetic fields in the magnetosphere in the frequency range from 100 Hz to several tens of MHz must be made in order to study throw out dynamics.

Answers to these questions will make possible a final explanation of the mechanism involved in the effect of corpuscular radiation from the sun on the earth.

References

1. Kellog, P. J., Nature, Vol. 183, p. 1295, 1959. /217
2. Parker, E., J. Geophys. Res., Vol. 65, p. 3117, 1960.
3. Herlofson, N., Phys. Rev. Letters, Vol. 5, p. 414, 1960.
4. Davis, L., and Chang, D. B., J. Geophys. Res., Vol. 67, p. 2169, 1962.
5. Tverskoy, B. A., Izv. AN. SSSR, ser. fiz., Vol. 28, p. 2026, 1964.
6. Tverskoy, B. A., Izv. AN. SSSR, ser. fiz., Vol. 28, p. 2029, 1964.
7. Tverskoy, B. A., Trudy 8-y Mezhdunarodnoy konferentsii po fizike kosmicheskikh luchey [Transactions of the 8th International Conference on Cosmic Ray Physics], Jaipur, India, 1963.
8. Tverskoy, B. A., Geomagnetism i aeronomiya, Vol. 4, p. 224, 1964.
9. Tverskoy, B. A., Geomagnetism i aeronomiya, Vol. 4, p. 436, 1964.
10. Tverskoy, B. A., Space Research, Vol. 4, p. 367, 1965.
11. Tverskoy, B. A., Geomagnetism i aeronomiya, Vol. 5, p. 793, 1965.
12. Tverskoy, B. A., Issledovaniya kosmicheskogo prostranstva [Space Research], p. 314, "Nauka," 1965.
13. Dungey, J. W., Hess, W. N., Nakada, M. P., J. Geophys. Res., Vol. 70, p. 3525, 1965.
14. Falthammer, C.-G., J. Geophys. Res., Vol. 70, p. 2503, 1965.
15. Nakada, M. P., Mead, G. D., J. Geophys. Res., Vol. 70, p. 4777, 1965.
16. Tsytovich, V. N., Geomagnetism i aeronomiya, Vol. 3, p. 616, 1963.
17. Trakhtengerts, V. Yu., Geomagnetism i aeronomiya, Vol. 3, p. 816, 1963.
18. Andronov, A. A., Trakhtengerts, V. Yu., Geomagnitism i aeronomiya, Vol. 4, p. 233, 1964.
19. Tverskoy, B. A., Proceedings of 9th International Conference on Cosmic Rays, London, 1965 (being printed).
20. Tverskoy, B. A., Geomagnetism i aeronomiya, Vol. 7, No. 2, 1967, (being printed).
21. Gardner, C., Goertzel, H., Grad, H., Moravets, C., Rose, M.,

Rubin, H., Geneva Conference on Atomic Energy, Paper No. 374, 1958.

22. Sagdeyev, R. Z., Sb. Voprosy teorii plazmy [Collection: Questions of Plasma Theory], Vol. 4, p. 20, Atomizdat, 1964.

23. Tverskoy, B. A., ZhETF, Vol. 46, p. 1653, 1964.

24. Ness, N. F., Scearce, C. S., Seek, J. B., J. Geophys. Res., Vol. 69, p. 3531, 1964.

25. Ness, N. F., J. Geophys. Res., Vol. 70, p. 2989, 1965.

26. Dolginov, Sh. Sh., Yeroshenko, Ye. G., Zhuzgov, L. N., Issledovaniya kosmicheskogo prostranstva [Space Research], p. 342, "Nauka," 1965. /21

27. Nishida, A., Cahill, L. J., J. Geophys. Res., Vol. 69, p. 2243, 1964.

28. Cahill, L. J., Space Research, Vol. 6, 1966 (being printed).

29. Zhigulev, V. N., Romishevskiy, Ye. A., DAN SSSR, Vol. 127, p. 100, 1959.

30. Kellog, P. J., J. Geophys. Res., Vol. 67, p. 3805, 1962.

31. Mead, G. D., J. Geophys. Res., Vol. 69, p. 1181, 1964.

32. Mead, G. D., Beard, D. B., J. Geophys. Res., Vol. 69, p. 1169, 1964.

33. Wolfe, J. H., Silva, R. W., Myers, M. A., Space Research, Vol. 6, 1966 (being printed).

34. Spreiter, J. R., Jones, W. P., J. Geophys. Res., Vol. 68, p. 3555, 1963.

35. Spreiter, J. R., Briggs, B. R., J. Geophys. Res., Vol. 67, p. 37, 1962.

36. Grad, H., Phys.of Fluids, Vol. 4, p. 1366, 1961.

37. Sigov, Yu. S., Tverskoy, B. A., Geomagnetism i aeronomiya, Vol. 3, p. 43, 1963.

38. Piddington, J. H., J. Geophys. Res., Vol. 65, p. 93, 1960.

39. Axford, W. I., Hines, C. O., Canad. J. Phys., Vol. 39, p. 1322, 1961.

40. Axford, W. I., Petschek, H. E., Siscoe, G. L., J. Geophys. Res., Vol. 70, p. 1231, 1965.

41. Parker, E., Dinamicheskiye protsessy v mezhplanetnoy srede [Dynamic Processes in the Interplanetary Medium], "Mir," 1965.

42. Pletnev, V. D., Skuridin, G. A., Shalimov, V. P., Shvachunov, I. I., Kosmicheskiye issledovaniya, Vol. 3, No. 2, 1965.

43. Pletnev, V. D., Skuridin, G. A., Shalimov, V. P., Shvachunov, I. I., Issledovaniya kosmicheskogo prostranstva [Space Research], p. 283, "Nauka," 1965.

44. Pletnev, V. D., Skuridin, G. A., Shalimov, V. P., Shvachunov, I. I., Space Research, Vol. 6, 1966 (being printed).

45. Kawashima, N., Fukushima, N., Planet. Space Science, Vol. 12, p. 1187, 1964.

46. Kawashima, N., Mori, S., Phys. of Fluids, Vol. 8, p. 378, 1965.

47. Bostic, W. H., Butfield, H., Brettschneider, M., J. Geophys. Res., Vol. 68, p. 5315, 1963.

48. Alfven, H., Danielson, L, Falthammer, C.-G., Zindberg, L., On the penetration of interplanetary plasma into the magnetosphere, Report on the symposium on plasma physics held at Catholic University, USA, 1963, preprint.

49. Khorosheva, O. V., Dissertation, NIIYaF, MGU, 1965.

50. Williams, D. J., Mead, G. D., J. Geophys. Res., Vol. 70, p. 3017, 1965.

51. Akasofu, S. J., Cain, J. C., Shapman, S., J. Geophys. Res., Vol. 66, /219 p. 4013, 1961.

52. Hoffman, R. A., Bracken, P. A., J. Geophys. Res., Vol. 70, p. 3555, 1965.

53. Yeroshenko, Ye. G., Issledovaniya kosmicheskogo prostranstva [Space Research], p. 365, "Nauka," 1965.

54. Shapman, S., Ferraro, V. C. A., Nature, Vol. 126, p. 129, 1930.

55. Yanovskiy, B. M., Zemnoy magnetizm [Earth Magnetism], Vol. 1, L, 1964.

56. Chepmen, S., "Solar Plasma, Geomagnetism, and the Auroras," Sb. Geofizika. Okolozemnoye kosmicheskoye prostranstvo [Collection: Geophysics. Near-Earth Cosmic Space], "Mir," 1964.

57. Krasoviskiy, V. I., Issledovaniya kosmicheskovo prostranstva [Space Research], p. 11, "Nauka," 1965.

58. Kadomtsev, B. B., Sb. Voprosy teorii plazmy [Collection: Questions of Plasma Theory], Vol. 2, p. 132, Atomizdat, 1963.

59. Kadomtsev, B. B., Rokotyan, V. Ye., DAN SSSR, Vol. 133, p. 68, 1960.

60. Bauer, S. J., Bluml, L. J., Donley, J. L., Fitzenreiter, R. J., Jackson, J. E., J. Geophys. Res., Vol. 69, p. 186, 1964.

61. Istomin, V. G., Issledovaniya kosmicheskogo prostranstva [Space Research], p. 192, "Nauka," 1965.

62. Taylor, H. A., Brace, L. H., Brinton, H. C., Smith, C. R., J. Geophys. Res., p. 68, p. 5339, 1963.

63. Bezrukikh, V. V., Gringauz, K. I., Issledovaniya kosmicheskogo prostranstva [Space Research], p. 177, "Nauka," 1965.

64. Benediktov, Ye. A., Getmantsev, G. G., Mityakov, N. A., Rapoport, V. O., Sazonov, Yu. A., Tarasov, A. F., Issledovaniya kosmicheskogo prostranstva [Space Research], p. 581, "Nauka," 1965.

65. Bowles, K. L., Science, Vol. 139, p. 389, 1963.

66. Carpenter, D. L., J. Geophys. Res., Vol. 68, p. 1675, 1963.

67. Gul'yel'mi, A. V., Geomagnetism i aeronomiya, Vol. 6, p. 135, 1966.

68. Serbu, G. P., Space Research, Vol. 5, p. 564, 1965.

69. Troitskaya, V. A., Bol'shakova, O. V., Matveyeva, E. T., Geomagnetism i aeronomiya, Vol. 6, p. 533, 1966.

70. Troitskaya, V. A., Transactions of the Toronto Meeting (XI General Assembly of the IUGG, 1957), p. 392, 1960.

71. Vernov, S. N., Chudakov, A. Ye., Vakulov, P. V., Gorchakov, Ye.,V., Logachev, Yu. I., Nikolayev, A. G., Rubinshteyn, I. A., Sosnovets, E. N., Ternovskaya, M. V., Issledovaniya kosmicheskogo prostranstva [Space Research], p. 433, "Nauka," 1965.

72. Vernov, S. N., Chudakov, A. Ye., UFN, Vol. 70, p. 585, 1960.

73. Heliwell, R. A., Gehrels, E., Proc. IRE, Vol. 46, p. 785, 1958.

74. Cain, J. C., Shapiro, I. R., Stolaric, J. D., Heppner, J. P., J. Geophys. Res., Vol. 66, p. 2677, 1961.

75. Gurnett, D. A., O'Brien, B. J., J. Geophys. Res., Vol. 69, p. 65, 1964.

76. Skarf, F. L., Crook, G. M., Frederics, R. W., J. Geophys. Res., Vol. 70, p. 3045, 1965. /220

77. Lew, J. S., J. Geophys. Res., Vol. 66., p. 2681, 1961.

78. Van Allen, J., Sb. Radiationneye poyasa zemli [Collection: The Earth's Radiation Belts], p. 10, IL, 1963.

79. MacIlvain, K., J. Geophys. Res., Vol. 66, p. 3681, 1961.

80. Nortrop, T. G., Teller, E., Phys. Rev., Vol. 117, p. 215, 1960.

81. Yershkovich, A. I., Shabanskiy, V. P., Antonova, A. Ye., Issledovaniya kosmicheskogo prostranstva [Space Research], p. 326, "Nauka," 1966.

82. Krymov,Yu. S., Tverskoy, B. A., Geomagnetism i aeronomiya, Vol. 4, p. 397, 1964.

83. Kadomtsev, B. B., Sb. Voprosy teorii plazmy [Collection: Questions of Plasma Theory], Vol. 4, p. 188, Atmizdat, 1964.

84. O'Brien, B. J., J. Geophys. Res., Vol. 68, p. 989, 1963.

85. Maehlum, B., O'Brien, B. J., J. Geophys. Res., Vol. 68, p. 997, 1963.

86. Frank, L. A., Van Allen, J. A., Macagno, E., J. Geophys. Res., Vol. 68, p. 3543, 1963.

87. Vernov, S. I., Chudakov, A. Ye., Vakulov, P. V., Gorchakov, Ye. V., Kuznetsov, S. N., Logachev, Yu. I., Nikolayev, A. G., Sosnovets, E. N., Rubinshteyn, I. A., Stolpovskiy, V. G., El'tekov, V. A., Issledovaniya kosmicheskogo prostranstva [Space Research], p. 394, "Nauka," 1965.

88. Kuznetsov, S. N., Sosnevets, E. N., Stolpovskiy, V. G., Issledovaniya kosmicheskogo prostranstva [Space Research], p. 420, "Nauka," 1965.

89. Vernov, S. N., Chudakov, A. Ye., Vakulov, P. V., Kuznetsov, S. N., Logachev, Yu. I., Sosnovets, E. N., Stolpovskiy, B. G., Issledovaniya kosmicheskogo prostranstva [Space Research], p. 425, "Nauka," 1965.

90. Fritz, T. A., Gurnett, D. A., J. Geophys. Res., Vol. 70, p. 2485, 1965.

91. Frank, L. A., J. Geophys. Res., Vol. 70, p. 1593, 1965.

92. Vernov, S. N., Mel'nikov, V. V., Savenko, I. A., Savin, B. I., Pervaya, T. I., Issledovaniya kosmicheskogo prostranstva [Space Research], p. 381, "Nauka," 1965.

93. Bezrukikh, V. V., Gringauz, K. I., Ozerov, V. D., Rybchinskiy, R. Ye., DAN SSSR, Vol. 131, p. 1301, 1960.

94. MacIlvain, C. E., Space Research, Vol. 1, p. 715, 1960.

95. MacDiarmid, J. B., Rose, D. C., Budsinsky, E., Canad. J. Phys., Vol. 39, p. 1888, 1961.

96. Gringauz, K. I., Khokhlov, M. Z., Issledovaniya kosmicheskogo prostranstva [Space Research], p. 467, "Nauka," 1965.

97. Savin. B. I., Proceedings of 9th International Conference on Cosmic Rays, London, 1965 (being printed).

98. Hones, J., J. Geophys. Res., Vol. 68, p. 1209, 1963.

99. Davis, L. R., Williamson, J. M., Space Research, Vol. 3, p. 365, 1963.

100. Van Allen, J. A., Frank, L. A., Hills, H. K., J. Geophys. Res., Vol. 69, /22 p. 2171, 1964.

101. Vernov, S. N., Gorchakov, Ye. V., Kuznetsov, S. M., Logachev, Yu. I., Sosnovets, E. N., Tverskoy, B. A., Chudakov, A. Ye., Proceedings of the 9th International Conference on Cosmic Rays, London, 1965 (being printed).

102. Bolyunova, A. D., Vaysberg, O. L., Gal'perin, Yu. I., Potapov, B. P., Temnyy, V. V., Shuyskaya, F. K., Issledovaniya kosmicheskogo prostranstva [Space Research], p. 406, "Nauka," 1965.

103. MacIlvain, C. E., Fillius, R. W., Phys. Rev. Letters, April, 1964.

104. Fillius, R. W., J. Geophys. Res., Vol. 71, p. 97, 1966.

105. MacIlvain, C. E., Science, Vol. 142, p. 355, 1963.

106. Freden, S. C., Blake, J. B., Paulikas, G. A., J. Geophys. Res., Vol. 70, p. 3113, 1965.

107. Vernov, S. N., Savenko, I. A., Tel'tsov, M. V., Shavrin, P. I., Issledovaniya kosmicheskogo prostranstva [Space Research], p. 460, "Nauka," 1965.

108. Davis, L. R., Hoffman, R. A., Williamson, J. M., J. Geophys. Res., Vol. 67, No. 13, 1962.

109. Frank, L. A., J. Geophys. Res., Vol. 70, p. 3533, 1965.

110. McDiarmid, B., Burrows, J. R., Rose, D. C., Wilson, M. D., Space Research, Vol, 4, p. 606, 1964.

111. MacIlvain, C. E., Space Research, Vol. 4, p. 385, 1965.

112. MacIlvain, C. E., Fillius, R. W., Valerio, J., Dave, A., Report of Department of Physics, University of California, March, 1964 (preprint).

113. Shabanskiy, V. P., Geomagnetizm i aeronomnya, Vol. 5, p. 969, 1965.

114. Dessler, A. J., O'Brien, B. J., Sb. Okolozemnoye kosmicheskoye prostranstvo, spravochnyye dannyye [Collection: Near-Earth Cosmic Space, Reference Data], p. 58, "Mir," 1966.

115. Freeman, J., J. Geophys. Res., Vol. 69, p. 1691, 1964.

116. Frank, L. A., Van Allen, J. A., J. Geophys. Res., Vol. 69, p. 3155, 1964.

117. Frank, L. A., J. Geophys. Res., Vol. 70, p. 4131, 1965.

118. Vernov, S. N., Savenko, I. A., Tverskaya, L. V., Shavrin, P. I., Geomagnetizm i aeronomiya, Vol. 3, p. 812, 1963.

119. Vernov, S. N., Chudakov, A. Ye., Vakulov, P. V., Gorchakov, Ye. V., Ignat'yev, P. P., Kuznetsov, S. N., Logachev, Yu. I., Lyubimov, G. P., Nikolayev, A. G., Okhlopkov, V. P., Sosnovets, E. N., Ternovskaya, M. V., Izv. AN SSSR, ser. fiz., Vol. 28, p. 2058, 1964.

120. Temnyy, V. V., Issledovaniya kosmicheskogo prostranstva [Space Research], p. 209, "Nauka," 1965.

121. Williams, D. J., Smith, A. M., J. Geophys. Res., Vol. 70, p. 541, 1965.

122. Paulikas, G. A., Freden, S. C., J. Geophys Res., Vol. 69, p. 1239, 1964.

123. Williams, D. J., Palmer, W. F., J. Geophys. Res., Vol. 70, p. 557, 1965. /222

124. O'Brien, B. J., J. Geophys. Res., Vol. 67, p. 3687, 1962.

125. O'Brien, B. J., Taylor, H., J. Geophys. Res., Vol. 69, p. 45, 1964.

126. Wincler, J. R., Bhavsar, P. D., Anderson, K. A., J. Geophys. Res., Vol. 67, p. 3717, 1962.

127. Brown, R. R., Barkus, J. R., Parsons, N. R., J. Geophys. Res., Vol. 70, p. 2599, 1965.

128. Vernov, S. N., Issledovaniya kosmicheskogo prostranstva [Space Research], p. 277, "Nauka," 1965.

129. Tverskoy, B. A., Geomagnetism i aeronomiya, Vol. 6, p. 585, 1966.

130. Gradshteyn, I. S., Ryzhik, I. M., Tablitsy integralov, summ, ryadov i proizvedeniy [Tables of Integrals, Sums, Series, and Products], Fizmatgiz, 1962.

131. Hess, W. J., Canfield, E., Lingenfelter, R., J. Geophys. Res., Vol. 66, p. 666, 1961.

132. Witteker, E. T., Watson, J., Kurs sovremennogo analiza [Course in Modern Analysis], Vol. 2, Fizmatgiz, 1963.

133. Vernov, S. N., Kuznetsov, S. N., Logachev, Yu. I., Report to the VI Assembly of COSPAR, Vienna, 1966 (will be published in Space Research).

134. Vernov, S. N., Savenko, I. A., Tel'tsov, M. V., Shavrin, P. I., Geomagnetism i aeronomiya, Vol. 6, 377, 1966.

135. Savenko, I. A., Tel'tsov, M. V., Shavrin, P. I., Geomagnetism i i aeronomiya, Vol. 6, p. 661, 1966.

136. Mikhailovskiy, A. V., Sb. Voprosy teorii plazmy [Collection: Questions of Plasma Theory], Vol. 3, p. 41, Atomizdat, 1963.

137. Vedenov, A. A., Velikhov, Ye. P., Sagdeyev, R. Z., UFN, Vol. 73, p. 701, 1961.

138. Akhiyezer, A. I., Akhiyezer, I. A., Polovin, R. V., Sitenko, A. G., Stepanov, K. N., Kollektiviye kolebannya v plazmy [Collective Oscillations in Plasma], Atomizdat, 1964.

139. Chang, D. B., Pearlstein, L. D., Rosenbluth, M. N., J. Geophys. Res., Vol. 70, p. 3085, 1965.

140. Vedenov, A. A., Velikhov, Ye.,P, Sagdeyev, R. Z., Yadernyi sintez, Vol. 1, p. 82, 1961.

141. Vedenov, A. A., Sb. Voprosy teorii plazmy [Collection: Questions of Plasma Theory], Vol. 3, p. 203, Atomizdat, 1963.

142. Sagdeyev, R. Z., Shafranov, V. D., ZhETF, Vol. 12, p. 130, 1961.

143. Seidl, M., Sunka, P., Phys. Rev. Letters, Vol. 11, p. 31, 1964.

144. Post, R. F., Perkins, W. A., Phys. Rev. Letters, Vol. 6, p. 85, 1961.

145. Galle, G., Sb. Geofizika [Collection: Geophysics], p.431, "Mir," 1964.

146. Shafranov, V. D., Sb. Voprosy teorii plazmy [Collection: Questions of Plasma Theory], Vol. 3, Atomizdat, 1963.

147. Francis, W., Carplus, R., J. Geophys. Res., Vol. 66, p. 3593, 1961.

148. Gendrin, R., Annales de Geophysique, Vol. 19, No. 3, 1963.

149. Nikole, M., Aeronomiya, "Mir," 1964.

150. Mihalov, J. D., White, R. S., J. Geophys. Res., Vol. 71, p. 2217, 1966. /223

151. Serlemitsos, P., J. Geophys. Res., Vol. 71, p. 61, 1966.

152. Anderson, K. A., Ness, N. F., J. Geophys. Res., Vol. 71, p. 3705, 1966.

153. MacIlvain, C. E., Trans. Amer. Geophys. Union, Vol. 47, p. 131, 1966.

154. Browton, W. L., Roberts, C. S., Trans. Amer. Geophys. Union, Vol. 47, p. 135, 1966.

155. Vernov, S. N., Kuznetsov, S. N., Logachev, Yu. I., Sosnovets, E. N., Geomagnetizm i aeronomiya, Vol. 7, 1967, (being printed).

156. Kennel, C. F., Petscheck, H. E., J. Geophys. Res., Vol. 71, p. 1, 1966.

Translated for the National Aeronautics and Space Administration under contract No. NASw-2038 by Translation Consultants, Ltd., 944 South Wakefield Street, Arlington, Virginia 22204.

NASA-Langley, 1971 - 29
Coml., Phila., Penn.

"The aeronautical and space activities of the United States shall be conducted so as to contribute . . . to the expansion of human knowledge of phenomena in the atmosphere and space. The Administration shall provide for the widest practicable and appropriate dissemination of information concerning its activities and the results thereof."

—NATIONAL AERONAUTICS AND SPACE ACT OF 1958

NASA SCIENTIFIC AND TECHNICAL PUBLICATIONS

TECHNICAL REPORTS: Scientific and technical information considered important, complete, and a lasting contribution to existing knowledge.

TECHNICAL NOTES: Information less broad in scope but nevertheless of importance as a contribution to existing knowledge.

TECHNICAL MEMORANDUMS: Information receiving limited distribution because of preliminary data, security classification, or other reasons.

CONTRACTOR REPORTS: Scientific and technical information generated under a NASA contract or grant and considered an important contribution to existing knowledge.

TECHNICAL TRANSLATIONS: Information published in a foreign language considered to merit NASA distribution in English.

SPECIAL PUBLICATIONS: Information derived from or of value to NASA activities. Publications include conference proceedings, monographs, data compilations, handbooks, sourcebooks, and special bibliographies.

TECHNOLOGY UTILIZATION PUBLICATIONS: Information on technology used by NASA that may be of particular interest in commercial and other non-aerospace applications. Publications include Tech Briefs, Technology Utilization Reports and Technology Surveys.

Details on the availability of these publications may be obtained from:

SCIENTIFIC AND TECHNICAL INFORMATION OFFICE

NATIONAL AERONAUTICS AND SPACE ADMINISTRATION

Washington, D.C. 20546